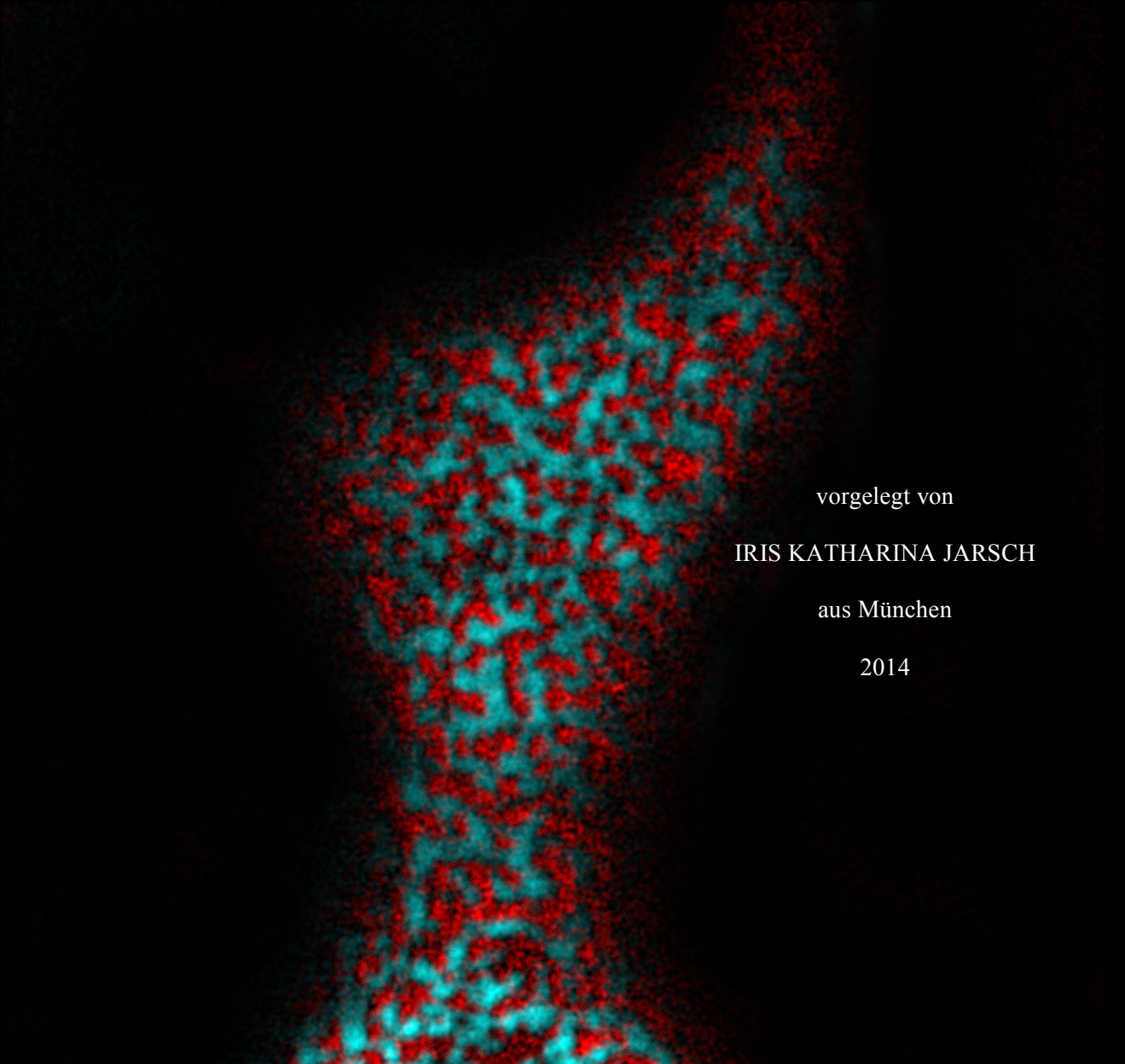


Dissertation
zum Erwerb des Doktorgrades
an der Fakultät für Biologie der
Ludwig-Maximilians-Universität München

Remorin proteins in *Arabidopsis thaliana*:
Markers for diverse membrane micro-domains
with roles in plant-microbe interactions



vorgelegt von

IRIS KATHARINA JARSCH

aus München

2014

Für meine Schwester Vroni

Die vorliegende Arbeit wurde im Bereich Genetik in der Arbeitsgruppe von Dr. Thomas Ott
(Lehrstuhl Prof. Dr. Martin Parniske) angefertigt.

Erstgutachter: Dr. Thomas Ott

Zweitgutachter: Prof. Martin Parniske

Tag der mündlichen Prüfung: 31.07.2014

Zusammenfassung:

Die Plasmamembran lebender Zellen stellt die Hauptbarriere für alle Arten von extrazellulären Signalen dar. Viele davon werden ins Innere der Zelle weitergeleitet, hier lösen sie im Kern transkriptionelle Veränderungen und damit die Anpassung der Zelle auf Proteinebene aus. Andere wiederum werden direkt erkannt und in unmittelbare molekulare Antworten umgewandelt, wie zum Beispiel die Sekretion von gespeicherten Stoffen oder Konformations-änderungen von Proteinen. Besonders in Pflanzen, welche durch ihre sesshafte Lebensweise auf die rechtzeitige und spezifische Erkennung von Umweltveränderungen angewiesen sind, hat sich ein höchst diverses Rezeptorsystem entwickelt. In der Ackerschmalwand *Arabidopsis thaliana*, der in dieser Arbeit verwendeten Modellpflanze, wurden 610 verschiedene Rezeptorproteine identifiziert, welche wiederum von zahlreichen interagierenden, und bis jetzt weitestgehend unerforschten Proteinen reguliert werden. Als entscheidendes Prinzip, dieses Aufgebot an membran-gebundenen Komponenten von Signalkaskaden zu organisieren, gilt inzwischen die zeitliche und lokale Kompartimentierung der Plasmamembran. Durch Akkumulation relevanter Bestandteile von biologischen Prozessen in sogenannten Membrandomänen werden kurze Reaktionszeiten und die unmittelbare Signalweiterleitung garantiert. Besonders wichtig bei solchen Prozessen sind sogenannte Gerüstproteine, welche als Adaptoren zwischen anderen Komponenten fungieren.

In dieser Arbeit wurden Remorine, eine Familie pflanzenspezifische Proteinen ohne bisher definierte Funktion, aufgrund ihrer Eigenschaft Membrandomänen zu markieren und ihrer mutmaßlichen Beteiligung an Pflanzen-Pathogen-Interaktionen, genauer untersucht.

Eine systematische Expression von Remorinen als Fluorophor-Fusionen mit anschließender hochauflösender mikroskopischer und quantitativer Untersuchung offenbarte, dass die meisten Remorine sich in deutlich unterschiedlichen Mustern an der Membran verteilen. Untersucht wurden dabei Parameter wie die Größe der erkennbaren Domänen, die Form, die Helligkeit, aus welcher auf die Proteinkonzentration rückgeschlossen werden kann, sowie die Domänendichte an der Membran. Diese Ergebnisse wurden von Kollokalisationsanalysen unterstützt, welche die Lokalisation in unterschiedlichen, koexistierenden Membrankompartimenten erkennen ließen. Ferner wurden die Eigenschaften der von Remorinen markierten Membrandomänen, wie zum Beispiel der Austausch an Proteinen mit der umgebenden Membran, sowie lokale und zeitliche Dynamik und Stabilität untersucht. Dabei konnte eine hohe Fluktuation einzelner Proteine zwischen Domäne und umliegender Membran, jedoch eine klare laterale Immobilität der gesamten Domäne nachgewiesen werden. Zusätzlich zeichneten sich die untersuchten

Domänen teilweise durch eine außerordentlich große zeitliche Stabilität aus, andere wiederum scheinen abhängig von bestimmten Stimuli zu entstehen.

Weitergehende Arbeiten dienten der Identifizierung der Funktion einzelner Bereiche der Proteine. Hierbei konnte die entscheidende Rolle des äußersten C-terminalen Bereichs, des so- genannten RemCAs (Perraki et al., 2012; Konrad et al., 2014) als Membrananker bestätigt werden. Zusätzlich wurden mit Hilfe eines Hefe-2-Hybrid Ansatzes zahlreiche neue Interaktoren für eine Auswahl von Remorinen identifiziert. Dabei wurde ein essentieller Rezeptor der basalen Immunantwort, BAK1 als Interaktor für Remorin 6.4 gefunden.

Zuletzt wurden einige wenige Remorine mit Hilfe von Mutantenlinien in einer genetischen Studie phänotypischen Analysen bezüglich ihrer Funktion bei Pflanzen-Pathogen Interaktionen unterzogen. Remorin 6.4 spielt hiernach eine Rolle bei der Immunantwort nach Befall mit virulenten Bakterien.

Die grundlegende Erkenntnis, dass in lebenden Zellen zahlreiche klar unterscheidbare Arten an Membrandomänen koexistieren, ist ein Meilenstein auf dem Weg zur Anerkennung einer neuen Vorstellung vom Aufbau der Zytoplasmamembran. Diese wird häufig noch als undifferenzierte zweidimensionale Flüssigkeit beschrieben, in welcher stellenweise sogenannte Lipidflöße, festere Strukturen aus Cholesterin und Sphingolipiden, die auch bestimmte Proteine beherbergen können, auftreten. Anhand der in dieser Arbeit gewonnenen Ergebnisse, sowie ähnlicher Studien in Hefe lässt sich nun folgendes Bild zeichnen: Es ist davon auszugehen, dass unterschiedliche Proteine, welche im selben biologischen Prozess involviert sind, in unmittelbarer Nachbarschaft oder sogar im selben Proteinkomplex in der Membran organisiert sind. Die Lipidzusammensetzung in der unmittelbaren Umgebung wird von diesen Proteinen bestimmt, bietet jedoch auch die Grundlage für die Bildung der Domäne, indem sie die Lokalisation der Komponenten in diesem Bereich fördert. Die zahlreichen an der Zellmembran gleichzeitig ablaufenden, unterschiedlichen Prozesse erfordern eine hochkomplexe, zeitlich und räumlich stark regulierte Kompartimentierung der Membran. Es kann vermutet werden, dass Remorine eine Rolle als Gerüstproteine bei der Ausbildung einer Auswahl dieser Domänen bilden. Im Fall von Remorin 6.4 ist das Protein für den Prozess der Flagellin-Erkennung und die unmittelbaren Abwehrantworten, welche nachweislich eine Präformierung der beteiligten Proteinkomplexe voraussetzen, notwendig.

Eidesstattliche Versicherung

Hiermit erkläre ich an Eides statt, dass ich die vorliegende Arbeit selbstständig, und ohne unerlaubte Hilfe von Dritten angefertigt habe.

München, den

(Iris Katharina Jarsch)

Erklärung

Ich habe weder anderweitig versucht, eine Dissertation einzureichen oder mich einer Doktorprüfung zu unterziehen, noch habe ich diese Dissertation oder Teile derselben einer anderen Prüfungskommission vorgelegt.

München, den

(Iris Katharina Jarsch)

Table of contents:

Zusammenfassung.....	5
Eidesstattliche Versicherung/ Erklärung	7
Introduction	17
1. The role of receptor-like kinases in plant signalling	17
2. Receptor mediated immunity and effector triggered immunity in plant pathogen interactions	21
Remorin proteins, a novel group of regulatory proteins in receptor-mediated signalling.....	26
3. Membrane compartmentalisation	29
3.1. The concept of membrane domain formation	29
3.2. Functional relevance of membrane compartmentalisation	33
3.3. Membrane compartmentalisation in plant biotic interactions	34
4. Aims of this work	36
Material and Methods.....	37
1. Methods	37
1.1. Recombinant DNA Methods.....	37
1.1.1. DNA amplification via polymerase chain reaction (PCR)	37
1.1.1.1. Analytical PCR	37
1.1.1.2. Preparative PCR.....	37
1.1.2. Fusion of DNA fragments via cut-ligation	38
1.1.3. Cloning of entry vectors	38
1.1.4. Creation of expression vectors.....	39
1.2. Protein expression for fluorescence microscopy.....	39
1.2.1. <i>A. tumefaciens</i> mediated transient transformation of <i>N. benthamiana</i>	39
1.2.2. <i>A. tumefaciens</i> mediated transient transformation of <i>A. thaliana</i>	40
1.3. Plant work	40
1.3.1. Sterilization of <i>A. thaliana</i> seeds	40
1.3.2. Plant growth conditions	40
1.3.3. Genotyping procedure for SALK T-DNA insertion lines	40
1.3.4. Generation of stable transgenic <i>A. thaliana</i>	41
1.3.5. DNA extraction from <i>A. thaliana</i> leaf material (short protocol)	41
1.3.6. ROS burst assay	42
1.3.7. Seedling growth inhibition assay	42
1.3.8. MAPK activation assay	42
1.3.9. Infection with <i>P. syringae</i>	43
1.3.10. Root growth inhibition assay with brassinolides	43

1.4.	Yeast work	43
1.4.1.	Yeast transformation.....	43
1.4.2.	GAL4 yeast-2-hybrid drop assay	43
1.5.	Protein work.....	44
1.5.1.	Protein separation via SDS-PAGE	44
1.5.2.	Western blot analysis	44
1.5.3.	Protein extraction from plant material and cell fractionation	45
1.5.4.	Co-immunoprecipitation from <i>A. thaliana</i> and <i>N benthamiana</i> leaf material ..	45
1.5.5.	Protein extraction from yeast.....	45
1.5.6.	Expression and purification of recombinant proteins from <i>E. coli</i>	46
1.5.7.	<i>In vitro</i> phosphorylation assay.....	46
1.6.	Plant treatment for imaging, image acquisition and processing	47
1.6.1.	Sample preparation and confocal microscopy	47
1.6.2.	PM counterstaining with FM® 4-64.....	47
1.6.3.	Plasmolysis	47
1.6.4.	Image processing	48
1.6.5.	Quantitative analysis of single domains	48
1.6.6.	Fluorescent recovery after photo bleaching (FRAP)	48
1.6.7.	Kymographs.....	48
1.6.8.	Co-localisation analysis	49
2.	Material.....	50
2.1.	Antibodies, antibody coated products	50
2.2.	Chemicals	50
2.3.	Enzymes and kits.....	50
2.4.	Buffers and solutions.....	51
2.4.1.	Antibiotic stock solutions	51
2.4.2.	Solutions for recombinant DNA techniques.....	51
2.4.2.1.	TOPO cloning reaction mix	51
2.4.2.2.	BP reaction mix	52
2.4.2.3.	LR reaction mix	52
2.4.2.4.	Reaction mix for analytical polymerase chain reaction (PCR).....	52
2.4.2.5.	Reaction mix for preparative PCR.....	52
2.4.2.6.	Reaction mix for cut-ligations in pENTR/D-BsaI	53
2.4.3.	DNA extraction buffer for <i>A. thaliana</i> leaf material (short protocol)	53
2.4.4.	Solutions for <i>Agrobacterium</i> mediated transformation of plant material.....	53
2.4.4.1.	Infiltration solution for <i>A. tumefaciens</i> mediated transient transformation of <i>N. benthamiana</i> or <i>A. thaliana</i>	53
2.4.4.2.	DEX-solution for pre-treatment of AvrPto-DEX inducible <i>A. thaliana</i>	54

2.4.4.3. Dipping solution for stable transformation of <i>A. thaliana</i>	54
2.4.5. Buffers and solutions for yeast work	54
2.4.5.1. Yeast transformation master mix	54
2.4.5.2. 10 x amino acid (AA) -stock solution	54
2.4.6. ROS reaction buffer	55
2.4.7. Buffers and Solutions for plant protein work	55
2.4.7.1. Lacus buffer for MAPK assay	55
2.4.7.2. <i>N. benthamiana</i> protein extraction buffer	55
2.4.7.3. Extraction buffer for co-immunoprecipitation from <i>N. benthamiana</i> and <i>A. thaliana</i>	56
2.4.7.4. Plant proteinase inhibitor cocktail	56
2.4.7.5. Kinase buffer for <i>in vitro</i> protein phosphorylation assays	57
2.4.8. Buffers for purification of His-tagged proteins from bacteria	57
2.4.8.1. Binding buffer	57
2.4.8.2. Washing buffer	57
2.4.8.3. Elution buffer	57
2.4.9. Buffers and Solutions for SDS-PAGE and Western Blotting	58
2.4.9.1. Solution for acrylamide – isotachopheresis gel (“stacking“ gel)	58
2.4.9.2. Solution for acrylamide – electrophoresis gel (“resolving” gel)	58
2.4.9.3. 6 x SDS loading dye	58
2.4.9.4. 10 x SDS running buffer	58
2.4.9.5. 10 x Transfer buffer for wet transfer	59
2.4.9.6. 10 x TBS	59
2.4.9.7. 10 x Semi-dry transfer buffer	59
2.4.9.8. Coomassie staining solution	59
2.4.9.9. Destaining solution	59
2.5. Media	60
2.5.1. Plant media MS solid/liquid medium for <i>A. thaliana</i> seedlings	60
2.5.2. Media for Yeast	60
2.5.2.1. YPAD solid/liquid	60
2.5.2.2. Selective dropout (SD) medium solid/liquid	60
2.5.3. Kings B medium for <i>P. syringae</i>	61
Results	62
1. Cell biological characterisation of the remorin protein family	62
1.1. Subcellular localisation	62
1.1.1. The N-terminal fusion of the proteins compared to a C-terminal fusion does not impair membrane localisation	63

1.1.2.	Localisation of remorin proteins to membrane domains is independent of the plant expression system or the promoter.....	66
1.1.3.	Remorin proteins label a variety of coexisting distinct membrane compartments.....	69
1.1.4.	AtREM1.2 and AtREM1.3 are organised in structures below the resolution limit of standard confocal microscopy.....	79
1.1.5.	Tissue specific labelling of membrane domains.....	80
1.1.6.	Remorin-labelled membrane compartments exhibit lateral stability.....	81
1.1.7.	Immobile and mobile fraction of the protein population undergo dynamic exchange.....	84
1.1.8.	The far C-terminal region of remorin proteins is necessary but not entirely sufficient for membrane binding.....	86
1.1.9.	Relocalisation.....	90
1.2.	Interactions with other proteins.....	91
1.2.1.	Remorin proteins are able to both homo- and hetero-oligomerise.....	91
1.2.2.	Arabidopsis remorin proteins interact with different receptor kinases.....	92
1.3.	Phosphorylation.....	96
1.3.1.	Remorins can be directly phosphorylated by receptor kinases.....	96
1.3.2.	Investigation of the role of phosphorylation on interaction with RLKs.....	97
2.	Towards the role of remorin proteins in plant pathogen interactions.....	100
2.1.	Creation of a T-DNA insertion line collection for <i>Arabidopsis thaliana</i> remorin proteins.....	100
2.2.	Generation of complemented mutant lines.....	101
2.3.	Phenotypical analysis of remorin mutants.....	102
2.3.1.	Experimental approaches.....	102
2.3.2.	Phenotypic analysis of AtREM1.2 and AtREM1.3 during plant-pathogen interactions.....	102
2.3.2.1.	<i>Atrem1.2-1</i> , <i>Atrem1.2-2</i> and <i>Atrem1.3-2</i> are knockout mutant lines.....	102
2.3.2.2.	FLS2 and BAK1 form an intact receptor complex after flg22 elicitation....	103
2.3.2.3.	The production of reactive oxygen species is unaltered in group 1 mutant lines.....	104
2.3.2.4.	MAP kinase activation.....	106
2.3.2.5.	Seedling growth inhibition.....	107
2.3.2.6.	Investigation of remorin mutant lines for phenotypes after infection with <i>Pseudomonas syringae</i>	107
2.3.3.	Investigation of AtREM6.4 function in BAK1-related biological processes.....	108
2.3.3.1.	<i>Atrem6.4-1</i> is a knockout mutant line.....	108
2.3.3.2.	FLS2-BAK1 interaction after flg22 elicitation is unaltered in <i>Atrem6.4-1</i> ..	109
2.3.3.3.	The production of ROS after flg22 treatment is reduced in <i>Atrem6.4-1</i> plants.....	110

2.3.3.4. <i>Atrem6.4-1</i> displays higher susceptibility towards infection with <i>P. syringae</i> <i>pv. Pto DC3000</i> compared to Col-0 wt	111
2.3.3.5. Investigation of <i>Atrem6.4-1</i> for defects in brassinolide signalling	112
Discussion	115
1. A global approach to investigate the cell biological aspects of remorin proteins provides insights into their possible biological function	115
1.1. Remorins are marker proteins for a multitude of coexisting, laterally stable membrane domains	115
1.2. Remorin proteins attach to the membrane via two mechanisms	117
1.3. The N-terminal region of the protein plays a role in formation of membrane domains and relocalisation	118
1.4. Remorin proteins – phosphorylation dependent scaffold proteins for RLKs	119
2. A phenotypical assessment of remorin mutants	122
2.1. The genetic approach to investigate the biological role of group one remorin proteins	122
2.2. <i>AtREM6.4</i> is involved in <i>flg22</i> induced ROS production but not in other BAK1- dependent processes as BR signalling	125
Abbreviations	128
Acknowledgements	134
Literature	136
Appendix	156

List of Figures:

FIG. 1: MECHANISMS OF REGULATION OF PRR COMPLEXES (MODIFIED FROM MONAGHAN AND ZIPFEL, 2012).....	20
FIG. 2: THE TWO LAYERS OF PERCEPTION IN ANIMAL AND PLANT INNATE IMMUNE SYSTEM (ADAPTED FROM NURNBERGER AND KEMMERLING, 2006; MONAGHAN AND ZIPFEL, 2012)	22
FIG. 3: ILLUSTRATION OF PTI AND ETI IN PLANTS AFTER ELICITOR TREATMENT OR PATHOGEN ATTACK (ADAPTED FROM ABRAMOVITCH ET AL., 2006; PANSTRUGA ET AL., 2009)	23
FIG. 4: ILLUSTRATION OF THE GUARD AND THE DECOY MODEL IN RECOGNITION OF EFFECTOR PROTEINS BY THE PLANT INNATE IMMUNE SYSTEM (ADAPTED FROM VAN DER HOORN AND KAMOUN, 2008).....	25
FIG. 5: SIMPLIFIED ILLUSTRATION OF THE REMORIN PROTEIN STRUCTURE ACCORDING TO A 3D MODEL OF SYMREM1..	27
FIG. 6: THE THREE MECHANISMS OF DYNAMIC MEMBRANE COMPARTMENTALISATION COEXISTING IN THE PLASMA MEMBRANE (KUSUMI, 2012).....	32
FIG. 7: THE N-TERMINAL TAG DOES NOT HINDER MEMBRANE ATTACHMENT OF REMORIN PROTEINS AND LEADS TO LOCALISATION IN MEMBRANE DOMAINS.....	65
FIG. 8: REMORIN EXPRESSION PATTERNS ACCORDING TO GENEVESTIGATOR DATABASE	67
FIG. 9: VARIATION IN EXPRESSION STRENGTH OR SYSTEM DOES NOT ALTER LOCALISATION OF ATREMS IN MEMBRANE DOMAINS.....	68
FIG. 10: REMORIN PROTEINS LABEL A VARIETY OF DISTINCT MEMBRANE DOMAINS.....	70
FIG. 11: QUANTITATIVE ANALYSIS OF DOMAIN PATTERNS.	71
FIG. 12 CHOICE OF REGIONS OF INTEREST FOR CALCULATION OF THE CO-LOCALISATION COEFFICIENTS	73
FIG. 13: THE PLANT PLASMA MEMBRANE DISPLAYS A WIDE SPECTRUM OF DISTINGUISHABLE COEXISTING MICRODOMAINS.	74
FIG. 14 RANGE OF CORRELATION BETWEEN DOMAINS LABELLED BY REMORIN PROTEINS.....	78
FIG. 15: FRAP EXPERIMENTS ON ATREM1.2 AND ATREM1.3 REVEAL LATERAL MOBILITY IN THE PLASMA MEMBRANE	80
FIG. 16: ATREM1.2 AND ATREM1.3 LOCALISE TO MEMBRANE MICRODOMAINS IN A TISSUE-SPECIFIC MANNER	81
FIG. 17 ATREM6.6 FILAMENTOUS STRUCTURES ARE STABLE OVER TIME	82
FIG. 18: MEMBRANE DOMAINS ARE LATERALLY IMMOBILE.....	83
FIG. 19: FRAP EXPERIMENTS ON REMORIN PROTEINS REVEAL DYNAMIC AND CONSTANT RECRUITMENT OF PROTEINS INTO IMMOBILE MEMBRANE DOMAINS.....	85
FIG. 21: INVESTIGATION OF TRUNCATION CONSTRUCTS TO DETERMINE THE ROLE OF THE DIFFERENT REMORIN PROTEIN REGIONS.....	89
FIG. 22: RELOCALISATION OF C-TERMINALLY AND N-TERMINALLY TAGGED ATREM6.4	91
FIG. 23: HOMO- AND HETEROOLIGOMERISATION OF ATREMS IN YEAST.....	92
FIG. 24: ATREM6.4 INTERACTS WITH BAK1 <i>IN PLANTA</i>	96
FIG. 25: <i>IN VITRO</i> PHOSPHORYLATION OF ATREM6.4 BY THE BAK1 KD	97
FIG. 26: MUTATIONS OF THE ANNOTATED PHOSPHORYLATION SITE OF ATREM6.4, T215, HAVE AN IMPACT ON INTERACTION WITH BAK1 IN MEMBRANE DOMAINS	98
FIG. 27: HOMOZYGOUS T-DNA INSERTION LINES IDENTIFIED FOR SEVERAL ATREMS	101

FIG. 28: IDENTIFICATION OF KNOCKOUT MUTANTS USING WESTERN BLOT ANALYSIS	103
FIG. 29 THE FLS2-BAK1 RECEPTOR COMPLEX FORMS NORMALLY IN GROUP 1 MUTANT LINES AFTER FLG22 TREATMENT	104
FIG. 30: REACTIVE OXYGEN PRODUCTION IS NOT ALTERED IN GROUP1 MUTANT LINES AFTER ELICITOR TREATMENT	105
FIG. 31: MAPK ACTIVATION IS NOT REDUCED IN GROUP 1 MUTANT LINES	106
FIG. 32: SEEDLING GROWTH INHIBITION IS UNALTERED IN GROUP 1 MUTANT LINES AFTER FLG22 TREATMENT	107
FIG. 33: THE <i>ATREM1.2-1/ATREM1.3-2</i> DOUBLE MUTANT SHOWS A MODERATE BUT SIGNIFICANTLY INCREASED SUSCEPTIBILITY TOWARDS INFECTION WITH <i>P. SYRINGAE PV. PTO DC3000</i>	108
FIG. 34: <i>ATREM6.4</i> TRANSCRIPT IS NOT DETECTABLE IN <i>ATREM6.4-1</i> MUTANTS	109
FIG. 35 THE FLS2-BAK1 RECEPTOR COMPLEX FORMS NORMALLY IN <i>ATREM6.4-1</i> AFTER FLG22 TREATMENT	110
FIG. 36: <i>ATREM6.4-1</i> IS IMPAIRED IN ROS BURST AFTER FLG22 ELICITATION	111
FIG. 37: <i>ATREM6.4-1</i> IS MORE SUSCEPTIBLE TO INFECTION WITH <i>P. SYRINGAE PV. PTO DC3000</i>	112
FIG. 38: <i>ATREM6.4-1</i> DOES NOT DISPLAY ALTERED REACTIONS TO BRASSINOLIDE TREATMENT	113

List of tables:

TABLE 1: CHANGES IN SUBCELLULAR LOCALISATION PATTERN WITH N-TERMINAL PROTEIN FUSIONS.....	63
TABLE 2: CO-LOCALISATION ANALYSIS OF CO-EXPRESSED PROTEIN PAIRS	75
TABLE 3: RESULTS OF A TARGETED Y2H GAL4 SCREEN FOR RLKS INTERACTING WITH ATREMS	93

Introduction

1. The role of receptor-like kinases in plant signalling

As sessile organisms, plants have been challenged in evolution to survive in an ever-changing environment. In order to adapt to environmental cues, both harmful and beneficial, they had to evolve mechanisms to detect a vast variety of external stimuli. Changes in physiology and development in response to stresses require high amounts of energy. Therefore the involved perception systems are both highly specialized as well as tightly regulated.

Receptor-like kinases (RLKs) in plants and the Pelle-kinases in animals have evolved from a common eukaryotic ancestor. While three and four members of the RLK/Pelle superfamily are annotated in mice and humans, respectively, the receptor repertoire with over 600 members has massively diversified in *Arabidopsis thaliana* (Shiu and Bleecker, 2001a, b, 2003; Gish and Clark, 2011). Most of the RLKs in plants unite an extracellular N-terminal domain and a C-terminal intracellular kinase domain in one plasma membrane-spanning protein. Others do not harbour a transmembrane region, and are therefore predicted to be of cytoplasmic localisation (RLCKs = receptor-like cytoplasmic kinase). Additionally, there are receptor-like proteins (RLPs) without an intracellular kinase domain, but resembling the extracellular domains of RLKs (Shiu and Bleecker, 2001a, b, 2003).

The general mechanisms, by which receptors perceive chemical signals and mediate the transduction from the outside of the cell to the intracellular lumen and the nucleus have been unravelled over the past decades both for animal as well as for plant receptor proteins (reviewed in Schlessinger, 2000; Pawson and Nash, 2000; Silverman and Maniatis, 2001; Imler and Hoffmann, 2001; Hoffmann and Reichhart, 2002; Gomez-Gomez and Boller, 2002). Ligand binding induces receptor oligomerisation and structural changes, which lead to auto-phosphorylation and/or trans-phosphorylation of the intracellular domain or interacting kinase proteins. This results in another structural change usually exposing the active site of the kinase to bind the substrate. The activated kinase then phosphorylates additional residues, usually within non-catalytic regions, which then provide binding sites for downstream targets (reviewed in Schlessinger, 2000; Pawson and Nash, 2000). Both animal as well as plant kinases, including RLKs, can be subdivided into RD and non-RD kinases (RD = arginine and aspartate) depending on the conservation of the amino-acid residue preceding the highly conserved

Introduction

aspartate in the catalytic loop of the kinase domain (Johnson et al., 1996; Nolen et al., 2004). Most RD kinases require auto-phosphorylation of the activation loop for full kinase activity. In contrast, non-RD kinases are not dependent on activation-loop auto-phosphorylation for kinase activation (Nolen et al., 2004).

The largest group among the plant RLKs is constituted by leucine-rich-repeat-RLKs (LRR-RLKs) (Shiu and Bleeker, 2001a, b, 2003). By now, a number of individual examples as well as transcriptome analyses have shown roles for LRR-RLKs in plant growth and development as well as reactions to biotic and abiotic stresses (Shiu and Bleeker, 2001a, b, 2003; Diévar and Clark, 2004; Kilian et al., 2007; Chae et al., 2009).

Paradigm examples for plant LRR-RLKs are the brassinosteroid (BR) receptor BRASSINOSTEROID INSENSITIVE 1 (BRI1), which is involved in hormone signalling (He et al., 2000; Kinoshita et al., 2005), and the pattern recognition receptors (PRRs) FLAGELLIN SENSITIVE-2 (FLS2) and EF-TU RECEPTOR-1 (EFR). FLS2 and EFR are involved in plant defence responses and are activated upon perception of segments of the bacterial flagellum and the elongation factor EF-Tu (Gómez-Gómez and Boller, 2000; Zipfel et al., 2006). Both ligands can be experimentally mimicked by the small peptides flg22 (Felix et al., 1999; Zipfel et al., 2004; Chinchilla et al., 2006) and elf18 (Kunze et al., 2004) respectively. Another LRR-RLK, BRI1-ASSOCIATED KINASE 1 (BAK1) was originally found in complex with BRI1 (Nam and Li, 2002; Li et al., 2002; Russinova, 2004), but has been shown to associate as a co-receptor with FLS2, EFR and supposedly additional PRRs (Heese et al., 2007b; Chinchilla et al., 2009; Chinchilla et al., 2007b; Postel et al., 2010). BAK1 belongs to a family of closely related and putatively redundant receptor kinases called SOMATIC EMBRYOGENESIS RECEPTOR KINASES (SERKs) (Albrecht et al., 2005; Albrecht et al., 2008; Chinchilla et al., 2007a; Colcombet et al., 2005; He et al., 2007; Hecht et al., 2001; Heese et al., 2007a; Karlova et al., 2006; Kemmerling et al., 2007). Since *bak1* knockout mutants display increased lesions upon pathogen infection and a premature senescence phenotype (Kemmerling et al., 2007; Jeong et al., 2010), additional roles for BAK1 in cell death control have been proposed (He et al., 2007, 2008).

BAK1 itself has not been shown to be involved in ligand recognition (Chinchilla et al., 2007a; Kinoshita et al., 2005). It has therefore been considered to act as a central regulator with scaffold function of the corresponding RLKs (Chinchilla et al., 2009; Postel et al., 2010). Interestingly, major differences between the interaction of BAK1 with the RD-kinase BRI1 and the non-RD-kinases FLS2 and EFR have been described

Introduction

(Dardick and Ronald, 2006). While kinase activities of both proteins are required during BAK1-BRI1 interaction, this feature is dispensable for the association of BAK1 with the two PRRs (Schulze et al., 2010; reviewed in Clouse, 2011; Schwessinger et al., 2011). Recent analyses of two *BAK1* alleles, *bak1-5* (Schwessinger et al., 2011) and *BAK1_{elg}* (Chung et al., 2012) as well as BAK1 phospho-sites (Oh et al., 2010; Wang et al., 2008) have shed light on the mechanistic specification of BAK1 signalling. Both mutants display only a single amino-acid exchange; yet, differential effects on plant defence, brassinosteroid (BR) responses and cell death control have been described.

While the mechanisms of signal transduction and regulation beyond the receptor complex formation are still largely unknown, several direct regulators of few RLKs have been identified. One paradigm example is BKI1 (BRI1 KINASE INHIBITOR 1), a specific inhibitor of BR signalling and a direct target of BRI1. It has been found to limit the interaction of BRI1 and BAK1 *in vitro*, hypothetically via steric hindrance, but dissociates from the plasma membrane (PM) upon brassinolide (BL) binding (Wang and Chory, 2006).

In plant immune signalling, FLS2, EFR and putatively BAK1 associate with the RLCK BOTRYTIS-INDUCED KINASE 1 (BIK1) and its paralogs PBS1, PBL1 and PBL2. BIK1 is phosphorylated by BAK1 after elicitation, and in return trans-phosphorylates both FLS2 and BAK1. Subsequently, it dissociates from the activated receptor complex (Lu et al., 2010; Zhang et al., 2010) (Fig. 1A). In line with this, *bik1* and *pbl* mutants are impaired in a number of immune responses. Interestingly, BIK1 and PBLs are dispensable for downstream kinase activation (Feng et al., 2012a). These results indicate not only that BIK1 is a positive regulator of some plant defence responses, but also that branching of downstream signalling pathways occurs directly at the receptor complex.

To complete the picture of differential regulation of signalling pathways, BIK1 has just recently been identified as an interactor of BRI1 as well. Here, it acts as a negative regulator, as *bik1* mutants display BL hypersensitivity phenotypes (Lin et al., 2013).

The role of phosphorylation in regulation of RLK-signalling has also been well studied for the rice pattern receptor kinase XANTHOMONAS RESISTANCE 21 (XA21). Although the bacterial elicitor that activates XA21 is still unknown (Lee et al., 2009; retracted), several constant interactors have been identified (Fig. 1B), including XB24. This kinase promotes phosphorylation at auto-regulatory residues, which keep XA21 inactive. Upon XA21 activation, XB24 dissociates and allows signalling (Chen et al., 2010a; Chen et al., 2010b). Association of XB15, leading to de-phosphorylation of the kinase domain, mediates receptor inactivation (Park et al., 2008).

Introduction

Recent studies also demonstrated that ubiquitination is negatively regulating receptor mediated signalling at the example of FLS2. The two E3-ubiquitin ligases PUB12 and PUB13 are recruited to the receptor complex by BAK1 post ligand perception. Subsequently, to terminate signalling, FLS2 is poly-ubiquitinated, leading to degradation (Lu et al., 2011).

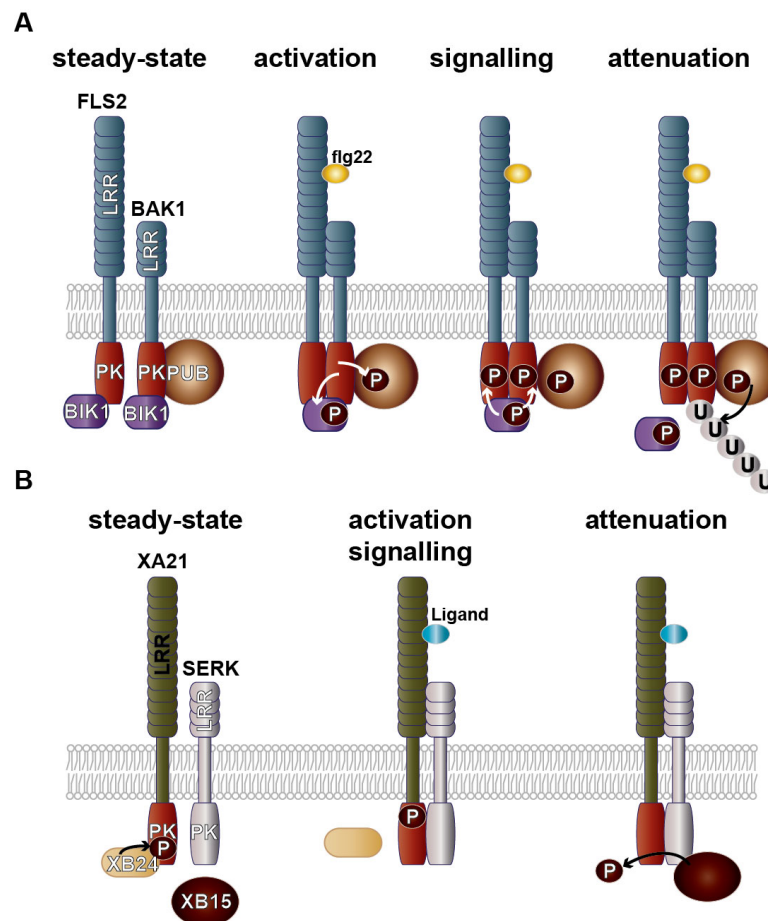


Fig. 1: Mechanisms of regulation of PRR complexes (modified from Monaghan and Zipfel, 2012)

In *A. thaliana*, FLS2 interacts constitutively with BIK1 and related PBLs (A). BAK1 interacts constitutively with the E3-ubiquitin ligases PUB12 and PUB13 and putatively also associates with BIK1. Upon flg22 binding, BAK1 interacts with FLS2 and trans-phosphorylates both BIK1 and PUB12/13. BIK1 then trans-phosphorylates BAK1 and FLS2 leading to full activation of the receptor complex before it dissociates. For attenuation of signalling, PUB12 and PUB13 poly-ubiquitinate FLS2, targeting it for degradation.

In rice, XA21 has been shown to constitutively interact with XB24 (B). XB24 promotes auto-phosphorylation at residues, which keep XA21 inactive. Ligand binding results in XB24 dissociation, putative dimerization of XA21 with a SERK family protein, XA21 phosphorylation at distinct residues and the activation of immune signalling. XB15 then dephosphorylates XA21 to attenuate signalling. Phosphorylation is annotated as black circles labelled 'P' and arrows indicate the direction of post-translational modifications. P = phosphorylation; PK = protein kinase

Additionally to the above-described mechanisms, endocytosis is a key process in regulation of receptor complexes. Both BRI1 and FLS2 are constitutively endocytosed (Ruscinova, 2004; Geldner et al., 2007). For the BRI1 receptor complex, the importance of internalisation for successful signalling has been a matter of debate for several years (Ruscinova, 2004; Geldner et al., 2007; Song et al., 2009). Recent studies showed that impairment of endosome formation enhanced BR signalling, indicating that indeed signalling takes place at the PM and endocytosis mediates receptor inactivation and subsequent degradation (Irani et al., 2012; Di Rubbo et al., 2013). For FLS2, internalisation has been studied in detail. Here, constitutive endocytosis is BAK1-independent and sensitive to brefeldin A (BFA), a drug, which interferes with the endosomal recycling pathway. In contrast, ligand-induced FLS2 endocytosis is BAK1-dependent and leads to BFA-insensitive endocytosis and subsequent degradation of the receptor (Robatzek and Saijo, 2008; Beck et al., 2012). These results show that FLS2 is both subject to a constant recycling process independent of activation, but also inactivated by endocytosis of the receptor complex to attenuate the signalling cascade.

2. Receptor mediated immunity and effector triggered immunity in plant pathogen interactions

Among the many dangers plants face in nature, infection by pathogens is one of the most challenging ones. Unlike animals, plants cannot rely on an adaptive immune system. Additionally, microbes evolve with unequally much higher rates, making it almost impossible for the plant to specifically recognize them and directly defend itself towards harmful microorganisms.

At a first glance, plant immunity seems simple: At the frontier, plants rely on pre-existing barriers present on the leaf surface such as wax layers, the cell wall itself or secreted molecules like enzymes or secondary metabolites (Zipfel and Felix, 2005). Yet, more importantly, plants share with animals one fundamental defence system: The basal, innate immunity. Here both animals and plants rely on two kinds of receptors, which lead to two independent sets of immune response (reviewed in Faulkner and Robatzek, 2012) (Fig. 2). The first step is mediated by the above described pattern recognition receptors at the PM. These receptors typically perceive conserved molecular patterns referred to as PAMPs or MAMPs (pathogen associated molecular patterns/microbe associated molecular patterns). These epitopes are invariant among whole classes of microbes, as they are part of molecules, which are fundamental to the pathogens fitness (Schwessinger and Zipfel, 2008). Receptor activation leads to active immune responses prior to host invasion (Boller and Felix, 2009).

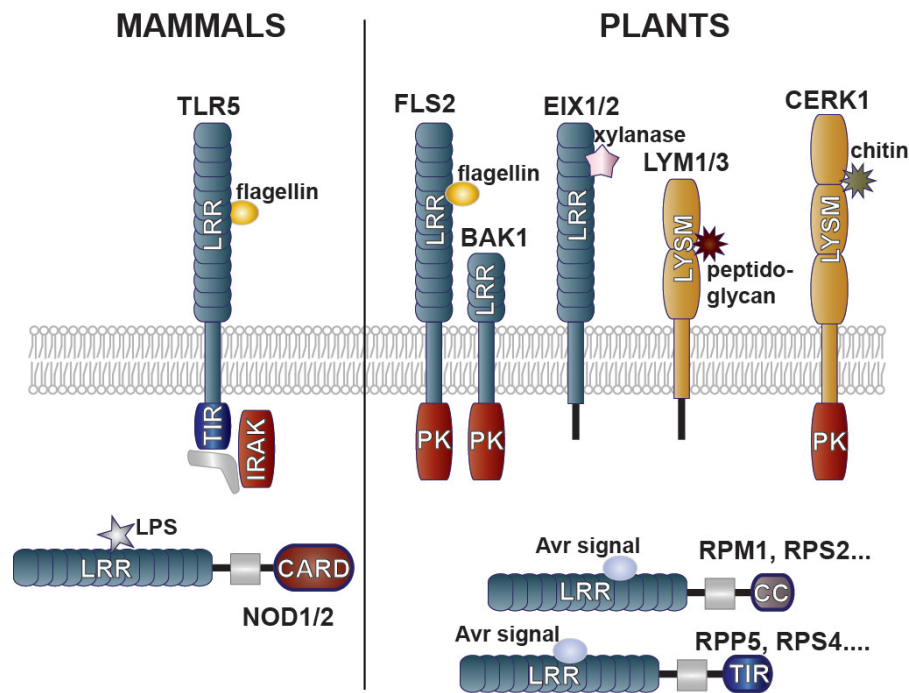


Fig. 2: The two layers of perception in animal and plant innate immune system (adapted from Nurnberger and Kemmerling, 2006; Monaghan and Zipfel, 2012)

Pattern recognition receptors at the plasma membrane bind conserved molecular patterns invariant among whole classes of microbes. Depicted examples are the TOLL-LIKE RECEPTOR 5 (TLR5) in mammals (Hayashi et al., 2001) as well as FLS2 and its co-receptor BAK1 in plants, which perceive flagellin. EIX1 and EIX2 are receptors for the fungal plant cell wall degradation enzyme xylanase tomato (Ron and Avni, 2004). Additionally to those LRR-receptors, a number of lysine-motif (LYSM)-RLKs has been identified. CERK1 from *A. thaliana* binds both the fungal cell wall component chitin (Miya et al., 2007; Iizasa et al., 2010; Petutschnig et al., 2010) as well as has been proposed to act as a co-receptor for the LYSM-RLPs LYM1 and LYM3 after peptidoglycan recognition (Willmann et al., 2011). A second layer of pathogen perception consists of the cytoplasmic nucleotide-binding site (NBS)-LRR receptors. In mammals, NOD1 and NOD2 bind lipo-poly-saccharide (LPS) (Inohara and Nunez, 2001). In plant cells, direct PAMP recognition at this stage has not been shown so far. However, NBS-LRR receptors act as so called resistance (R) proteins, indirectly sensing cell biological changes provoked by bacterial avirulence (Avr) factors. CC = coiled coil; TIR = toll and interleukin receptor motif; PK = protein kinase; CARD = caspase activation and recruitment domain.

The second step involves cytoplasmic receptor proteins that indirectly perceive bacterial effector proteins inside the plant cell. The recognition ultimately leads to a hypersensitive response mediating resistance (Jones and Dangl, 2006; Chisholm et al., 2005).

FLS2 and EFR are model PAMP-receptors. Activation by pathogens or the respective elicitors flg22 and elf18 leads to a stereotypic set of downstream responses (Boller and Felix, 2009) (Fig. 3). Seconds after ligand perception, FLS2 and BAK1 form a heterodimer and phosphorylation takes place (Schulze et al., 2010). Subsequently, ion fluxes across the PM occur and intracellular Ca^{2+} concentration increases (Schwacke and Hager, 1992; Tavernier et al., 1995). After two minutes, the RESPIRATORY

Introduction

BURST OXIDASE HOMOLOG D (RBOHD) mediated production of reactive oxygen species, the oxidative burst, can be measured at the leaf surface (Miller et al., 2009).

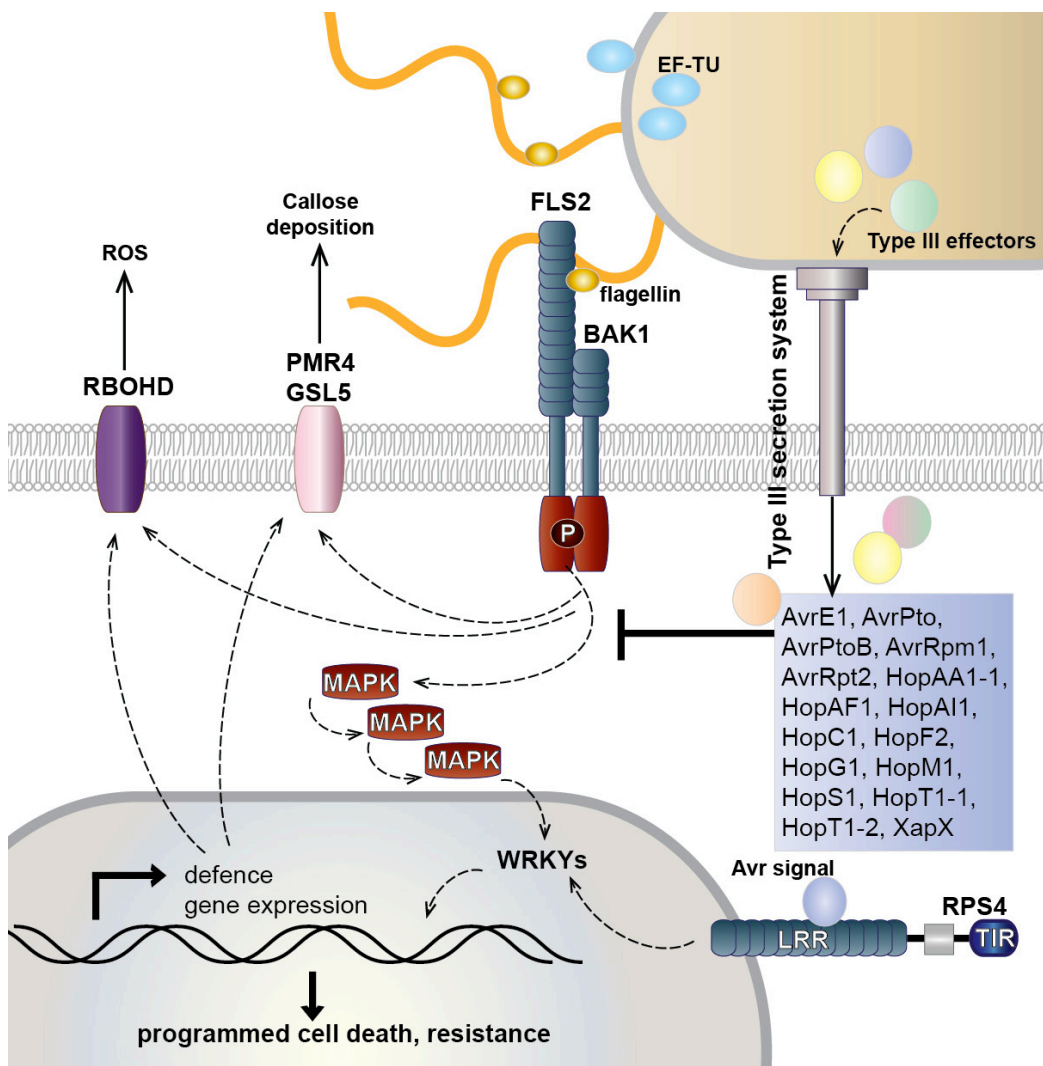


Fig. 3: Illustration of PTI and ETI in plants after elicitor treatment or pathogen attack (adapted from Abramovitch et al., 2006; Panstruga et al., 2009)

The *A. thaliana* PRR FLS2 recognises the flg22 peptide of flagellin. PRR activation leads to receptor heteromerisation, which triggers signalling events that lead to the upregulation of over 300 plant genes (Asai et al., 2002; Navarro et al., 2004; Thilmony et al., 2006). A complete signal transduction cascade downstream of the receptor complex has been shown by Asai and colleagues. Activation of the mitogen-activated protein kinase (MAPK) pathway and several WRKY transcription factors leads to the expression of PAMP induced genes (Asai and Yoshioka, 2008; Asai et al., 2002). Phenotypes that are associated with activated basal defences include cell wall fortifications by callose deposition and the production of reactive oxygen species (ROS). Delivery of effector proteins through the type III secretion system into plant cells a strategy applied by pathogens, which have successfully entered the leaf to target PRR-mediated defences (He et al., 2006; Hauck et al., 2003; Li et al., 2005; Oh and Collmer, 2005; Metz et al., 2005). Modifications on effector targets are recognized in resistant plant species by NB-LRR type receptors like the resistance against *Pseudomonas syringae* 4 (RPS4) protein. It perceives targeting of the enhanced disease resistance 1 (EDS1) complex by AvrRps4 and triggers a hypersensitive response via WRKY transcription factors (Bhattacharjee et al., 2011). TIR = toll and interleukin receptor motif, P = phosphorylation.

Introduction

Reactive oxygen species (ROS) both acidify the leaf surface and serve as a signal accelerator for cell-to-cell communication (reviewed by Lamb and Dixon, 1997; Miller et al., 2009) (Fig. 3). Activation of the MAPK cascade leads to transcriptional changes (Asai et al., 2002; reviewed by Zhang and Klessig, 2001; reviewed by Tena et al., 2001) (Fig. 3). Ultimate plant defence responses are for example stomatal closure (Melotto et al., 2006) and callose deposition (Gomez-Gomez et al., 1999; Brown et al., 1998; Luna et al., 2011).

All those reactions can be seen as means to strengthen the pre-existing barriers on the plant surface (Zipfel and Felix, 2005). The goal is to successfully prevent the pathogen from entering the plant cell and/or proliferating in the intercellular space. Therefore, PTI only rarely leads to a hypersensitive response and ultimate death of the infected tissue.

Yet, successful pathogens survive the initial pre-existing and inducible immune system and inject effector proteins via their type-III secretion system into the host cell (reviewed in Alfano and Collmer, 2004). Effector proteins can be enzymes or even transcription factors, which aim to alter cellular processes in favour of the pathogen. They also target essential components of the plant innate immune system, which, consequently, results in effector-triggered susceptibility (Gohre and Robatzek, 2008; Gohre et al., 2008).

In response to effector injection, plants have added a second layer of plant innate immunity based on intracellular components, mostly nucleotide-binding (NB)-LRR-type proteins encoded by so-called resistance (R) genes (Meyers et al., 2003). These proteins indirectly recognize pathogen effectors delivered into host cells during infection by detection of modifications on typical effector targets.

Effector targets, of which the plant cell recognizes modifications, have been termed “guardees”, the R proteins “guard proteins”. Activation of guard proteins lead to effector triggered immunity (ETI) (Fig. 4C). The effector perception mechanism postulated by the Guard Model proposes an explanation on how multiple effectors could be perceived indirectly if they target the same guardee. Thus a relatively small R gene repertoire would be able to recognize the broad diversity of pathogens that attack plants (Dangl and Jones, 2001). It has been proposed that the guardee is indispensable for the virulence function of the effector protein in the absence of the cognate R protein, consequently leading to effector-triggered susceptibility (ETS) (Fig. 4A). Supporting evidence for the Guard Model has accumulated over the past decade with the description of several classical guarded effector targets like *A. thaliana* RIN4 and PBS1 (Jones and Dangl, 2006)

Introduction

New data on additional targets of Avr proteins suggested a modification to the Guard hypothesis, proposing that some host targets of effectors act as decoys to detect pathogen effectors via R proteins (Fig. 4D) but are dispensable for effector function (Zhou and Chai, 2008) (Fig. 4B).

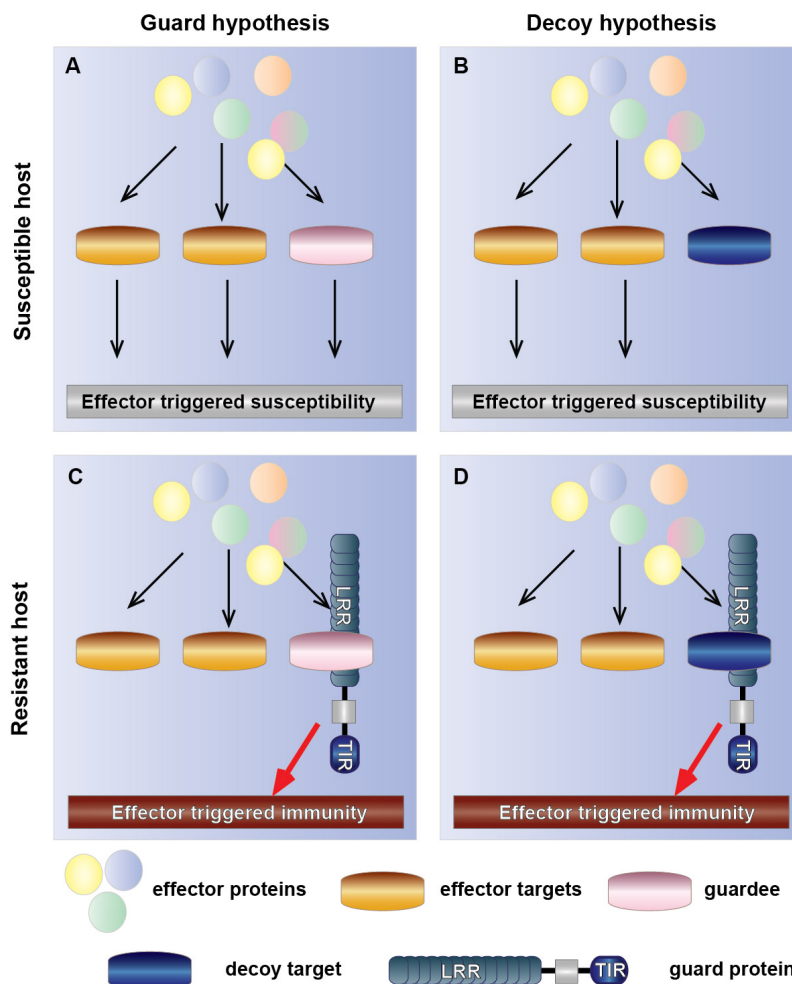


Fig. 4: Illustration of the Guard and the Decoy Model in recognition of effector proteins by the plant innate immune system (adapted from van der Hoorn and Kamoun, 2008)

The Guard Model sees the guardee as one of many effector targets indispensable for pathogen virulence in susceptible hosts (A), which is monitored by the resistant plant to perceive infection (C). In the decoy model, plants provide a protein dispensable for pathogen fitness and therefore not underlying negative selective forces in susceptible genotypes (B). In resistant phenotypes, targeting of the decoy is perceived by the guard protein, leading to effector-triggered immunity.

Remorin proteins, a novel group of regulatory proteins in receptor-mediated signalling

Remorins are plant-specific proteins comprising a multi-gene family in all land-plants with 16 different members in *A. thaliana* (Raffaele et al., 2007). Originally found to be differentially phosphorylated upon application of poly-galacturonoids (PGN) in potato (Farmer et al., 1989), remorins were suggested to play roles in cell-to-cell signalling and plant defence (Reymond et al., 1996). Remorins are PM associated (Farmer et al., 1989; Jacinto et al., 1993; Reymond et al., 1996; Marmagne et al., 2004; Mongrand et al., 2004; Sazuka et al., 2004; Nelson et al., 2006; Valot et al., 2005; Valot et al., 2006) and phosphorylated by a PM-associated protein-kinase (E. Farmer, P. Bariola, pers. communication). Although they were demonstrated to bind a number of poly-anions including DNA, which led to an annotation as DNA-binding proteins (Alliotte et al., 1989; Reymond et al., 1996), there is currently no *in vivo* evidence for a biological function related to these observations.

Remorins have recently been phylogenetically investigated and divided into six subgroups based on their protein-structure. All members of the protein-family harbour the highly conserved C-terminal region with a canonical remorin-signature. This region contains both a number of highly conserved positively charged residues as well as a predicted coiled-coil domain (Reymond et al., 1996; Raffaele et al., 2007). It is the main contributor to protein-protein interactions (Tòth et al., 2012; Marin et al., 2012). Also, for StREM1.3 the far C-terminal region (remorin C-terminal anchor = REMCA) has been shown to mediate PM localisation (Perraki et al., 2012a).

Additionally to this invariable part, most remorins feature a highly diverse N-terminal region (Raffaele et al., 2007). This part of the protein is mostly intrinsically disordered (Marin and Ott, 2012; Marin et al., 2012). It is subject to differential phosphorylation (Benschop et al., 2007; Keinath et al., 2010; Marin et al., 2012) and may serve regulatory functions during protein-protein interactions (Tòth et al., 2012; Marin et al., 2012).

Several studies have linked remorin proteins to plant-microbe interactions. Studies on StREM1.3 showed binding of the TRIPLE GENE BLOCK Protein1 (TBP1) of the Potato Virus X (PVX) and an influence on virus movement through plasmodesmata (Raffaele et al., 2009).

Introduction

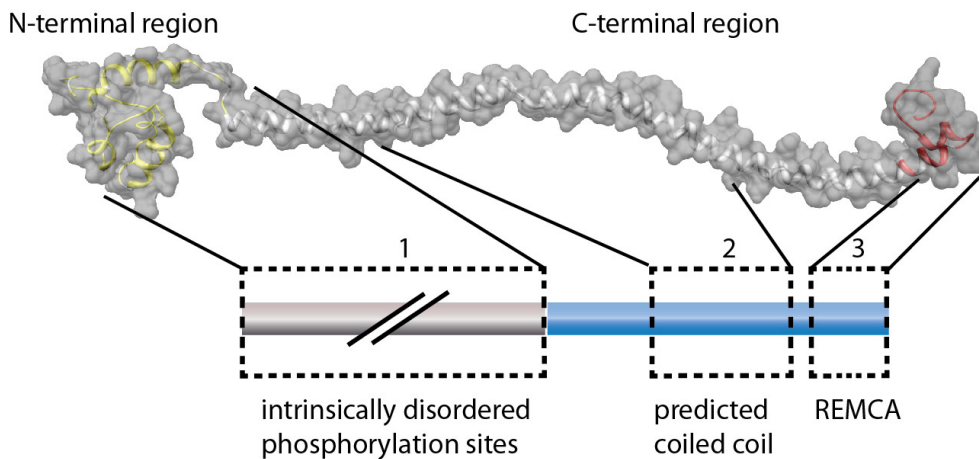


Fig. 5: Simplified illustration of the remorin protein structure according to a 3D model of SYMREM1

All remorin proteins harbour the highly conserved C-terminal region. This region contains a predicted coiled-coil domain (2) and the plasma membrane attachment site (3). The N-terminal region is highly variable in both length and amino-acid composition for most remorins, while it is completely absent in members of the phylogenetic group 3. This part of the protein is intrinsically disordered and can be phosphorylated in order to regulate protein-protein interactions (1) (modified from Konrad et al., 2014)

SYMBIOTIC REMORIN 1 (SYMREM1), a remorin of the phylogenetic class 2, was found to be involved in the establishment of the symbiosis between rhizobia and legumes (Lefebvre et al., 2010; Tòth et al., 2012). SYMREM1 is strongly up-regulated in *Medicago truncatula* roots (Lefebvre et al., 2007; Lefebvre et al., 2010) after perception of the nodulation factors (Nod factors or NFs), strain-specific lipopolyoligosaccharide signalling molecules secreted by bacteria prior to root hair infection. A *symrem1* knockout mutant in *M. truncatula* was shown to be impaired in the formation of nitrogen-fixing nodules (Lefebvre et al., 2010). In line with that, a microscopical analysis of fluorophore fusion constructs demonstrated SYMREM1 localisation to the host derived membrane surrounding symbiosomes inside fully developed nodules of *M. truncatula* and *Lotus japonicus* (Lefebvre et al., 2010; Tòth et al., 2012). Additional immuno-labelling experiments with antibodies against the native SYMREM1 protein also confirmed its localisation to infection thread membranes in *M. truncatula* (Lefebvre et al., 2010). SYMREM1 was also shown to directly interact with the major RLKs required for rhizobial invasion, NOD FACTOR RECEPTOR 1 (NFR1), NOD FACTOR RECEPTOR 5 (NFR5) and SYMBIOSIS RECEPTOR-LIKE KINASE (SYMRK) in *L. japonicus* (Tòth et al., 2012) as well as with the respective putative orthologs RLKs in *M. truncatula* (Lefebvre et al., 2010). Both NFR1 and SYMRK kinase domains phosphorylate SYMREM1 *in vitro* (Tòth et al., 2012).

There is further accumulating evidence that other members of the remorin protein family are involved in plant–microbe interactions (reviewed in Jarsch and Ott, 2011) as

Introduction

several remorins are differentially regulated during host invasion by pathogenic bacteria. Primarily transcripts of group 1b remorins were reported to be altered in *A. thaliana* upon infection with *Pseudomonas syringae* (Nelson et al., 2006; Widjaja et al., 2009) and after inoculation of *Lycopersicon hirsutum* with *Clavibacter michiganensis* (Coaker et al., 2004).

In a large-scale proteomic approach to identify differentially phosphorylated proteins involved in early plant defence signalling after elicitation with bacterial or fungal PAMPs, the *A. thaliana* remorin AtREM1.3 was found to be phosphorylated in a flg22-dependent manner. Interestingly, phospho-peptides of remorins AtREM1.2, AtREM5.1, AtREM6.1, AtREM6.2, and AtREM6.4 were also detected. However, for the latter five proteins, the increase in phosphorylation status was not significant compared to mock treated samples (Benschop et al., 2007).

It has also been suggested that remorin proteins are involved in ETI (reviewed in Jarsch and Ott, 2011). AtREM1.2 is significantly up-regulated in an RPM1-dependent manner in plants overexpressing the bacterial effector AvrRPM1. RPM1 is the (NB)-LRR type receptor recognising AvrRPM1-mediated hyper-phosphorylation of the classical effector target RPM1 INTERACTING PROTEIN 4 (RIN4) (Mackey et al., 2002). Additional isoforms of AtREM1.2 were found in the infection-mimicking overexpression state, indicating that differential phosphorylation of AtREM1.2 is dependent on AvrRPM1 (Widjaja et al., 2009). Furthermore, it was reported that AtREM1.2 interacts with RIN4 itself (Liu et al., 2009). Being targeted by several *P. syringae* effector proteins, RIN4 is the paradigmatic example for a host target that is guarded by NB-LRR resistance proteins. Two different type III effectors, AvrRpm1 and AvrB (Boyes et al., 1998), interact with RIN4 and induce hyper-phosphorylation, which leads to RPM1-mediated resistance (Mackey et al., 2002). A third effector, AvrRpt2, a cysteine protease (Axtell et al., 2003; Kim et al., 2005) that is activated inside the host cell (Coaker et al., 2005), directly targets and cleaves RIN4. AvrRpt2 triggered resistance is dependent on another NB-LRR type receptor, RPS2. It is possible that remorins are targets of bacterial effectors themselves, as a putative cleavage sequence of AvrRpt2 in AtREM6.1 has already been published (Chisholm et al., 2005). However, this *in silico* prediction is not yet proven experimentally.

Several group 1 remorin proteins as well as SYMREM1 are described as membrane domain marker proteins. Proteomic analyses after extraction of detergent resistant membrane (DRM) fractions from *A. thaliana* and *M. truncatula* (Kierszniowska et al., 2009; Laloi et al., 2007; Lefebvre et al., 2007; Mongrand et al., 2004; Morel et al., 2006; Raffaele et al., 2009) or extraction of plasmodesmata membranes, which are defined by

a very specific membrane compartment (Salmon and Bayer, 2012), have shown remorins to be enriched in those samples. Additionally to that, the localisation of remorin proteins to membrane domains has been shown microscopically for StREM1.3 as a fluorophore fusion in *Nicotiana benthamiana* (Raffaele et al., 2009) as well as for SYMREM1 after immune-gold labelling in *M. truncatula* (Lefebvre et al., 2010).

3. Membrane compartmentalisation

3.1. The concept of membrane domain formation

The interest in membrane compartmentalisation has been rising over the past decades, as our understanding of molecular processes has led to an increasingly complex and detailed picture of biological systems. It is by now accepted that efficient and specific reactivity within biological pathways requires highly specialised environments, accumulation of certain molecules, and small distances.

In their discussion on the structure of cell membranes, Singer and Nicolson 1972 presented a model of the physical generalities of membrane organisation, which is still valid for many aspects. Any known membrane in living organisms can be described as a two-dimensional liquid. This liquid is composed of both proteins and lipids. Yet, while proteins had obvious roles in cell biological processes as transport and signalling, the latter were believed to play no more than a passive role as structural elements - acting as framework and solvent for the functional components. Moreover, in this fluid mosaic model, the membrane was believed to be essentially homogeneous (Singer and Nicolson, 1972).

This view was subject to a revolutionary change, when in 1997 Simons and Ikonen critically discussed the dramatic impact of lipid clustering and targeted trafficking on protein localisation and phenomena as cell polarity and caveolae formation (Harder and Simons, 1997). In their model, called the “lipid raft hypothesis”, glycosphingolipids laterally associate with each other by interaction of their carbohydrate head groups. The space between the larger molecules is filled with stabilizing cholesterol. As a consequence, membrane phases separate into co-existing liquid ordered and liquid disordered areas (Hancock et al., 2006). This leads to tightly packed clusters of lipids (the so-called rafts) surrounded by the less tighter and more fluid environment of unsaturated sphingolipids and phospholipids (Simons and Ikonen, 1997). It was proposed that proteins are either included or excluded from either of the two phases, providing a mechanism of spatial separation of distinct protein populations (Ikonen et al., 2008). Again, this model provides mechanistic explanations for cell biological

Introduction

phenomena, which are still as relevant as back then. Yet, it also has its drawbacks and does not fill the blanks for several questions directly arising. First of all, it is restricted to the extracellular leaflet of the bilayer, as glycosphingolipids as well as the proteins discussed are not found in the intracellular part of the membrane. Secondly, it does not consider an active role for proteins in membrane compartmentalisation but elevates lipids to the role of the determining agent of membrane domain formation.

The lipid raft model gave rise to new approaches on how to study the described membrane compartments. Based on the assumption that lipid rafts were more stable than disordered regions in the membrane, a method to extract detergent resistant membrane (DRM) fractions was established. It was used as a approach to investigate lipid and protein content of extracted ordered membrane compartments. Yet, a number of scientists not only convincingly demonstrated that the method *per se* might be inadequate to differentiate between ordered and disordered membrane areas due to artificial lipid and protein clustering (Heerklotz et al., 2002, Munro et al, 2003). Additionally, the understanding of membrane compartments has changed, moving towards the idea that indeed there may be a multitude of coexisting membrane domains with divers biological functions in signalling, membrane trafficking and endocytosis (Jacobson et al., 2007). Smaller membrane domains are able to cluster into more stable (signalling) platforms upon the perception of certain stimuli and crosslinking (Kusumi et al., 2005; Kusumi et al., 2004; Kusumi and Suzuki, 2005; Hammond et al., 2005; Lingwood et al., 2008; Hogue et al., 2011).

By now, the definition of membrane rafts is as follows: Rafts are “small (10–200 nm), heterogeneous, highly dynamic, sterol-enriched and sphingolipid-enriched domains that compartmentalize cellular processes. Small rafts can sometimes be stabilized to form larger platforms through protein-protein and protein-lipid interactions” (Pike, 2006).

It was shown that, due to their specific properties such as lipid composition, rigidity and thickness, a number of transmembrane and membrane-associated proteins preferentially localise to those rafts. Post-translational modifications like S-acylation and myristoylation target proteins to sterol-rich membrane compartments at the inner leaflet of the PM. Fusion with a glycosylphosphatidylinositol (GPI) – anchor fosters protein association with membrane rafts at the outer leaflet of the PM (Schroeder et al., 1994, Varma and Mayor, 1998, Zacharias et al., 2002). Transmembrane proteins themselves then massively influence dynamics and rigidity of an emerging domain by slowing down diffusion, inhibiting lateral movement of smaller proteins and interactions with the cell wall and the cytoskeleton (reviewed in Kusumi et al., 2012).

Introduction

Next to membrane-internal forces, external factors influence membrane composition and structure as well as protein localisation and mobility. One major factor of course is targeted protein trafficking, which has been thoroughly researched in animal epithelial cells as a model system. Here, the PM forms two major distinct compartments, the apical and the baso-lateral domain (Mostov et al, 2003; Janssens and Chavrier, 2004). This polar differentiation is achieved by targeted recruitment of different cargos to these domains. Newly synthesized proteins are sorted into vesicles that discriminate between apical and basal domains. Furthermore, proteins are selectively retained at their position or, in case of mis-localisation, endocytosed, respectively (Rodriguez-Boulán et al., 2005). In plants, those processes are directly connected to an auxin gradient, which is both dependent on as well as a prerequisite for cell polarity (Went et al, 1974; Friml et al., 2003). Regulation of cell polarity is therefore achieved by the asymmetric localisation of auxin efflux carriers (Galweiler et al., 1998; Wisniewska et al., 2006; Petrasek et al., 2006). Key components here are the polarly distributed PINFORMED (PIN) proteins, which were identified as auxin-regulators involved in a variety of developmental processes (Chen et al., 1998, Luschnig et al., 1998, Muller et al., 1998, Utsuno et al., 1998; Friml et al., 2002a, 2002b, 2003; Benkova et al., 2003; Reinhardt et al., 2003; Blilou et al., 2005; Sauer et al., 2006; Scarpella et al., 2006)

Several models propose roles for the cytoskeleton in membrane compartmentalisation. Interaction between membrane proteins and the cytoskeleton laterally immobilize protein complexes. Furthermore, larger proteins and protein clusters, which are prevented in diffusion by the actin/microtubule network are lining up to it. In this way, they act themselves as fences and (temporarily) prevent diffusion of other membrane localised proteins and rafts (membrane-skeleton fence and anchored-protein picket model) (Kusumi and Sako, 1996; Sako et al., 1998; Kusumi et al., 1998; Fujiwara et al., 2002; Kusumi et al., 2004). The different layers of cell-internal mechanisms for membrane compartmentalisation have recently been reviewed by Kusumi and colleagues. They coupled raft formation, protein-complex establishment and compartmentalisation by the membrane cytoskeleton to a three-tiered architecture of the PM (Kusumi et al., 2012) (Fig. 6). The so-called “hop-diffusion”, the specific movement pattern proteins would adopt when being temporarily confined in cytoskeleton-bordered membrane compartments has already been experimentally demonstrated for a number of proteins (Sako and Kusumi, 1995; Kusumi et al., 2005, reviewed in Urbanus and Ott, 2012)

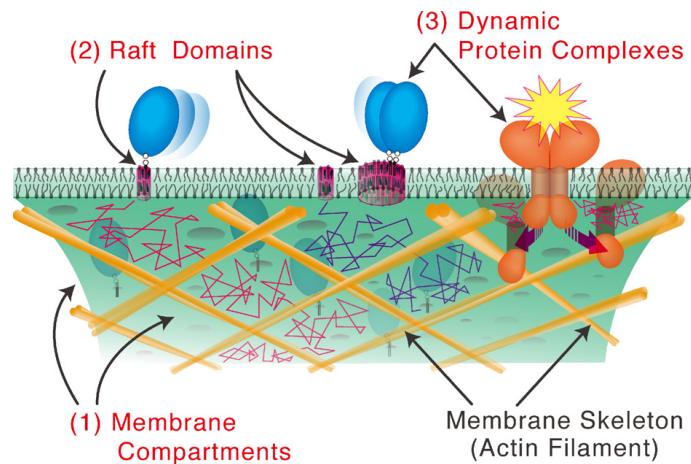


Fig. 6: The three mechanisms of dynamic membrane compartmentalisation coexisting in the plasma membrane (Kusumi, 2012).

As membrane compartments formed by the cytoskeleton can be as large as several hundred nm, single proteins, protein clusters as well as several single rafts can be accommodated in them. Single molecules can dynamically associate with rafts, which slows down their diffusion speed. Hop-diffusion occurs between cytoskeleton-bordered compartments. Both kinds of protein dynamics are decreased upon protein oligomerisation and multi-complex formation.

An additional, external factor for membrane compartmentalisation specific for plants and fungi is the cell wall. Recent studies with fluorescently tagged PM localised proteins showed a significant influence of the cell wall on protein mobility even if there was no extracellular protein domain which could interact with the latter. Interestingly, the pattern of cellulose deposition could be directly linked to protein dynamics in the PM. These data indicate that membrane compartmentalisation can actively be regulated by localisation-specific cell wall synthesis (Martiniere et al., 2012). Two other studies describe the targeted trafficking of the cellulose synthase along the microtubule network (Gutierrez et al., 2009, Crowell et al., 2009). Also, mobility of membrane compartments containing active cellulose synthase is directly dependent on microtubule dynamics and is increased during different kinds of stresses (Gutierrez et al., 2009). The manipulation of PM protein mobility by a specific cell wall pattern is reminiscent of the Casparian strip, a band of very specifically produced cell wall material found by Robert Caspary in the 19th century. The Casparian strip is characteristic for the root epidermis and functions as a barrier for water and ions (Enstone et al., 2002). The so-called CASPARIAN STRIP MEMBRANE DOMAIN PROTEINS (CASPs) are a set of novel proteins which were found to specifically localise beneath this cell wall structure, where they immobilise. These data indicate the formation of a specific membrane domain underlying this cell wall accumulation. Different *casp* mutants also display defects in Casparian strip formation (Roppolo et al., 2011).

3.2. Functional relevance of membrane compartmentalisation

There are several examples of well-documented functional importance of membrane domains by now. One of them revolves around the *Chlorella kessleri* hexose-proton symporter HEXOSE UPTAKE 1 (HUP1). HUP1 shows a dot-like distribution in the PM in the homologous system as well as upon heterologous expression in yeast. Mutant yeast strains lacking ergosterol (*erg6*) or sphingolipids (*lcb1-100*), however, show a homogeneous distribution of HUP1 (Grossmann et al., 2006). Moreover, correlating with loss of membrane domain localisation, the catalytic activity of HUP1 is impaired in *erg6* cells. These results indicate that localisation of HUP1 to membrane clusters is important for protein function. In earlier experiments, it had already been demonstrated that membrane domain association is decreased for a number of microdomain associated proteins in ergosterol and sphingolipid yeast mutant strains (Bagnat and Simons, 2002b). Consequently, these strains are also impaired in membrane polarisation at the mating projection (Bagnat and Simons, 2002a, 2002b).

Profound alterations in cell polarity and protein localisation were also obtained with *A. thaliana* sterol biosynthesis mutants, leading to severe developmental phenotypes. The ergosterol biosynthesis mutants *smt1* and *smt1^{orc}*, which lack the enzyme STEROL METHYLTRANSFERASE 1, accumulate abnormal amounts of cholesterol (Diener, 2000, Willemsen 2003). As a result, these mutant lines show defects in the establishment of proper cell polarity, leading to a mislocalisation of the previously mentioned auxin efflux carrier-proteins PIN1 and PIN3 but also AUX1. The latter is an auxin influx carrier, which is also usually asymmetrically localised in specific cell types and serves as a cell polarity marker protein (Friml et al., 2002a; Friml et al., 2002b; Galweiler et al., 1998; Muller et al., 1998; Swarup et al., 2001). As a consequence of the cellular alterations in *smt1^{orc}*, polar auxin transport is reduced leading to defects in growth and development (Willemsen et al., 2003).

Similar results were obtained with the so-called *hydra* mutants. *HYDRA1* and *HYDRA2* encode enzymes essential for sterol biosynthesis. These mutant lines exhibit altered concentrations of sitosterol, campesterol and stigmasterol and are hypersensitive to auxin. Also here, the authors provide a model, in which membrane function influences protein localisation to correctly regulate hormone signalling (Souter et al., 2002)

A well-elaborated example linking directed vesicle transport and protein localisation in membrane domains is the inward-rectifying K⁺ channel KAT1. When being expressed in the heterologous *N. benthamiana* system, KAT1 is distributed in immobile membrane domains in the PM and exhibits a distinct radial pattern in turgid guard cells in *Vicia*

Introduction

faba (Sutter et al., 2006; Homann et al., 2007). While the described distinct pattern of KAT1 in guard cells could be attributed to interactions with the plant cell wall, the association of KAT1 with membrane domains seems to depend on other factors. It was demonstrated that both localisation as well as lateral mobility of the protein were profoundly changed upon overexpression of a dominant-negative fragment (Sp2) of the SOLUBLE N-ETHYLMALEIMIDE-SENSITIVE FACTOR ATTACHMENT RECEPTOR (SNARE) protein, SYP121. SNARE proteins occur at vesicle and target membranes and maintain mechanisms for targeted trafficking, recognition, docking and fusion (Pratelli et al., 2004). KAT1 was shown to be homogeneously distributed and highly mobile in the respective cells (Sutter et al., 2006). These data implicate a role for SNAREs in the distribution and dynamics of KAT1 at the PM.

Furthermore, it was shown that the phytohormone abscisic acid selectively triggers KAT1 endocytosis in specialized vesicles excluding other proteins. This indicates inducible membrane compartmentalisation upon stress signals (Sutter et al., 2007).

3.3. Membrane compartmentalisation in plant biotic interactions

The establishment of specialised membrane compartments is a specific response to pathogens in plants defence. A number of proteins localise in focal accumulations beneath fungal appressoria. Fluorophore-tagged versions of the SNARE-proteins SYP121 (PEN1), SYP122 and ROR2 are homogeneously distributed at the PM prior to fungal attack, but accumulate in circular domains of several μm beneath fungal entry points (Assaad et al., 2004, Bhat et al., 2005). Similar observations have been made for the heptahelical defence modulator MLO (Bhat et al., 2005) as well as for the cell death regulator BAX Inhibitor-1 (Eichmann et al., 2006). Interestingly, the reverse observation can be made for several PM localised proteins after infection on *A. thaliana* or *N. benthamiana* by the oomycetes *Hyaloperonospora parasitica* or *Phytophthora infestans*. While FLS2 or PEN1 label both *H. parasitica* haustoria-surrounding plant PM as well as peripheral PM, PIP1 and ACA8 are depleted from the haustorial entry sites. As partially reverse observations were made at *P. infestans* haustoria, it can be concluded that specialised membrane microdomains are formed at oomycete entry sites in a pathogen-species dependent manner (Lu et al., 2012).

A striking example for dynamic membrane domain localisation of a plant protein has recently been published. In analogy to SYMREM1, the *M. truncatula* membrane resident flotillin FLOT4 is required for root nodule symbiosis (Haney and Long 2010). A fluorophore-tagged version of the protein was coexpressed with a fluorophore fusion of the predicted Nod factor receptor LYSINE MOTIF RECEPTOR KINASE 3 (LYK3),

Introduction

the putative homolog of NFR1 (Haney et al., 2011). Both proteins localise to diverse membrane domains in the PM of *M. truncatula* roots. Interestingly, the proteins did not co-localise until stimulation of the roots with *Sinorhizobium meliloti*. In stimulated roots, stable, immobile membrane domains formed, which contained both previously separated proteins (Haney et al., 2011).

In human cells, membrane rafts have been shown to play crucial roles in pathogenic interactions. They are essential for the signalling processes in B-cell and T-cell activation (reviewed in Alonso and Millan, 2001). Nevertheless, they can also be hijacked by a number of pathogens. Both microbes and viruses use raft-mediated endocytotic machineries as entry sites into the cell (reviewed in Rosenberger et al., 2000; Pelkmans et al., 2005 and Hartlova et al., 2010). The accumulation of important signalling molecules such as components being required for cytoskeleton reorganisation in membrane domains is likely to be attractive for invading microbes.

Being non-plant specific, the above-mentioned reggie/flotillin proteins have already been extensively studied in mammalian cells. Both in plants and in animals, members of the reggie/flotillin protein family have been shown to play a role in clathrin-independent endocytosis. Interestingly they were also shown to be localised on host-derived membranes surrounding intracellular microorganisms. These data gave first indications for raft-mediated endocytosis as a possible entry point for microorganisms (Panter et al., 2000; Dermine et al., 2001; Saalbach et al., 2002; Glebov et al., 2006; Murphy et al., 2007; Li et al., 2008; Korhonen et al., 2012; reviewed in Urbanus and Ott, 2012).

A number of viruses, bacteria and protozoans have been shown to display a specific set of surface proteins, which enable them to directly interact with membrane rafts. One example is the omnipresent uropathogen *Escherichia coli*, which has been demonstrated to bind CD48, a GPI-anchored raft-localised surface molecule, via the bacterial adhesion molecule FimH prior to invasion of macrophages and mast cells (Baorto et al., 1997; Shin et al., 2000; Parton and Richards, 2003). Similar observations have been made for *Salmonella enteritica*, which induces the accumulation of cholesterol and the GPI-anchored raft-localised surface molecule CD55 at its entry site. Inside the cell, this pathogen replicates in cholesterol-rich vacuoles, indicating further implications of membrane rafts in pathogen survival (Catron et al., 2002; Knodler and Steele-Mortimer, 2003; Knodler et al., 2003). It seems that most pathogens utilize host mechanisms involved in phagocytosis and bacterial transport to lysosomes but evade degradation once inside the cell (reviewed in Hartlova et al., 2010).

4. Aims of this work

The presented work aimed to take a substantial approach on the function and mechanisms of remorin proteins *in planta*. Most functional analyses on these proteins have so far been performed on rather difficult model organisms. Consequently we chose to address those fundamental questions in the most established and best investigated plant model organism – *Arabidopsis thaliana*.

Three different approaches were taken:

A thorough cell biological investigation concentrated on the subcellular localisation of each single member of the protein family. In the frame of this approach, we also aimed to explore the potential of *Arabidopsis thaliana* remorin proteins as markers to investigate the dynamic diversity of the living plant plasma membrane microscopically. Systematic co-expression and subsequent co-localisation experiments were performed to reveal the range of different membrane domains labelled by remorin proteins. Additionally this thesis aimed to investigate the different characteristics of membrane microdomains such as lateral stability and protein dynamics within the domains.

Secondly, in a more biochemical line of attack, a directed Y2H screen aimed to identify interacting receptor-like kinases. Further, truncations and mutations on the protein level were performed to elaborate functions of the different protein regions including phosphorylation of the N-terminal domain.

Finally, we aimed to address the role of remorin proteins from a genetic side of view. A phenotypic analysis of selected homozygous knockout mutants focused on different biological situations the proteins might be involved in, namely treatments with microbial elicitors or with actual plant pathogens.

Material and Methods

1. Methods

1.1. Recombinant DNA Methods

1.1.1. DNA amplification via polymerase chain reaction (PCR)

1.1.1.1. Analytical PCR

Standard PCR for verification of constructs or bacterial strains (colony PCR) was performed with TAQ polymerase. 20 μ l of PCR reaction mix (2.4.2.4) were incubated in a Thermo-Cycler using the following program:

Step	Temperature	Time
1. Initial denaturation/bacterial lysis	95°C	2 min
2. Denaturation	95°C	10 - 30 s
3. Primer annealing	2°C below melting temperature of the primer	10 - 30 s
4. Elongation	72°C	1 min/1 kb length of the template
5. Final Elongation	72°C	5 min

Steps 2-4 were repeated 34 times. Modifications for non-standard templates included additives as CES enhancer or variations of the MgCl₂ concentration.

1.1.1.2. Preparative PCR

Standard PCR for preparative amplification of sequences from cDNA or genomic DNA was performed with Phusion HF polymerase. 20 μ l of PCR reaction mix (2.4.2.5) were incubated in a Thermo-Cycler using the following program:

Step	Temperature	Time
1. Initial denaturation/bacterial lysis	95°C	2 min
2. Denaturation	95°C	10 - 30 s
3. Primer annealing	2°C below melting temperature of the primer	10 - 30 s
4. Elongation	72°C	15 s/1 kb length of the template

separately with BsaI restriction site containing primers and combined into a modified pENTR-D via a cut-ligation reaction (see chapter 1.1.2, Jarsch et al., 2014).

Gateway-compatible entry vectors were created both with and without stop codon via TOPO cloning (Invitrogen) or BP reaction (Invitrogen) according to the respective manual. As modifications, volumes of expensive components of the kits were cut down to the minimum (see 2.4.2.1 and 0).

1.1.4. Creation of expression vectors

As destination vectors for overexpression in *A. thaliana* or *N. benthamiana* vectors from the pAM-PAT series (Lefebvre et al., 2010) and pUbi-YFP:GW (Konrad et al., 2014) were used, respectively. For expression of C-terminally tagged constructs under control of the putative endogenous promoter a modified (promoter-less) pH7YGW2 (GENT) was used. N-terminally tagged constructs under control of the endogenous promoter were expressed in the pGWB1 (Nakagawa et al., 2007).

For the GAL4 yeast 2 hybrid (Y2H) assays, gateway-compatible versions of the matchmaker (Invitrogen), pGADT7 and pGBKT7 were used. Both vectors are suitable for N-terminal fusions. Constructs of *A. thaliana* soluble kinases (ASKs) in pBT9 were obtained from Claudia Jonak (Vienna).

1.2. Protein expression for fluorescence microscopy

1.2.1. *A. tumefaciens* mediated transient transformation of *N. benthamiana*

For *in planta* localisation of fluorophore-tagged fusion proteins and protein-protein interaction studies in *N. benthamiana*, *A. tumefaciens* mediated transient transformation was performed as described earlier (Tóth et al., 2012). Two strains were used: *GV3101 C58 mp90RK* for constructs in pAM-PAT:35S and pH7YGW2, and *Agl1* for constructs in pUbi and pGWB1-based vectors. Briefly, bacterial strains carrying the constructs of choice were cultured in liquid LB under appropriate antibiotic selection over night (ON). Bacteria were harvested by centrifugation at 6,500 x g and resuspended in infiltration solution (2.4.4.1). For pUbi-YFP constructs a final OD₆₀₀ of 0.01 and for pAM-PAT-35SSCFP/YFP constructs a final OD₆₀₀ of 0.2-0.4 was used. An *A. tumefaciens Agl1* strain containing a construct mediating expression of the viral silencing inhibitor P19 (Koncz et al., 1989; Voinnet et al., 2003) was added to each sample at a final OD₆₀₀ of 0.1. The solution was incubated for 2 h in the dark, subsequently plants were syringe-infiltrated at the youngest fully expanded leaves.

1.2.2. *A. tumefaciens* mediated transient transformation of *A. thaliana*

A. tumefaciens mediated transient transformation of *A. thaliana* was performed in stable transgenic lines expressing AvrPto under control of a dexamethasone (DEX)-inducible promoter as described previously (Hauck et al., 2003; Tsuda et al., 2012). Five to six weeks old plants grown under short-day conditions were sprayed with a 2 μ M DEX-solution containing 0.04% Silwett-77 24 h prior to transformation (2.4.4.2). Preparation of the infiltration solution and infiltration of leaves was performed as described for *A. tumefaciens* mediated transformation of *N. benthamiana* in chapter 1.2.1.

1.3. Plant work

1.3.1. Sterilization of *A. thaliana* seeds

Seeds were incubated in 70% ethanol with 0.5 % Tween 20 in a 1.5 ml reaction tube for 10 – 15 min and occasionally vortexed. The supernatant was replaced twice with 96% Ethanol for 2 min. Subsequently the seeds were transferred onto sterile Whatman paper and dried under a sterile fume hood.

1.3.2. Plant growth conditions

A. thaliana seeds for all experiments were ethanol-sterilized, sown on ½ MS plates containing 1 % sugar (2.5.1) and vernalised for two days at 4°C in the dark. Subsequently, plates were transferred for germination to long-day conditions (16h light/8h dark) at 22°C/18°C for day/night cycles. Seedlings designated for transfer to earth were picked two days post germination. Plants required for bacterial infection, oxidative burst assays or AvrPto-DEX inducible *A. thaliana* lines (Tsuda et al., 2012) used for transient protein expression were grown in a climate chamber five to six weeks under short-day conditions (16h dark/8h light) with 18°C/75% humidity and 20°C/60% humidity for night/day cycles, respectively. *A. thaliana* plants used for the production of synchronized seed batches were grown under long-day conditions (16h light/8h dark) in the greenhouse for 8 weeks, then dried for 2 more weeks prior to seed harvest.

N. benthamiana plants used for transient expression of proteins were grown 4-5 weeks in the greenhouse prior to transformation.

1.3.3. Genotyping procedure for SALK T-DNA insertion lines

Seeds of lines heterozygous for an annotated T-DNA insertion in or close to the coding sequence of remorin genes were ordered from ABRC and grown in the greenhouse. Leaf

material was harvested from 3 weeks old plants for DNA extraction (1.3.5) and subsequent genotyping analysis via analytical PCR (1.1.1.1). Depending on the annotated location of the insertion, either primers for the coding region or the promoter were used. In total, 4 PCRs were performed for each sample: One to amplify the wt allele with gene or promoter specific primers, two more to amplify the T-DNA insertion region and one control PCR. Depending on the insertion direction an amplicon for the T-DNA was obtained with a T-DNA specific primer and either the gene or promoter specific forward or the reverse primer, respectively. If possible, T-DNA amplicons were extracted from gel and sequenced to verify or, if necessary, re-annotate the insertion position. Homozygous plants were then processed for seed harvest and approximately 50 seeds were subjected to a selection on kanamycin containing plates to verify homozygosity of the insertion. Heterozygous plants were self-crossed, grown for seed production and re-entered into the screening pipeline.

1.3.4. Generation of stable transgenic *A. thaliana*

A. thaliana lines for stable transformation with *A. tumefaciens* were grown for 4 weeks under long-day conditions (8h dark/16h light) in the greenhouse. Shoots were cut back and plants were regrown for one more week prior to floral dipping (Clough et al., 1998). In brief, buds and floral meristems were dipped in infection solution (2.4.4.3) containing the *A. tumefaciens* strain of choice. Plants were laid horizontally in a tray, then covered with foil and incubated in dark over night. Selection of stable transformants was performed according to Harrison et al., 2006. Seeds were ethanol sterilized, sown on ½ MS plates (1 % sugar) containing 15 µg/ml hygromycin B and vernalised for 2 days in the dark at 4°C. Subsequently, the seeds were subjected to 6 h light at 22°C, 48 h dark and 24-48 h light at 18-22°C for night-day conditions. Etiolated, greening seedlings were picked for further processing.

1.3.5. DNA extraction from *A. thaliana* leaf material (short protocol)

For extraction of DNA from *A. thaliana* leaves, one leaf per plant was harvested, ground in liquid nitrogen and solubilized in 500 µl *A. thaliana* DNA extraction buffer (2.4.3). After centrifugation at 14,000 x g for 10 min, 350 µl of the supernatant were transferred to a fresh 1.5 ml reaction tube containing 350 µl isopropanol. The solution was mixed by inversion and spun down for 15 min at 14,000 x g. The supernatant was discarded and the pellet dried for 30 min on bench-top. Subsequently the pellet was resolubilized in H₂O and vortexed for 30 min for resolubilization. To remove any debris, the sample

was centrifuged one more time for 10 min at 14,000 x g and the supernatant transferred to a fresh reaction tube.

1.3.6. ROS burst assay

The measurement of oxidative burst was performed on 5 weeks old *A. thaliana* plants according to Schwessinger et al., 2011. Seedlings were grown under short-day conditions (16h dark/8h light) with 18°C/75% humidity and 20°C/60% humidity for night and day rhythm. For biological replicates, 24 leaf discs were analysed per line, harvested 24 h prior to the experiments and kept in water over night. To trigger the oxidative burst, 100 µl of reaction mix (2.4.6) were applied. Luminescence was detected using a 96-well plate reader over a 30 min time-period.

1.3.7. Seedling growth inhibition assay

Analysis of seedling growth inhibition by PAMP treatment was performed according to Schwessinger et al., 2011. As a modification, seedlings were transferred from solid to liquid medium seven days after germination and grown for 14 more days prior to fresh weight measurement. Shortly, 12 replicates per line and treatment were analysed, with three seedlings per well in a 12-well plate. For treatment, 2 ml of MS medium containing concentrations of flg22 or elf18 in the range of 10 nM to 1 µM, respectively, were used in one well.

1.3.8. MAPK activation assay

Seedlings were germinated for seven days on MS plates prior to transfer to liquid MS and grown for 7 more days. For treatment with water, 100 nM elf18 or 100 nM flg22, six replicates of two seedlings each were taken. Samples for 0, 5, 10 and 30 min after treatment were pooled and frozen in liquid nitrogen. Plant material was ground and solubilized in Lacus buffer (2.4.7.1). After centrifugation at 16,000 x g at 4°C, the supernatant was syringe-filtered and SDS-loading buffer was added. Western blot analysis was performed after semi-dry transfer. Blocking was performed with TBS-T (5% milk) before the membrane was washed vigorously with TBS with 0.05 % Tween20 (TBS-T) and the α -P p42/44 MAPK primary antibody was incubated with TBS-T (5% BSA). Again the membrane was washed before incubation with α -rabbit-HRP trueblot secondary antibody in TBS-T (5% milk).

1.3.9. Infection with *P. syringae*

Infection with bacterial pathogens was performed according to Schwessinger et al., 2011. Plants were grown for 5 weeks under short-day conditions (see 1.3.2). Wildtype *Pseudomonas syringae* DC3000 was sprayed with an OD₆₀₀ of 0.02, while the *P. syringae* DC3000 COR⁻ mutant was sprayed with an OD₆₀₀ of 0.2. Two days after infection three leaf discs of 4 mm diameter were harvested per plant and pooled. For each treatment and line, four plants were used. Samples were ground in 10 mM MgCl₂, subjected to serial dilutions and plated on Kings B Medium (2.5.3) containing the respective antibiotics. Colonies were counted two days after infection.

1.3.10. Root growth inhibition assay with brassinolides

A. thaliana seedlings were ethanol sterilized and sown on ½ MS solid medium containing 1 ng brassinolide or mock, respectively. Seeds were then stratified in the dark at 4 °C for 2 days and subsequently grown vertically for 7 days under long-day conditions. Seedlings were transferred to a new plate to stretch roots. Images were taken from whole plates and root length was measured using the ImageJ software.

1.4. Yeast work

1.4.1. Yeast transformation

Yeast transformation was performed according to Tòth et al., 2012. In brief, an over night culture was started in 20 ml YPAD (2.5.2.1). The next day, the culture was refreshed and diluted to an OD₆₀₀ of 0.2, calculating 20 ml for 10 transformations. After reaching an OD₆₀₀ of 0.6 - 0.8, the culture was centrifuged at 700 x g for 5 min and the pellet kept on ice. For each transformation, 300 µl of the yeast transformation master mix (2.4.5.1) were combined with the purified plasmids (approximately 200 ng each). Subsequently, each yeast pellet was dissolved in 1 ml ice-cold water and 100 µl of the solution were added to the master mix. After vigorous vortexing and 45 min heat-shock at 42°C, the transformation-mix was centrifuged at 700 x g for 5 min and the supernatant removed. The pellet was dissolved in 100 µl 0.9 % NaCl₂ and plated on SD medium (2.5.2.2) containing the respective amino acid combination for selection.

1.4.2. GAL4 yeast-2-hybrid drop assay

For interaction tests between soluble proteins in yeast, both constructs of interest were cloned into the matchmaker vector pair and co-transformed into the pJ69-4a strain. At

least 10 colonies from the transformed yeast were pooled and grown over night in 100 μ l of liquid SD –LW medium (2.5.2.2) in a 96-well plate. Subsequently a dilution series of 10^{-1} , 10^{-2} , 10^{-3} , 10^{-4} and 10^{-5} was performed. For the drop test, a set of selective media consisting of SD –LW, SD –LWH and SD –LWH containing 5–30 mM 3-Aminotriazol (3-AT) were used.

1.5. Protein work

1.5.1. Protein separation via SDS-PAGE

SDS-gels for acrylamide-gel-electrophoresis were cast and run with a vertical BioRad system. For protein separation, a discontinuous buffer system was used, combining a standard acrylamide-electrophoresis gel (2.4.9.2) for protein separation with an acrylamide-isotachphoresis gel (2.4.9.1) for protein stacking on top. Acrylamide concentrations varied depending on the type of experiment and the size of the proteins of interest.

SDS-gels with separated proteins were either stained with Coomassie Brilliant Blue (2.4.9.8) and destained (2.4.9.9) for visualisation of total protein content or processed for Western blot analysis (1.5.2).

1.5.2. Western blot analysis

For wet transfer, the PVDF membrane was hydrated first in 100% EtOH and then soaked in 1 x wet transfer buffer (0) together with Whatman paper, sponges and the gel. The transfer was performed either for two hours at 120 V or over night at 40 V.

For semi-dry transfer, the gel was first incubated in semi-dry transfer buffer for at least 15 min to exchange contained water by glycerol. Then the membrane was hydrated in EtOH and together with Whatman paper soaked in semi-dry transfer buffer. The transfer was performed for 1 h at 25 V.

Membranes were blocked for 1 h in TBS-T supplemented with 5% milk powder. The primary antibody was incubated over night in TBS-T (5% milk) at 4°C while gently shaking. Subsequently the membrane was washed 3 times quickly, then 3 times 10 min with TBS-T. In the following, the membrane was incubated 2 h with the secondary antibody in TBS-T with 5% milk. The membrane was washed 3 times quickly and 3 times 10 min with TBS-T. Protein detection was performed using chemiluminescent reagent (Luminogen, GE Healthcare) on a Fusion detection camera (Peqlab).

1.5.3. Protein extraction from plant material and cell fractionation

Leaf material expressing the proteins of interest was harvested, frozen in liquid nitrogen, and ground thoroughly. 2 ml of fine plant tissue powder was solubilized in 3 ml of extraction buffer (2.4.7.2). After 15 min centrifugation at 3500 rpm (4°C) and subsequent Miracloth filtration, the supernatant was centrifuged at 100,000 x g for 1h. Microsomal pellets were resolubilized in extraction buffer. Protein content of samples from crude extract, soluble fraction and microsomal fraction were measured in replicates using a Bradford assay. Samples were adjusted to equal protein concentrations with extraction buffer and subsequently mixed with 5 x SDS loading buffer. Western blot analysis was performed after SDS-PAGE and wet transfer as described before (1.5.2).

1.5.4. Co-immunoprecipitation from *A. thaliana* and *N. benthamiana* leaf material

A. thaliana seedlings were grown on plate for 5 days, then transferred to liquid MS medium for 7-10 more days. Before freezing in liquid nitrogen, plantlets were treated for 5 min with 100 nM of flg22 or mock, respectively. The leaf material was ground and at least 5 ml of fine tissue powder was solubilized in 3 ml of extraction buffer (2.4.7.3). After 15 min centrifugation at 3500 rpm (4°C) the samples were filtered through Miracloth.

In the meantime, 25 µl per reaction of magnetic GFP-trap® (Chromotek) or anti-rabbit agars beads (trueblot eBioscience) were equilibrated by sedimentation of the beads and replacement of the supernatant by 1 ml extraction buffer. After vortexing, another sedimentation step and discarding of the supernatant, agarose beads were coated with 15 µl rabbit antibody by incubation for 10 min on ice.

Protein samples were incubated for 2 h in the cold with antibody-coated agarose-beads or magnetic GFP-trap®, respectively. Beads were washed 3 times with extraction buffer and subsequently taken up in 1x SDS-loading buffer. Elution was performed at 52°C for 10 min. Protein separation was carried out via SDS-PAGE using an 8 % acrylamide gel. Western blot analysis was performed after wet transfer as described before (1.5.2).

1.5.5. Protein extraction from yeast

For whole protein extraction from yeast, single colonies of the strains of interest were inoculated in 10 ml SD-LW medium (2.5.2.2) and grown over night at 28-30°C. The cultures were harvested by centrifugation at 700 x g for 5 min at room temperature

(RT). The pellet was dissolved 1 ml of 1mM EDTA, transferred into a fresh 1.5 ml reaction tube and centrifuged again at 11,000 x g for 1 min. The pellet was overlaid with 200 μ l of 2 M NaOH, then incubated on ice for 10 min. 200 μ l of 50 % TCA were added, the sample mixed thoroughly and then incubated for 2 h on ice. Subsequently, the sample was subjected to centrifugation for 20 min with 14,000 x g (4°C). The supernatant was discarded, the pellet washed with 200 μ l ice-cold acetone and sedimented again at 14,000 x g (4°C) for 20 min. The pellet was then resuspended in 200 μ l 5% SDS by vortexing, then mixed with an equal volume of 2x SDS sample buffer for yeast. After incubation at 37°C with shaking for 15 min, the sample was centrifuged once more at 14,000 x g for 5 min and the supernatant transferred to a fresh tube. Western blotting was performed after SDS-PAGE and wet transfer as described before (1.5.2)

1.5.6. Expression and purification of recombinant proteins from *E. coli*

All proteins purified for this work were expressed as HIS-tagged versions in the bacterial expression vector pET42. Single colonies of *E. coli* Rosetta strains carrying the respective constructs were inoculated in 20 ml LB with antibiotics and grown over night at 37°C shaking. The culture was refreshed in 200 ml with an OD₆₀₀ of 0.18. Induction was performed with 0.2 mM IPTG when OD₆₀₀ had reached 0.6. Subsequently, the culture was incubated for 2 hours at 21°C. Cells were harvested by centrifugation for 15 min at 4,000 rpm and 4°C. The pellet was washed once with 0.9% NaCl for storage at -20°C. To proceed, pellets were defrosted on ice and resuspended in 10 ml binding buffer (2.4.8.1). Cells were broken up by three times transfer through a french press at 1260 PSI. The now clear lysate was centrifuged for 15 min at 13,000 rpm and 4°C to remove cell debris and non-lysed cells. The supernatant was mixed with 300 μ l equilibrated Metal Talon Affinity Matrix and incubated for 30 min –1h at 4°C on a rotor. Subsequently, the solution was transferred onto a column and the flow-through discarded. The beads were washed 3 times with 5 ml washing buffer (2.4.8.2). Elution was performed by 5 times incubation with 500 μ l elution buffer (2.4.8.3) for 5 min. Flow-through was collected in separate reaction tubes and stored at 4°C.

Samples for analytical SDS-PAGE were taken before induction, before harvesting, from the first flow-through, from the first and third washing step and from each elution.

1.5.7. *In vitro* phosphorylation assay

For *in vitro* phosphorylation assays, proteins were either purified from bacteria (1.5.6) or immuno-precipitated from plant material (1.5.4). Recombinant proteins were used in

an amount of 2 ng, while proteins extracted from plants were not eluted but taken bound to the beads. The proteins of interest and 0.5 -1 μ l of radioactive ATP (containing γ^{32} P) were filled up with kinase buffer (0) to a reaction volume of 20 μ l and incubated for 1 h. The sample was supplemented with 5 μ l of 5 x SDS-sample buffer and heated to 95°C for 5 min. Proteins were then subjected to standard SDS-gel electrophoresis (1.5.1) and stained with Coomassie Brilliant. After destaining, the gel was spread on Whatman paper, covered with foil, vacuum dried for 2 h at 80°C and exposed to a phosphor-screen over night. Image acquisition was performed on a Typhoon Trio Variable Mode Imager.

1.6. Plant treatment for imaging, image acquisition and processing

1.6.1. Sample preparation and confocal microscopy

For microscopical analysis, leaf discs were cut from the plant, mounted on glass slides and imaged directly. Standard confocal microscopy was performed with a Leica TCS SP5 CLSM using an Argon-Laser. Images were taken with a Leica DFC350FX digital camera. For single pictures of PM surfaces, 2 line averages were used. Pictures for co-localisation analysis were captured using sequential scans between lines.

CFP was excited with a wavelength of 456 nm. Emission was detected for 475 to 520 nm. YFP was excited with 514 nm wavelength and emission was detected from 525 to 580 nm.

1.6.2. PM counterstaining with FM® 4-64

The styryl dye FM® 4-64 was solubilized in water to a stock concentration of 100 μ M. For sample staining, the leaf disc was syringe infiltrated with a working solution of 10 μ M, mounted on a glass slide and imaged right away. Excitation was performed at 565 nm and emission was detected from 650 - 750 nm to exclude chloroplast auto-fluorescence.

1.6.3. Plasmolysis

Plasmolysis of leaf epidermal cells in *N. benthamiana* was performed to visually differentiate between apoplast and PM localisation. Leaf discs were syringe infiltrated with 300 mM mannitol, mounted on glass slides in the same solution and imaged after 5-10 min incubation time.

1.6.4. Image processing

Image processing was performed with ImageJ or Fiji. For membrane close-ups, pictures of single infiltrations were subjected to background subtraction with a rolling ball radius of 100 pixels and subsequent auto-adjusting of brightness and contrast.

1.6.5. Quantitative analysis of single domains

For quantitative image analysis of individually expressed proteins, 10 images were segmented to differentiate between background and domains using a Macro including background subtraction and thresholding (see appendix). The Fiji plugin Watershed was applied to separate overlapping intensities. The resulting image was used as a mask for an overlay on the original image. All quantitative measurements were then performed on the unprocessed image. Average values for domain size, mean domain intensity, circularity, and density were depicted as box plots using R. Statistical analysis was performed in R using ANOVA and Tukey's honestly significant difference.

1.6.6. Fluorescent recovery after photo bleaching (FRAP)

For FRAP analysis, samples were prepared for standard confocal microscopy (1.6.11.6.1) but imaged with lowest laser intensities to avoid overall sample bleaching. The analysis was performed using FRAP Wizard implemented in the Leica LAS AF software. One frame was scanned prior to bleaching. Bleaching was performed on a circular ROI of 5 μm in diameter in 10 frames with 100% laser intensity (approximately 15 s). For single-domain bleaching, this ROI was decreased to 2 μm . Fluorescence recovery was imaged in 30-s intervals over 10 frames. FRAP values were fitted as described previously (Spira et al., 2012) using a simple exponential fit of $y=a*(1.0*\exp(bx))$. Half times [$t_{1/2}=\ln(0.5)/b$] and mobile fractions [$M_f=(a*100)/I_{\text{norm}}$] were calculated for all FRAP experiments with a coefficient of determination higher than 0.97. Surface plots were calculated from single ROIs in ImageJ.

1.6.7. Kymographs

For kymographs, films were acquired over a timeframe of at least 20 min. Z-stacks with 15-18 slices of 1 μm thickness were taken every 2 min.

Single images from Z-stacks of each time-point were combined into stacks and transformed into Z-projects with maximal intensities in Fiji (see appendix). All ten Z-project images were then again combined into a stack and corrected for eventual lateral

shift of the sample via the Fiji Plugin StackReg (see appendix). A line of 20 μm was drawn and the kymograph created via the Reslice [/] tool of Fiji.

1.6.8. Co-localisation analysis

For co-localisation analysis, single images were subjected to a Mean Blur Filter of 2 pixels and a background subtraction with a rolling ball radius of 20 pixels. Intensity correlation analysis was performed on selected areas excluding regions without signal, with auto-fluorescence or cell wall reflections. Both the Pearson co-localisation coefficient (Rr) (Manders et al., 1992) and the squared overlap coefficient (R^2) (Manders et al., 1993) were calculated using the respective Plugin from WCIF for ImageJ.

2. Material

2.1. Antibodies, antibody coated products

Antibody	Dilution	Company
α -GFP rabbit polyclonal	1:5000	Rockland
α -P-p44/42 MAPK rabbit (T202/Y204)	1:3000	Cell Signaling Technologies
α -FLS2 rabbit	1:2000	Self-raised by C. Zipfel, TSL
α -BAK1 rabbit	1:5000	Self-raised by C. Zipfel, TSL
α -HA-HRP rat	1:2000	Roche
α -myc mouse	1:3000	Roche
α -rabbit HRP trueblot rabbit	1:10000	eBioscience
α -mouse HRP		Biomol
GFP-Trap® magnetic beads	25 μ l per reaction	Chromotek
GFP-Trap® agarose beads	25 μ l per reaction	Chromotek

2.2. Chemicals

This table list a set of chemicals and reagents acquired specifically for a number of plant treatments and microscopical analyses performed in this work:

Product	Company
Luminol	Sigma Aldrich
flg22	Genscript
K-252- α	Biomol
FM® 4-64	Invitrogen
Oryzalin	Sigma Aldrich
Paclitaxel	Sigma Aldrich
Protease inhibitor for bacterial proteins	Roche

2.3. Enzymes and kits

This table list a set of enzymes and enzyme containing kits acquired specifically the reactive oxygen burst assay as well as recombinant DNA methods. Standard restriction enzymes for classical cloning steps were obtained from New England Biolabs and are not listed here.

Product	Company
Horseradish peroxidase (HRP)	Fluka
Topo clonase kit	Invitrogen
LR clonase mix II	Invitrogen
BP clonase mix II	Invitrogen

2.4. Buffers and solutions

All buffers and solutions were prepared with water as a solvent unless stated otherwise.

2.4.1. Antibiotic stock solutions

Antibiotic	Stock concentration
Ampicillin	100 mg/ml
Carbenicillin	50 mg/ml
Chloramphenicol	34 mg/ml
Gentamicin	25 mg/ml
Hygromycin	50 mg/ml
Kanamycin	50 mg/ml
Rifampicin	50 mg/ml
Spectinomycin	100 mg/ml
Streptomycin	200 mg/ml
Zeocin	25 mg/ml

Rifampicin was diluted in methanol as a solvent. All other antibiotics were dissolved in H₂O. All stocks were sterile filtrated with 0.45 µm disposable filters and diluted 1000x before use.

2.4.2. Solutions for recombinant DNA techniques

2.4.2.1. TOPO cloning reaction mix

Component	Amount
PCR product	1 µl
Salt stock solution	0.5 µl
Topo vector	0.5 µl

2.4.2.2. BP reaction mix

Component	Amount
PCR product	150 ng (or 3 µl max.)
Entry vector	150 ng (or 1 µl max.)
BP clonase	0.75 µl
TE buffer pH 8.0	2.25 µl

2.4.2.3. LR reaction mix

Component	Amount
Entry vector	150 ng (or 1 µl max.)
Destination vector	150 ng (or 1 µl max.)
LP clonase	0.75 µl
TE buffer pH 8.0	2.25 µl

2.4.2.4. Reaction mix for analytical polymerase chain reaction (PCR)

Component	Amount
TAQ polymerase (5 U/µl)	0.05 µl
dNTPs (10 mM each)	0.2 µl
MgCl ₂ (50 mM)	0.2 µl
Forward primer (10 pmol/µl)	0.4 µl
Reverse primer (10 pmol/µl)	0.4 µl
10 x Standard TAQ buffer	2 µl
Template	5-10 ng (1 µl max.)
Sterile MQ-H ₂ O	add. 20 µl

The reaction mix was prepared on ice. For colony PCR, a single colony was picked with a sterile 10µl tip and dipped into the reaction solution instead of adding template.

2.4.2.5. Reaction mix for preparative PCR

Component	Amount
Phusion polymerase (2 U/µl)	0.2 µl
dNTPs (10 mM each)	0.2 µl
MgCl ₂ (50 mM)	0.2 µl
Forward primer (10 pmol/µl)	0.4 µl

Material and Methods

Reverse primer (10 pmol/ μ l)	0.4 μ l
5 x HF phusion buffer	4 μ l
Template	5-10 ng (1 μ l max.)
Sterile MQ-H ₂ O	add. 20 μ l

The reaction mix was prepared on ice.

2.4.2.6. Reaction mix for cut-ligations in pENTR/D-BsaI

Component	Amount
pENTR/D-BsaI	1 μ l (50 ng/ μ l)
pCR-product	1-3 μ l (50 – 150 ng/ μ l)
BsaI	1 μ l
10 x T4 DNA –ligase buffer	1.5 μ l
T4 DNA ligase	2 μ l
Sterile MQ-H ₂ O	add. 15 μ l

The reaction mix was prepared on ice.

2.4.3. DNA extraction buffer for *A. thaliana* leaf material (short protocol)

Component	Amount
Tris/HCl pH 9.0	200 mM
LiOAc	400 mM
EDTA	25 mM
SDS	1 % (w/v)

2.4.4. Solutions for *Agrobacterium* mediated transformation of plant material

2.4.4.1. Infiltration solution for *A. tumefaciens* mediated transient transformation of *N. benthamiana* or *A. thaliana*

Component	Amount
MgCl ₂	10 mM
MES KOH pH 5.6	10 mM
Acetosyringone	150 μ M
Agrobacteria	Appropriate OD

2.4.4.2. DEX-solution for pre-treatment of AvrPto-DEX inducible *A. thaliana*

Component	Amount
DEX	2 μ M
EtOH	1 %
Silwett-77	0.04 %

2.4.4.3. Dipping solution for stable transformation of *A. thaliana*

Component	Amount
Sucrose	5 %
Silwett-77	0.05 %
Agrobacteria	Pellet from overnight culture

2.4.5. Buffers and solutions for yeast work

2.4.5.1. Yeast transformation master mix

Component	Amount
PEG 3350 50%	240 μ l
LiOAc (1M)	36 μ l
ss-DNA (2mg/ml)	27 μ l

PEG 3350 was sterilized using a 0.45 μ m disposable filter. LiAc was autoclaved at 120 °C for 20 min. ss-DNA was dissolved in sterile MQ-H₂O and incubated at 95°C for 10 min prior use.

2.4.5.2. 10 x amino acid (AA) -stock solution

Component	Amount
L-arginine HCl	200 mg/l
L-isoleucine	300 mg/l
L-lysine HCl	300 mg/l
L-methionine	200 mg/l
L-phenylalanine	500 mg/l
L-threonine	2000 mg/l
L-tyrosine	300 mg/l
L-uracil	200 mg/l
L-valine	1500 mg/l

Material and Methods

Combined ingredients were autoclaved for 20 min at 120°C.

2.4.6. ROS reaction buffer

Component	Amount
Luminol	100 μ M = 17 μ g/ml
HRP	10 μ g/ml
PAMP	100 mM

2.4.7. Buffers and Solutions for plant protein work

2.4.7.1. Lacus buffer for MAPK assay

Component	Amount
Tris HCl pH 7.5	50 mM
NaCl ₂	100 mM
MgCl ₂	10 mM
EGTA	15 mM
Na ₂ MoO ₄ (<i>add fresh before use</i>)	1 mM
NaF (<i>add fresh before use</i>)	1 mM
Na ₃ VO ₄ (<i>add fresh before use</i>)	0.5 mM
β -glycerol-phosphate	30 mM
IGEPAL (=NP-40)	0.1 %
PMSF (<i>add fresh before use</i>)	0.5 mM
Proteinase inhibitor cocktail (<i>add fresh before use</i>)	1 %
Calculin A (<i>add fresh before use</i>)	100 nM
DTT (<i>add fresh before use</i>)	2 mM

2.4.7.2. *N. benthamiana* protein extraction buffer

Component	Amount
Tris/MES pH 8	50 mM
EDTA	20 mM
Sucrose	0.5 M
DTT (<i>add fresh before use</i>)	5 mM
Plant proteinase inhibitor cocktail (<i>add fresh before use</i>)	1%

PMSF (<i>add fresh before use</i>)	0.5 mM
Na ₂ MoO ₄ (<i>add fresh before use</i>)	1 mM
NaF (<i>add fresh before use</i>)	1 mM
Na ₃ VO ₄ (<i>add fresh before use</i>)	0.5 mM

2.4.7.3. Extraction buffer for co-immunoprecipitation from *N. benthamiana* and *A. thaliana*

Component	Amount
Tris HCl pH 7.5	50 mM
NaCl ₂	150 mM
Glycerol	10%
EDTA	2 mM
DTT (<i>add fresh before use</i>)	5 mM
Plant proteinase inhibitor cocktail (<i>add fresh before use</i>)	1%
IGEPAL (NP-40)	1 %
PMSF (<i>add fresh before use</i>)	0.5 mM
Na ₂ MoO ₄ (<i>add fresh before use</i>)	1 mM
NaF (<i>add fresh before use</i>)	1 mM
Na ₃ VO ₄ (<i>add fresh before use</i>)	0.5 mM

2.4.7.4. Plant proteinase inhibitor cocktail

Component	Amount
AEBSF (4-2-Aminoethyl Benzene Sulfonyl Fluoride)	20 mM
Bestatin Hydrochloride	70 µM
Pepstatin A	70 µM
Leupeptin Hydrochloride	1 mM
E-64 (Trans-Epoxy succinyl-L-Leucylamido-(4-Guanidino)Butane)	140 µM
Phenanthroline (1-10-Phenanthroline Monohydrate)	140 µM

2.4.7.5. Kinase buffer for *in vitro* protein phosphorylation assays

Component	Amount
HEPES pH7.5	100 mM
MgCl ₂	10 mM
β-mercaptoethanol	0.1 %

2.4.8. Buffers for purification of His-tagged proteins from bacteria

2.4.8.1. Binding buffer

Component	Amount
Tris HCl	10 mM
NaCl	150 mM
Protease inhibitors	1 tablet/100 ml

→ adjust to pH 8.0

2.4.8.2. Washing buffer

Component	Amount
Tris HCl	10 mM
NaCl	300 mM
Imidazole	10 mM
Protease inhibitors	1 tablet/100 ml

→ adjust to pH 8.0

2.4.8.3. Elution buffer

Component	Amount
Tris HCl	10 mM
NaCl	400 mM
Imidazole	150 mM
Protease Inhibitors	1 tablet/100 ml

→ adjust to pH 8.0

2.4.9. Buffers and Solutions for SDS-PAGE and Western Blotting

2.4.9.1. Solution for acrylamide – isotachopheresis gel (“stacking“ gel)

Component	Amount
Tris HCl pH 6.8	0.18 M
Acrylamide	5 %
SDS	0.1 %
APS	0.1 %
TEMED	0.1 %

2.4.9.2. Solution for acrylamide – electrophoresis gel (“resolving” gel)

Component	Amount
Tris HCl pH 8.8	0.36 M
Acrylamide	8 – 15%
SDS	0.1%
APS	0.1%
TEMED	0.04%

2.4.9.3. 6 x SDS loading dye

Component	Amount
Tris HCl pH 6.8	120 mM
Glycerol	50%
SDS	6%
Bromophenol blue	0.05%

2.4.9.4. 10 x SDS running buffer

Component	Amount
Tris	30 g/l = 3% (w/v)
Glycine	144 g/l = 14.4% (w/v)
SDS	10 g/l = 1% (w/v)

2.4.9.5. 10 x Transfer buffer for wet transfer

Component	Amount
Tris	30 g/l = 3% (w/v)
Glycine	144 g/l = 14.4% (w/v)
HCl	add. pH 8.3

2.4.9.6. 10 x TBS

Component	Amount
Tris	24 g/l = 3% (w/v)
NaCl	80 g/l = 8% (w/v)
HCl	add. pH 7.6

2.4.9.7. 10 x Semi-dry transfer buffer

Component	Amount
Tris	116.4 g
Glycerol	58.6 g (=25%)
SDS	7.5 g
H ₂ O	add 2 l

2.4.9.8. Coomassie staining solution

Component	Amount
EtOH	10% (v/v)
Acidic acid	10% (v/v)
Coomassie	0.25% (w/v)

2.4.9.9. Destaining solution

Component	Amount
EtOH	30% (v/v)
Acidic acid	10% (v/v)

2.5. Media

2.5.1. Plant media MS solid/liquid medium for *A. thaliana* seedlings

Component	Amount
Basal Salt Mixture Murashige & Skoog Medium	2.2 g/l = 0.22 % (w/v)
Sucrose	10 g/l = 1% (w/v)
Bacto-agar (<i>for solid medium</i>)	8 g/l = 0.8 % (w/v)

Combined ingredients were autoclaved for 20 min at 120°C.

2.5.2. Media for Yeast

2.5.2.1. YPAD solid/liquid

Component	Amount
Bacto yeast extract	10 g/l = 1% (w/v)
Bacto peptone	20 g/l = 1% (w/v)
Glucose monohydrate (<i>add after autoclaving</i>)	20 g/l = 1% (w/v)
Adenine sulphate	10 g/l = 1% (w/v)
Bacto agar (<i>for solid media</i>)	20 g/l = 2% (w/v)

Combined ingredients were autoclaved for 20 min at 120°C. Glucose was autoclaved separately as a 20% stock solution for 15 min at 115°C and added before use.

2.5.2.2. Selective dropout (SD) medium solid/liquid

Component	Amount
10 x YNB stock solution	10% (v/v) = 0.67 g final
10 x AA stock solution	10% (v/v)
Glucose	20 g/l = 2 % (w/v)
Bacto agar (<i>for solid medium</i>)	20 g/l = 2% (w/v)

YNB was sterilized using a 0.22 µm steritop filter. Glucose was autoclaved as a 40% stock solution for 15 min at 115°C All other components were autoclaved for 20 min at 120°C before use.

2.5.3. Kings B medium for *P. syringae*

Component	Amount
Bacto peptone	20 g/l = 2% (w/v)
K ₂ HPO ₄	1.5 g/l = 0.15% (w/v)
MgSO ₄	1.5 g/l = 0.15% (w/v)
Bacto Agar	10 g/l = 1% (w/v)

→ adjust to pH 7.2

Combined ingredients were autoclaved for 20 min at 120°C.

Results

1. Cell biological characterisation of the remorin protein family

Recent data from microscopical and biochemical approaches confirmed the association of remorin proteins with the PM. SYMREM1 was found on infection thread membranes and surrounding symbiosomes in legumes (Lefebvre et al., 2010). StREM1.3 was localised in plasmodesmata controlling viral movement in tobacco (Raffaele et al., 2009, Perraki et al., 2012a). While remorin proteins were found to be enriched in DRM fractions before (Mongrand et al., 2004), membrane domain localisation of SYMREM1 was shown via electron microscopy after immuno-gold labelling (*M. truncatula*) (Lefebvre et al., 2010) and expression of StREM1.3 as fluorophore fusions (*N. benthamiana*) ((Raffaele et al., 2009, Perraki et al., 2012a). Furthermore, remorins interact with a very specific set of proteins found at the above mentioned locations: The RLKs important for establishment of the root nodule symbiosis in *M. truncatula* (Lefebvre et al., 2010) and TBP, which is important for spreading of the virus from cell to cell in *N. benthamiana* ((Raffaele et al., 2009).

However, no systematic evaluation of remorin localisation has been conducted, although this protein family displays great sequence diversity. To assess membrane localisation patterns throughout the remorin protein family and to address the question of an overall domain co-existence in living plant cells, a systematic survey of *A. thaliana* remorin proteins was initiated.

1.1. Subcellular localisation

In a recent study, ten out of the 16 *A. thaliana* remorin family members were cloned and expressed as C-terminally tagged fluorophore fusion proteins in *N. benthamiana*. These experiments revealed an association with the PM for the majority of the proteins, but a number of additional subcellular compartments were also labelled (Jarsch, 2009). Results from microscopical analyses on truncation constructs indicated that few residues within the C-terminus of remorins are required for membrane binding (Konrad et al., 2014). In contrast, the N-terminal region was dispensable for PM attachment even though it was important for interaction with downstream signalling components (Sylvain Raffaele, Katalin Tóth, Thomas Ott, personal communication). In both cases, the attachment of a large tag such as GFP and its derivatives potentially alters functionality or subcellular localisation of the proteins. To test whether the fusion

Results

direction influences remorin function and localisation, N-terminal fusions were created for all proteins.

1.1.1. The N-terminal fusion of the proteins compared to a C-terminal fusion does not impair membrane localisation

To compare C-terminally and N-terminally tagged constructs, 15 out of 16 members of the family were cloned and heterologously expressed via *A. tumefaciens* mediated transient transformation of *N. benthamiana* leaf epidermal cells. AtREM1.1 was not included, as both Geninvestigator data as well as q-PCR experiments did not indicate significant expression *in planta* (Jarsch et al., 2014).

Table 1: Changes in subcellular localisation pattern with N-terminal protein fusions

Comparison of the subcellular localisation of C-terminally and N-terminally tagged constructs of remorin family members when being ectopically expressed in *N. benthamiana*.

Gene ID	Protein	Localisation with C-term. Tag	Localisation with N-term. tag
At3g61260	AtREM1.2	Cytoplasmic, PM	PM
At2g45820	AtREM1.3	Cytoplasmic, PM	PM
At5g23750	AtREM1.4	Cytoplasmic, PM	PM
At1g69325	AtREM3.1	Cytoplasmic, nuclear, nucleolar	PM, slightly cytoplasmic, nuclear, nucleolar
At4g00670	AtREM3.2	PM, nuclear, nucleolar	PM
At3g57540	AtREM4.1	PM, slightly cytoplasmic	PM
At2g41870	AtREM4.2	PM, slightly cytoplasmic	PM
At1g45207	AtREM5.1	PM	PM
At2g02170	AtREM6.1	PM	PM
At1g30320	AtREM6.2	PM	PM
At1g53860	AtREM6.3	Aggregations at the PM	PM
At4g36970	AtREM6.4	PM	PM
At1g67590	AtREM6.5	PM	PM
At1g13920	AtREM6.6	PM, nuclear, nucleolar	PM, nuclear, nucleolar
At5g61280	AtREM6.7	Cytoplasmic aggregations, nuclear, nucleolar	PM, cytoplasmic, nuclear, nucleolar

Results

As expected, a clear shift towards a tighter membrane localisation was observed for N-terminally tagged constructs. Group 1 remorins, which showed both cytoplasmic and PM localisation when being tagged C-terminally (Fig. 7A, Table 1), exclusively labelled the membrane when being expressed as N-terminally tagged versions (Fig. 7E, Table 1). These data are in agreement with data from several proteomic approaches on PM preparations from *N. benthamiana* and *A. thaliana* plant material where these remorins were exclusively associated with the membrane fraction (Marmagne et al., 2004; Mongrand et al., 2004; Nelson et al., 2006; Sazuka et al., 2004; Valot et al., 2006; Watson et al., 2003).

Similar observations were made for AtREM3.2 (Fig. 7F, Table 1), which displayed fluorescent signal both at the PM and in the nucleus (Fig. 7B) when being expressed with a C-terminal tag. Additionally, some remorin proteins showed the tendency to form aggregations when being tagged C-terminally (AtREM6.3, AtREM6.7) (Fig. 7C, Table 1). This effect was not observed when expressing them N-terminally fused to the fluorophore (Fig. 7G, Table 1). Nevertheless, the majority of the remorin family members were not affected in membrane attachment by a C-terminal fusion (Fig. 7D, Table 1) (AtREM4.1, AtREM4.2, AtREM5.1, AtREM6.1, AtREM6.2, AtREM6.4, AtREM6.5).

Strikingly, in addition to the above-described change in stringency of membrane attachment, an alteration in localisation within the membrane was observed. When analysing the samples via high-resolution confocal laser-scanning microscopy most C-terminally tagged constructs were homogeneously distributed. In contrast, the majority of N-terminally tagged versions of remorin proteins displayed a specific pattern in the PM. While AtREM1.2 was more diffusely, yet non-homogeneously distributed (Fig. 7I), other family members exhibited spherical and laterally immobile domains in between a non-domain-localised, diffuse protein fraction (Fig. 7J-L). Although the C-terminal tag did not inhibit membrane binding for most remorin proteins, it was concluded that it did alter sub-membranous targeting to membrane domains.

Results

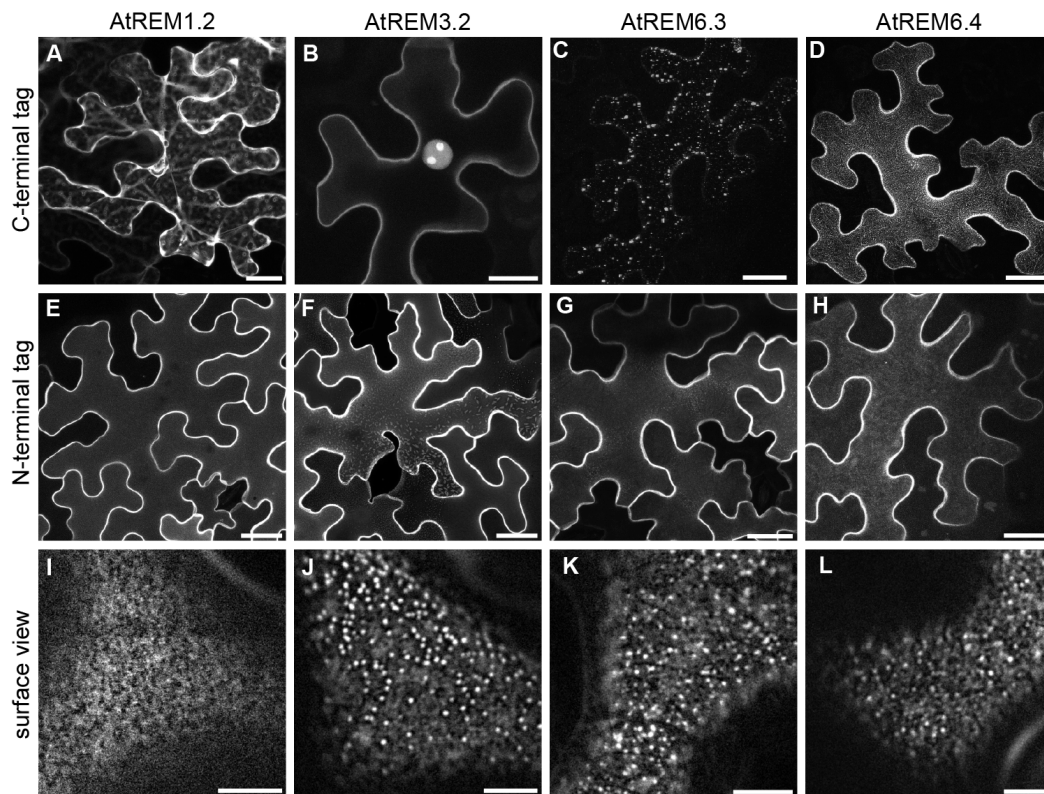


Fig. 7: The N-terminal tag does not hinder membrane attachment of remorin proteins and leads to localisation in membrane domains

When being expressed as C-terminal fluorophore fusion proteins (**A-D**), remorin proteins often displayed subcellular localisations additional to membrane binding such as cytosolic localisations (**A**), nuclear and nucleolar labelling (**B**) or aggregations at the plasma membrane (**C**). N-terminally tagged, all of them exhibited exclusive labelling of the plasma membrane (**E-H**). A top view onto the upper plane of the plasma membrane revealed localisation in distinct, spherical membrane domains for AtREM3.2 (**J**), AtREM6.3 (**K**) and AtREM6.4 (**L**), while AtREM1.2 displayed a more diffuse distribution (**I**). All constructs were expressed as CFP/YFP fusions in *N. benthamiana* under control of the CaMV 35S promoter. Images are either combined Z-stacks (**A-H**) or single planes (**I-L**); Scale bars represent 15 μm (**A-H**) and 5 μm (**I-L**).

To ultimately test whether C- or N-terminally tagged constructs are impaired in localisation, folding or interaction with other proteins, a comparison between both fusion directions for functional complementation of the mutant phenotype was performed for AtREM6.4. An *Atrem6.4* T-DNA knockout line, which did no longer express AtREM6.4 was transformed with either a C-terminally or a N-terminally tagged fluorophore fusion and subjected to phenotypic analysis. It clearly demonstrated that only the N-terminally fused version was able to restore the wildtype phenotype (for details, see chapter 2.3.2.3).

As a consequence of these observations, N-terminal fusion constructs were preferably used for all future cell biological approaches.

Results

1.1.2. Localisation of remorin proteins to membrane domains is independent of the plant expression system or the promoter

To verify that the localisation of N-terminally tagged remorin fusions to membrane domains was not caused by overexpression or the use of the heterologous *N. benthamiana* system, two control experiments were performed.

In the most elaborate approach, three transgenic lines were created. T-DNA insertion lines (see chapt. 2.1.) for AtREM1.2, AtREM1.3 and AtREM6.4 were transformed with N-terminally tagged YFP fusions under control of a 2 kb fragment of the endogenous promoter (2.2). All three lines were shown to be knockout mutants prior to use (for more details see chapters 2.3.2.1 and 2.3.3.1). Special focus was put on group 1, as the localisation pattern of AtREM1.2 significantly differed from that of other remorin proteins (Fig. 7). While both AtREM1.2 and AtREM1.3 were expressed in all tissues in levels microscopically comparable to CaMV-35S-driven constructs, AtREM6.4 was significantly lower expressed. No YFP-fluorescence was detectable in 5-7 days old seedlings, but could be microscopically analysed in 3-4 week old plants in rosette leaves and in cauline leaves of older plants. These expression patterns resemble transcript levels of these genes in wildtype plants, where AtREM1.2 and AtREM1.3 were found to be highly expressed, while levels of AtREM6.4 were found to be about 40 fold lower (Fig. 8).

In all investigated tissues, AtREM1.2 and AtREM1.3 showed a diffuse but inhomogeneous distribution (Fig. 9A-B). By contrast, AtREM6.4 displayed a localisation in clear dot-like, laterally immobile membrane domains (Fig. 9C).

In a second approach, the influence of overexpression on membrane domain formation was tested. A subset of proteins was expressed under control of the constitutively active CaMV-35S promoter in an *A. thaliana* line carrying a *proDEX:AvrPto* construct (Fig. 9D-L). After dexamethasone (DEX) treatment, this line expresses the bacterial effector AvrPto, which targets and degrades FLS2 and EFR (Xiang et al., 2008) but not BAK1 (Xiang et al., 2011). As a consequence, these plants can be easily used for *A. tumefaciens* mediated transient transformation.

Independent of expression strength, AtREM1.2, AtREM1.3 and AtREM6.4 displayed the same membrane localisation pattern as seen in *N. benthamiana* or the *A. thaliana* mutant background (Fig. 9D-F).

Results

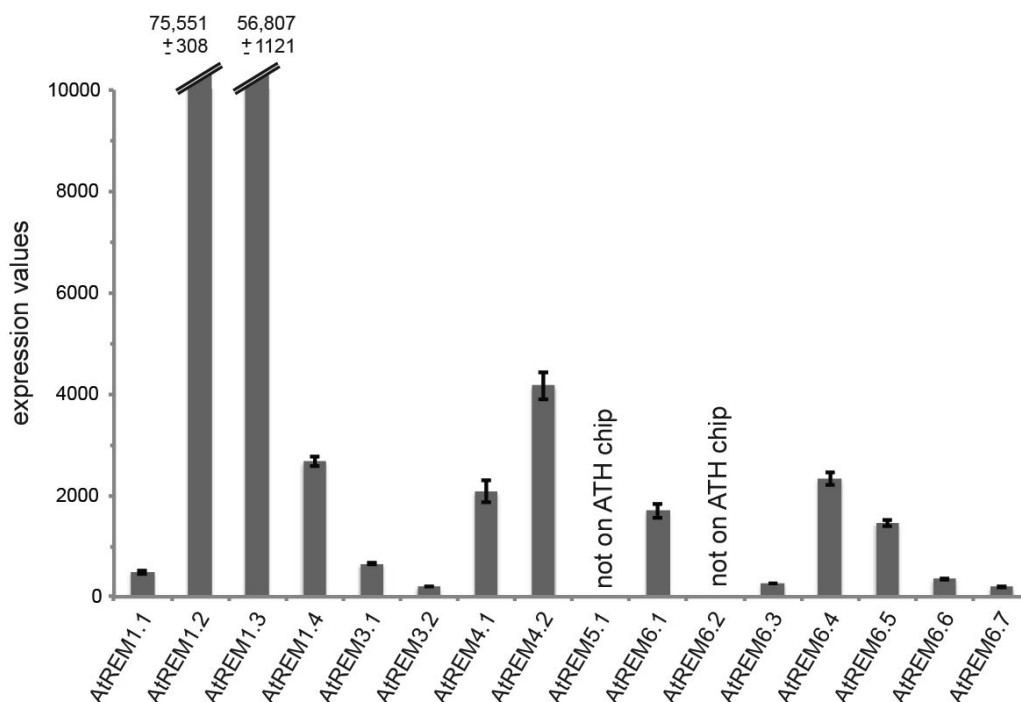


Fig. 8: Remorin expression patterns according to Genevestigator database

Data were obtained from the publically available Genevestigator database (<https://www.genevestigator.com/gv/plant.jsp>). Expression patterns were determined in Col-0 seedlings by Leivar and colleagues and deposited in the repository with the identifiers GSM768250, GSM768251, GSM768252. Error bars represent standard errors of three independent biological experiments. ATH chip = *A. thaliana* Affymetrix chip.

Group 1 remorin proteins did not label distinct domains but showed an diffuse, irregular distribution while AtREM6.4 localised to clear, immobile domains. To further verify that domain formation was also visible in *A. thaliana* an additional set of six proteins from different subgroups of the protein family were subjected to expression and microscopical analysis. Encouragingly also all additionally tested constructs from groups 3, 4, 5 and 6 showed clear labelling of spherical membrane compartments in *proDEX:AvrPto A. thaliana* plants (Fig. 9G-L).

No differences in localisation patterns were observed when comparing all tested systems. These results indicated that indeed the *N. benthamiana* system was suitable for transient expression and subcellular investigation of *A. thaliana* remorin proteins. Consequently, the latter was chosen for all future cell biological investigations, as it is the most convenient to transiently express proteins and also co-express several construct in a reproducible manner.

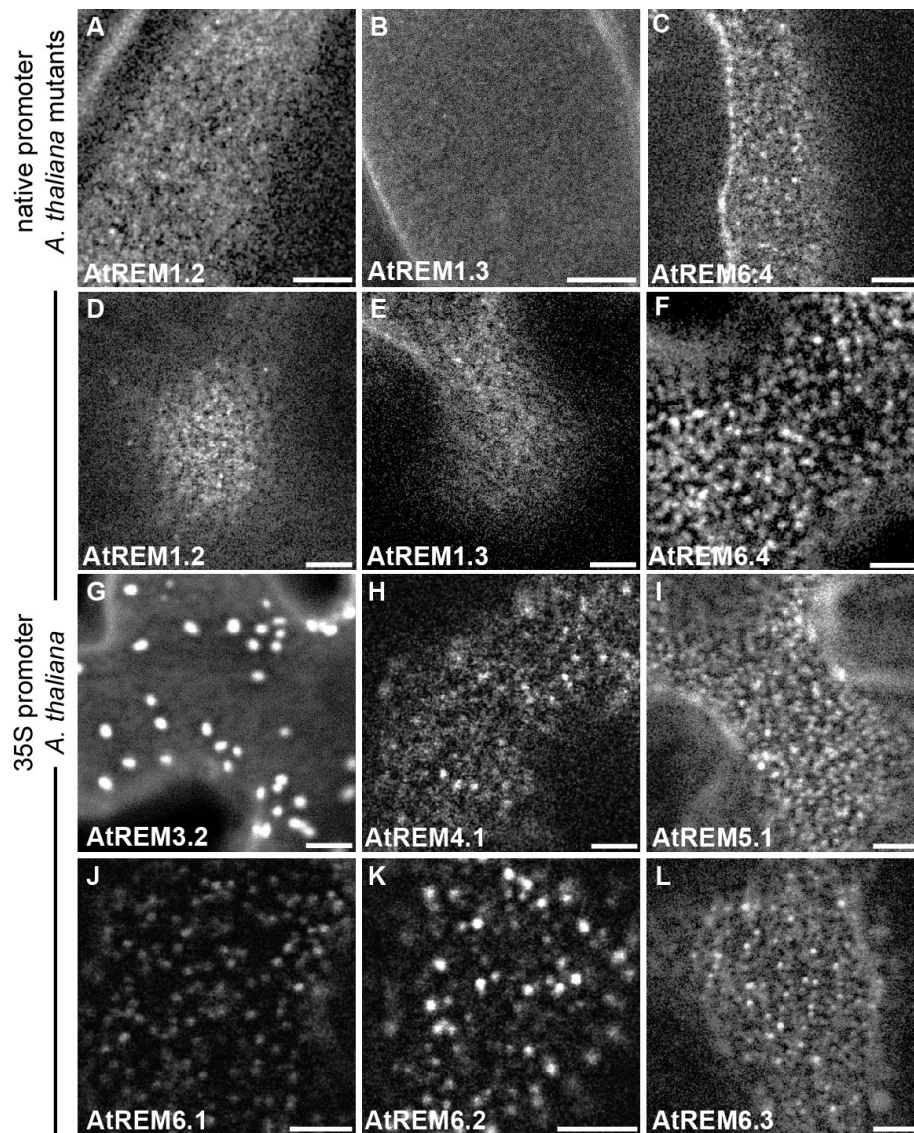


Fig. 9: Variation in expression strength or system does not alter localisation of AtREMs in membrane domains

Expression of AtREM1.2, AtREM1.3 and AtREM6.4 constructs under the control of their endogenous promoters (A-C) in the respective mutant backgrounds or under control of the CaMV 35S promoter in *A. thaliana proDEX:AvrPto* (D-F) does not change localisation patterns compared to *N. benthamiana* (Fig. 7). Additionally tested remorin proteins from group 3, 4, 5 and 6 also show labelling of distinct immobile spherical domains when expressed under control of the CaMV 35S promoter in *A. thaliana proDEX:AvrPto* (G-L). All constructs were N-terminally tagged to YFP. Scale bars indicate 5 μ m.

Results

1.1.3. Remorin proteins label a variety of coexisting distinct membrane compartments

As shown above remorin proteins label distinct membrane compartments in living plant cells. Therefore, the question was raised, whether the whole remorin family in its manifoldness could be reflective of the diversification of the domain landscape of the plant PM. Consequently, the next goal was, to assess the whole range of membrane compartments being labelled by remorin proteins.

Extensive optimization of the expression conditions revealed that the use of low optical densities (ODs) of *A. tumefaciens* cultures for infiltration as well as the selection of lowly expressing cells for confocal microscopy provided the most native conditions. In highly expressing cells, domains became less clear as non-domain-bound protein fraction accumulated within the inter-domain space. Otto and colleagues, when microscopically analysing flotillin micro-domains in the plasma membrane of mammalian cells made similar experiences. Here, they demonstrated rapid saturation of flotillin membrane domains and an accumulation of fluorescence in the surrounding membrane area, resulting in significantly deteriorated imaging conditions (Otto and Nichols, 2011).

Interestingly, remorin proteins showed similar domain patterns among members within the same phylogenetic group. The remaining group 1 remorin, AtREM1.4 was diffusely distributed over the PM, similar to AtREM1.2 and AtREM1.3 (Fig. 10A). Also AtREM3.1 showed a more homogeneous distribution (Fig. 10B). In contrast, AtREM3.2, another remorin protein lacking the non-structured, variable N-terminal region, often formed clear dot-like domains (Fig. 7J). All other proteins from group 4, 5 and 6 show a variety of spherical, immobile domains (Fig. 10C-J). Two additionally expressed proteins, KAT1 (Sutter et al., 2006) and FLOT1A (Borner et al., 2005; Li et al., 2012), chosen for their published accumulation in membrane domains, also localised to the membrane in the previously observed patterns (Fig. 10K, L).

Results

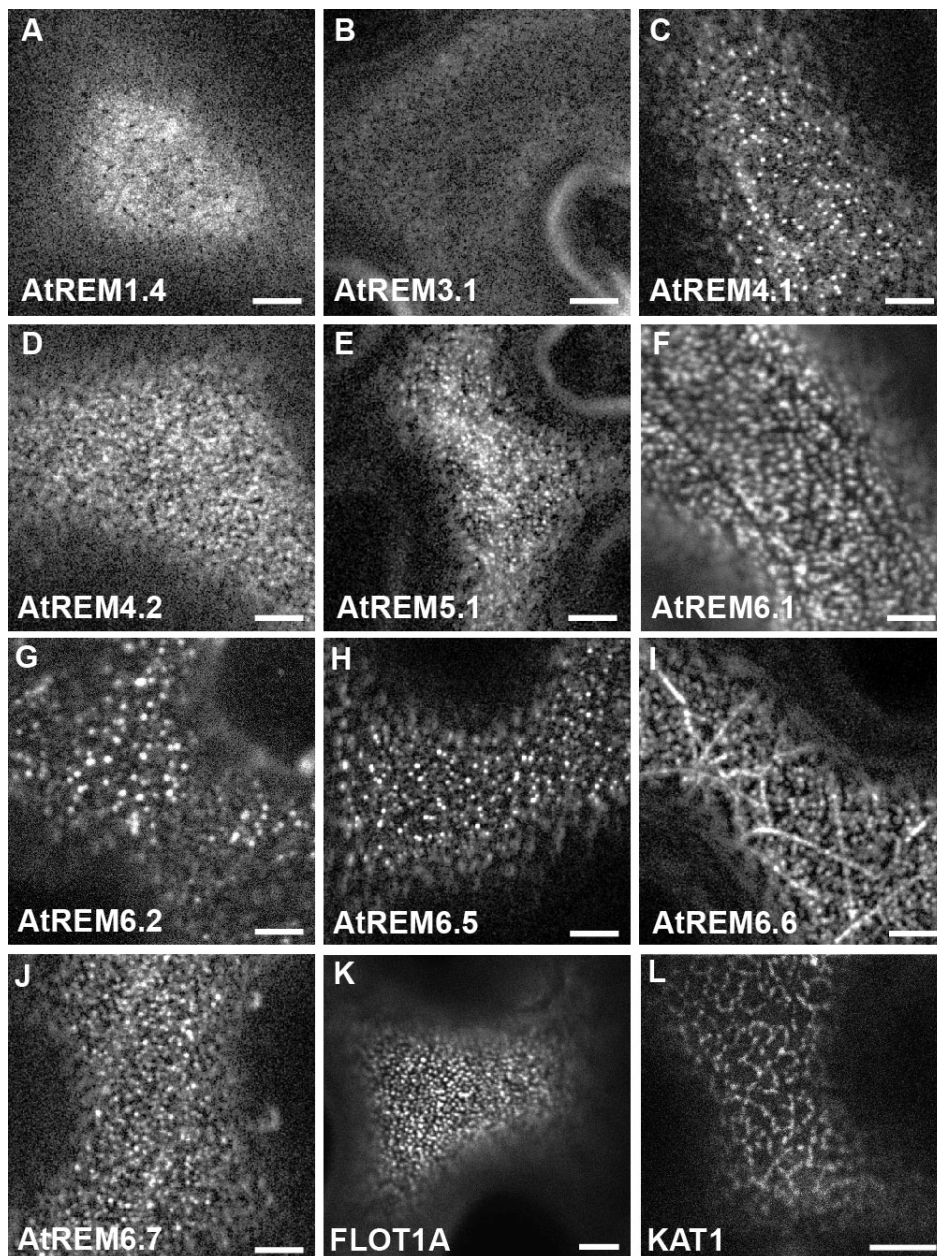


Fig. 10: Remorin proteins label a variety of distinct membrane domains

Confocal imaging of 10 remorin proteins and two additional membrane microdomain marker proteins (A-L). While no distinct foci could be resolved for AtREM1.4 (A) and AtREM3.1 (B), all other proteins labelled distinct and immobile membrane domains when being ectopically expressed in *N. benthamiana* leaf epidermal cells. Scale bars indicate 5 μm .

To define the observed patterns more precisely, quantitative image analysis was performed on all investigated proteins. The aim was to determine a set of parameters in order to be able to assess similarities and differences between the observed domains in a quantitative way. Mean domain size in square μm , the average domain circularity on a scale between 0 and 1 (with 1 representing a perfect circle), average domain density as well as mean domain intensity were addressed using ImageJ. It has to be kept in mind

Results

that no statistical investigation on how different expression levels might influence any of the above mentioned parameters has been performed.

Both mean domain size (Fig. 11A) and domain density (Fig. 11B) varied significantly between the different constructs, and confirmed the observed diverse patterns. For example AtREM3.2 forms fewer, but larger domains, while group four and five remorin proteins localize to smaller, numerous domains. A similar observation was made for FLOT1A, which displays a localisation in bigger, brighter and less densely packed membrane compartments, in contrast to which the closely related, newly cloned FLOT1B (Jarsch et al., 2014) exhibits more domains per square micrometre, but they are significantly less bright and significantly smaller.

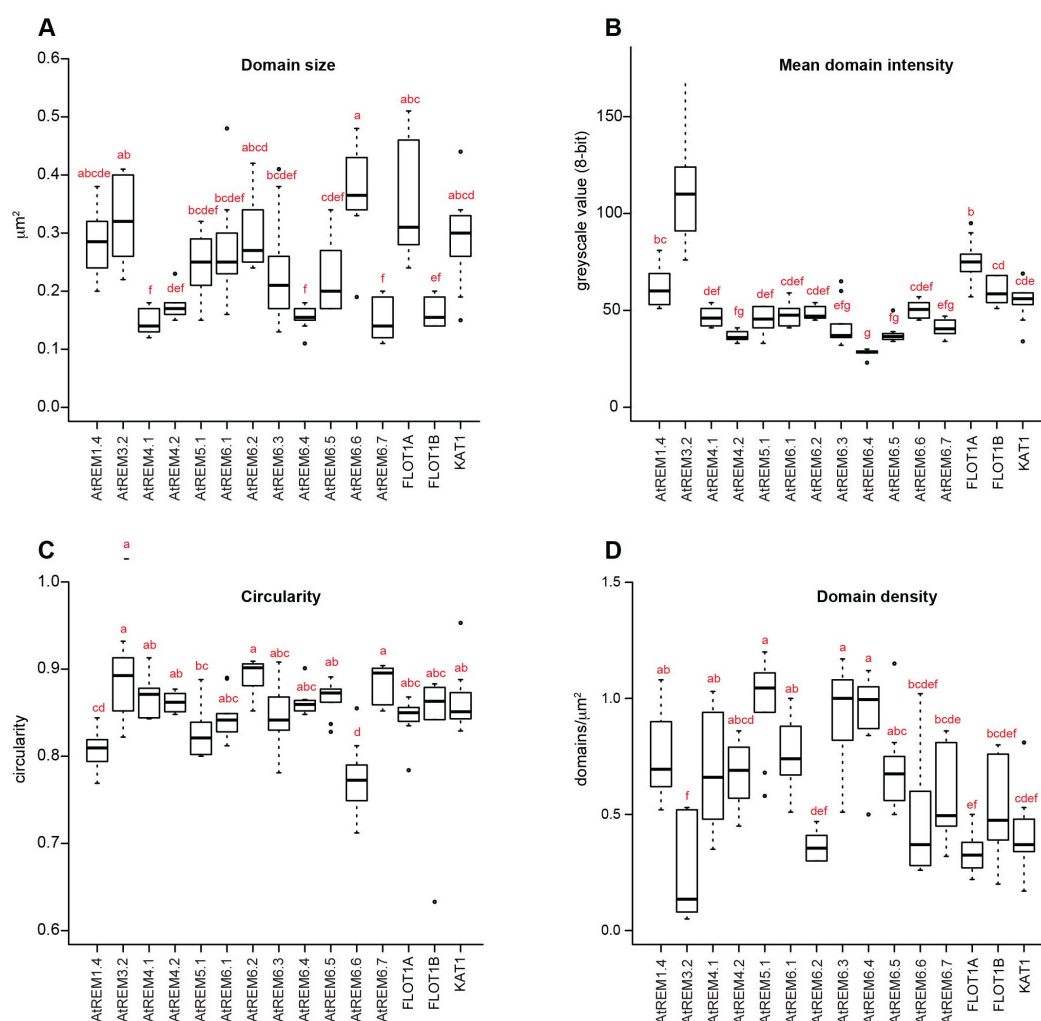


Fig. 11: Quantitative analysis of domain patterns.

Domains labelled by the investigated marker proteins were analysed for average size (A), mean average intensity (B), their average circularity (C) and the average domain density. While no distinct foci could be resolved for AtREMAAtREM1.2, AtREM1.3 and AtREM3.1 all other proteins labelled distinct membrane domains, which were encompassed by the segmentation procedure. Significant differences were determined with a one-way ANOVA and Tukey'sHSD in R.

Results

Interestingly, while neither AtREM1.2 nor AtREM1.3 structures were encompassed using the standard procedure for the image segmentation due to their diffuse nature, AtREM1.4 localisation obviously was containing elements, which were captured during the process. The membrane compartments, which were distinguishable here, were of larger nature and significantly less circular than others (Fig. 11C).

On average, domain shape did not vary significantly, as most of the remorin proteins labelled roundish compartments. Also, most of them had similar intensities, indicating a similar protein concentration inside the domains. Here, AtREM3.2 stood out with significantly higher mean domain intensity, a feature, which was also obvious in the microscopy images.

To further assess domain diversity and to define domain heterogeneity in a comparative manner, an extensive cross-comparison between single remorin proteins was performed. For each single experiment, a pair of proteins with different fluorophore fusions (one tagged to CFP, one to YFP) was co-expressed. This approach aimed to understand, whether the labelled domains co-localised with each other or whether the proteins localised to independent sites at the PM. A total number of 524 co-localisations were successfully performed for 45 protein pairs, with at least 8 repetitions each. Single images were subjected to a background subtraction using a rolling ball radius of 20 pixels, as background has drastic influence on the calculation of the co-localisation coefficients.

For calculations, regions of interest were chosen, where both channels showed fluorescent signal and the membrane domains were in focus, excluding part of the picture with no signal, auto-fluorescence or cell wall reflections. Both standard Pearson correlation coefficient R_r (Manders et al., 1992) as well as the squared overlap coefficient R^2 (Manders et al., 1993) were calculated. The Pearson correlation coefficient has a theoretical range from -1 to 1. Negative values describe exclusion of measured intensities, while values around 0 are obtained by samples that display random distribution. Values above 0 can be considered as positive correlation, meaning co-localisation. This way to assess co-localisation in fluorescent probes has been critically discussed, as negative and very low Pearson values are often difficult to interpret and sometimes vary depending on intensity differences between both channels (Zinchuk et al., 2007). Consequently, the squared overlap coefficient (also used in recent co-localisation studies (Spira et al., 2012) was included. Here, values range from 0 for low co-localisation to 1 for perfect co-localisation. It has to be considered that the strength of the Manders overlap coefficient, which makes it superior to the Pearson correlation coefficient for some purposes (namely its insensitivity to intensity differences) also

Results

makes it extremely sensitive for background noise, a reason why some researchers still prefer the Pearson coefficient (Adler and Parmryd, 2010).

Simulations to assess expected values for randomly distributed protein patterns were performed for each investigated protein pair individually by horizontally or vertically flipping one of the two images (Fig. 12). In cases where intensities did not overlap to larger extents after reflection, images were additionally rotated (Fig. 12K). Again, only areas in focus, with signal in both channels and without auto-fluorescence or cell wall reflections were chosen for calculations.

As expected, values for randomized samples ranged between 0.2-0.4 for the squared Manders overlap coefficient, and perfectly around 0 for the Pearson correlation coefficient (Fig. 12F, L, R, X, Table 2). For statistic analyses the Student Ttest was performed to assess significance of positive or negative correlation of protein pairs compared to the simulated random patterns (Table 2).

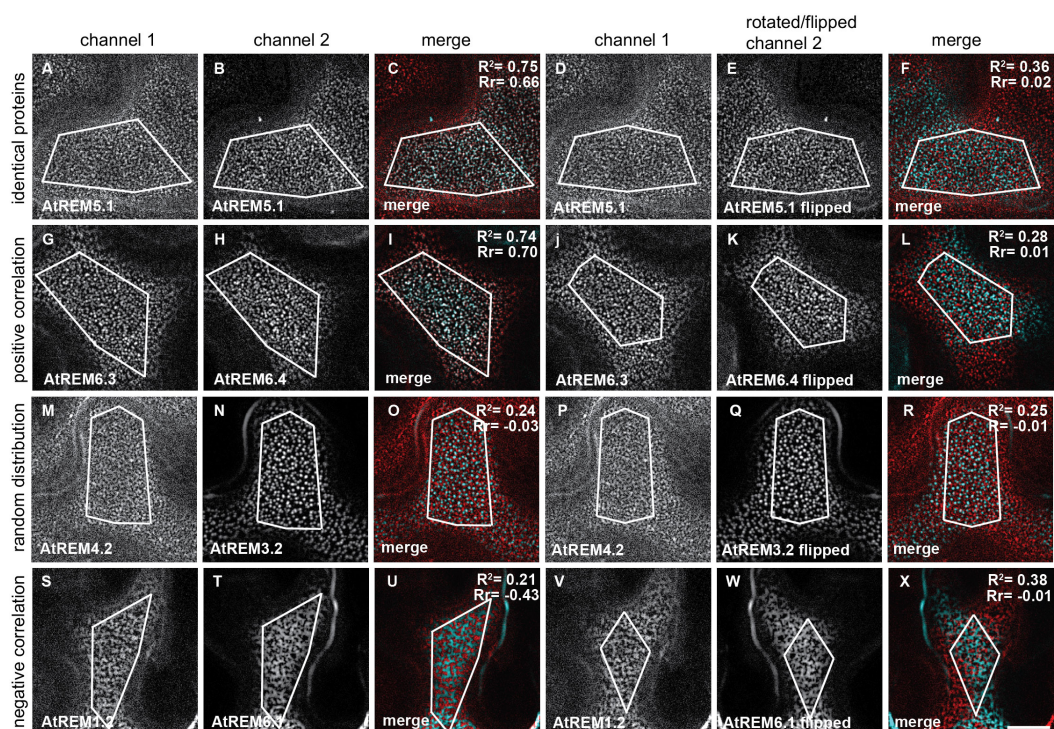


Fig. 12 Choice of regions of interest for calculation of the co-localisation coefficients

Four examples of remorin protein pairs investigated for their co-localisation patterns ranging from positive correlation (G-L) over random distribution (M-R) to negative correlation. Average Pearson correlation coefficients (Rr) as well as squared correlation coefficients (R²) for this protein pair (Table 2) are provided in the top right corner of the merged images. Identical proteins were used as control (A-F). White borders represent regions of interest used for calculation. Scale bar = 10 μm.

Results

To assess the maximum values that could be expected in our experimental settings, nine different protein pairs were tested, where the same remorin was expressed as two different fluorophore fusions (e.g. YFP:AtREM6.4 and CFP:AtREM6.4). Pearson values of 0.5 to 0.6 as well as R^2 values of 0.6 to 0.7 were obtained (Fig. 13A-F, Table 2). An exception is AtREM1.2, the values of which are (although significantly different from the randomized samples) clearly lower than for other identical pairs. This is due to the diffuse distribution, where the algorithms used in this study cannot make a clear difference between random localisation and positive correlation.

Several protein pairs displayed similarly high degrees of co-localisation (AtREM6.2 with AtREM6.5, AtREM6.4 with AtREM6.3, AtREM6.2 with AtREM6.1, AtREM4.1 with AtREM4.2 and AtREM5.1 with AtREM6.4) (Fig. 13G-L; Table 2). Notably, positive correlation of distribution seems more likely to occur between proteins of close phylogenetic proximity, namely between proteins of the same or of neighbouring groups (Fig. 13; Table 2).

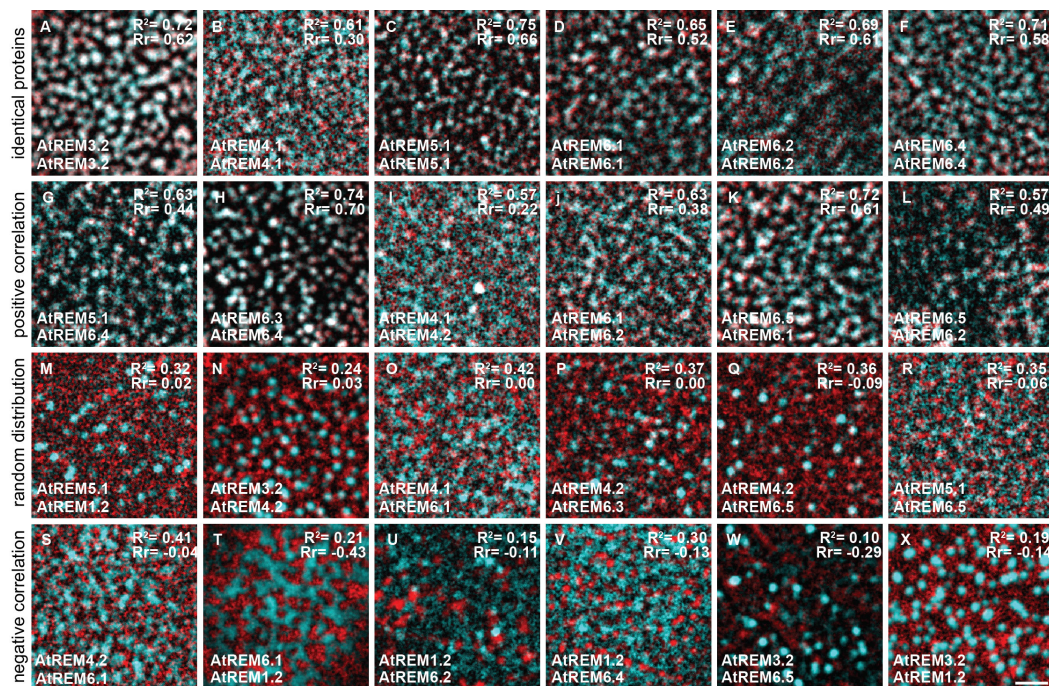


Fig. 13: The plant plasma membrane displays a wide spectrum of distinguishable coexisting microdomains.

Co-localisation analysis was performed by co-expression of two proteins fused to YFP and CFP respectively. Presented are representative images of proteins showing positively correlated distribution patterns (G-L), random distribution (M-R) or negatively correlated distribution patterns (S-X). Average Pearson correlation coefficients (R_r) as well as squared correlation coefficients (R^2) for this protein pair (Table 2) are provided in the top right corner of the images. As a proof of principle, co-expression of the same protein fused to different fluorophores resulted in highest correlation coefficients (A-F). Scale bars indicate 2 μ m.

Results

While a number of protein pairs displayed non-correlated distribution patterns (Fig. 13M-R; Table 2), several investigated remorin proteins obviously localised to domains, which excluded other remorin proteins (Fig. 13S-X; Table 2). This was most prominently the case for AtREM1.2, which was clearly excluded from all group 6 remorin labelled membrane compartments (Fig. 13T, U, V, X; Table 2). Also AtREM3.2 did not show a positively correlated distribution pattern with any of the tested other proteins (Fig. 13N, W, X; Table 2).

Notably, both correlation coefficients indicated the same kind of distribution relation for most of the tested proteins. Exceptions are cases, with range minimally above 0 for the Pearson co-localisation coefficient, and between 0.2 and 0.4 for the squared Manders overlap coefficient. While statistics did not indicate a significant difference to the randomized samples for the latter and therefore pointed towards a non-correlated distribution, the Pearson values were significantly divers (Table 2). This was the case with samples that displayed rather low intensities in one channel, showing the weakness of the Pearson correlation coefficient for pairs with larger intensity differences between both images.

To illustrate the diversity of the membrane domains labelled by remorin proteins, the results were additionally combined in a diagram, which shows the level of overlap of each single remorin protein with the other tested proteins. Again it is illustrated that both AtREM1.2 and AtREM3.2 either exclude or are excluded from the domains labelled by other tested remorins. In contrast, both group 4 and group 5 remorins localised to less exclusive domains, as other proteins are either included into those domains in a non-correlated way, or actively accumulate together in the respective compartments. Interestingly, group 6 remorin proteins showed the broadest range of correlation patterns with other family members.

Table 2: Co-localisation analysis of co-expressed protein pairs

Data points were obtained from co-expression and image acquisition of two remorin proteins fused to CFP and YFP, respectively. Images were processed using the Intensity Correlation Analysis plugin of WCIF ImageJ. Squared Manders Overlap Coefficient (R^2) (Spira et al., 2012) as well as Pearson Correlation Coefficient (R_r) values were calculated both for directly merged images as well as for randomized image pairs. Average values for at least 8 repetitions are displayed, with protein pairs were sorted into groups according to their significant difference to randomizing simulations; std. err. = standard error; rd = randomized. Groups are sorted according to the R^2 values from highest to lowest.

Results

Protein pair	sq. Manders		Pearson		sq. Manders		Pearson		sq. Manders		Pearson	
	R ²	std. err.	Rr	std. err.	n	rd R ²	rd std. err.	rd Rr	rd std. err.	n	ttest R ²	ttest Rr
AIREM5.1xAIREM5.1	0.752	0.020	0.661	0.026	11	0.364	0.021	0.016	0.012	10	3.47E-11	6.20E-15
AIREM3.2xAIREM3.2	0.718	0.022	0.617	0.038	15	0.360	0.016	0.017	0.010	19	8.04E-14	1.30E-16
AIREM6.4xAIREM6.4	0.711	0.022	0.582	0.021	9	0.432	0.011	-0.003	0.006	11	6.46E-10	8.82E-17
AIREM6.2xAIREM6.2	0.687	0.018	0.607	0.021	17	0.365	0.013	0.054	0.015	11	9.02E-13	5.67E-17
AIREM6.1xAIREM6.1	0.653	0.007	0.524	0.015	13	0.352	0.008	0.002	0.008	15	1.67E-20	2.08E-22
AIREM4.2xAIREM4.2	0.635	0.009	0.332	0.012	8	0.476	0.005	-0.005	0.008	10	1.94E-11	2.93E-12
AIREM6.5xAIREM6.5	0.618	0.010	0.397	0.022	9	0.418	0.011	-0.015	0.010	11	1.28E-10	4.98E-13
AIREM4.1xAIREM4.1	0.609	0.006	0.303	0.012	8	0.459	0.005	-0.003	0.006	10	7.65E-13	5.32E-14
AIREM1.2xAIREM1.2	0.498	0.007	0.027	0.007	10	0.477	0.007	-0.017	0.004	11	3.66E-02	3.15E-05

identical proteins

Protein pair	sq. Manders		Pearson		sq. Manders		Pearson		sq. Manders		Pearson	
	R ²	std. err.	Rr	std. err.	n	rd R ²	rd std. err.	rd Rr	rd std. err.	n	ttest R ²	ttest Rr
AIREM6.4xAIREM6.3	0.737	0.024	0.698	0.032	12	0.282	0.016	0.012	0.007	12	1.52E-13	4.70E-16
AIREM6.5xAIREM6.1	0.717	0.013	0.605	0.024	11	0.382	0.010	0.027	0.009	10	3.42E-14	5.11E-15
AIREM6.4xAIREM5.1	0.633	0.029	0.435	0.054	11	0.412	0.015	0.030	0.008	11	1.33E-06	3.51E-07
AIREM6.2xAIREM6.1	0.628	0.017	0.382	0.029	8	0.411	0.021	0.017	0.009	11	6.54E-07	1.37E-10
AIREM6.5xAIREM6.2	0.572	0.025	0.487	0.036	13	0.238	0.014	-0.010	0.009	12	4.69E-11	6.11E-12
AIREM4.2xAIREM4.1	0.569	0.007	0.217	0.014	10	0.465	0.005	-0.005	0.003	10	1.65E-10	1.21E-11
AIREM6.3xAIREM5.1	0.513	0.012	0.222	0.014	15	0.408	0.012	-0.004	0.006	15	7.80E-07	7.68E-15
AIREM6.5xAIREM6.2	0.492	0.013	0.217	0.016	10	0.385	0.011	-0.002	0.004	10	6.83E-06	8.75E-11
AIREM6.3xAIREM6.1	0.446	0.008	0.251	0.010	12	0.302	0.009	-0.002	0.010	13	3.40E-11	9.97E-15
AIREM6.1xAIREM5.1	0.434	0.009	0.286	0.009	11	0.275	0.009	0.001	0.005	11	5.84E-11	8.13E-18
AIREM6.4xAIREM4.1	0.423	0.017	0.070	0.016	9	0.384	0.009	-0.007	0.004	21	3.70E-02	7.92E-07
AIREM6.5xAIREM4.1	0.401	0.009	0.104	0.012	13	0.330	0.009	-0.004	0.008	9	3.44E-05	1.71E-06
AIREM6.4xAIREM6.2	0.366	0.028	0.188	0.031	12	0.274	0.021	0.015	0.011	12	1.94E-02	5.43E-05
AIREM6.3xAIREM6.2	0.298	0.010	0.139	0.016	10	0.238	0.014	-0.010	0.009	12	3.66E-03	3.36E-08

positive co-localization

Results

Protein pair	sq. Manders		Pearson		sq. Manders		Pearson		random co-localization		sq. Manders		Pearson	
	R ²	std. err.	Rr	std. err.	n	rd R ²	rd std. err.	rd Rr	rd std. err.	n	rd R ²	rd std. err.	ttest R ²	ttest Rr
	AtREM6.1xAtREM4.1	0,424	0,009	-0,002	0,005	9	0,409	0,014	-0,007	0,007	9	0,409	0,014	4,00E-01
AtREM5.1xAtREM4.1	0,417	0,009	0,039	0,006	19	0,396	0,008	-0,006	0,003	19	0,396	0,008	8,24E-02	3,84E-08
AtREM6.4xAtREM6.1	0,381	0,013	-0,002	0,010	10	0,366	0,011	-0,005	0,004	13	0,366	0,011	3,84E-01	7,88E-01
AtREM6.3xAtREM4.2	0,374	0,009	0,003	0,007	10	0,366	0,012	-0,005	0,006	12	0,366	0,012	5,87E-01	4,01E-01
AtREM6.5xAtREM4.2	0,361	0,019	0,087	0,010	13	0,312	0,022	-0,005	0,006	10	0,312	0,022	1,10E-01	4,88E-08
AtREM6.5xAtREM5.1	0,354	0,029	0,058	0,011	10	0,322	0,024	-0,011	0,003	10	0,322	0,024	3,90E-01	1,60E-05
AtREM4.2xAtREM1.2	0,353	0,007	-0,027	0,005	12	0,356	0,009	-0,018	0,007	12	0,356	0,009	8,37E-01	2,39E-01
AtREM5.1xAtREM4.2	0,353	0,010	0,045	0,021	12	0,333	0,010	0,012	0,008	12	0,333	0,010	3,33E-01	1,60E-01
AtREM5.1xAtREM1.2	0,318	0,011	-0,019	0,003	11	0,319	0,012	-0,020	0,004	11	0,319	0,012	9,54E-01	8,85E-01
AtREM4.2xAtREM3.2	0,239	0,021	-0,031	0,013	11	0,246	0,017	-0,007	0,005	11	0,246	0,017	7,88E-01	1,10E-01
AtREM6.2xAtREM5.1	0,133	0,008	0,050	0,007	18	0,116	0,009	0,002	0,005	17	0,116	0,009	1,53E-01	1,28E-06
AtREM6.2xAtREM4.1	0,132	0,005	0,014	0,007	12	0,122	0,005	-0,011	0,004	12	0,122	0,005	1,03E-01	5,25E-03
AtREM6.1xAtREM4.2	0,410	0,005	-0,042	0,009	10	0,436	0,006	-0,003	0,006	10	0,436	0,006	2,89E-03	2,79E-03
AtREM6.3xAtREM1.2	0,373	0,011	-0,117	0,011	15	0,434	0,004	-0,005	0,006	14	0,434	0,004	2,52E-05	2,52E-09
AtREM6.4xAtREM1.2	0,296	0,014	-0,128	0,026	11	0,353	0,006	0,010	0,008	12	0,353	0,006	9,82E-04	2,84E-05
AtREM6.5xAtREM6.4	0,286	0,012	-0,009	0,012	13	0,385	0,011	-0,002	0,004	10	0,385	0,011	6,41E-06	6,29E-01
AtREM6.5xAtREM1.2	0,208	0,013	-0,368	0,027	10	0,357	0,008	-0,019	0,009	11	0,357	0,008	5,12E-09	8,21E-11
AtREM6.1xAtREM1.2	0,207	0,016	-0,432	0,047	15	0,383	0,012	-0,012	0,010	14	0,383	0,012	2,29E-09	4,98E-09
AtREM3.2xAtREM1.2	0,193	0,014	-0,136	0,017	11	0,247	0,016	0,004	0,009	11	0,247	0,016	2,00E-02	4,04E-07
AtREM6.2xAtREM3.2	0,191	0,023	-0,153	0,021	12	0,265	0,018	0,003	0,009	12	0,265	0,018	1,70E-02	6,06E-07
AtREM6.2xAtREM1.2	0,153	0,006	-0,106	0,032	10	0,192	0,011	-0,017	0,010	10	0,192	0,011	5,61E-03	1,64E-02
AtREM6.5xAtREM3.2	0,102	0,011	-0,291	0,019	13	0,217	0,015	0,004	0,008	13	0,217	0,015	1,60E-06	2,46E-13

Results

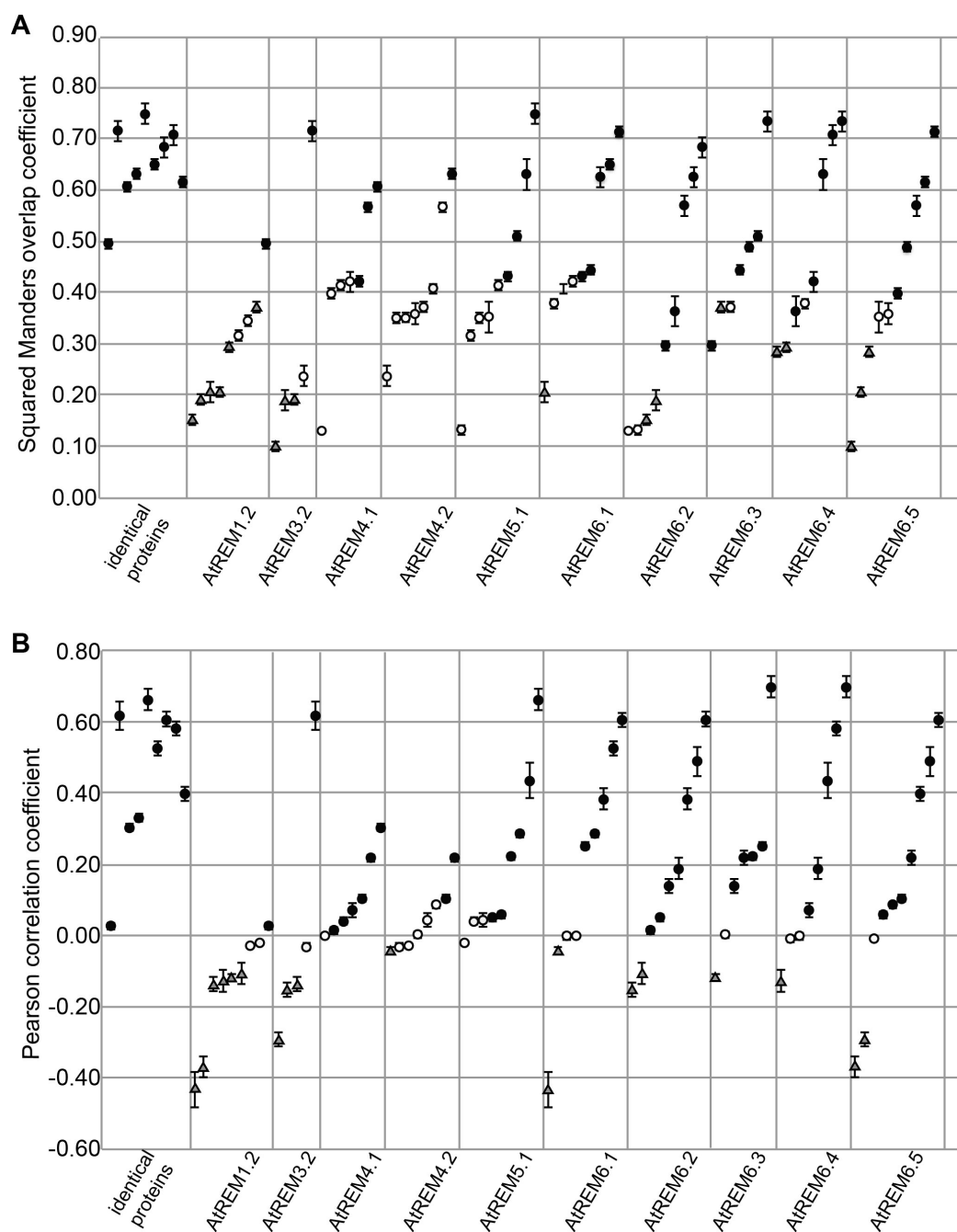


Fig. 14 Range of correlation between domains labelled by remorin proteins

Data points from **Table 2** were sorted for each single investigated protein from lowest to highest. Presented are values for the Squared Manders Overlap Coefficient (R^2) (Spira et al., 2012) (**A**) as well as Pearson Correlation Coefficient (R_r) values (**B**). According to statistics for each protein pair, data points are presented as circles with black filling (positive correlation), circled with white filling (no correlation) and triangles with grey filling (negative correlation).

Results

1.1.4. AtREM1.2 and AtREM1.3 are organised in structures below the resolution limit of standard confocal microscopy

In all assays performed so far, group 1 remorin proteins and AtREM3.1 displayed clearly different localisation patterns compared to any other member of the family. As described above, group 1 remorin proteins were not targeted into distinct membrane domains in *N. benthamiana* leaves. Also, no micro-domains were observed in mature rosette leaves in stable transgenic *A. thaliana* lines where AtREM1.2 and AtREM1.3 were expressed under the control of their own promoters. As previously published localisation data of group 1 remorins from other species (Perraki et al., 2012b; Raffaele et al., 2009) show clear labelling of domains, AtREM1.2 and AtREM1.3 were investigated in more detail. This approach followed the hypothesis that those proteins were organized in domains of a size below resolution of confocal microscopy. Fluorescence recovery after photo-bleaching (FRAP) experiments were performed on AtREM1.2 (Fig. 15A) and AtREM1.3 (Fig. 15B) expressed under control of their endogenous promoters in the respective mutant backgrounds (2.2). Centripetal recovery of bleached areas was observed within a timeframe of 150 s.

These data suggest that the diffuse structures labelled by *A. thaliana* group 1 remorins are mobile within the PM under the used experimental conditions. These results were confirmed in parallel by total internal reflection fluorescence microscopy (TIRFM) analysis of the same genetic material by Sebastian Konrad (Jarsch et al., 2014). Due to the higher spatiotemporal resolution, AtREM1.2 and AtREM1.3 were found to label small, highly mobile domains. This supports the described findings from the FRAP experiments, which show recovery of the bleached areas in a timeframe close to recovery rates reported for single S-acylated proteins in the PM (Martiniere et al., 2012).

Results

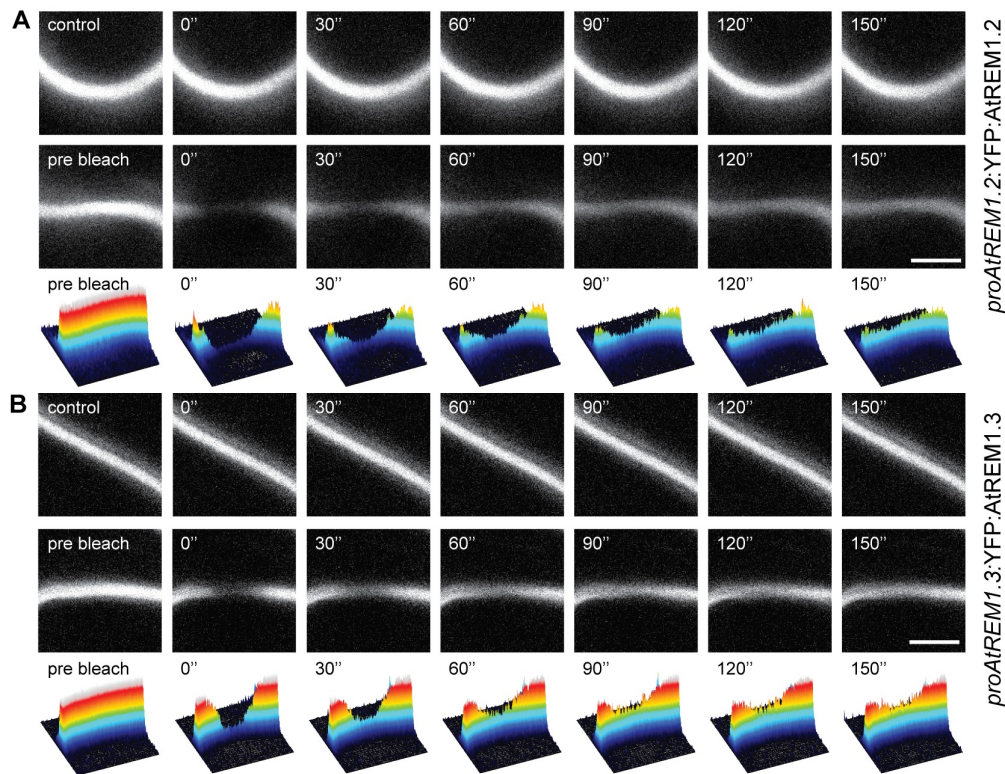


Fig. 15: FRAP experiments on AtREM1.2 and AtREM1.3 reveal lateral mobility in the plasma membrane

FRAP experiments on complemented mutants expressing AtREM1.2 (A) and AtREM1.3 (B) under control of their native promoters as YFP fusion proteins. Images were taken prior to bleaching (pre-bleach) and post bleaching fluorescence recovery was monitored in 30 s intervals. Concentric fluorescence recovery was monitored 150 s after bleaching indicating lateral recovery at a speed close to free diffusion. Scale bars indicate 2 μ m.

1.1.5. Tissue- or stimulus-specific labelling of membrane domains

The question was raised, whether domain formation of group 1 remorin proteins would occur only under certain biological conditions. Thus it was tested whether membrane domains may be labelled in a tissue-specific manner. For this, different tissues were imaged in five days old seedlings that were grown under sterile conditions. In both cases, no distinct membrane domains could be observed when imaging cells of the leaf and root epidermis (Fig. 16A, B, top and bottom). By contrast occasionally, the proteins were targeted to distinct membrane domains in elongating hypocotyl cells (Fig. 16A, B, middle lane). There, they labelled immobile foci in the plasma membrane that were similar in distribution and pattern as observed for other remorin proteins. These data suggest that membrane domains are dynamically formed or disintegrated under different environmental conditions or developmental stages.

Results

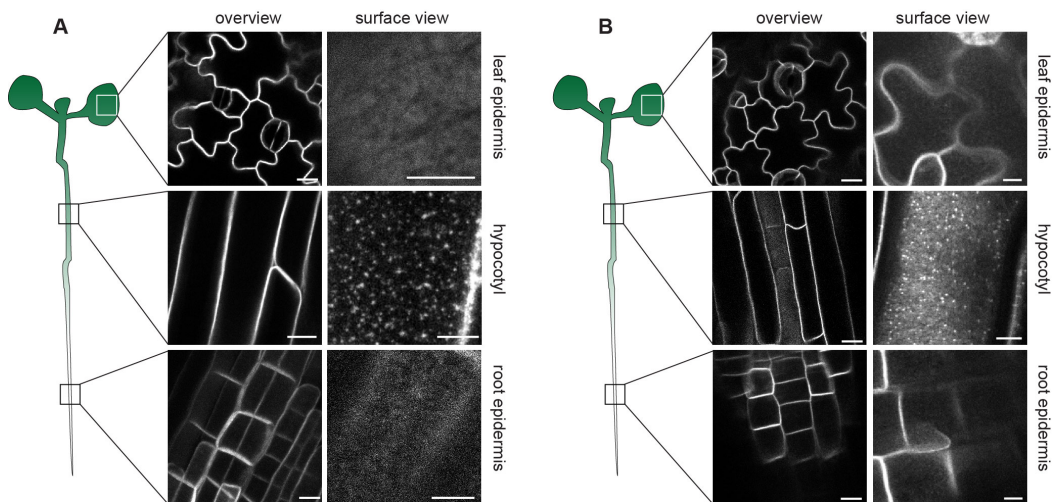


Fig. 16: AtREM1.2 and AtREM1.3 localise to membrane microdomains in a tissue-specific manner

AtREM1.2 (**A**) and AtREM1.3 (**B**) were expressed under the control of their endogenous promoters in the respective mutant backgrounds. Upper planes of leaf epidermal cells (upper panels), elongating hypocotyl cells (middle panels) and root epidermal cells (lower panels) were imaged in five days old seedlings the proteins as N-terminally tagged YFP fusion proteins. Scale bars indicate 10 μm (left columns) and 5 μm (right columns).

1.1.6. Remorin-labelled membrane compartments exhibit lateral stability

Lateral mobility has been greatly discussed for membrane domains. Current definitions describe membrane rafts as small, highly mobile domains (Pike, 2006). In human and mammalian cells it is now well accepted that raft clusters can be laterally immobile within the membrane. Several factors contribute to domain immobility: (i) Simple oligomerisation reduces movement of protein complexes in the plasma membrane; (ii) Membrane domains can contain a proportion of proteins with extracellular protein parts interacting with the cell wall; (iii) Intracellular protein domains can be connected to the cytoskeleton where the microtubule and the actin network act as barriers that prevent lateral movement of larger clusters (picket fence theory) (reviewed by Kusumi et al., 2012).

As the observed remorin labelled domains were found to be stationary, at least in the timeframe of minutes, long-time imaging was performed to investigate whether those membrane compartments display slow dynamics over time (e.g. expansion, reduction, etc.). Time-lapse imaging was performed over a timeframe of 20 min, with single z-stacks containing 15-18 slices of 1 μm thickness acquired every 2 min. Kymographs were created from shift-corrected stacks (see material and methods) over a length of 20 μm (Fig. 18). All remorin proteins were investigated. As controls, again the two proteins published to form domains in the plasma membrane, FLOT1A and KAT1, as well as the newly cloned FLOT1B (Jarsch et al., 2014) were co-investigated.

Results

As expected, AtREM1.2, AtREM1.3 and AtREM3.1 did not show formation of stable membrane compartments over time. The kymographs showed a completely homogeneous distribution of the first two proteins, whereas AtREM3.1 displayed moving stretches of additional cytoplasmic fluorescence. Interestingly, AtREM1.4 showed a tendency to form membrane areas where protein concentration was slightly increased, and therefore fluorescence was accumulating. Those compartments were stable for a fraction of the investigated timeframe, but they did not persist throughout the whole 20 min.

AtREM3.2, AtREM4.1, AtREM4.2, AtREM5.1, AtREM6.1, AStREM6.2, AtREM6.3, AtREM6.4, AtREM6.5, AtREM6.7, FLOT1A, FLOT1 and KAT1 all formed clear, laterally immobile membrane compartments of highly increased protein content which persist over the investigated 20 min timeframe. Additionally to that, in several cases, areas of increased fluorescence could be observed, which did not display homogeneous persistence in the kymographs. Here bright pixels alternate with darker pixels, indicating minimal lateral movement to the sides. This behaviour of domains is reminiscent of the previously observed movement patterns for rafts and domains within cytoskeletal compartments in the plasma membrane (Sako and Kusumi, 1995, Kusumi et al., 2005, reviewed in Urbanus and Ott, 2012).

AtREM6.7, FLOT1A and KAT1 clearly exhibit a second population of compartments with high protein content, which are laterally mobile and showed up as single dots in the kymographs. From these data alone, it cannot be excluded that the observed structures are cytoplasmic.

AtREM6.6 is a special case, as it both displayed stable domains in the plasma membrane as well as filamentous structures, which moved marginally throughout the investigated 20 min timeframe (Fig. 17A-D).

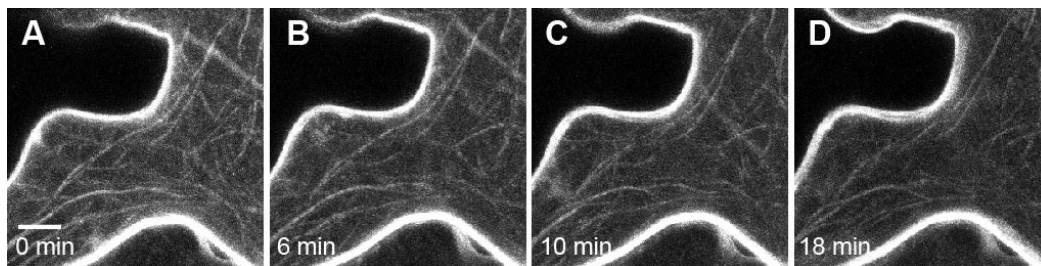


Fig. 17 AtREM6.6 filamentous structures are stable over time

When expressed in *N. benthamiana*, AtREM6.6 forms both membrane domains as well as long, filamentous structures additionally to some cytoplasmic fluorescence (A-D). Those structures, reminiscent of cytoskeleton show only slow dynamics. Confocal z-stacks with 1 μm slice-thickness were acquired over 20 min; scalebar = 10 μm

Results

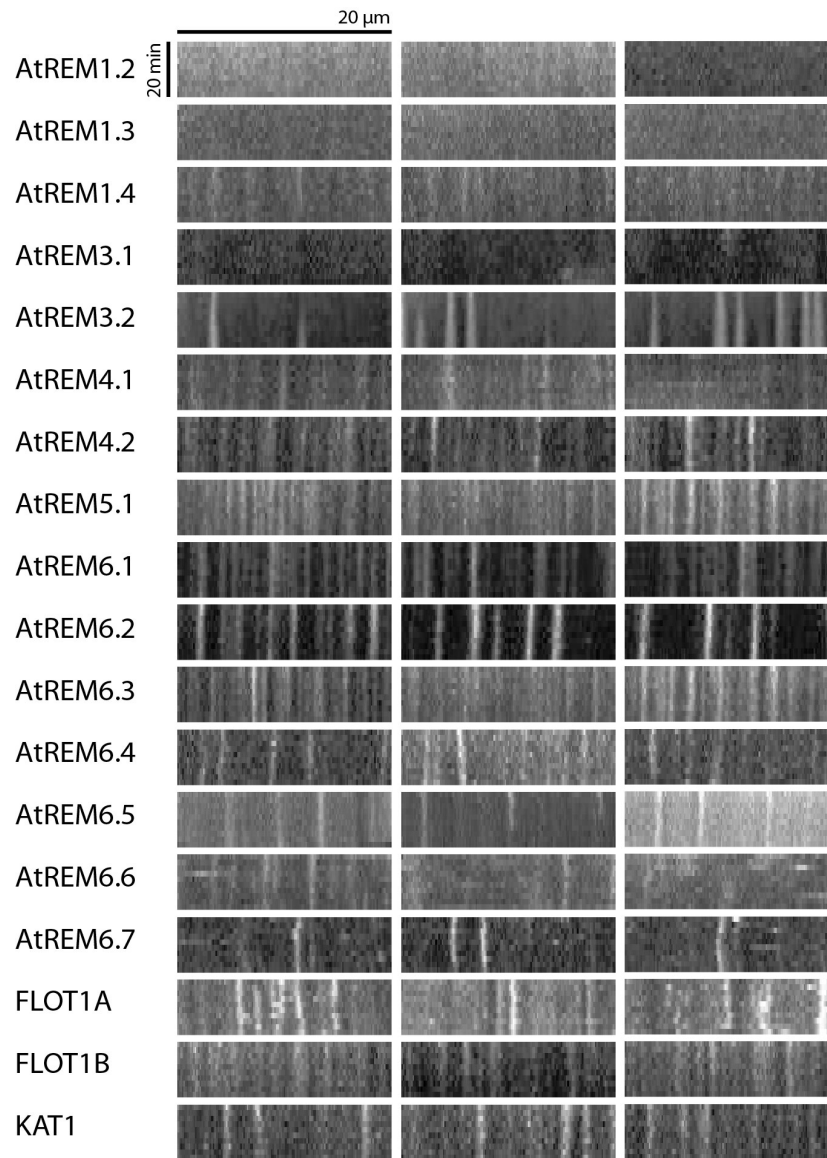


Fig. 18: Membrane domains are laterally immobile

Kymographs for 15 remorin proteins as well as FLOT1A, FLOT1B and KAT1 expressed in *N. benthamiana*. Three random examples for each construct are shown. Films were recorded over 20 min, with one pixel line representing a z-stack of 15-18 slices of 1 μm thickness. Scale bar indicates 20 μm.

Results

1.1.7. Immobile and mobile fraction of the protein population undergo dynamic exchange

In all investigated cases the membrane regions between the observed stable membrane domains were decorated by an additional, diffusely distributed, non-domain bound protein fraction (Fig. 7I-L, Fig. 9C,F-L, Fig. 10C-I, Fig. 18A-F). This raised the question, whether these two protein populations, the domain-bound and the “free” fraction, were excluding each other, or whether there was continuous exchange between the two compartments. To characterise the lateral mobility of remorin proteins in more detail, extensive fluorescence recovery after photobleaching (FRAP) analysis was performed on a subset of seven proteins (Fig. 19). For this, a circular region of interest (ROI) was bleached by high-intensity laser emission for 10 frames (15 s) (Image acquisition was performed by Thomas Ott). Fluorescence recovery on membrane surface areas was assessed over 5 min in 30-s intervals, and data were normalized to a reference ROI of equal size that was placed in close proximity to the bleached one. To compare these data with a cytosolic protein, a soluble YFP was expressed in addition. In all samples, fluorescence recovered mono-exponentially with coefficient of determination (R^2) > 0.97 (Fig. 19A). Both recovery half time (Fig. 19B) as well as the mobile fraction (Fig. 19C), meaning the percentage of total protein, which is diffusing within the membrane, were calculated. In general, membrane surfaces labelled by remorin proteins recovered within short timeframes, yet significantly slower compared with the cytosolic YFP control. Half-times of 24.3 +/- 1.4 s for AtREM6.6 filaments to 47.7 +/- 1.9 s for AtREM6.2 and 12.4 +/- 2.6 s for free YFP, respectively (Fig. 19B), were calculated. However, significant differences were observed between the proteins, with AtREM6.2 being the most slowly diffusing protein. In the case of AtREM3.2, no difference in fluorescence recovery between the domain-associated fraction and the homogeneously PM-labelling fraction was observed (Fig. 19A, B). Moreover, when bleaching single membrane domains labeled by AtREM3.2, proteins accumulated in the same position (Fig. 19D) while non-domain-labeled PM segments recovered homogeneously (Fig. 19E). This indicates a physical structure underlying protein accumulation in these distinct positions. Interestingly, AtREM6.6 again showed a significantly different pattern. While the domain-localized protein fraction overall recovered slowly, the halftime of filament-associated AtREM6.6 was significantly lower (Fig. 19B). This was also reflected in the mobile fraction, which was significantly increased for filament-associated AtREM6.6, while no differences were observed between the other Remorin proteins (Fig. 19B).

Results

These results indicate that laterally immobile membrane domains like the ones labelled by remorin proteins are in constant, dynamic exchange with the surrounding membrane area and recruit proteins from a non-domain bound mobile fraction. Lateral dynamic of all tested proteins was comparable to the diffusion speed of typical plasma membrane-bound proteins.

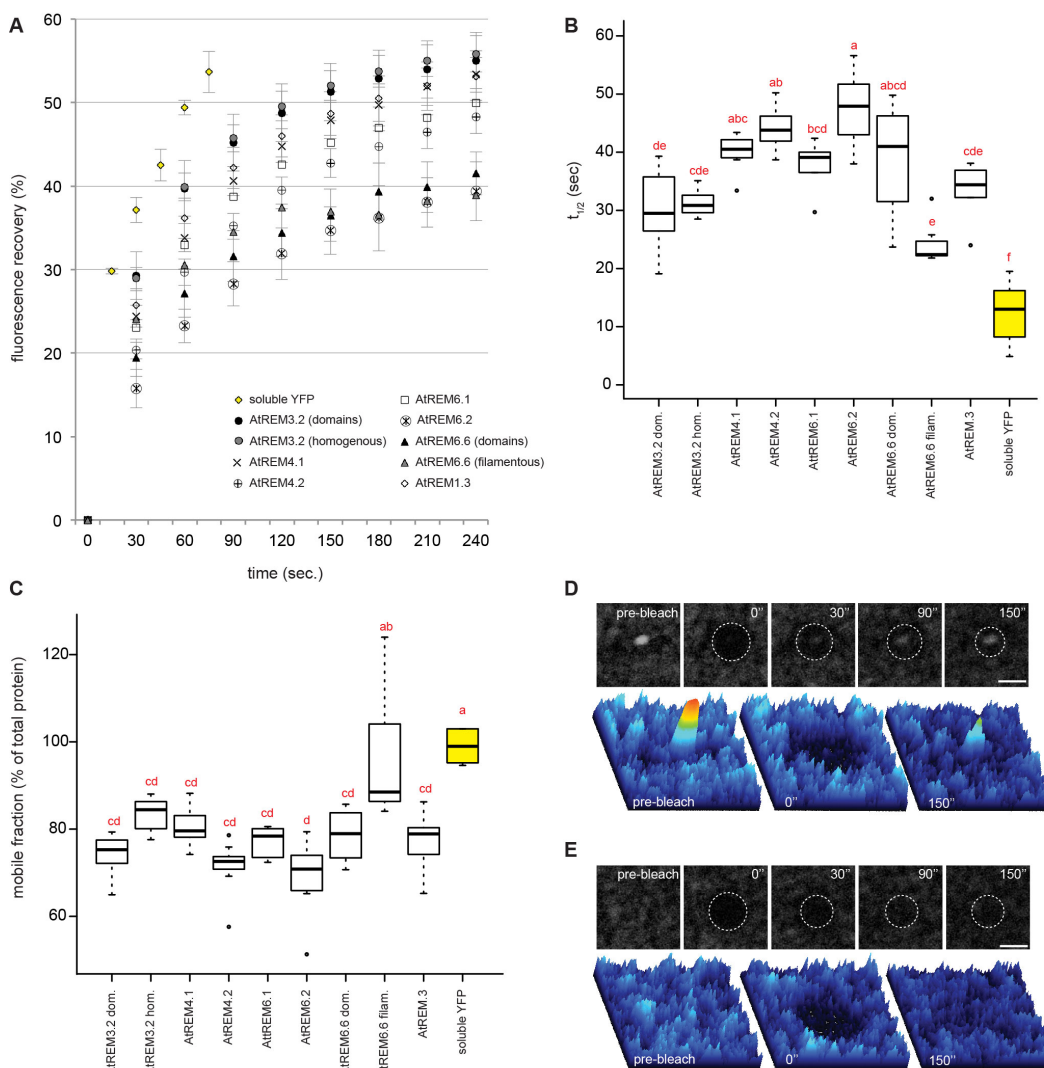


Fig. 19: FRAP experiments on remorin proteins reveal dynamic and constant recruitment of proteins into immobile membrane domains

FRAP experiments were performed on membrane domains labelled by a subset of remorin proteins in *N. benthamiana* leaf epidermal cells to visualize protein dynamics over time. Fluorescence was measured in a minimum of 12 independently bleached ROIs and standardized to a control ROI in the vicinity (A). Recovery half-times (B) as well as mobile fractions (C) were calculated and significances in differences were assessed by a one-way ANOVA followed by a Tukey's HSD test in R. Bleaching of a single domain of AtREM3.2 illustrated recovery of micro-domains (D). Images were taken prior to bleaching (pre-bleach) and post bleaching fluorescence recovery was monitored over time. Dashed circles indicate halo-like photo-bleached areas. Plasma membrane segments without any immobile membrane domains centripetally recovered within 90 s indicating replenishment by lateral diffusion (E). Fluorescence recovery of membrane domains occurred at a laterally fixed position (D). Intensity plots are provided for three time points below the images. Scale bars indicate 2 μ m.

Results

1.1.8. The far C-terminal region of remorin proteins is necessary but not entirely sufficient for membrane binding

In order to identify the functions of the different regions of remorin proteins a number of truncation constructs were assembled for expression as fluorophore fusions in *N. benthamiana* (Fig. 20). Recent experiments from our lab had shown that the conserved C-terminal region not only harbours a putative coiled-coil region important for protein-protein interactions (Raffaele et al., 2007) but also the membrane attachment site (Konrad et al., 2014).

A first set of constructs was used to determine, whether the far C-terminal part of the protein (REMCA = remorin C-terminal anchor) was indeed responsible for PM binding throughout the protein family. Deletion mutants of AtREM1.2, AtREM1.3, AtREM4.2, AtREM6.1 and AtREM6.4, lacking the REMCA (AtREM1.2¹⁻¹⁸³, AtREM1.3¹⁻¹⁶¹, AtREM4.2¹⁻²⁴³, AtREM6.1¹⁻¹⁴⁵³, and AtREM6.4¹⁻³⁸⁴) (Fig. 20) were expressed in *N. benthamiana* for microscopical analysis. Indeed, membrane localisation was lost, and most of the signal was cytoplasmic, with additional nuclear localisations (Fig. 21A-D, I-J) in these mutant variants. To further verify loss of membrane attachment, PM counterstaining with the styryl dye FM® 4-64 was performed for both full length AtREM1.3 and AtREM6.1 as well as for AtREM1.3¹⁻¹⁶¹ and AtREM6.1¹⁻⁴⁵³. FM® 4-64 signal did clearly co-localise with the signal from the full-length constructs both before (Fig. 21E-F) and after plasmolysis (Fig. 21G-H). These data confirmed membrane binding of wildtype remorin proteins. In contrast, no co-localisation was observed for FM® 4-64 and AtREM1.3¹⁻¹⁶¹ or AtREM6.1¹⁻⁴⁵³ (Fig. 21I-J), indicating full loss of membrane localisation by removal of the REMCA region.

For AtREM6.4 additional constructs were created: The N-terminal region alone (AtREM6.4¹⁻²⁹⁹), the C-terminal region alone (AtREM6.4³⁰⁰⁻⁴²⁷), the C-terminal region lacking the REMCA (AtREM6.4³⁰⁰⁻³⁸⁴) and the REMCA alone (AtREM6.4³⁸⁵⁻⁴²⁷). As expected, AtREM6.4¹⁻²⁹⁹ did not bind to the plasma membrane but displayed cytoplasmic localisation as it lacked the REMCA peptide (Fig. 21K). AtREM6.4³⁰⁰⁻⁴²⁷ associated with the plasma membrane, where it was homogeneously distributed (Fig. 21L). AtREM6.4³⁰⁰⁻³⁸⁴ formed long, filamentous bundles, matching with the predictions of the C-terminal region consisting to large parts of a coiled coil region functioning in protein-protein interactions and oligomerisation (Raffaele et al., 2007, Tòth et al., 2012) (Fig. 21M). The AtREM6.4³⁸⁵⁻⁴²⁷ construct bound almost completely to the PM, but showed additional aggregates or vesicles in the cytoplasm as well as nuclear fluorescence (Fig. 21N), indicating a less stringent binding as AtREM6.4³⁰⁰⁻⁴²⁷.

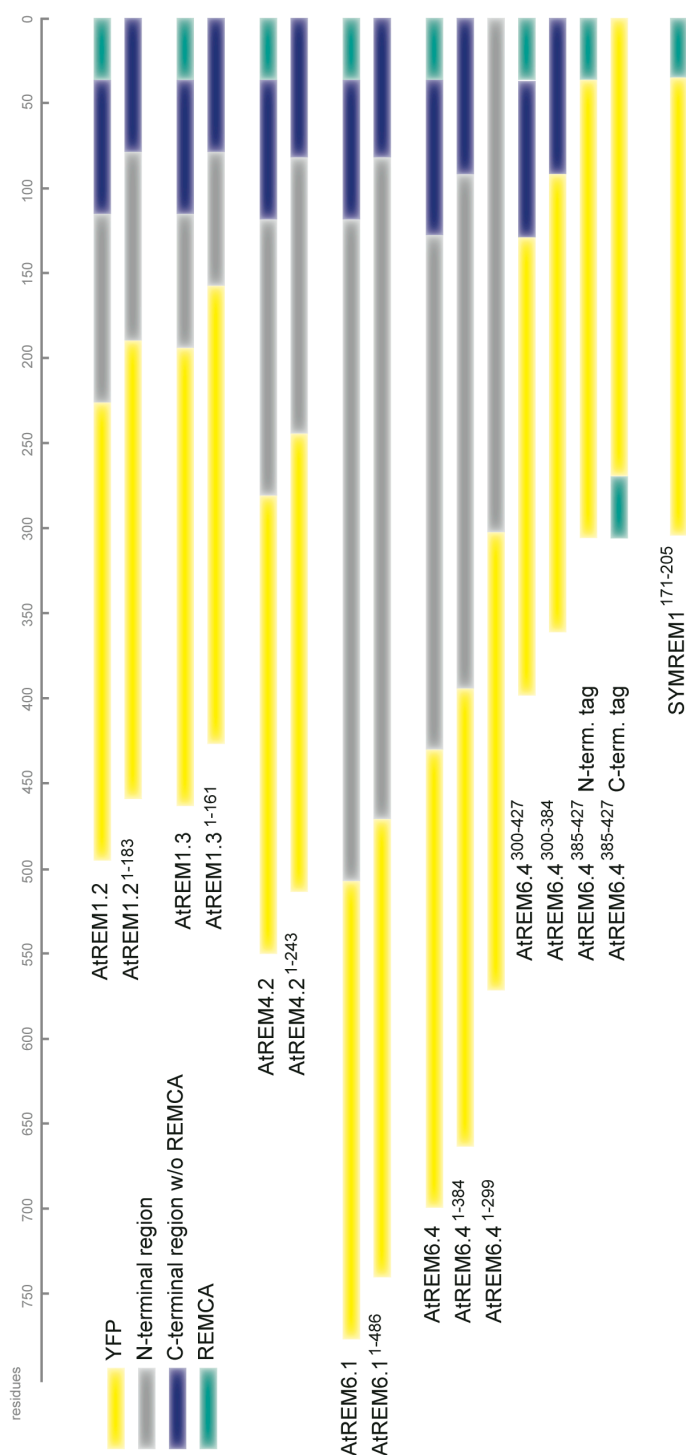


Fig. 20: Truncation constructs of remorin proteins used for cell biological approaches to determine the function of the different protein regions

Schematic representation of several YFP:AtREM fusion constructs. REMCA-devoid variants AtREM1.2¹⁻¹⁸³, AtREM1.3¹⁻¹⁶¹, AtREM4.2¹⁻²⁴³, AtREM6.1¹⁻⁴⁵³, and AtREM6.4¹⁻³⁸⁴ were created to investigate the role of the far C-terminal part of the protein in membrane binding. Additional deletion constructs of AtREM6.4 as well as the SYMREM1 REMCA construct (AtREM6.4¹⁻²⁹⁹, AtREM6.4³⁰⁰⁻⁴²⁷, AtREM6.4³⁰⁰⁻³⁸⁴, AtREM6.4³⁸⁵⁻⁴²⁷ and SYMREM1¹⁷¹⁻²⁰⁵) were employed to assess contributions of other protein regions to membrane attachment. Yellow bars = YFP tag; grey bars = variable N-terminal region; blue bars = conserved C-terminal region without REMCA, including putative coiled coil-region; green bars = REMCA

Results

In previous experiments together with Sebastian Konrad (LMU), a set of transgenic *A. thaliana* lines had been created, carrying CaMV 35S driven constructs of all cloned full-length remorin proteins as well as a set of REMCA constructs both in WT and, if available, in the respective mutant backgrounds (described in 2.1). At least 20 transformed seedlings per construct were microscopically investigated for fluorescence. However, in all of the transformed WT lines the transgenes were silenced. Interestingly, some REMCA constructs were successfully expressed in their respective mutant backgrounds (data not shown). These results raised the question, whether REMCA can interfere with the native proteins. To investigate, whether REMCA can be driven to the plasma membrane by oligomerisation with the wildtype protein, a C-terminally tagged AtREM6.4³⁸⁵⁻⁴²⁷ construct, which had completely lost plasma membrane localisation (see appendix) was co-expressed with the full-length protein. Indeed, the construct was recruited to the plasma membrane (Fig. 21O), and co-localised with the membrane domains labelled by the full-length protein (Fig. 21P).

To confirm these results, the SYMREM1 REMCA (SYMREM¹⁷¹⁻²⁰⁵) which is completely membrane localised in wildtype *M. truncatula* (Konrad et al., 2014), was expressed both transiently in AvrPto-DEX inducible *A. thaliana* (Fig. 21Q-R) as well as in a stable transgenic *A. thaliana* line with wildtype background (Fig. 21S-T) under control of the pUbi promoter. In both cases, the protein showed membrane localisation. Nevertheless additional cytoplasmic and nuclear localisation was visible. These data confirm the hypothesis that remorin proteins are targeted to the PM primarily via the REMCA. Nevertheless, additional regions in the C-terminal part of the protein support this localisation, probably via protein-protein interactions. In expression systems lacking the full-length protein, complete membrane attachment of a REMCA-only construct is obviously not achieved (Fig. 21N, S-T).

Results

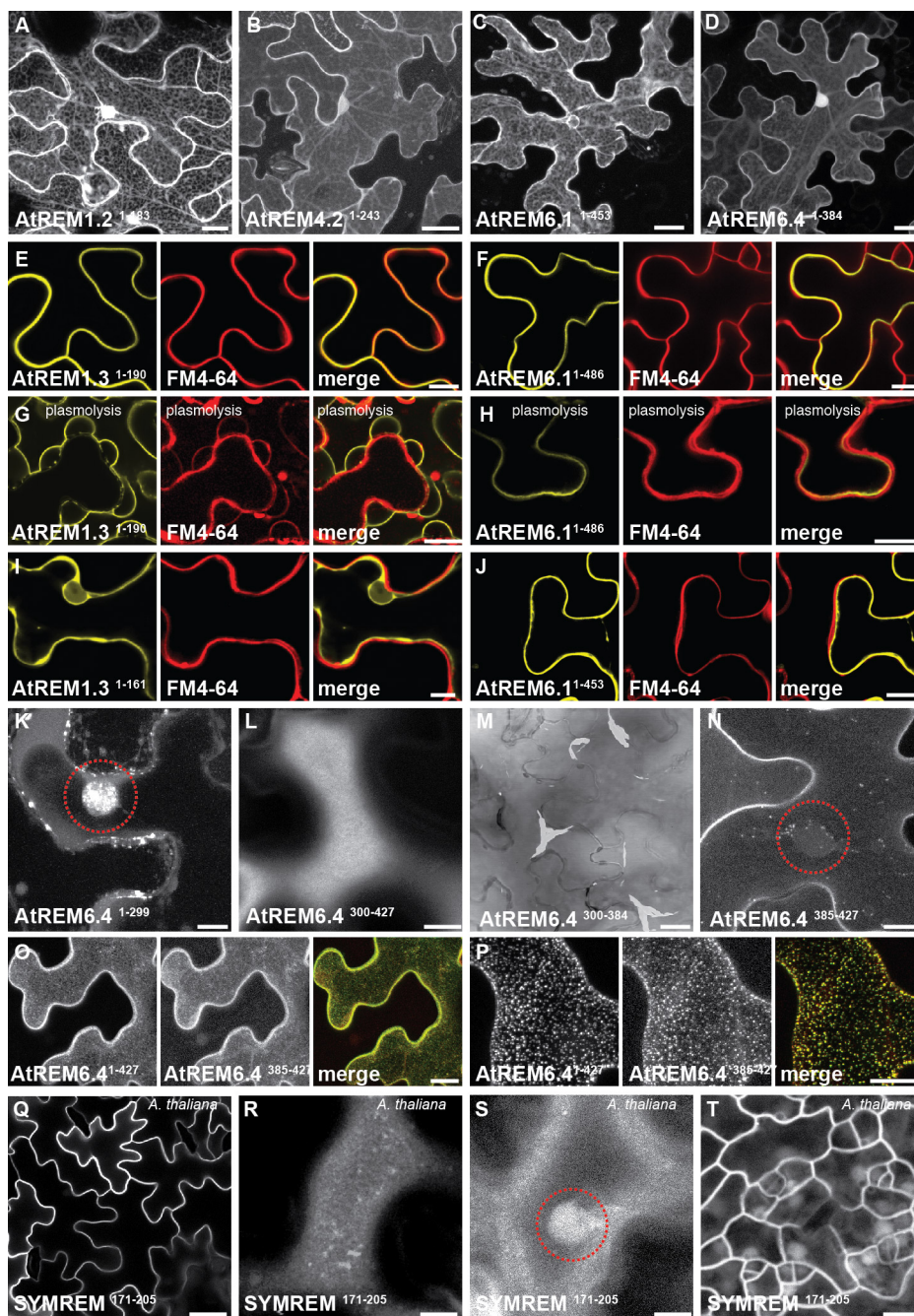


Fig. 21: Investigation of truncation constructs to determine the role of the different remorin protein regions

REMCA-devoid variants AtREM1.2¹⁻¹⁸³, AtREM4.2¹⁻²⁴³, AtREM6.1¹⁻⁴⁵³, and AtREM6.4¹⁻³⁸⁴ localise to the cytoplasm when being expressed under control of the CaMV 35S in leaf epidermal cells of *N. benthamiana* (A-D). Full-length AtREM1.3 (E, G) and AtREM6.1 (F, H) co-localises with PM counterstaining with the styryl dye FM® 4-64 both before (E-F) as well as after induction of plasmolysis (G-H). No co-localisation was observed between FM® 4-64 and the truncated variants AtREM1.3¹⁻¹⁶¹ (I) and AtREM6.1¹⁻⁴⁵⁸ (J).

Additional truncation constructs of AtREM6.4 reveal more details about the functions of the protein regions: AtREM6.4¹⁻²⁹⁹ localises to the cytoplasm and the nucleus (K) while AtREM6.4³⁰⁰⁻⁴²⁷ is homogeneously distributed over the plasma membrane (L). AtREM6.4³⁰⁰⁻³⁸⁴ forms long, flexible bundles of filaments (merged with bright field image to show cell boards) (M). AtREM6.4³⁸⁵⁻⁴²⁷ localises to the plasma membrane but additionally to the cytoplasm and the nucleus (N).

A non-membrane-bound REMCA-construct, AtSYMREM¹⁷¹⁻²⁰⁵ (C terminally tagged) can be

Results

recruited to the PM (**O**) and even into domains (**P**) by co-expression with the full-length protein. Transient (**Q-R**) and stable expression (**S-T**) of the SYMREM-REMCA under control of the pUbi promoter in *A. thaliana* reveals targeting to the membrane (**Q-T**) but also to the nucleus (**S-T**).

Nuclei are highlighted by red circles (**K, N, U**). Scale bars indicate 15 μm (**A-D, M, O-Q, T**) and 10 μm (**E-J, K-L, N, R-S**).

1.1.9. Relocalisation

For most remorin proteins, the localisation pattern in the PM did not change significantly over time during microscopy (Fig. 18). Interestingly, for a small number of remorins, a significant change in domain size could be observed in a timeframe of 30 min to one hour after sample preparation (e.g. leaf disc excision and submersion in water between object plate and cover slide). Most prominently, this was the case for AtREM6.4. Being initially distributed over the membrane in small, distinct, spherical domains (Fig. 22A, C), it often relocalised to larger domain clusters (Fig. 22B, D). Interestingly, during this process, the membrane area surrounding the domains was depleted of the freely diffusing protein fraction, indicating an active recruitment into the growing domains over time. Larger domains disintegrated over 4-6 hours. This behaviour was independent of the fusion direction, as both C-terminally (Fig. 22A-B) as well as N-terminally tagged constructs (Fig. 22C-D) showed this characteristic change in localisation.

Often the C-terminally tagged construct of AtREM6.4 relocalised not only to the above-mentioned larger domains, but additionally filamentous, network-like structures, which appeared similar to cytoskeleton (Fig. 22B). In rare cases, this was also observed with the N-terminally tagged construct (Fig. 22D). This indicates either a less stringent binding to the PM favours relocalisation to the observed structures, or that the N-terminal tag is interfering with such attachment. Co-localisation experiments with the microtubule marker MAP4 unfortunately remained inconclusive due to aggregation of MAP4 upon co-expression with AtREM6.4 (data not shown).

To investigate, which region of the protein was important for this relocalisation behaviour, a truncation construct lacking the N-terminal region of the protein, both tagged C- and N-terminally was investigated. These experiments were performed by Christina Weiß during a laboratory rotation in frame of her Master studies under my supervision. In both cases, no relocalisation was observed, indicating that the N-terminal region is essential for protein relocalisation (Weiß, 2013, LMU, Munich).

Results

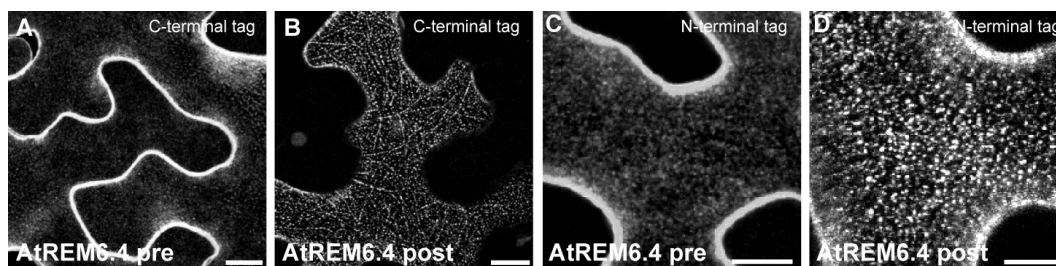


Fig. 22: Relocalisation of C-terminally and N-terminally tagged AtREM6.4

Relocalisation of C-terminally (A-B) and N-terminally (C-D) tagged AtREM6.4 into bigger domains was observed after a timeframe of 30 min to 2 hours of microscopy. pre = before relocalisation; post = after relocalisation; Scale bars indicate 10 μm .

To assess whether stress responses during these experiments caused the relocalisation of the AtREM6.4 protein, a number of abiotic stimuli such as wounding, heat, light and osmotic stresses were tested. Leaf discs were imaged after cutting or squeezing the leaf 1 hour prior to microscopy, incubation of the whole plant at 37°C for 30 min, transfer to a 300 $\mu\text{mol}/\text{m}^2$ light chamber for 30 min or water infiltration 1 hour prior to imaging. None of the tested treatments yielded in relocalisation prior to microscopy (data not shown). Merely the combination of the excision of the leaf disc as well as infiltration with water for microscopy resulted in the characteristic change in membrane patterning.

1.2. Interactions with other proteins

1.2.1. Remorin proteins are able to both homo- and hetero-oligomerise

It has been shown before that remorin proteins can form homo-oligomers when being purified from plant material or recombinantly expressed in bacteria (Bariola et al., 2004; Reymond et al., 1996). This is supported by results from a yeast-2-hybrid (Y2H) screen, where remorin hetero- and homo-oligomers were detected (Yamada et al., 1998) as well as previously published BiFC data showing both homo and hetero-oligomerisation of the SYMREM1 orthologs from *M. truncatula* and *L. japonicus* when being ectopically expressed in *N. benthamiana* (Tòth et al., 2012). In previous work (Jarsch, 2009) the ability of *A. thaliana* remorin proteins to form homo- and heterooligomers throughout the whole family had already been tested using Bimolecular Fluorescence Complementation (BiFC). In this system, interactions between all tested proteins were found, indicating a general possibility of hetero-oligomerisation, but also raising doubts concerning the specificity of the experimental setup due to the lack of appropriate negative controls. To address this question more stringently, a small set of proteins was cloned into vectors for a GAL4 Y2H interaction assay. Interestingly, AtREM1.2 and AtREM1.3 both formed homo-oligomers, but also interacted with each other (Fig. 23A-D). Nevertheless, none of the two proteins was able to interact with AtREM3.1 (Fig.

Results

23E-F). AtREM3.1 can form homo-oligomers (Fig. 23G), indicating also the functionality of the construct. These results show that remorin proteins are able to form homo-oligomers as well as hetero-oligomers with closely but not distantly related family members. Together with the data obtained from the co-localisation experiments they also indicate functional redundancy between similar remorin proteins.

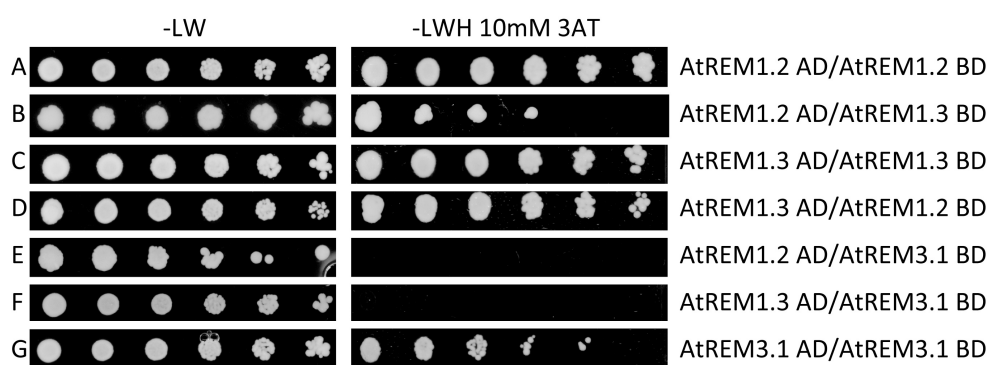


Fig. 23: Homo- and heterooligomerisation of AtREMs in yeast

Remorin proteins are able to form homooligomers in yeast two hybrid assays (**A-C, G**). Closely related remorins hetero-oligomerise (**B, D**), while interaction between phylogenetically distinct proteins could not be seen (**E, F**). -LW = transformation control on selective dropout medium without leucine and tryptophan; -LWH 10 mM 3-aminotriazol = interaction test on selective dropout medium without leucine, tryptophan and histidine but supplemented with 10 mM 3-aminotriazol.

1.2.2. *A. thaliana* remorin proteins interact with different receptor kinases

One of the goals of this work was to identify new interaction partners for *A. thaliana* remorins proteins. Here, remorin proteins were used as tools to identify new players in plant-pathogen interaction pathways that act together in signalling complexes at the PM.

In the frame of the presented work, the identification of interaction partners at the PM was addressed using a library of GAL4 Y2H clones containing the cytoplasmic domains of 55 receptor kinases from *A. thaliana* that were preselected for putative involvement in plant defence (Birgit Kemmerling, University of Tübingen). A targeted screen was performed for AtREM1.2, AtREM1.3, AtREM3.1, AtREM3.2, AtREM4.1, AtREM4.2 and an AtREM6.4¹⁻³⁸⁴ construct. The REMCA-devoid construct of AtREM6.4 was chosen to increase the fraction of soluble protein in the yeast cytoplasm. Each putative interactor was directly co-transformed with the respective remorin construct into the yeast strain pJ69-4a by a single transformation reaction. For drop-out selection SD-LW, SD-LWH 10 mM 3-AT and SD-LWH 20 mM 3-AT solid media were used. As a consequence of the stringent selection conditions, few but strong interactors were

Results

identified. All of them were independently confirmed and also tested for putative auto-activity. Table 3 shows the combined results.

Table 3: Results of a targeted Y2H Gal4 screen for RLKs interacting with AtREMs

A. thaliana remorin coding sequences (CDS) were fused to the GAL4 activation domain in the pGADT7 vector and subjected to a one-to-one screen with 55 RLKs putatively involved in plant defence (Birgit Kemmerling). Rows with red background indicate constructs that were found to be auto-active in the used experimental conditions; cells marked with 1 indicated the combination was successfully tested. Cells with grey background represent weak interactions or interactions, which have not been confirmed. Cells in yellow indicate strong interactions, which were confirmed in independent repetitions. KDSC = Kinase domain soluble construct

pGBKT7	pGADT7						
	AtREM1.2 CDS	AtREM1.3 CDS	AtREM3.1 CDS	AtREM3.2 CDS	AtREM4.1 CDS	AtREM4.2 CDS	AtREM6.4 ¹⁻²⁹⁹ CDS
At1g51820KDSC	1	1	1	1	1		1
At4g28490KDSC	1	1	1	1	1	1	1
At3g28450KDSC	1	1	1	1	1		1
At2g13790KDSC	1	1	1		1		1
At5g48380KDSC	1	1	1	1	1	1	1
At1g51860KDSC	1	1	1	1	1	1	1
At1g56140KDSC	1	1	1	1	1		1
At3g02880KDSC	1	1	1	1	1		1
At1g51790KDSC	1	1	1	1	1	1	1
At1g09970KDSC	1	1	1				1
At1g17750KDSC	1	1	1		1		1
At5g53320KDSC	1	1	1	1	1	1	1
At1g17230KDSC	1	1	1	1	1		1
At1g34420KDSC	1	1	1	1	1	1	1
At1g55610KDSC	1	1	1	1	1		1
At1g56130KDSC	1	1	1	1	1		1
At2g13800KDSC	1	1	1		1	1	1
At1g53420KDSC	1	1	1	1	1		1
At2g41820KDSC	1	1	1	1	1		1
At2g24130KDSC	1		1	1	1		1
At1g67510KDSC	1	1	1	1	1		1
At1g66830KDSC	1	1	1	1	1		1
At1g73080KDSC	1	1	1	1	1		1
At1g56120KDSC	1	1	1	1	1		1
At1g71830KDSC	1	1	1		1	1	1
At1g24650KDSC	1	1			1		1
At5g25930KDSC	1	1	1		1		1
At2g25790KDSC	1	1	1	1	1		1
At1g53440KDSC	1	1	1	1	1		1
At1g51870KDSC	1	1	1	1	1	1	1
At1g51800KDSC	1	1	1		1		1
At1g53430KDSC	1	1	1	1	1	1	1
At3g14840KDSC	1	1	1	1	1		1
At1g12460KDSC	1	1	1	1	1	1	1

Results

pGBKT7	pGADT7						
	AtREM1.2 CDS	AtREM1.3 CDS	AtREM3.1 CDS	AtREM3.2 CDS	AtREM4.1 CDS	AtREM4.2 CDS	AtREM6.4 ¹⁻²⁹⁹ CDS
At4g33430KDSC	1	1	1	1	1		1
At1g69270KDSC	1	1	1	1	1		1
At4g03390KDSC	1	1		1			1
At1g69990KDSC	1	1		1			1
At2g23300KDSC	1	1		1	1	1	1
At3g13380KDSC	1	1	1	1			1
At3g56100KDSC	1	1	1	1	1		1
At5g07280KDSC	1	1	1	1	1		1
At3g25560KDSC	1	1	1	1	1		1
At1g34210KDSC	1	1	1	1	1		1
At1g75640KDSC	1	1	1	1	1		1
At5g59670KDSC	1	1	1	1	1		1
At1g51880KDSC	1	1	1		1		1
At3g46370KDSC	1	1	1	1	1		1
At2g31880KDSC	1	1	1	1	1		1
At3g47580KDSC	1	1	1	1	1		1
At1g51830KDSC	1	1	1	1	1		1
At1g35710KDSC	1	1	1	1	1	1	1
At3g02130KDSC	1	1	1	1	1	1	1
At5g46330KDSC	1	1		1		1	1
At1g51850KDSC	1	1			1	1	1

Reproducible interactions with RLKs were found for AtREM1.2, AtREM3.1, AtREM3.2 and AtREM6.4. Two of these interactors were investigated in more detail.

One of the most interesting interactions was observed between AtREM1.2 and the LRR-RLK, At1g53440 (Table 3), which has been shown to be unregulated upon flg22 treatment (Zipfel, Tübingen, 2006). A T-DNA insertion mutant (Salk_130548.42.45.x) was obtained for this gene and preliminary experiments showed a strong insensitivity phenotype in seedling growth inhibition assays with flg22. Strikingly, an almost identical kinase, At1g53430 was included in the screen, but did not interact with AtREM1.2. Additionally both kinases did not interact with AtREM1.3. The further phenotypical characterization of both kinases and the investigation of their interaction with remorins were carried out by Corinna Hofer in her Master thesis project under my supervision (Hofer, 2012).

Among the eight putative interaction partners found for AtREM6.4, BAK1 (At3g33430) was the so far most intensively researched one. This receptor had been independently tested for interaction with AtREM6.4 in a Bimolecular Fluorescence Complementation (BIFC) approach. Here, four of the most prominent RLKs from *A. thaliana*, BRI1,

Results

BAK1, EFR and FLS2 had been investigated in respect for complex formation with remorin proteins in *N. benthamiana*. While a homogeneously distributed fluorescence was observed for BRI1, EFR and FLS2, which eventually represented background signal, BAK1 was the only protein interacting in specific laterally stable domains in the membrane with AtREM6.4 (Fig. 24A). While testing different truncation constructs (Fig. 20) to evaluate the regions of AtREM6.4 essential for interaction with BAK1, even an AtREM6.4¹⁻³⁸⁴ construct lacking the REMCA showed complex formation in the BIFC system. Also here, labelling of laterally immobile membrane domains was visible (Fig. 24E), indicating recruitment of the proteins into a BAK1-AtREM6.4 complex in specific immobile membrane compartments even independent of membrane binding by the remorin protein.

As a third independent approach, a co-immunoprecipitation experiment was performed to verify the interaction of AtREM6.4 and BAK1 *in planta*. In this case, C-terminally tagged remorin constructs were used, as these experiments were performed prior to the decision to preferably work with N-terminally tagged constructs. AtREM6.4 C-terminally fused to YFP was co-expressed with BAK1 fused to a His-HA tag.

The AtREM6.4-YFP fusion protein was immunoprecipitated using magnetic GFP-Trap®, and the samples were analysed via Western-Blot for co-bound His-HA-tagged BAK1. While AtREM6.4 was generally well detectable after protein-extraction procedures where the membrane was kept intact (e.g. in microsomal fractions), AtREM6.4 was not detected in crude extracts after procedures using detergents. It was concluded that AtREM6.4 aggregated and probably precipitated, as soon as it was depleted of its hydrophobic environment. This may be predominantly caused by the large intrinsically disordered N-terminal region of the AtREM6.4 protein (Marin and Ott, 2012).

In experiments where AtREM6.4 was successfully immunoprecipitated, co-bound BAK1 was visualised via Western blot analysis (Fig. 24F).

So far, attempts using material from a complemented mutant expressing AtREM6.4 under control of the endogenous promoter and trying to detect BAK1 with a native antibody were not successful, as AtREM6.4 was not detectable in the IP fraction (data not shown).

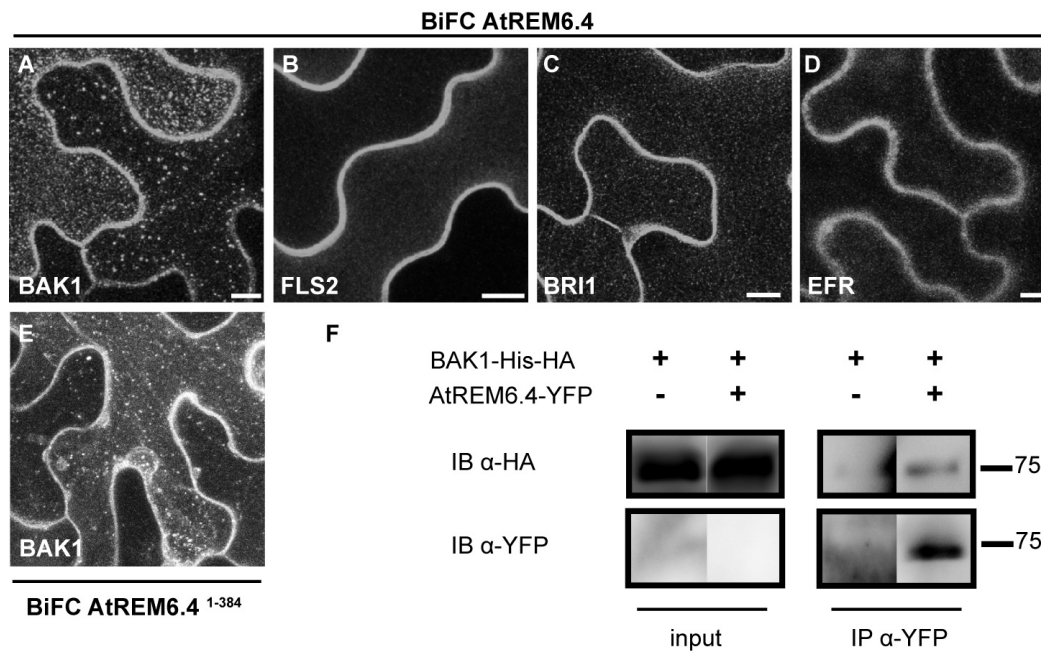


Fig. 24: AtREM6.4 interacts with BAK1 in planta

AtREM6.4 interacted with BAK1 in distinct domains in the plasma membrane when being tested in the BiFC system (A). BiFC signal with other receptors displayed a homogeneous distribution pattern (B-D). Also an AtREM6.4¹⁻³⁸⁴ construct shows interaction with BAK1 in membrane domains (E). Full length AtREM6.4-YFP was immunoprecipitated using GFP®-Trap and blotted using an α -GFP antibody (F). Bound BAK1-HIS-HA was detected using an α -HA antibody. All constructs were expressed in *N. benthamiana*. Scale bars represent 10 μ m.

1.3. Phosphorylation

1.3.1. Remorins can be directly phosphorylated by receptor kinases

Remorin proteins interact with receptor kinases at the PM and are differentially phosphorylated upon external stimuli (Lefebvre et al., 2010, Tóth et al., 2012, reviewed in Jarsch and Ott, 2011, Marin and Ott, 2012). Therefore, the direct phosphorylation of remorins by the kinase domain (KD) of BAK1 was tested in an *in vitro* kinase assay (experiments were performed together with Macarena Marín, LMU; purification of AtREM6.4 from inclusion bodies as well as refolding was carried out by Macarena Marín). BAK1 KD as well as AtREM1.3 and AtREM6.4 were purified from bacteria and subjected to *in vitro* phosphorylation. BAK1 KD showed strong auto-phosphorylation as well as a weak trans-phosphorylation of AtREM1.3 (Fig. 25). Interestingly, although added in amounts almost not visible in the Coomassie Brilliant Blue stained SDS-PAGE, AtREM6.4 showed strong integration of radioactivity, indicating hyper-phosphorylation by the BAK1 KD (Fig. 25).

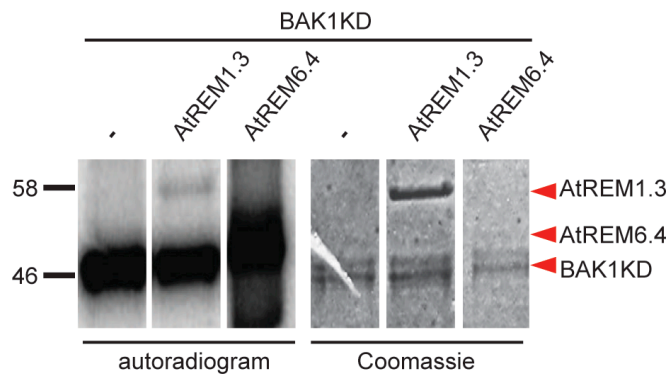


Fig. 25: *In vitro* phosphorylation of AtREM6.4 by the BAK1 KD

BAK1 KD displays strong auto-phosphorylation (lane 1). While AtREM1.3 (lane 2) is only weakly phosphorylated, AtREM6.4 shows very strong integration of radioactivity (lane 3). Coomassie Brilliant Blue staining shows that equal amounts of BAK1KD have been used.

1.3.2. Investigation of the role of phosphorylation on interaction with RLKs

AtREM6.4 harbours one annotated *in vivo* phosphorylation site, threonine 215 (T215), which resides in the middle of the intrinsically disordered N-terminal region of the protein. Phosphorylated peptides were found both in untreated plants as well as after flg22 application (Benschop et al., 2007), indicating a constitutive phosphorylation of this residue. Mutations of T215 to glutamate (T215D) and alanine (T215A) were performed to create both a phosphomimic as well as a phosphoablative variant of AtREM6.4, respectively. Both mutant constructs were overexpressed in *N. benthamiana* to assess, whether subcellular localisation or relocalisation of the proteins was altered. These experiments were performed by Christina Weiß during a laboratory rotation in frame of her Masters studies under my supervision.

As no differences in localisation or relocalisation compared to the wildtype protein were observed (Weiß, 2013, LMU, Munich), interaction patterns of the mutant proteins with BAK1 using the BiFC system were investigated.

Indeed, when BAK1 was fused to the N-terminal and the AtREM6.4T215A to the C-terminal half of YFP, interaction did no longer occur in the previously seen laterally stable domains, but appeared homogeneously distributed over the PM. By contrast, an increase in domains was observed when using the AtREM6.4T215D version. These results are to be considered preliminary, as experiments were performed only twice.

Results

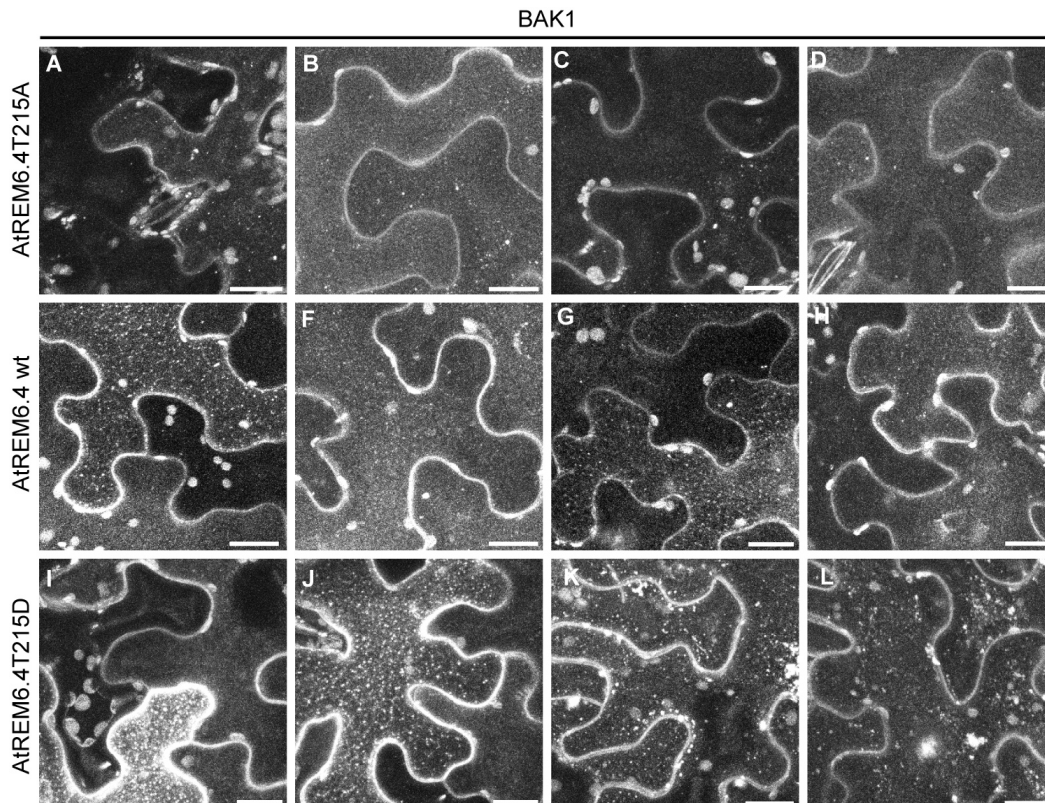


Fig. 26: Mutations of the annotated phosphorylation site of AtREM6.4, T215, have an impact on interaction with BAK1 in membrane domains

Representative images showing interaction of AtREM6.4 wt and mutant constructs in the BiFC system. While the wt (**E-H**) often displayed interaction with BAK1 in a dotted pattern, this was dramatically reduced with the AtREM6.4T215A construct (**A-D**). AtREM6.4T215D displayed even stronger dot-formation than the wildtype construct (**I-L**). Scale bar = 10 nm.

Results

In this part of the study, I was able to show that N-terminally tagged fluorophore fusions constructs of remorin proteins label microdomains in the plasma membrane of 0.1 – 0.4 μm^2 size. By quantitative image analysis, I determined differences between these domains using domains size, mean domain intensity, circularity and density as parameters. I further verified the labelling of diverse membrane domains by remorin proteins by a large-scale co-expression analysis, showing that the plasma membrane of plants displays a plethora of coexisting membrane compartments. The observed domains were laterally immobile and showed dynamic exchange of proteins with the surrounding membrane as demonstrated with FRAP experiments. For group 1 remorin proteins, domains formation in a tissue-specific manner was shown.

In the frame of a project in the laboratory to investigate the determinant for membrane localisation of remorin proteins I demonstrated that the REMCA region is indeed necessary for association of the protein to the PM throughout the whole family. Nevertheless, additional factors like protein-protein-interactions are likely to contribute to this process.

Finally, a targeted yeast to hybrid screen yielded several putatively interacting RLKs for a subset of the remorin protein family. Two of them were pursued for further characterisation, At1g53440 for AtREM1.2 and BAK1 for AtREM6.4. The first one was successfully taken up as a separate project by Corinna Hofer. The interaction between AtREM6.4 and BAK1 was independently confirmed by BIFC and Co-IP *in planta* as well as by an *in vitro* kinase assay.

It remains to be confirmed, whether this interaction as well as the accumulation of the protein complex in membrane microdomains is indeed dependent on a phosphorylation at residue T215 of AtREM6.4.

2. Towards the role of remorin proteins in plant pathogen interactions

The second major part of the here presented work aimed to assess the biological function of *A. thaliana* remorin proteins during plant-microbe interactions. For this, mutant lines for a number of the investigated proteins were identified. A subset was selected for further phenotypic investigations under different experimental conditions focusing on plant-pathogen interactions.

2.1. Creation of a T-DNA insertion line collection for *Arabidopsis thaliana* remorin proteins

Designated to provide a broad basis for future systematic genetic approaches on *A. thaliana* remorin proteins, a library of T-DNA insertion lines was created, including mutant lines for 11 of the 16 *A. thaliana* remorin family members. With technical assistance by Jessica Folgmann a common workflow for the screening of segregating T-DNA insertion lines was established. Available T-DNA insertion lines for remorin genes provided by the SALK institute were obtained. Plants were grown for seed-production and subjected to a PCR-based genotyping procedure to identify homozygous individuals. A subset of T-DNA-derived PCR-amplicons was sequenced to verify the annotated T-DNA insertion site. In total, 13 independent mutant alleles for 11 different remorin proteins were identified and brought to homozygosity. SALK insertion lines all derive from a Col-0 background. Additionally, one Flag-T-DNA insertion line in the Wassilevskija ecotype background for AtREM3.2, *Atrem3.2-4*, was ordered and brought to homozygosity. This ecotype does not harbour a functional FLS2 receptor, consequently it is not suitable for flg22-based defence experiments.

Double mutants were created from *Atrem1.2-1* and *Atrem1.3-2* as well as from *Atrem6.4-1* and *Atrem6.7-1* by crossing. Additionally, a triple mutant from *Atrem1.2-1/Atrem1.3-2* with *Atrem1.4-3* was initiated (now continued by Macarena Marin).

Results

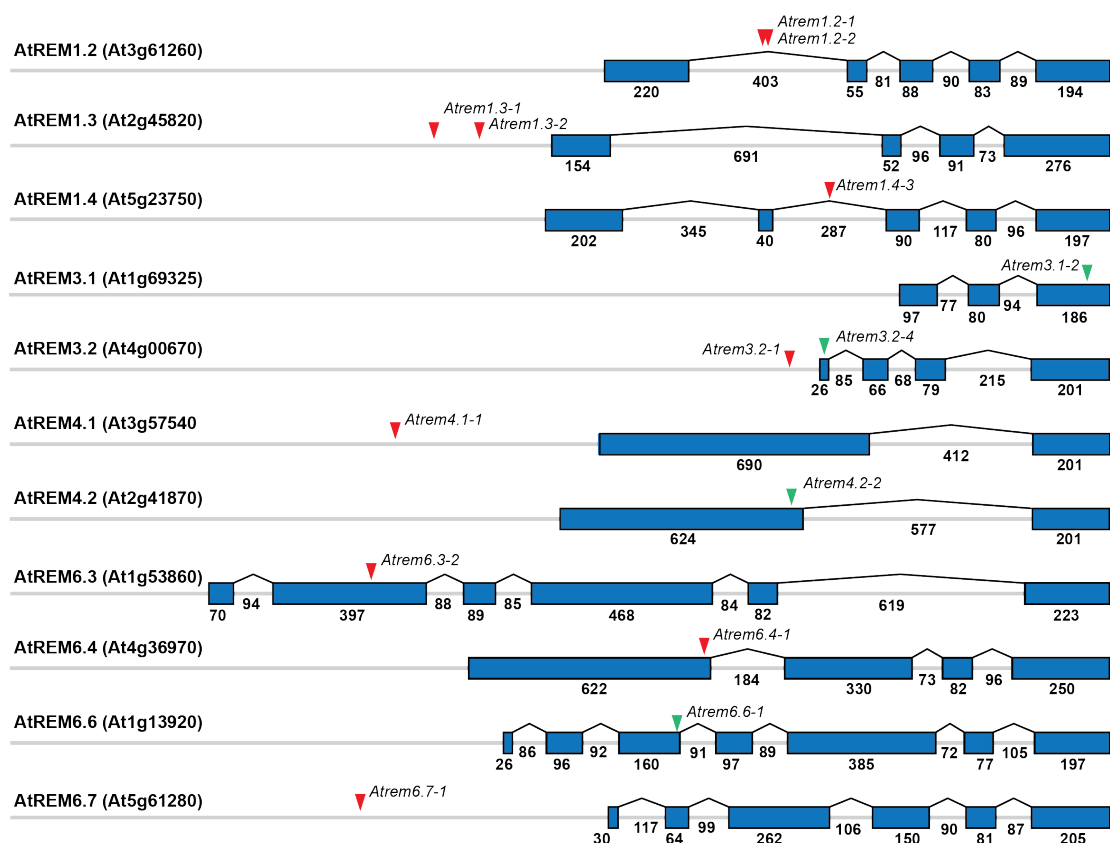


Fig. 27: Homozygous T-DNA insertion lines identified for several AtREMs

Illustration of the structures of the genomic regions of 11 remorin alleles and the sites of the T-DNA insertion. Blue bars indicate exons, topped space in between introns. The length of the different sequences is indicated in number of nucleotides below. Red arrows = insertion sites of the T-DNA for given alleles as annotated by the SALK institute. Green arrows = insertion sites of the T-DNA for given alleles as identified via sequencing of PCR amplicons derived from the T-DNA-border.

2.2. Generation of complemented mutant lines.

It is crucial to confirm that phenotypes of the identified T-DNA insertion lines were caused indeed by a disruption of the respective remorin gene. Therefore, a subset of the identified mutant lines, chosen for further phenotypic investigations, were transformed with genomic versions of the respective genes fused to YFP to be expressed under control of their endogenous promoters. Additionally, these lines were used to verify the functionality of fluorophore-tagged fusion constructs. *Atrem1.2-2*, *Atrem1.3-2* and *Atrem6.4-1* were stably transformed with constructs expressing the protein both with N-terminal (e.g. *proAtREM:YFP:AtREM*) as well as with C-terminal tags (e.g. *proAtREM:AtREM:YFP*).

2.3. Phenotypical analysis of remorin mutants

2.3.1. Experimental approaches

Defence responses to the model PAMP flg22 are among the best-dissected pathways in plant signalling. In the respective mutant lines, each single step of the signalling cascade can be experimentally assessed by a variety of well-established assays, in order to investigate the position of a protein in the signalling pathway.

In this study, early responses after PAMP treatment including receptor oligomerisation, ROS production and MAPK activation were assessed.

Additionally, long time responses to PAMPs were tested in a so-called seedling growth inhibition (SGI) assay. The SGI assay makes use of the fact that seedlings concentrate their resources on growth and development in the absence of pathogens, while the perception of a biotic threat causes a reprogramming of their cellular processes. The plant ceases to grow but invests in defence. This reaction can be easily assessed by measuring fresh weight after incubation with a bacterial elicitor.

In this part of the project, the focus was put on three specific remorin proteins in two independent approaches. AtREM1.2 and AtREM1.3 were chosen, as both proteins or their orthologs are transcriptionally regulated during pathogen attack or application of bacterial elicitors such as flg22 (Navarro et al., 2004, Coaker et al., 2004). Also, both are differentially phosphorylated in an elicitor- or R-gene dependent manner (Benschop et al., 2007, Keinath et al., 2010, Widjaja et al., 2009).

AtREM6.4 was chosen due to its interesting cell biological aspects like domain formation and relocalisation and the physical interaction with BAK1.

None of the plants with mutant alleles associated with AtREM1.2, AtREM1.3 and AtREM6.4 had shown a visible growth-related or developmental phenotype.

2.3.2. Phenotypic analysis of AtREM1.2 and AtREM1.3 during plant-pathogen interactions

2.3.2.1. *Atrem1.2-1*, *Atrem1.2-2* and *Atrem1.3-2* are knockout mutant lines

To phenotypically analyse mutant lines of AtREM1.2 and AtREM1.3, each two different alleles from the previously created library of T-DNA insertion lines were chosen (see chapter 2.1). All four lines were subjected to additional analyses to ensure that the plants were true knockout mutants and did not express the native protein. Seeds

Results

were germinated on plates and grown for 10 days. For each assay, five whole seedlings were pooled and processed for protein separation via SDS-PAGE. Western Blot analysis using a group 1 remorin specific, polyclonal antibody (Sylvain Raffaele, LIPM, Toulouse) was performed. While no expression of the respective native proteins could be detected in *Atrem1.2-1*, *Atrem1.2-2* and *Atrem1.3-2*, full protein amounts were visible in *Atrem1.3-1*. This line was excluded from further experiments.

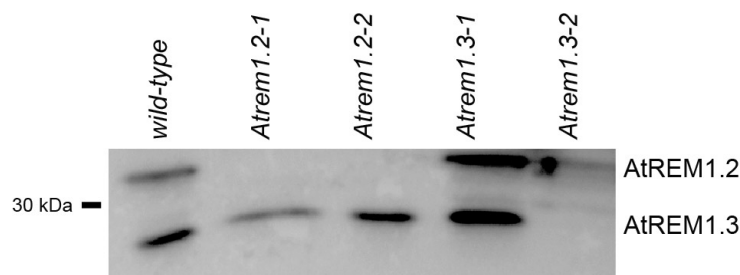


Fig. 28: Identification of knockout mutants using Western Blot analysis

Western Blot analysis was performed on crude extracts of 7 days old seedlings using a group 1 remorin specific antibody. Both in *Atrem1.2-1* as well as in *Atrem1.2-2*, expression of the protein is completely abolished compared to the wildtype (lanes 1-3). While this is also the case in *Atrem1.3-2*, full protein amounts are still detectable in *Atrem1.3-1* (lanes 4-5). Remorin proteins were detected via a group 1 specific, polyclonal antibody (Sylvain Raffaele, Bordeaux).

2.3.2.2. FLS2 and BAK1 form an intact receptor complex after flg22 elicitation

AtREM1.2 and AtREM1.3 are among the 10 % highest expressed genes in *A. thaliana* (Raffaele et al., 2007). One idea on the role of AtREM1.2 and AtREM1.3 was, that both proteins are essential for membrane compartmentalisation in general, and therefore crucial for correct localisation and recruitment of receptor proteins within the PM. Establishment of receptor oligomers is the first known output of ligand perception by the plant and can be easily assessed by immunoprecipitation of one player and investigation of bound co-receptors by Western-Blot analysis. Consequently, the formation of an intact FLS2-BAK1 complex after elicitor treatment was tested in Col-0 wt, *Atrem1.2-1*, *Atrem1.2-2*, *Atrem1.3-2* and the *Atrem1.2-1/Atrem1.3-2* double mutant (Fig. 29A-B). Seedlings were treated with flg22 for 5 min and then subjected to IP of either FLS2 (Fig. 29A) or BAK1 (Fig. 29B). Both receptors were detected in high amounts in the IP fraction by Western Blot analysis. While co-immunoprecipitation of the respective co-receptor was not visible before flg22 treatment, dimerization was shown after elicitation for all lines. No difference in receptor complex formation was detected between wt and mutant lines. These results indicate that FLS2-BAK1-dimerisation upon flg22 perception is independent on group 1 remorin proteins.

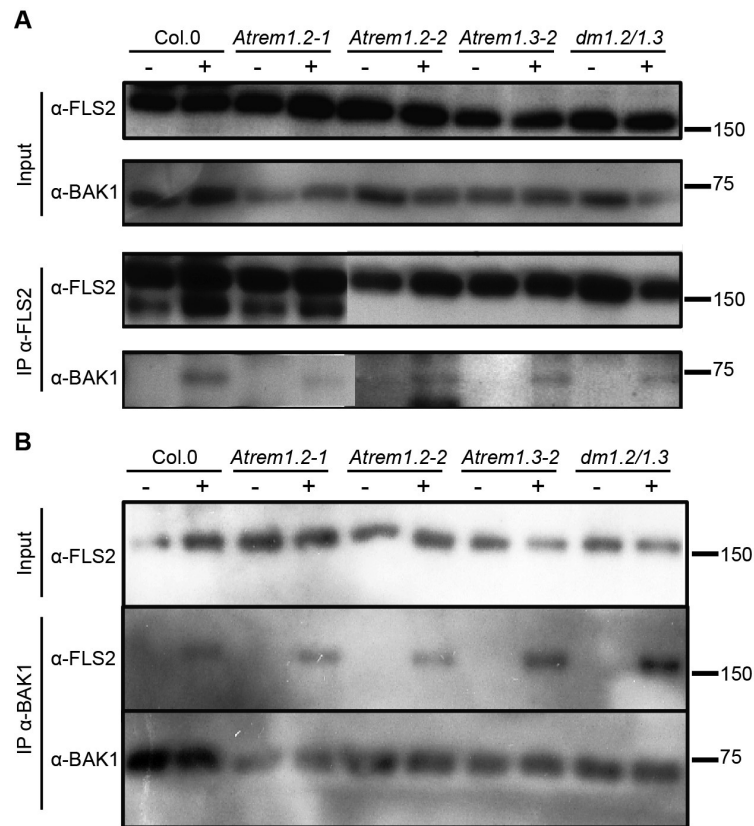


Fig. 29 The FLS2-BAK1 receptor complex forms normally in group 1 mutant lines after flg22 treatment

Immunoprecipitation of FLS2 (A) and BAK1 (B) from *A. thaliana* seedlings treated with H₂O (-) or 100 nM flg22 (+) for 5 min. Both receptors can be detected in high amounts in the IP fraction. No co-immunoprecipitation of the respective partner for the receptor complex can be detected in water treated samples. After flg22 treatment, both FLS2 and BAK1 are co-immunoprecipitated. No difference to Col-0 wt was determined for group1 mutants (A-B). *dm1.2/1.3* = double mutant *Atrem1.2-1/Atrem1.3-2*.

2.3.2.3. The production of reactive oxygen species is unaltered in group 1 mutant lines

After receptor dimerization, another ultimate early response of the plant immune system is the production of reactive oxygen species on the leaf surface. Acidification of the extracellular space is both a direct measure of pathogen elimination as well as a signal for further downstream responses of the plant cell (Miller et al., 2009). The occurrence of the oxidative burst upon flg22 treatment can be measured using an HRP/luminol assay. H₂O₂ production is detectable about 2 min after elicitation with a maximum at 10 min after a rather steep rise. The response curve then decreases in a gentle slope and reaches background level after 30 min. Total photon counts are calculated over the whole time of the measurement, ranging from 0 to 30 min after elicitation.

Results

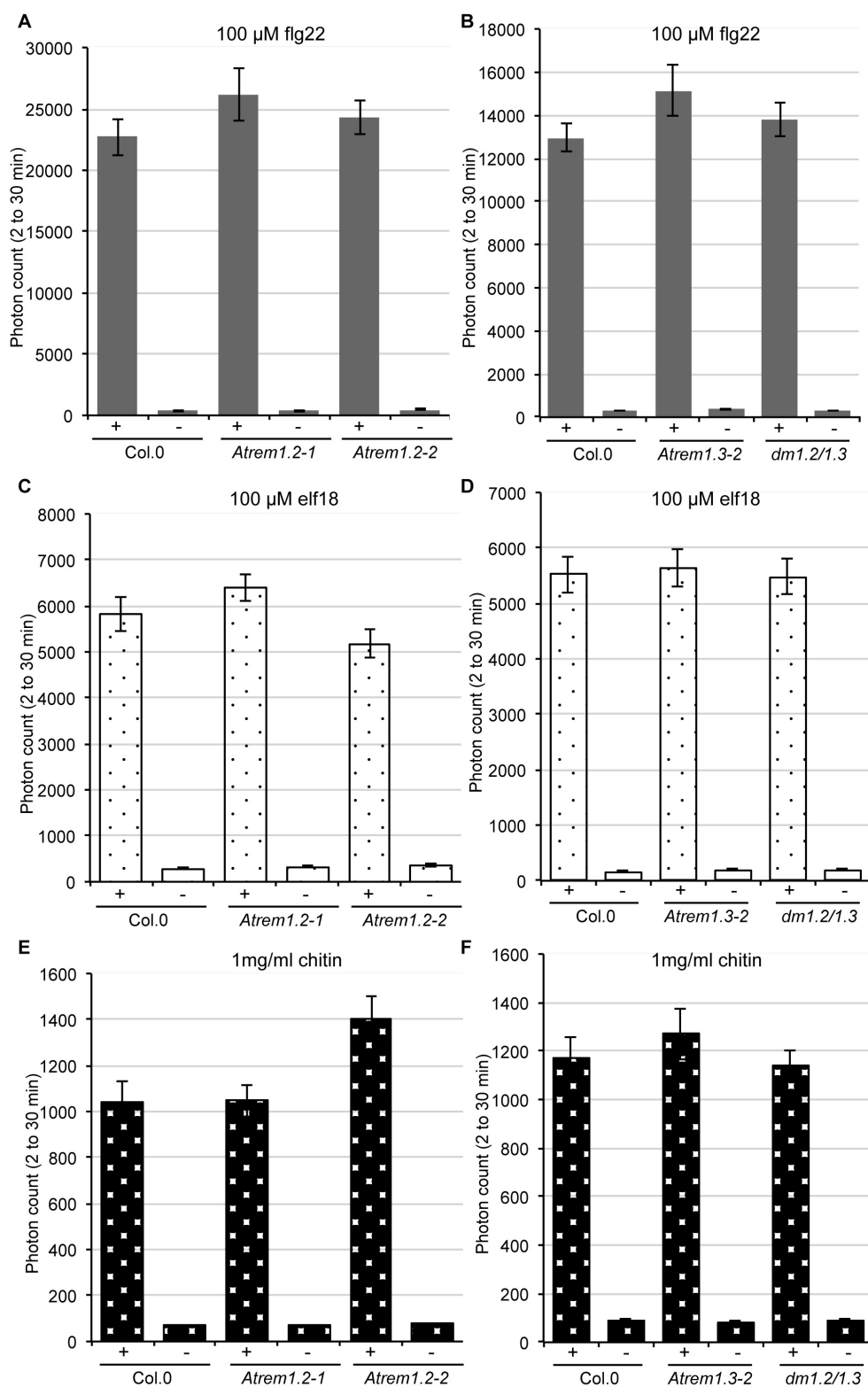


Fig. 30: Reactive oxygen production is not altered in group1 mutant lines after elicitor treatment

Total photon counts from ROS burst measurements. *Atrem1.2-1* and *Atrem1.2-2* (A, C, E) as well as in *Atrem1.3-2* and the *Atrem1.2-1/Atrem1.3-2* double mutant (B, D, F) were compared to Col-0 wt both with (+) and without (-) elicitor treatment. Three different elicitors were tested; flg22 (A-B), elf18 (C-D) and chitin (E-F). No difference between the different lines was detected. n = 32; error bars represent standard error between biological replicates.

Results

Col-0 wt, *Atrem1.2-1*, *Atrem1.2-2*, *Atrem1.3-2* and the *Atrem1.2-1/Atrem1.3-2* double mutant were investigated in collaboration with the lab of Cyril Zipfel, Norwich. Here, three different elicitors were tested, namely flg22 (Fig. 30A-B), elf18 (Fig. 30C-D) and chitin (Fig. 30E-F). All experiments were repeated four times independently. No significant difference between the mutant lines and the wildtype were observed.

2.3.2.4. MAP kinase activation

The activation of the MAPK cascade after flg22 and elf18 treatment was tested for *Atrem1.2-1*, *Atrem1.2-2*, *Atrem1.3-2* and the *Atrem1.2-1/Atrem1.3-2* double mutant in comparison to Col-0 wild type. Phosphorylation status of the proteins was investigated 0, 5, 10 and 30 min after application of the elicitor. In the wildtype plants, little phosphorylation was detectable at time-point 0. The phosphorylation status increased after 5 min and reached its maximum 10 min after elicitation. After 30 min, the activation started to decrease. So far, no clear defect in activation of this signalling pathway was detected in the tested remorin mutants (Fig. 31). Yet, the *Atrem1.2-1/Atrem1.3-2* double mutant showed a slightly increased phosphorylation after 30 min in both treatments. To closer investigate a possible deregulation, repetitions of this experiment will be performed with samples from more time points and including the *Atrem1.2-1/Atrem1.3-2/Atrem1.4-3* triple mutant.

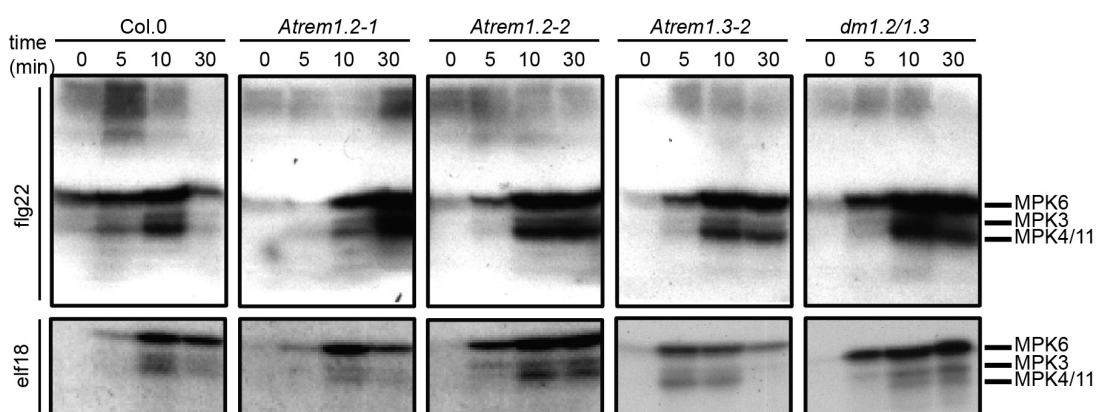


Fig. 31: MAPK activation is not reduced in group 1 mutant lines

Western Blot analysis to detect MAPK phosphorylation in group1 mutant lines compared to wildtype after flg22 and elf18 treatment. Samples were harvested 0, 5, 10 and 30 min after elicitation. Phosphorylation of proteins was visualized using an α -P-p44/42 MAPK rabbit (T202/Y204) antibody. n = 12.

Results

2.3.2.5. Seedling growth inhibition

Seedling growth inhibition assays were carried out with *Atrem1.2-1*, *Atrem1.2-2*, *Atrem1.3-2* and the *Atrem1.2-/Atrem1.3-2* double mutant in comparison to Col-0 wildtype. Flg22 concentrations of 10 nM, 100 nM and 1 μ M were used. While growth of the flg22-insensitive *fls2* mutant was unaltered, wt and group 1 mutant lines showed similarly strong growth inhibition correlating with elicitor concentrations.

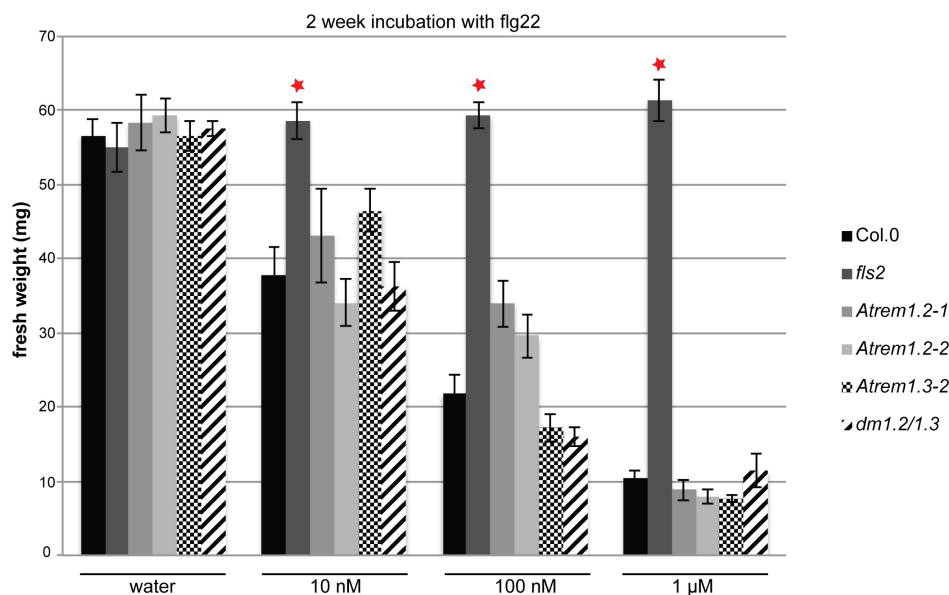


Fig. 32: Seedling growth inhibition is unaltered in group 1 mutant lines after flg22 treatment

Seedlings were transferred to liquid MS containing different concentrations of flg22 7 days post germination. After two weeks of incubation, fresh weight was determined. No significant differences between *rem* lines and wt were determined. $n = 18$. Red stars indicate significant differences *fls2* compared to the wt with $p < 0.01$; error bars represent standard error between biological replicates.

2.3.2.6. Investigation of remorin mutant lines for phenotypes after infection with *Pseudomonas syringae*

After the evaluation of several specific cellular outputs of elicitor recognition by the plant through RLKs in remorin mutant plants, the overall susceptibility towards plant pathogens was tested by infection with *P. syringae* DC3000 strains. By application of the wildtype bacterial strain and subsequent analysis of infection success by assessment of bacterial proliferation, the combined effects of PTI and ETI can be investigated. By using mutant strains of the bacterial pathogen, again a differentiation in defence processes coinciding with the different steps of the infection can be archived. In this study, a *P. syringae* strain lacking the bacterial effector molecule coronatin (PtoDC3000

Results

Cor-) was used. This substance is produced by the microorganism to trigger the reopening of plant stomata, a step essential to invade the intercellular space (Melotto et al., 2006). While *Atrem1.2-1*, *Atrem1.2-2* and *Atrem1.3-2* did not show a significant difference in infection strength by the pathogen, the *Atrem1.2-1/Atrem1.3-2* double mutant displayed a weakly but significantly higher susceptibility compared to the wildtype. Due to the weak phenotype, it was decided to include the *Atrem1.2-1/Atrem1.3-2/Atrem1.4-3* triple mutant, which is currently in segregating T1, before investing further in group 1 phenotyping. The lack of differences after *PtoDC3000 Cor-* infection indicated that any differences observed with the virulent stains are depending on processes happening independent of stomatal closure and eventually after the pathogen enters the leaf.

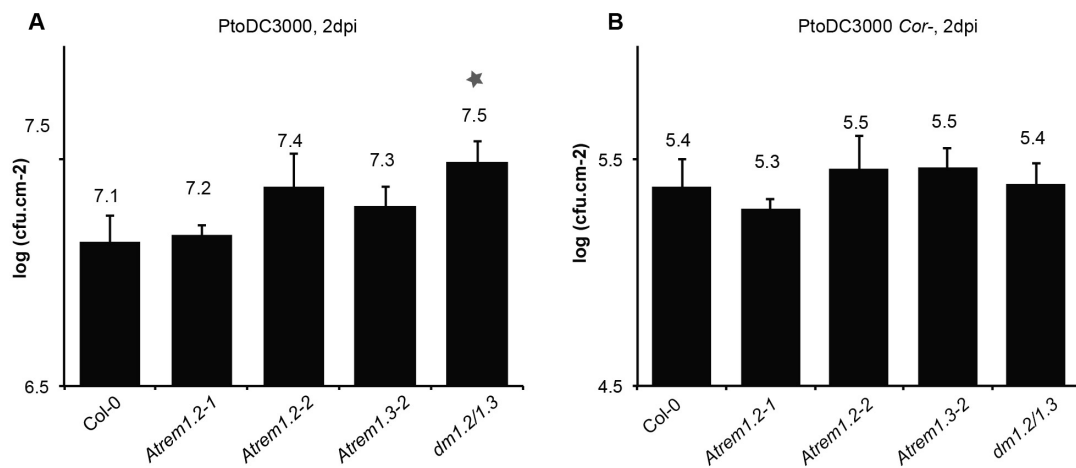


Fig. 33: The *Atrem1.2-1/Atrem1.3-2* double mutant (dm) shows a moderate but significantly increased susceptibility towards infection with *P. syringae pv. PtoDC3000*

The *Atrem1.2-1/Atrem1.3-2* dm displays higher bacterial infection after spray-inoculation with *PtoDC3000* (A). The phenotype is not visible after infection with *PtoDC3000 Cor-* (B). n = 4, p = 0.05; error bars represent standard error between biological replicates.

2.3.3. Investigation of AtREM6.4 function in BAK1-related biological processes

2.3.3.1. *Atrem6.4-1* is a knockout mutant line

Similar to the above-described analysis of the group1 remorin mutant lines for native gene expression prior to phenotypical investigations, *Atrem6.4-1* was tested for expression of *AtREM6.4*. As no antibody was available for AtREM6.4, transcript levels were determined in seedlings in collaboration with Susan Urbanus (LMU Munich). Primers for a 70 bp sequence spanning the junction of the first and the second exon were used for q-RCR. Expression was normalized to transcript levels of ubiquitin. While

Results

AtREM6.4 transcript was detected in whole Col-0 adult rosette leaf material, no expression was quantified in the same tissue of the *Atrem6.4-1* line. These data show that these plants are indeed knockout mutants.

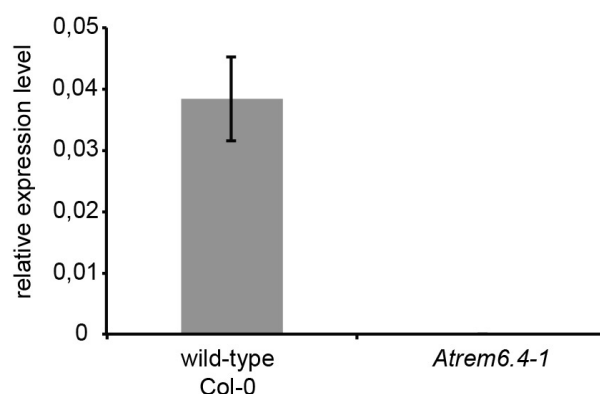


Fig. 34: *AtREM6.4* transcript is not detectable in *Atrem6.4-1* mutants

AtREM6.4 transcript levels were determined in wildtype and *Atrem6.4-1* whole leaf tissue of 3 week old plants. No *AtREM6.4* transcripts were detected in the mutant line. n = 2; error bars represent standard error between biological replicates.

2.3.3.2. FLS2-BAK1 interaction after flg22 elicitation is unaltered in *Atrem6.4-1*

It was shown previously that BAK1 forms an interaction with AtREM6.4 *in planta* (Fig. 24), which may be dependent on the phosphorylation of a specific residue in the N-terminal region of the remorin (Fig. 26). As a co-receptor of several known RLKs, BAK1 is heavily regulated by co-bound proteins (see introduction). As it was likely that the interaction of the remorin protein with BAK1 is constitutive, it was of interest, whether AtREM6.4 is modulating BAK1 recruitment to the FLS2 complex. Similar to the group 1 mutant lines, this was tested via a co-immunoprecipitation approach.

Atrem6.4-1 as well as the putatively complemented line carrying the *proAtREM6.4:YFP:AtREM6.4* construct were tested for alterations in BAK1-FLS2 receptor complex formation after flg22 treatment (Fig. 29C). BAK1 was immunoprecipitated from flg22 treated 2 weeks old seedlings. Co-immunoprecipitation of FLS2 was analysed by Western Blot. No changes between wildtype and mutants could be detected. These results indicate that receptor-interaction upon flg22 perception is unaltered in the *Atrem6.4-1* line and therefore independent of AtREM6.4. A second possibility would be redundancy between related remorin proteins and AtREM6.4.

Results

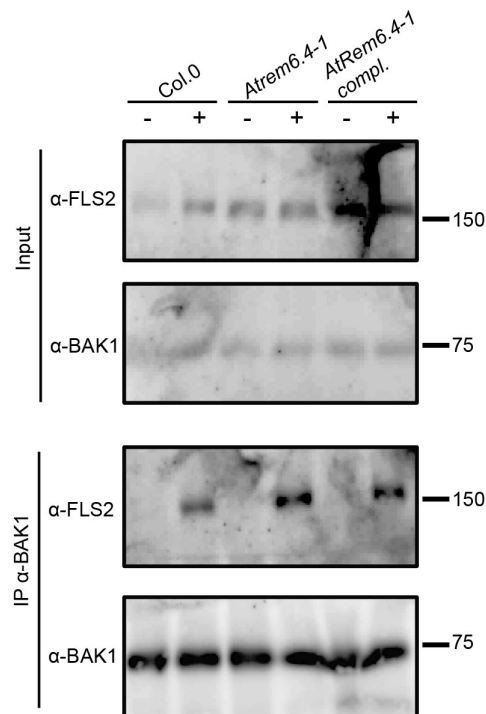


Fig. 35 The FLS2-BAK1 receptor complex forms normally in *Atrem6.4-1* after flg22 treatment

Immunoprecipitation of BAK1 from *A. thaliana* seedlings treated with H₂O (-) or 100 nM flg22 (+) for 5 min. BAK1 can be detected in high amounts in the IP fraction. No co-immunoprecipitation of FLS2 can be detected in water treated samples. After flg22 treatment, both FLS2 is co-immunoprecipitated. No difference to Col-0 wt could be determined for *Atrem6.4-1* or *proAtREM6.4:YFP:AtREM6.4/Atrem6.4-1*. *Atrem6.4-1 compl.* = *proAtREM6.4:YFP:AtREM6.4/Atrem6.4-1*.

2.3.3.3. The production of ROS after flg22 treatment is reduced in *Atrem6.4-1* plants

Similarly to the group 1 mutant lines, *Atrem6.4-1* was subjected to a ROS burst assay to assess immediate downstream signalling events after receptor dimerization. Col-0 wt, *fls2*, *Atrem6.4-1* as well as both a *proAtREM6.4:AtREM6.4:YFP/Atrem6.4-1* line and a *proAtREM6.4:YFP:AtREM6.4/Atrem6.4-1* were tested.

Atrem6.4-1 shows a significant reduction in ROS production (Fig. 36A-B), which could not be complemented by the C-terminally tagged AtREM6.4 construct in *proAtREM6.4:AtREM6.4:YFP/Atrem6.4-1* (Fig. 36A).

In contrast, the *proAtREM6.4:YFP:AtREM6.4/Atrem6.4-1* line expressing the N-terminally tagged version of AtREM6.4 showed recovery of the wildtype phenotype (Fig. 36B), indicating complementation and therefore biological functionality of this construct. These results indicate that ROS production upon flg22 elicitation is dependent on AtREM6.4.

Results

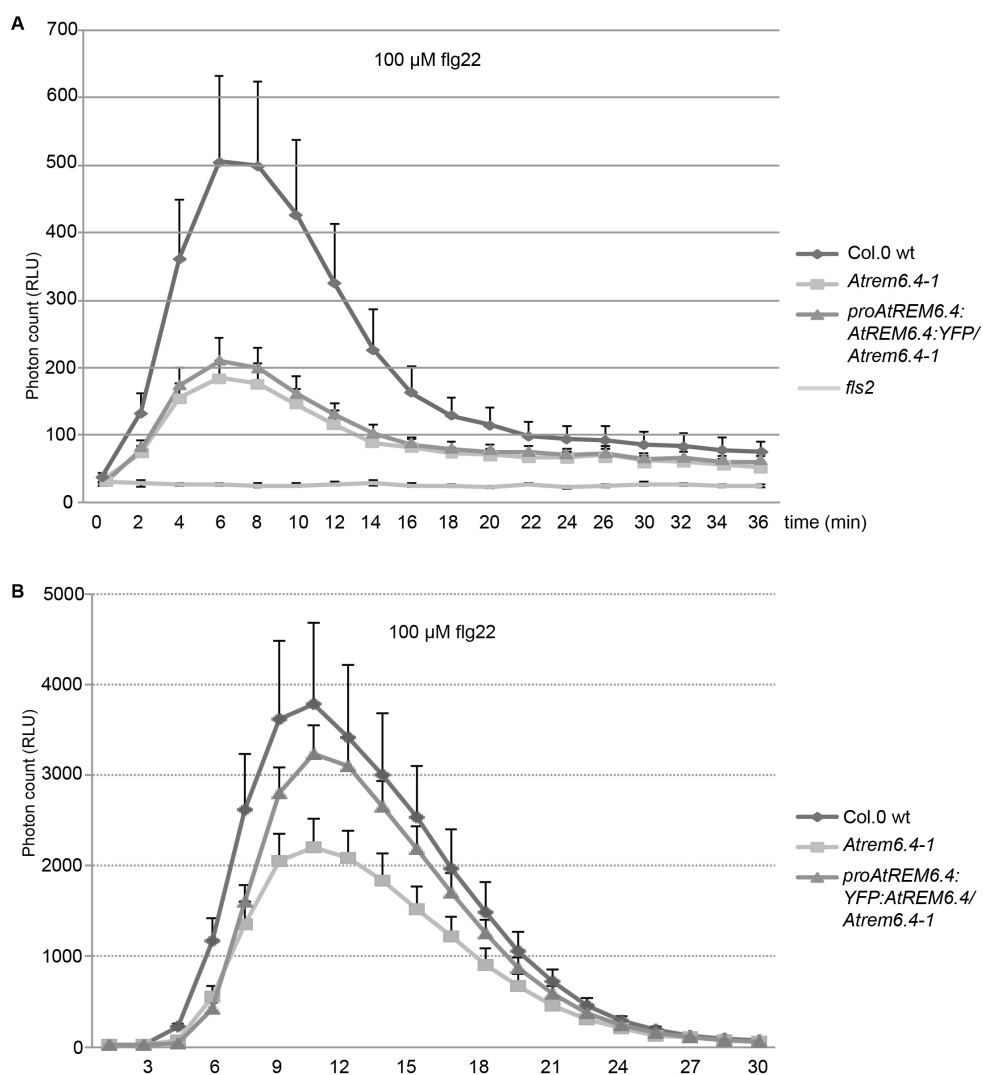


Fig. 36: *Atrem6.4-1* is impaired in ROS burst after flg22 elicitation

Measurements of oxidative burst after flg22 elicitation over a timeframe of 30 min. *Atrem6.4-1* shows a clear decrease in H₂O₂ production (A-B). While the homozygous *proAtREM6.4:AtREM6.4:YFP/Atrem6.4-1* line does not display a difference to the mutant line (A), the segregating *proAtREM6.4:YFP:AtREM6.4/Atrem6.4-1* line shows partial complementation (B). These results indicate functionality of the N-terminally tagged construct. n = 24; error bars indicate standard error between biological replicates,

2.3.3.4. *Atrem6.4-1* displays higher susceptibility towards infection with *P. syringae* pv. *Pto DC3000* compared to Col-0 wt

Experiments carried out with isolated PAMPs indicated a defect of *Atrem6.4-1* knockout mutants in ROS production after elicitation, but not for other investigated early defence responses. To confirm these data, also *Atrem6.4-1* were infected with *P. syringae* to assess a putative phenotype of the plants during a challenge by a true plant pathogen. Here, only the virulent strain *P. syringae* pv. *PtoDC3000* was used.

Results

Atrem6.4-1 reproducibly showed a significant difference compared to the wildtype after infection with *P. syringae*. In all repetitions, the mutant was more susceptible and showed higher growth rates of the bacteria. The phenotype could be described as intermediate to the one of the *fls2* receptor mutant.

Also, two homozygous *proAtREM6.4:YFP:AtREM6.4/Atrem6.4-1* lines showed a phenotype comparable to the wildtype. These results show that the observed differences are caused by the knockout of the *AtREM6.4* gene as well as prove the functionality of the N-terminally tagged fluorophore fusion of the AtREM6.4 protein.

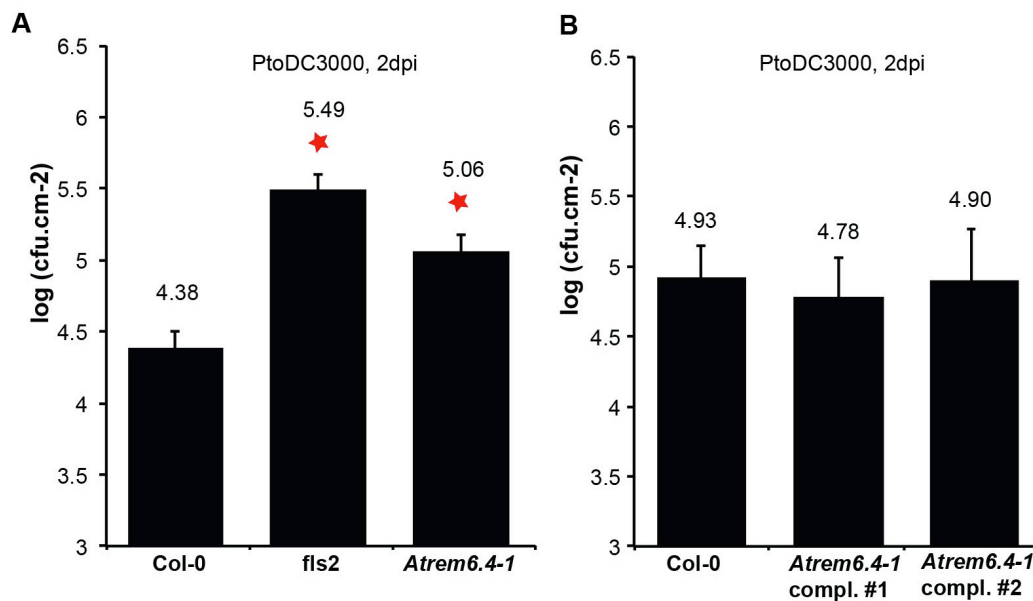


Fig. 37: *Atrem6.4-1* is more susceptible to infection with *P. syringae* pv. *PtoDC3000*

Atrem6.4-1 displays higher bacterial infection after were spay-inoculation with PtoDC3000. The phenotype is intermediate to the one of the *fls2* receptor mutant in comparison to Col-0 wt (A). Two homozygous *proAtREM6.4:YFP:AtREM6.4/Atrem6.4-1* lines (*Atrem6.4-1* compl.) complement the phenotype (B). n = 8, p = 0.05; error bars represent standard error between biological replicates.

2.3.3.5. Investigation of *Atrem6.4-1* for defects in brassinolide signalling

BAK1 is a co-receptor of both BRI1 and different pattern recognition receptors including FLS2 (reviewed in Chinchilla et al., 2009). Therefore it is involved in plant defence as well as in growth and development. As AtREM6.4 is interacting with BAK1 and the *Atrem6.4-1* knockout mutant shows a higher susceptibility towards plant pathogens, it was of major interest, whether an additional alteration in brassinolide perception could be observed. *Atrem6.4-1*, *proAtREM6.4:YFP:AtREM6.4/Atrem6.4-1*

Results

and wildtype plants were subjected to a root growth inhibition assay using 1nM brassinolide. Perception of externally applied brassinolide leads to growth inhibition in young seedlings. Root length was measured in seven days old seedlings. No significant difference between the tested lines were observed comparing non-treated to treated plants (Fig. 38). So far obtained data indicates that AtREM6.4 is involved plant defence specific processes involving BAK1.

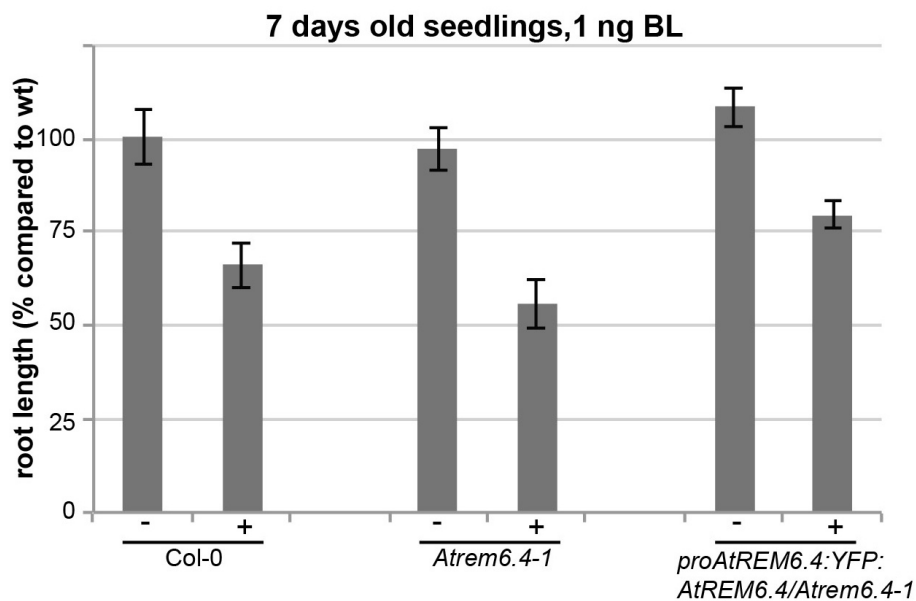


Fig. 38: *Atrem6.4-1* does not display altered reactions to brassinolide treatment

Atrem6.4-1 seedlings do not show alterations in reaction to treatment with brassinolides compared to Col-0 wt. Root length was measured 7 days post germination on brassinolide containing medium. n = 30; error bars represent standard error between biological replicates.

Results

A phenotypic investigation of remorin mutants from group one revealed that *Atrem1.2* and *Atrem1.3* single knockout mutants as well as a *Atrem1.2/Atrem1.3* double mutant do not show a specific phenotype for several early steps of PTI after flg22 and/or elf18 or chitin elicitation. The dimerization of FLS2 and BAK1 as well as the ROS burst and MAPK activation are likely to be independent of group 1 remorin proteins. Nevertheless, a slightly but significantly increased susceptibility towards the virulent form of the plant pathogen *P. syringae* was observed.

While receptor dimerization upon flg22 application seems to be also independent of AtREM6.4, the *Atrem6.4-1* mutant line showed a significantly reduced production of reactive oxygen species upon elicitation. Also, the infection with *P. syringae* pv. *PtoDC3000* resulted in a significantly higher bacterial proliferation on the mutant line compared to the Col-0 wt.

A stable transgenic line expressing AtREM6.4 C-terminally fused to YFP under control of its putative native promoter in the *Atrem6.4-1* mutant background did not display the wildtype phenotype. Yet, a similar construct with AtREM6.4 tagged N-terminally was able to complement both the ROS as well as the infection phenotype.

Referring to the previously shown interaction of AtREM6.4 with BAK1, the involvement of AtREM6.4 in brassinolide signalling was investigated. No difference between the mutant line and Col-0 wildtype was found.

Discussion

1. A global approach to investigate the cell biological aspects of remorin proteins provides insights into their possible biological function

1.1. Remorins are marker proteins for a multitude of coexisting, laterally stable membrane domains

As the critical view on investigation of membrane compartmentalisation by biochemical methods such as DRM extraction has been rising over the recent years, live cell imaging based approaches turned out to be methods of choice to assess membrane domain diversity in living cells. A number of cell biological studies revealed domain localization of PM-associated proteins such as Remorins (Lefebvre et al., 2010; Raffaele et al., 2009), Flotillins (Haney and Long, 2010; Li et al., 2012), the potassium channel KAT1 (Sutter et al., 2006; Reuff et al., 2010), the anion channel SLAC1 HOMOLOG3 (SLAH3) (Demir et al., 2013), the LysM receptor LYK3 (Haney et al., 2011) the NADPH oxidase RBOHD (Lherminier et al., 2009), and the exocyst protein SECA3 (Zhang et al., 2013). So far, all studies in plants were restricted to the analysis of individual proteins or a single protein pair. The co-existence of domains with diverse protein populations was first shown with the LYK3 – FLOT4 pair in *M. truncatula*, which localises to different membrane compartments prior to ligand binding (Haney et al., 2011). In agreement with its proposed function as a scaffold protein, the flotillin then co-localises with the previously mobile domains of the receptor, putatively acting as an enhancer of domain platform assembly and mediating anchoring of membrane domains to the cytoskeleton (Langhorst et al., 2007).

Recently, a broad approach using 49 membrane-localised proteins in yeast has demonstrated the dynamic and diverse membrane domain landscape in single cell organisms (Spira et al., 2012). Also, the tendency of proteins with similar structure and putatively related functions in overlapping domains was shown, indicating that certain types of membrane domains may serve in specific biological processes.

During my doctorate, I demonstrated the co-existence of different membrane compartments in living plant tissue for the first time (Fig. 13, Fig. 14, Table 2). Taking advantage of the diversification of remorin proteins in *A. thaliana*, a number of constructs were created, which can serve as a marker-set for diverse membrane

Discussion

compartments. Quantitative image analysis allowed the specific characterisation of these domains, defining parameters like size, shape and even extent of protein accumulation (Fig. 11). Kymographs showed both that these domains are mostly laterally immobile, but also that they persist at least over a timeframe of 20 min (Fig. 18). Nevertheless, dynamic changes in size and shape as well as domain clearance and constitution of new domains were observed (Fig. 18). It can be concluded that the observed membrane compartments are not equal to the previously described membrane rafts in mammalian cells. The latter are by now considered to be only a few nm large and highly mobile, coming down to single protein complexes surrounded by a specific lipid shell (Anderson and Jacobson, 2002; Edidin et al., 2003; Simons and Gerl, 2010; Spira et al., 2012). In contrast, the domains observed for remorin proteins rather fit to what is commonly described as a “raft cluster”, where single rafts connect via protein-protein interactions and association to the cytoskeleton (Lingwood and Simons, 2010; Tanner et al., 2011). Consequently, it can be hypothesized that also in plants smaller rafts in sizes below the resolution of confocal imaging may exist. Indications for that are provided by the data obtained for AtREM1.2 and AtREM1.3 via FRAP (Fig. 15) and TIRFM (Jarsch et al., 2014). It remains to be determined, whether the non-domain-bound, freely diffusing protein fraction of other remorin proteins is also organized in similar, small, highly mobile domains. If this were the case, those smaller domains would be dynamically recruited to structures providing lateral immobility for the development of microdomain clusters as described for several plant and fungal proteins (reviewed by Tanner 2011). This hypothesis is supported by results from this work showing dynamic exchange of proteins between the membrane domain and the surrounding non-bound protein fraction (Fig. 19).

It can be assumed that the diverse membrane domains labelled by remorin proteins indeed contain a specific set of proteins required for different cell biological processes at the PM. In this case, remorins represent a unique marker-set for the purpose of investigating the events in individual membrane compartments connected to specific cellular functions. Recent results by Demir and colleagues, who showed that the slow anion channel 1 homolog 3 (SLAH3) is recruited to domains labelled by AtREM1.3 by the calcium-dependent protein kinase 21 (CPK21), support this hypothesis (Demir et al., 2013). Even more interestingly, the function of the channel is impaired when being localised to membrane areas apart from the described AtREM1.3 labelled domains. These experiments are a first step into an effective use of remorin proteins as markers for distinct membrane domains *in planta*.

Discussion

Interestingly, the observed membrane domain localisation for AtREM1.2 and AtREM1.3 in *A. thaliana* leaves shown by Demir and colleagues could not be seen in the here presented study. This may be the case due to the different treatment of plants (e.g. cell bombardment with gold-particles in the described case) (Demir et al., 2013).

It can be taken for certain that the diversity in membrane compartmentalisation observed with remorin proteins as markers is only a tiny proportion of the diversity of domains that may actually exist in plant plasma membranes. The true situation is bound to be tremendously more complex!

1.2. Remorin proteins attach to the membrane via two mechanisms

It has been a long lasting debate, whether and if so, how remorin proteins bind to the membrane and if this is taking place via direct interaction with lipids or protein-protein interactions. Recent results from experiments performed mutant version of StREM1.3 in *N. benthamiana* showed that both a deletion as well as heavy mutations in the last 35 amino acids lead to the loss of membrane attachment, indicating that this far C-terminal region of the remorin is essential for membrane localisation (Perraki et al., 2012a). It was hypothesised, that remorin proteins bind to the membrane in a two-step process, establishing a first association via a stretch of amino acids forming an amphipatic-like helix when being exposed to lipid environment. This stretch lies just in front of the last few hydrophobic aminoacids, which consequently insert directly into the lipid bilayer, stabilizing the interaction and binding the protein strongly to the membrane (Perraki et al., 2012a). To confirm these results, truncated versions of several remorin proteins from the different phylogenetic groups have been analysed in this study, demonstrating that indeed the REMCA is the main determinant for membrane localisation of remorin proteins (Fig. 21). The expression of the REMCA N-terminally fused to fluorophores showed also that this part of the protein conducts their localisation to the PM (Fig. 21).

Yet, the model presented by Perraki and colleagues was inconsistent with recent studies on S-acylation (formerly palmitoylation), showing that at least AtREM1.2 and AtREM1.3 bear this post-translational lipid-modification at the very last cysteine residues, suggesting a additional, if not controversial mechanism of the REMCA function (Hemsley et al., 2013). A profound investigation into S-acylation in remorin proteins from our lab demonstrated now, that this mechanism is indeed a common means of remorin membrane association. Probably it is even the main means of the plasma membrane specificity of their localisation, as S-acylation is likely to be conferred after initial membrane association by a plasma membrane resident PROTEIN ACYL TRANSFERASE (PAT) (Konrad et al., 2014). This reversible modification may

also provide the necessary dynamic needed for signalling at the plasma membrane but also for a putative role in the nucleus (Marin et al., 2012).

A prominent example for S-acylated proteins involved in signalling at the plasma membrane are small GTPases of the Rho of plants (ROP) family. Rho6, which plays a role in abscisic acid signalling, is rapidly S-acylated upon stimulation and is enriched in DRM fractions upon activation (Sorek et al., 2010).

Still, the observation has been made that the REMCA does not entirely bind to the PM when being expressed in a background lacking the respective full-length protein (Fig. 21). This indicates that an initial contact to the PM via protein-protein interactions may be necessary for the S-acylation event performed by membrane resident enzymes (Bharadwaj and Bizzozero, 1995). This hypothesis has been strengthened by the demonstration that an AtREM6.4 REMCA construct, which had lost membrane association due to a C-terminal tag, could be fully relocalised to the PM and even into domains by coexpression with the full length protein (Fig. 21). Additionally, an AtREM6.4 construct lacking the REMCA could be observed to associate with an interacting receptor kinase in membrane domains in the BiFC system despite the deletion of the membrane attachment region (Fig. 24). So far obtained data indicate that remorin proteins connect to the PM both via S-acylation and protein-protein interactions, explaining that their binding strength in washing experiments was close to transmembrane proteins (Perraki et al., 2012a). Yet, the membrane attachment mechanism is not sufficient to confer membrane domain specificity, as the REMCA alone does not localize to defined membrane compartments (Konrad et al., 2014).

1.3. The N-terminal region of the protein plays a role in formation of membrane domains and relocalisation

While the terminal amino acids of remorin proteins are indispensable for tight membrane attachment via S-acylation, it is quite obvious that such a specific modification cannot be the causative principle for localisation into distinguishable domains. Here, truncation constructs of SYMREM1 and AtREM6.4 have shed light on the role of the different protein regions. While the REMCAs of SYMREM1 or AtREM6.4 does not localise to visible domains, also the C-terminal region alone does not label any membrane compartments above confocal resolution. It seems that the N-terminal region is required for domain formation in this case (Fig. 21). Also, relocalisation into larger compartments as observed for full length AtREM6.4 seems to be dependent on the presence of the N-terminal region (Christina Weiß, 2012). This is in agreement with results for AtREM3.1, one of the two remorin proteins which do not contain a protein

Discussion

region comparable to the N-termini of the other family members, and which does also not form visible domains. These results stand in contrast to the domain formation observed for the other remorin protein lacking a N-terminal region, AtREM3.2. Still, considering that AtREM3.2 labelled domains do not co-localise with any other domain containing remorin proteins, it may well be that AtREM3.2 forms those domains interacting with a completely unrelated membrane domain protein via its coiled-coil.

It has recently been demonstrated that the N-terminal region of AtREM1.3 plays a role in regulating protein-protein interactions (Marin et al., 2012). The hypothesis that it functions as a regulatory domain is strengthened by the findings that it includes many post-translational modifications and molecular recognition features (MoRFs) (Marin and Ott, 2012; Marin et al., 2012). Data obtained in the here presented study is not sufficient to show which of the two following hypothesis may be correct:

1. The N-terminal region is essential for correct localisation to membrane domains via protein-protein interactions.
2. The N-terminal region also regulates domain constitution and clustering in a stimulus-dependent manner. Its intrinsic disorder and its flexible nature can confer dynamism to protein-protein interactions and therefore to domain formation itself.

1.4. Remorin proteins – phosphorylation dependent scaffold proteins for RLKs

The importance of phosphorylation for remorin signalling has been postulated for long. It has been described that remorins are differentially phosphorylated upon external stimuli in potato (Farmer et al., 1989; Reymond et al., 1996) and *A. thaliana* (Benschop et al., 2007; Widjaja et al., 2009). Furthermore, it was shown in *L. japonicus* that SYMREM1 can be phosphorylated *in vitro* by the kinases it interacts with *in vitro* (Tóth et al., 2012). Yet, it has not been experimentally proven that phosphorylation of certain residues has a biological function, until recent works showed that phosphorylation of S66 in the otherwise intrinsically disordered N-terminal region of AtREM1.3 decreases the interaction with importin α proteins (Marin et al., 2012).

Additionally to those sites mapped after external stimulation, a great number of phosphorylated residues have been found in the control (non-stimulated) condition, indicating constitutive phosphorylation of large stretches in the N-terminal region of remorin proteins (reviewed in Marin and Ott, 2012).

Discussion

In independent studies, AtREM1.2 and AtREM1.3 have been demonstrated to be phosphorylated upon flg22 application (Benschop et al., 2007) as well as to be recruited to DRM fractions, similar to the flg22 receptor FLS2 itself (Keinath et al., 2010). In another study, flg22 application has been shown to induce decreased mobility of the FLS2 receptor, suggesting a change in submembraneous localisation and protein-protein or protein-lipid interactions upon receptor activation (Ali et al., 2007, Ali and Reddy, 2008). This behaviour is reminiscent of observations made for the already introduced flotillin proteins and the putative Nod factor receptor LYK3 in *M. truncatula*. Both proteins localise in mobile punctate structures in the PM when being co-expressed as fluorophore tagged constructs in *M. truncatula* roots. Interestingly, the proteins do not co-localise until stimulation of the root with NF or *Sinorhizobium meliloti*. While the full-length fusion proteins then label co-localising immobile domains, FLOT4 mislocalisation is observed in a LYK3 kinase-dead mutant line. These results indicate that the observed relocation process is dependent on phosphorylation events downstream of LYK3 and has been interpreted to serve regulatory functions during signalling (Haney et al., 2011). Nevertheless, experiments, which show whether a tagged version of the kinase dead protein would still co-localise with FLOT4, or whether FLOT4 is directly phosphorylated by LYK3 have not been performed.

In this study, direct phosphorylation of AtREM6.4 but not AtREM1.3 by the BAK1 kinase domain has been demonstrated *in vitro* (Fig. 25). Also, both proteins interact (directly or indirectly) *in planta*, as shown by BiFC and Co-IP experiments (Fig. 24). Interestingly, the BiFC signal for the AtREM6.4 – BAK1 protein complex was concentrated in membrane microdomains (Fig. 24). Moreover, a decrease in domain formation in BiFC has been observed, when using a phosphoablative mutant construct of AtREM6.4 (Fig. 26). Consistently, the reverse effect was seen when performing the same experiment with a phosphomimic mutant version of AtREM6.4, where more domains were observed (Fig. 26).

It can be hypothesized that phosphorylation at certain residues of remorin proteins regulates interaction with other proteins. The phosphorylation at T215 of AtREM6.4 may be a positive regulator of the complex-formation with BAK1. Data obtained from phosphoproteomic analyses before and after flg22 elicitation suggest this phosphorylation is constitutive. It remains to be analysed, which additional residues are phosphorylated by BAK1 after stimulation. Current working models are that these modifications result in conformational changes either providing further interactions sites to recruit downstream signalling components or stabilizing existing complexes and the subcellular localisation in microdomains.

Discussion

Interestingly, the above-mentioned works from Demir and colleagues described group 1 remorins in distinct, completely immobile domains that also did not recover after FRAP treatment in *N. benthamiana* (Demir et al., 2013). In this study, a localisation of AtREM1.2 and AtREM1.3 in small, highly mobile domains below confocal resolution was observed (Fig. 15). Domain formation was shown to occur occasionally in a putatively tissue or stimulus-dependent manner in the hypocotyl of six days old seedlings. Also, for many other remorin protein investigated for domain persistence, domains appearance, changes in size and form as well as domain clearance were demonstrated (Fig. 18). Additionally, dynamic exchange of proteins between domains and the surrounding membrane was observed in FRAP experiments, as well as additional relocalisation for AtREM6.4 (Fig. 22). These findings fortify the idea, that labelling of membrane microdomains by remorin proteins is stimulus-dependent. In cases where these membrane compartments are always visible, these stimuli may be constitutively present. In the case of group 1, the biological processes requiring domain formations seem to be more dynamic, and the constitution of membrane compartments is restricted to specific tissues under certain conditions.

Dynamic rearrangements in the plasma membrane under certain biological conditions have not only be shown for the already mentioned case of FLOT4 and LYK3 in *M. truncatula* which label a shared, laterally immobile membrane compartment after NF treatment (Haney et al., 2011). Also PIN3, one of the previously mentioned auxin efflux carriers with a role in tropism was observed to relocalised to a different subcellular membrane domain in response to changes in gravity (Friml et al., 2002b). Recent studies demonstrated the alteration of the localisation of the RESPIRATORY BURST OXIDASE HOMOLOG D (RBOHD) in membrane domains upon different treatments (Hao et al., 2014). Being initially distributed in small, dynamic spots with heterogeneous diffusion coefficients addition of a NADPH inhibitor caused a significant reduction in mobility coinciding with reduced oligomerisation state. By contrast, an activation of RBOHD by Ca^{2+} addition or phosphorylation increased both the diffusion coefficient as well as the dimerization state, an observation which could be repeated by treatment with salt. Here, RBOHD also visibly accumulated in larger membrane compartments prior to endocytosis (Hao et al., 2014).

As discussed before, the question of the influence of remorin proteins on domain constitution and/or maintenance has not been solved in this study. The direct role of several lipid species (mainly sterols) in membrane compartmentalisation and especially localisation of certain proteins in their specific submembranous location has been demonstrated impressively with mutant strains both in yeast (Grossmann et al., 2006;

Bagnat and Simons 2002a, 2002b) and in plants (Diener et al., 1000; Willemsen et al., 2003; Souter et al., 2002; Sutter et al., 2006). By contrast, scientific evidence of the determining role of the presence of one specific protein in the formation of a specific domain is still missing. The best means to addressing the function of a protein in membrane compartmentalisation so far is the investigation of lipid organization by Laurdan (6-Dodecanoyl-2-Dimethylaminonaphthalene) – staining. Laurdan integrates specifically in membrane areas of increased order, providing the possibility to investigate differences in lipid order between samples by 2-photon microscopy (Bagatolli and Gratton, 2000; Gaus et al., 2003). Laurdan staining has been used successfully in a recent study to visually investigate lipid packing and dynamics in the oligodendroglial plasma membrane (Fitzner et al., 2006). Here, it was shown that neurons induce a dramatic lipid condensation at the oligodendroglial membrane, forming a domain which is enriched both in cholesterol as well as in galactosylceramide. This change in lipid organisation was not observed in mice mutants lacking the myelin basic protein, indicating a role of the latter in this type of plasma membrane rearrangement. Yet, the function may be an indirect one, similar to the PINs which mediate the establishment of an auxin gradient and therefore cell polarity and the formation of the apical and basolateral domains (Went et al., 1974; Friml et al., 2003).

It may be of interest to test the influence of remorin proteins on membrane domain formation in a similar manner, using both mutant lines as well as overexpression in *N. benthamiana*.

2. A phenotypical assessment of remorin mutants

2.1. The genetic approach to investigate the biological role of group one remorin proteins

AtREM1.2 and AtREM1.3 had been chosen as priority candidates for closer phenotypic investigations due to their rich history in literature and the clear links to plant defence (reviewed in Jarsch and Ott, 2010) compared to other members of the protein family.

Most highly expressed of all remorins, AtREM1.2 and AtREM1.3 are ubiquitously present throughout the whole plant life in all tissues. Numerous broadly based analyses of group 1 remorin proteins after elicitor or pathogen treatment like transcriptomics (Navarro et al., 2004, Journot-Catalino et al., 2006, Coaker et al., 2004), phosphoproteomics (Benschop et al., 2007) and proteomics on DRM fractions (Keinath et al., 2010; Kierszniowska et al., 2009) associate them with early steps in PTI. Additionally, the interaction of AtREM1.2 with the RIN4 complex (Liu et al., 2009) and

Discussion

the AvrRPM1 dependent differential phosphorylation indicate a putative involvement in ETI (Widjaja et al., 2009).

In this study, the first of the two possibilities was assessed. The chosen mutant alleles were tested for the establishment of a receptor-hetero-complex after ligand binding (Fig. 29), the production of reactive oxygen species at the leaf surface (Fig. 30), and the activation of the MAPK-signalling cascade (Fig. 31). Yet, neither the single knock-out mutants of AtREM1.2 and AtREM1.3, nor a double mutant of both proteins showed a significant difference compared to the wildtype in one of the investigated processes in early plant defence.

Nevertheless, a small but significant increase in susceptibility upon infection with *P. syringae* pv. *PtoDC3000* could be observed with the AtREM1.2/AtREM1.3 double mutant (Fig. 33).

Both AtREM1.1 and AtREM1.4 are significantly lower expressed than AtREM1.2 and AtREM1.3. Also, the Western Blot analyses with a group 1 specific antibody did not show a visible upregulation of both proteins in the mutant backgrounds. Therefore the increase in significance for the observed phenotypes using a triple or even quadruple mutant is expected to be rather low compared to the existing double mutant line.

In fact, the obtained results point towards a role of AtREM1.2 and AtREM1.3 in a so far not investigated component of plant defence. This could be a directly connected process like callose deposition or defence gene regulation. The severe defect in callose deposition of *ricky-1* (Hofer, LMU, 2012), the mutant line of the RLK interacting with AtREM1.2 in yeast (Table 3), speaks for the former. The mutant lines created in this study are currently investigated for phenotypes in this aspect of PTI. Callose deposition is no longer defined as an early process in plant defence responses. Its regulation requires both changes in ion fluxes across the membrane directly after elicitation as well as transcriptional regulation and changes in hormone status (Gómez-Gómez et al., 1999; Brown et al., 1998; Luna et al., 2011).

With increasing refinement of forward and reverse genetics, recent publications have shown that PTI indeed employs specific regulators that play a role in distinct processes of the different responses. One example is the already introduced BIK1 protein, which positively regulates various immune responses following BAK1 activation, but does not seem to be involved in MAPK phosphorylation (Feng et al., 2012b). Another example is the lectin receptor kinase VI.2. This RLK is transcriptionally up-regulated upon pathogen attack or PAMP treatment (Singh et al., 2012). Mutants are impaired in

Discussion

MAPK signalling and subsequent defence gene upregulation, but not in BIK1 phosphorylation or ROS production (Singh et al., 2012).

A role for remorin proteins further downstream in signalling pathways beneath the membrane was initially proposed by Alliotte and colleagues. They characterised AtREM1.3 as an unspecific DNA-binding protein (ADbp) with biochemical similarities to histone H1 in humans and pea (Alliotte et al., 1989). AtREM1.3 transcript was significantly increased in an auxin-dependent manner. Interestingly, both AtREM1.2 and AtREM1.3 were found as interactors of the cytokinin-dependent *Arabidopsis* response regulator 4 (ARR4) several years later in a yeast-two-hybrid screen (Yamada et al., 1998). This cytoplasmic and nuclear protein is expressed in all aerial parts of the plant upon perception of white or red light (Sweere et al., 2001). Interestingly, the ARR4 induction can be reversed by pulses of far-red light and is reduced in mutants of the red/far-red reversible photoreceptor phytochrome B (phyB) (Sweere et al., 2001). Phytochromes are synthesized in the cytoplasm as a red light photoreceptor (Pr) in dark periods. Upon absorption of light, a conversion to the active, far-red light absorbing form (Pfr) takes place. Subsequently, the protein trans-locates to the nucleus (Neff and Chory, 1998; Nagy and Schafer, 2000). Phytochrome B specifically is involved in seed germination and seedling de-etiolation under continuous red light, as well as in the shade avoidance response. ARR4 was shown to physically interact with phyB specifically and is believed to stabilize the active form in the nucleus (Sweere et al., 2001). Also cyanobacterial phytochrome has been demonstrated to exhibit light-regulated histidine kinase activity (Yeh et al., 1997), only weak serine-threonine kinase activity could be associated with plant phytochromes (Schneider-Poetsch, 1992; Yeh et al., 1997). The link to remorin proteins cannot only be drawn via the interaction with ARR4, but also via the association of AtREM1.3 with importin proteins. Coexpression of the remorin with Importin α 3 resulted in co-localisation in the nucleus. Furthermore, the physical interaction of both proteins is regulated by the differential phosphorylation of the N-terminal region of AtREM1.3 (Marin et al., 2012).

These data may suggest that the role of group 1 remorin proteins in plant microbe interactions is rather an indirect one. If the proteins were involved in regulation of growth and development of the plant, mutants of AtREM1.2 and AtREM1.3 may be deregulated in reorganization processes of the plant development program after pathogen attack. Also, the phosphorylation of AtREM1.2 in AvrRPM1 overexpression lines does not necessarily imply an active role in ETI. The hypothesis, that remorin proteins are indeed effector targets has been raised before (Chisholm et al., 2005) and is fed by the idea, that the large intrinsically disordered stretches and the low conservation

between family members in the N-terminal region are both a consequence of effector recognition as well as a way to evade it (Tòth et al., 2012; reviewed in Marin and Ott, 2012). The crosstalk between hormonal pathways and plant immunity has been extensively researched and is an inevitable consequence of plants lacking specialized cells to carry out immune functions (reviewed in Spoel and Dong, 2012). Therefore, reprogramming of growth and development processes aim to prioritise defence pathways for the time of an attack. On the other hand, pathogens employ hormone mimicry as a virulence strategy. The most prominent example is the already mentioned bacterial phytotoxin coronatin (Bender et al., 1999, Melotto et al., 2006). It structurally resembles jasmonic acid (JA) (Staswick et al. 2008). Additionally to mimicking JA signalling and suppressing salicylic acid (SA)- mediated defence responses (Koornneef and Pieterse, 2008), coronatin induces transcriptional and physiological changes related to auxin (Uppalapati et al., 2005). A similar strategy is pursued by *P. syringae* when injecting the effector AvrRpt2, which promotes auxin biosynthesis. Interestingly, exogenous application of auxin increased plant susceptibility, while auxin biosynthesis mutants displayed higher resistance to *P. syringae* (Chen et al., 2007; Navarro et al., 2006; Wang et al., 2007), indicating a negative role of auxin in plant immunity.

2.2. AtREM6.4 is involved in flg22 induced ROS production but not in other BAK1-dependent processes as BR signalling

Although AtREM6.4 is differentially phosphorylated upon elicitor treatment (Benschop et al., 2007), this protein has never been investigated in more detail and does not have a history in scientific literature.

In this study, AtREM6.4 has drawn attention due to its remarkable cell biological characteristics. Apart from the localisation in laterally immobile microdomains, a relocalisation into enlarged membrane compartments as well as occasional filament formation was observed (Fig. 9, Fig. 18, Fig. 22).

The putative phosphorylation-dependent interaction with BAK1 *in vivo* in microdomains in the plasma membrane (Fig. 26) led to the conclusion, that AtREM6.4 is involved in BAK1-dependent signalling processes *in planta*. Here the best-studied examples are basal plant defence triggered by a selection of microbial elicitors as well as brassinolide signalling. While no defect of the respective remorin mutant line in oligomerisation of FLS2 and BAK1 after flg22 treatment was observed (Fig. 35), a decrease in the following ROS burst was shown (Fig. 36). Consequently, *Atrem6.4-1* mutant plants display higher sensitivity to infection with the virulent plant pathogen *P.*

Discussion

syringae Pto DC3000 (Fig. 37). Interestingly, an altered reaction of the mutant to external BL treatment was not detectable (Fig. 38).

The current working model places AtREM6.4 as a constitutive interactor of BAK1 in the preformed receptor-complex. The existence of such a receptor pre-complex has been postulated after recent studies had shown, that trans-phosphorylation of FLS2 by BAK1 can already be detected after a timeframe as short as 5 s (Schulze et al., 2010). As even faster measurements were not possible due to experimental limitations, it can be hypothesized, that the first signalling processes happen directly after ligand binding. The prerequisite for that, of course, is a preformed protein complex at the plasma membrane (Schulze et al., 2010, reviewed Monaghan and Zipfel, 2012)

Additional evidence supporting the pre-existence of receptor-oligomers has been shown in BR signalling. It was recently demonstrated, that, while BR application significantly increases receptor-dimer-formation, a good proportion of BRI1 and BAK1 molecules heterooligomerise without the presence of the ligand. It was proposed, that preassembly of the proteins is essential for signalling (Bucherl et al., 2013).

Also, while it was formerly believed that BAK1 is not involved in direct recognition of brassinolide or flg22, crystal structures of the respective protein-peptide trimers have revealed at least physical contact between the ligand and the extracellular LRR domains of the so called co-receptor (Sun et al., 2013a, 2013b). Finally, RBOHD has just recently been found to co-immunoprecipitate with the members of the hypothesized pre-complex prior to elicitation (Kadota et al., 2014). There is no indication so far for involvement of RBOHD in brassinolide signalling.

It remains still to be investigated, to which extent additional, BAK1-involving plant defence processes are affected in the *Atrem6.4-1* mutant line. Additionally, a complementation assay with the introduced phosphorylation-site mutant constructs (Fig. 26) will be performed to verify the importance of AtREM6.4-BAK1 interaction for PTI.

Here we propose, that AtREM6.4 interacts in a preassembled receptor-complex exclusively with BAK1 molecules that have formed heterooligomers with FLS2 and putatively other BAK1 dependent PAMP-receptors. Upon stimulation, AtREM6.4 may be further phosphorylated at additional residues and mediates/stabilizes interactions with downstream targets like RBOHD. The hypothesis would state also, that such preassembled receptor complexes accumulate in specific membrane environments, forming large, laterally stable microdomains, which are microscopically visible when using fluorescently labelled proteins. The latter may happen constitutively, or in a stimulus-dependent manner.

Discussion

As remorin proteins seemingly do not stabilize the receptor-complex itself, their function is most likely either:

1. The promotion of membrane compartmentalisation and the formation of raft clusters via protein-protein-interactions, or
2. the provision of interaction hubs for downstream signalling components, or
3. a dual role combining both functions.

In either way, the long proposed role of remorin proteins acting as scaffold proteins in signalling at the plant plasma membrane would still be consistent with current data.

While the diverse patterns of remorin proteins may be of great value for future microscopical analysis of membrane compartmentalisation, the evaluation of the co-localisation data will also be of help for further phenotyping investigations of the different family members. Most likely, those proteins sharing their positions in the same domains in the plasma membrane are involved in closely related biological processes.

Abbreviations

3-AT	3-Aminotriazol
35S	Promoter of the 35S RNA of the Cauliflower mosaic virus
α -	Anti- (for antibodies)
<i>A. thaliana</i>	<i>Arabidopsis thaliana</i>
ABRC	<i>Arabidopsis</i> Biological Resource Center
ACA8	<i>ARABIDOPSIS</i> AUTOINHIBITED Ca ²⁺ -ATPase
AEBSF	4-(2-Aminoethyl) benzenesulfonyl fluoride hydrochloride
APS	Ammoniumperoxodisulphate
ARR4	<i>ARABIDOPSIS</i> RESPONSE REGULATOR 4
ASK	<i>ARABIDOPSIS</i> SOLUBLE KINASE
AUX1	AUXIN TRANSPORTER PROTEIN 1
Avr	Avirulence factor
AtREM	<i>ARABIDOPSIS THALIANA</i> REMORIN
BAK1	BR11 ASSOCIATED KINASE 1
BFA	Brefeldin A
BiFC	Bimolecular fluorescence complementation
BIK1	BOTRYTIS-INDUCED KINASE 1
BKI1	BR11 INHIBITOR KINASE 1
BL	Brassinolide
BR	Brassinosteroide
BR11	BRASSINOLIDE INSENSITIVE 1
BSA	Bovine serum albumin
BsaI	<i>Bacillus stearothermophilus</i> 20241 I
C-terminus	Carboxy-terminus
Ca ²⁺	Calcium
CaMV	Cauliflower mosaic virus
CARD	Caspase activation and recruitment domain
CASP	CASPARIAN STRIP PROTEIN
CD48/55	CLUSTER OF DIFFERENTIATION 48/55
cDNA	Coding DNA
cds	Coding sequence
CERK1	CHITIN ELICITOR RECEPTOR KINASE 1

Abbreviations

CES	Combinatorial enhancer solution
CFP	Cyan fluorescent protein
CLSM	Confocal laser scanning microscopy
Co-IP	Co-immunoprecipitation
<i>Cor⁻</i>	Coronatin deficient mutant
CPK21	CALCIUM DEPENDENT PROTEIN KINASE 21
DEX	Dexamethasone
dm	Double mutant
DNA	Deoxyribonucleic acid
dNTP	di-nucleotide triphosphate
DRM	Detergent resistant membrane
DTT	dithiothreitol
E-64	(1S,2S)-2-(((S)-1-((4-guanidinobutyl)amino)-4-methyl-1-oxopentan-2-yl)carbonyl)cyclopropanecarboxylic acid
EDTA	Ethylene diamide tetraacetic acid
EFR	EF-Tu receptor
EF-Tu	Elongation factor thermo unstable
EGTA	Ethylene glycol tetraacetic acid
EIX1/2	Ethylene-inducing xylanase receptor 1/2
elf18	EF-Tu-like factor 18
<i>erg6</i>	Ergosterol deficient mutant 6
ETI	Effector triggered immunity
EtOH	Ethanol
ETS	Effector triggered susceptibility
flg22	flagellin 22
FLOT	FLOTILLIN
FLS2	FLAGELLIN SENSITIVE 2
FRAP	Fluorescence recovery after photo-bleaching
GAL4	Transcription factor 4 for the galactosidase operon
GFP	Green fluorescent protein
GPI	Glycosyl-Phosphatidyl-Inositol
GSL5	Glycan synthase-like 5
GW	Gateway
H	Histidine
HEPES	4-(2-hydroxyethyl)-1-piperazineethanesulfonic acid
HF	High fidelity
His	Histidine

Abbreviations

HRP	Horse radish peroxidase
HUP1	HEXOSE UPTAKE 1
IP	Immunoprecipitation
IRAK	INTERLEUCIN RECEPTOR-ASSOCIATED KINASE
K ⁺	Potassium
KAT1	<i>ARABIDOPSIS THALIANA</i> K ⁺ CHANNEL
kb	Kilobase
KD	Kinase domain
KDSC	Kinase domain soluble construct
K ₂ HPO ₄	Potassium phosphate
L	Leucine
LB	Lysogeny broth
<i>lcb1-100</i>	Long chain base biosynthesis protein1-100 deficient mutant
LioAc	Lithium acetate
LP	Lipopolysaccharides
LRR	Leucine-Rich-Repeat
LWHA	Leucine-Tryptophan-Histidine-Adenine
LYM1/2	LYSINE MOTIF PROTEIN 1/2
LYK3	LYSINE MOTIF KINASE 3
LYSM	Lysine motif
M	Molar
mg	Milligramm
ml	Millilitre
µm	Micrometre
mM	Millimolar
<i>M. truncatula</i>	<i>Medicago truncatula</i>
MAMP	Microbe associated molecular pattern
MAP4	MICROTUBULE ASSOCIATED PROTEIN 4
MAPK	MITOGEN ACTIVATED PROTEIN KINASE
MES	2-(N-morpholino)ethanesulfonic acid
MgCl ₂	Magnesium chloride
MgSO ₄	Magesium sulphate
min	Minute(s)
MLO	MILDEW RESISTANCE LOCUS O
MoRF	Molecular recognition factor
MQ	Milli-Q

Abbreviations

<i>M. truncatula</i>	<i>Medicago truncatula</i>
MtSYMREM1	MEDICAGO TRUNCATULA SYMBIOTIC REMORIN 1
MS	Murashige&Skoog
<i>N. benthamiana</i>	<i>Nicotiana benthamiana</i>
N-terminus	Amino-terminus
NaCl	Sodium chloride
NaF	Sodium fluoride
Na ₂ MoO ₄	Sodium molybdate
Na ₃ VO ₄	Sodium orthovanadate
ng	Nanogramm
NBS-LRR	Nucleotide-binding-site leucine-rich-repeat
NF	Nodulation factor
NFR1/5	NOD FACTOR RECEPTOR 1/5
nM	Nanomolar
nm	Nanometre
Nod	Nodulation
NOD1/2	NUCLEOTIDE BINDING OLOGOMERIZATION DOMAIN 1/2
OD	Optical density
P19	Tomato bush stunt virus protein with 19kDa
PAGE	Polyacrylamide gel electrophoresis
PAMP	Pathogen associated molecular pattern
PAT	PROTEIN FATTY ACYLTRANSFERASE
PBL1/2	PBS1-LIKE 1/2
PBS1	AvrPBHB SUSCEPTIBLE 1
PCR	Polymerase chain reaction
PEG	Polyethylene glycol
PEN1	PENETRATION 1
Pfr	Photoreceptor for far-red light
PGN	Peptidoglycan
PIN	PINFORMED
PIP1	PLASMA MEMBRANE INTRINSIC PROTEIN 1
PK	Protein kinase
PM	Plasma membrane
PMR4	POWDERY MILDEW RESISTANT 4
PMSF	Phenylmethanesulfonylfluoride
Pr	Photoreceptor for red light

Abbreviations

<i>proAtREM</i>	Promotor sequence of an <i>Arabidopsis thaliana</i> remorin
PUB12/13	PLANT U-BOX 12/13
PTI	PAMP-triggered immunity
<i>PtoDC3000</i>	<i>Pathovar tomato DC3000</i>
PVC	Polyvinyl chloride
PVX	Potato virus X
q-PCR	Quantitative PCR
R ²	Overlap coefficient
R gene	Resistance gene
RBOHD	RESPIRATORY BURST OXIDASE HOMOLOG D
RD	Arginine-glutamate
rd	random
REMCA	Remorin C-terminal anchor
RIN4	RPM1 INTERACTING PROTEIN 4
RLCK	Receptor-like cytosolic kinase
RLK	Receptor-like kinase
RLP	Receptor-like protein
ROI	Region of interest
ROR2	REQUIRED FOR MILDEW RESISTANCE LOCUS O-SPECIFIED RESISTANCE
ROS	Reactive oxygen species
rpm	Rounds per minute
RPM1	RESISTANCE TO <i>PSEUDOMONAS MACULICOLA</i> 1
RPS2/4/5	RESISTANCE TO <i>PSEUDOMONAS SYRINGAE</i> 2/4/5
Rr	Pearson co-localisation coefficient
RT	Room temperature
s	Second(s)
SD medium	Selective dropout medium
SDS	Sodium dodecyl-sulphate
SERK	SOMATIC EMBRYOGENESIS RECEPTOR KINASE
SGI	Seedling growth inhibition
SLAH3	SLAC1 HOMOLOG 3
<i>smt1</i>	Sterolmethyltransferase deficient mutant 1
SNARE	SOLUBLE N-ETHYLMALEIMIDE-SENSITIVE

Abbreviations

	FACTOR ATTACHMENT RECEPTOR
ssDNA	Single stranded DNA
std. err.	Standard error
StREM1.3	<i>SOLANUM TUBEROSUM</i> REMORIN 1.3
SYMREM1	SYMBIOTIC REMORIN 1
SYMRK	SYMBIOTIC RECEPTOR KINASE
SYPI21/122	SYNTAXIN RELATED PROTEIN 121/122
T	Threonine
T-DNA	Transposable DNA
TAQ – Polymerase	<i>Thermus aquaticus</i> polymerase
TBP1	TRIPLE GENE BLOCK PROTEIN 1
TBS	Tris buffered saline
TBS-T	Tris buffered saline with 0.05% TWEEN 20
TCA	Trichloroacetic acid
TE	Tris-EDTA buffer
TEMED	Tetramethylethylenediamine
TIR	Toll and interleukin receptor motif
TIRFM	Total internal reflection fluorescence microscopy
TLR5	TOLL-LIKE RECEPTOR 5
TWEEN 20	Polyoxyethylene (20) sorbitan monolaurate
V	Volt
W	Tryptophan
WCIF	Wright Cell Imaging Facility
WT	wildtype
XA21	XANTHOMONAS RESISTANCE 1
XB15/24	XA21 BINDING PROTEIN 15/21
Y2H	Yeast-2-hybrid
YFP	Yellow fluorescent protein
YNB	Yeast nitrogen base
YPAD	Yeast extract peptone adenine dextrose

Acknowledgements

As, I guess, any doctorate, also my time in the lab featured all the facets of science and life. Spending, what in the end sums up to quite a big part of your life in a few rooms, together with a few people, concentrating hard on the tiniest part of a small one of the many big questions plaguing humanity - this is bound to let anything expand: problems seem unbearable, answers close to redemption, solutions either within one's grab or maddening far away. Looking back, everything appears so much easier, and I would like to thank the people who helped me reach that stage:

First of all, I would like to thank my supervisor, Dr. Thomas Ott, for giving me the opportunity to conduct this study in his lab, for his constant support and encouragement. During the 5 years I worked on this very interesting project, I always had the feeling, you trusted my opinion concerning important decisions and we developed the project together based on respect for each other's needs. Thank you very much for that, Thomas! I suppose, it is difficult for a group leader, to direct an employee who asks both for guidance as well as for a good portion of freedom, and I hope the results of my work will show your way to handle it was right.

Next, I would like to thank the other members of my thesis advisory committee, Prof. Dr. Martin Parniske, Prof. Dr. Ralf Hückelhoven, Prof. Dr. Thomas Lahaye and Dr. Ruth Eichmann. It is a compliment to a student, if such a team of experts both spends willingly so much time on the evaluation of the project as well as takes its job to consult on problems so seriously! Thank you for being both unmercifully critical, but still always letting shine through that you believed in my work!

I had the pleasure to work with a number of great colleagues, who shared not only my "fate" but also many a scientific thought. After so much time together, both at the bench, in the office, on conferences, on retreats, in seminars, meetings and so on, it feels good if you can consider the people you shared so many both positive and negative moments with, as friends. Thank you, Katalin, Tom, Mac, Claudia, Tina, Martina, Basti and Janett for all these so important discussions not only about our projects, but also about any other issue arising in the life of a PHD student.

Many thanks also to the students I had the pleasure to supervise: Elle Dittmer, who both worked as a student helper on the mutant library as well as did her Bachelor thesis on group 3 remorins with Macarena and me. Alex Buschle, who not only surprised me

Acknowledgements

during his Forschungspraktikum with his widespread interest and profound scientific intellect, but also left me stunned by his extraordinary documentation and organisational work. Corinna Hofer, who, with great enthusiasm and ambition, took up a side-project of mine as a Master student, and not only made it her own in no time, but hopefully will be rewarded soon for her efforts by publishing her results on RICKY. “Little Tom” Seehofer, who started in our group as a student helper, assisting me on the genotyping for the AtREM1.2/AtREM1.3 double mutant – I am still sad that you did not continue your studies with us! Thank you also, Chrissy Weiß, for your valuable work on AtREM6.4 during your Forschungspraktikum. Being the only student working directly on my project, the faultlessness of your work was a relief!

Thank you very much to Karl-Heinz and Jessica, not only for excellent technical assistance, but also for the “ok, give it to me” in moments, when the amount of work is just too much for that day.

Many thanks also to Thomas, Katalin, Martina and Macarena for proofreading parts or the entirety of this thesis.

During the time of my doctorate, I was lucky to be supported by my family and my boyfriend. Thank you Mama, thank you Papa, for giving me the opportunity to study and also for backing me up lovingly in all the examination phases - including this last one. In the end, many thanks to Simon, who showed so much patience and endurance especially during the difficult times – I love you!

Literature

- Abramovitch, R.B., Anderson, J.C., and Martin, G.B. (2006). Bacterial elicitation and evasion of plant innate immunity. *Nature Reviews Molecular Cell Biology* 7, 601-611.
- Adler, J., and Parmryd, I. (2010). Quantifying Colocalization by Correlation: The Pearson Correlation Coefficient is Superior to the Mander's Overlap Coefficient. *Cytom Part A* 77A, 733-742.
- Albrecht, C., Russinova, E., Hecht, V., Baaijens, E., and de Vries, S. (2005). The *Arabidopsis thaliana* SOMATIC EMBRYOGENESIS RECEPTOR-LIKE KINASES1 and 2 control male sporogenesis. *The Plant Cell* 17, 3337-3349.
- Albrecht, C., Russinova, E., Kemmerling, B., Kwaaitaal, M., and de Vries, S.C. (2008). *Arabidopsis* SOMATIC EMBRYOGENESIS RECEPTOR KINASE proteins serve brassinosteroid-dependent and -independent signaling pathways. *Plant Physiology* 148, 611-619.
- Alfano, J.R., and Collmer, A. (2004). Type III secretion system effector proteins: double agents in bacterial disease and plant defense. *Annual Review of Phytopathology* 42, 385-414.
- Ali, G.S., Prasad, K.V.S.K., Day, I., and Reddy, A.S.N. (2007). Ligand-dependent reduction in the membrane mobility of FLAGELLIN SENSITIVE2, an *arabidopsis* receptor-like kinase. *Plant & Cell Physiology* 48, 1601-1611.
- Ali, G.S., and Reddy, A. (2008). PAMP-triggered immunity: Early events in the activation of FLAGELLIN SENSITIVE2. *Plant Signaling & Behavior* 3, 423-426.
- Alliotte, T., Tiré, C., Engler, G., Peleman, J., Caplan, A., Van Montagu, M., and Inzé, D. (1989). An Auxin-Regulated Gene of *Arabidopsis thaliana* Encodes a DNA-Binding Protein. *Plant Physiology* 89, 743-752.
- Alonso, M.A., and Millan, J. (2001). The role of lipid rafts in signalling and membrane trafficking in T lymphocytes. *Journal of Cell Science* 114, 3957-3965.
- Anderson, R.G., and Jacobson, K. (2002). A role for lipid shells in targeting proteins to caveolae, rafts, and other lipid domains. *Science* 296, 1821-1825.
- Asai, S., and Yoshioka, H. (2008). The role of radical burst via MAPK signaling in plant immunity. *Plant Signaling & Behavior* 3, 920-922.
- Asai, T., Tena, G., Plotnikova, J., Willmann, M.R., Chiu, W.L., Gomez-Gomez, L., Boller, T., Ausubel, F.M., and Sheen, J. (2002). MAP kinase signalling cascade in *Arabidopsis* innate immunity. *Nature* 415, 977-983.
- Assaad, F.F., Qiu, J.L., Youngs, H., Ehrhardt, D., Zimmerli, L., Kalde, M., Wanner, G., Peck, S.C., Edwards, H., Ramonell, K., *et al.* (2004). The PEN1 syntaxin defines a novel cellular compartment upon fungal attack and is required for the timely assembly of papillae. *Molecular Biology of the Cell* 15, 5118-5129.
- Axtell, M.J., Chisholm, S.T., Dahlbeck, D., and Staskawicz, B.J. (2003). Genetic and molecular evidence that the *Pseudomonas syringae* type III effector protein AvrRpt2 is a cysteine protease. *Molecular Microbiology* 49, 1537-1546.
- Bagatolli, L. A. and Gratton, E. (2000). Two photon fluorescence microscopy of coexisting lipid domains in giant unilamellar vesicles of binary phospholipid mixtures. *Biophysical Journal* 78 (1); 290-305.

Literature

- Bagnat, M., and Simons, K. (2002a). Cell surface polarization during yeast mating. *Proc Natl Acad Sci USA* *99*, 14183-14188.
- Bagnat, M., and Simons, K. (2002b). Lipid rafts in protein sorting and cell polarity in budding yeast *Saccharomyces cerevisiae*. *Biological Chemistry* *383*, 1475-1480.
- Baorto, D.M., Gao, Z., Malaviya, R., Dustin, M.L., van der Merwe, A., Lublin, D.M., and Abraham, S.N. (1997). Survival of FimH-expressing enterobacteria in macrophages relies on glycolipid traffic. *Nature* *389*, 636-639.
- Bariola, P.A., Retelska, D., Stasiak, A., Kammerer, R.A., Fleming, A., Hijri, M., Frank, S., and Farmer, E.E. (2004). Remorins form a novel family of coiled coil-forming oligomeric and filamentous proteins associated with apical, vascular and embryonic tissues in plants. *Plant Molecular Biology* *55*, 579-594.
- Beck, M., Zhou, J., Faulkner, C., MacLean, D., and Robatzek, S. (2012). Spatio-temporal cellular dynamics of the *Arabidopsis* flagellin receptor reveal activation status-dependent endosomal sorting. *The Plant Cell* *24*, 4205-4219.
- Bender, C.L., Alarcon-Chaidez, F., and Gross, D.C. (1999). *Pseudomonas syringae* phytotoxins: mode of action, regulation, and biosynthesis by peptide and polyketide synthetases. *Microbiology and Molecular Biology Reviews* : MMBR *63*, 266-292.
- Benkova, E., Michniewicz, M., Sauer, M., Teichmann, T., Seifertova, D., Jurgens, G., and Friml, J. (2003). Local, efflux-dependent auxin gradients as a common module for plant organ formation. *Cell* *115*, 591-602.
- Benschop, J.J., Mohammed, S., O'Flaherty, M., Heck, A.J.R., Slijper, M., and Menke, F.L.H. (2007). Quantitative phosphoproteomics of early elicitor signaling in *Arabidopsis*. *Molecular & Cellular Proteomics* *6*, 1198-1214.
- Bharadwaj, M., and Bizzozero, O.A. (1995). Myelin P0 glycoprotein and a synthetic peptide containing the palmitoylation site are both autoacylated. *Journal of Neurochemistry* *65*, 1805-1815.
- Bhat, R.A., Miklis, M., Schmelzer, E., Schulze-Lefert, P., and Panstruga, R. (2005). Recruitment and interaction dynamics of plant penetration resistance components in a plasma membrane microdomain. *Proc Natl Acad Sci USA* *102*, 3135-3140.
- Bhattacharjee, S., Halane, M.K., Kim, S.H., and Gassmann, W. (2011). Pathogen effectors target *Arabidopsis* EDS1 and alter its interactions with immune regulators. *Science* *334*, 1405-1408.
- Blilou, I., Xu, J., Wildwater, M., Willemsen, V., Paponov, I., Friml, J., Heidstra, R., Aida, M., Palme, K., and Scheres, B. (2005). The PIN auxin efflux facilitator network controls growth and patterning in *Arabidopsis* roots. *Nature* *433*, 39-44.
- Boller, T., and Felix, G. (2009). A renaissance of elicitors: perception of microbe-associated molecular patterns and danger signals by pattern-recognition receptors. *Annu Rev Plant Biol* *60*, 379-406.
- Borner, G.H., Sherrier, D.J., Weimar, T., Michaelson, L.V., Hawkins, N.D., Macaskill, A., Napier, J.A., Beale, M.H., Lilley, K.S., and Dupree, P. (2005). Analysis of detergent-resistant membranes in *Arabidopsis*. Evidence for plasma membrane lipid rafts. *Plant Physiology* *137*, 104-116.
- Boyes, D.C., Nam, J., and Dangl, J.L. (1998). The *Arabidopsis thaliana* RPM1 disease resistance gene product is a peripheral plasma membrane protein that is degraded coincident with the hypersensitive response. *Proc Natl Acad Sci USA* *95*, 15849-15854.

Literature

- Brown, I., Trethowan, J., Kerry, M., Mansfield, J., and Bolwell, G.P. (1998). Localization of components of the oxidative cross-linking of glycoproteins and of callose synthesis in papillae formed during the interaction between non-pathogenic strains of *Xanthomonas campestris* and French bean mesophyll cells. *Plant Journal* *15*, 333-343.
- Bucherl, C.A., van Esse, G.W., Kruijs, A., Luchtenberg, J., Westphal, A.H., Aker, J., van Hoek, A., Albrecht, C., Borst, J.W., and de Vries, S.C. (2013). Visualization of BRI1 and BAK1(SERK3) membrane receptor heterooligomers during brassinosteroid signaling. *Plant Physiology* *162*, 1911-1925.
- Catron, D.M., Sylvester, M.D., Lange, Y., Kadekoppala, M., Jones, B.D., Monack, D.M., Falkow, S., and Haldar, K. (2002). The Salmonella-containing vacuole is a major site of intracellular cholesterol accumulation and recruits the GPI-anchored protein CD55. *Cellular Microbiology* *4*, 315-328.
- Chae, L., Sudat, S., Dudoit, S., Zhu, T., and Luan, S. (2009). Diverse transcriptional programs associated with environmental stress and hormones in the *Arabidopsis* receptor-like kinase gene family. *Molecular Plant* *2*, 84-107.
- Chen, R.J., Hilson, P., Sedbrook, J., Rosen, E., Caspar, T., and Masson, P.H. (1998). The *Arabidopsis thaliana* AGRAVITROPIC 1 gene encodes a component of the polar-auxin-transport efflux carrier. *Proc Natl Acad Sci USA* *95*, 15112-15117.
- Chen, X., Chern, M., Canlas, P.E., Jiang, C., Ruan, D., Cao, P., and Ronald, P.C. (2010a). A conserved threonine residue in the juxtamembrane domain of the XA21 pattern recognition receptor is critical for kinase autophosphorylation and XA21-mediated immunity. *The Journal of Biological Chemistry* *285*, 10454-10463.
- Chen, X., Chern, M., Canlas, P.E., Ruan, D., Jiang, C., and Ronald, P.C. (2010b). An ATPase promotes autophosphorylation of the pattern recognition receptor XA21 and inhibits XA21-mediated immunity. *Proc Natl Acad Sci USA* *107*, 8029-8034.
- Chen, Z., Agnew, J.L., Cohen, J.D., He, P., Shan, L., Sheen, J., and Kunkel, B.N. (2007). *Pseudomonas syringae* type III effector AvrRpt2 alters *Arabidopsis thaliana* auxin physiology. *Proc Natl Acad Sci USA* *104*, 20131-20136.
- Chinchilla, D., Bauer, Z., Regenass, M., Boller, T., and Felix, G. (2006). The *Arabidopsis* receptor kinase FLS2 binds flg22 and determines the specificity of flagellin perception. *The Plant Cell* *18*, 465-476.
- Chinchilla, D., Shan, L., He, P., de Vries, S., and Kemmerling, B. (2009). One for all: the receptor-associated kinase BAK1. *Trends in Plant Science* *14*, 535-541.
- Chinchilla, D., Zipfel, C., Robatzek, S., Kemmerling, B., Nurnberger, T., Jones, J.D., Felix, G., and Boller, T. (2007a). A flagellin-induced complex of the receptor FLS2 and BAK1 initiates plant defence. *Nature* *448*, 497-500.
- Chinchilla, D., Zipfel, C., Robatzek, S., Kemmerling, B., Nurnberger, T., Jones, J.D.G., Felix, G., and Boller, T. (2007b). A flagellin-induced complex of the receptor FLS2 and BAK1 initiates plant defence. *Nature* *448*, 497-500.
- Chisholm, S.T., Dahlbeck, D., Krishnamurthy, N., Day, B., Sjolander, K., and Staskawicz, B.J. (2005). Molecular characterization of proteolytic cleavage sites of the *Pseudomonas syringae* effector AvrRpt2. *Proc Natl Acad Sci USA* *102*, 2087-2092.
- Chung, Y., Choe, V., Fujioka, S., Takatsuto, S., Han, M., Jeon, J.S., Park, Y.I., Lee, K.O., and Choe, S. (2012). Constitutive activation of brassinosteroid signaling

Literature

- in the *Arabidopsis* elongated-D/bak1 mutant. *Plant Molecular Biology* *80*, 489-501.
- Clouse, S.D. (2011). Brassinosteroid signal transduction: from receptor kinase activation to transcriptional networks regulating plant development. *The Plant Cell* *23*, 1219-1230.
- Coaker, G., Falick, A., and Staskawicz, B. (2005). Activation of a phytopathogenic bacterial effector protein by a eukaryotic cyclophilin. *Science* *308*, 548-550.
- Coaker, G.L., Willard, B., Kinter, M., Stockinger, E.J., and Francis, D.M. (2004). Proteomic analysis of resistance mediated by Rcm 2.0 and Rcm 5.1, two loci controlling resistance to bacterial canker of tomato. *Molecular Plant-Microbe Interactions* *17*, 1019-1028.
- Colcombet, J., Boisson-Dernier, A., Ros-Palau, R., Vera, C.E., and Schroeder, J.I. (2005). *Arabidopsis* SOMATIC EMBRYOGENESIS RECEPTOR KINASES1 and 2 are essential for tapetum development and microspore maturation. *The Plant Cell* *17*, 3350-3361.
- Crowell, E.F., Bischoff, V., Desprez, T., Rolland, A., Stierhof, Y.D., Schumacher, K., Gonneau, M., Hofte, H., and Vernhettes, S. (2009). Pausing of Golgi bodies on microtubules regulates secretion of cellulose synthase complexes in *Arabidopsis*. *The Plant Cell* *21*, 1141-1154.
- Dangl, J.L., and Jones, J.D. (2001). Plant pathogens and integrated defence responses to infection. *Nature* *411*, 826-833.
- Dardick, C., and Ronald, P. (2006). Plant and animal pathogen recognition receptors signal through non-RD kinases. *PLoS Pathogens* *2*, e2.
- Demir, F., Horntrich, C., Blachutzik, J.O., Scherzer, S., Reinders, Y., Kierszniowska, S., Schulze, W.X., Harms, G.S., Hedrich, R., Geiger, D., *et al.* (2013). *Arabidopsis* nanodomain-delimited ABA signaling pathway regulates the anion channel SLAH3. *Proc Natl Acad Sci USA* *110*, 8296-8301.
- Dermine, J.F., Duclos, S., Garin, J., St-Louis, F., Rea, S., Parton, R.G., and Desjardins, M. (2001). Flotillin-1-enriched lipid raft domains accumulate on maturing phagosomes. *The Journal of Biological Chemistry* *276*, 18507-18512.
- Di Rubbo, S., Irani, N.G., Kim, S.Y., Xu, Z.Y., Gadeyne, A., Dejonghe, W., Vanhoutte, I., Persiau, G., Eeckhout, D., Simon, S., *et al.* (2013). The clathrin adaptor complex AP-2 mediates endocytosis of brassinosteroid insensitive1 in *Arabidopsis*. *The Plant Cell* *25*, 2986-2997.
- Diévert, A., and Clark, S.E. (2004). LRR-containing receptors regulating plant development and defense. *Development* *131*, 251-261.
- Eddidin, M. (2003). The state of lipid rafts: from model membranes to cells. *Annual review of biophysics and biomolecular structure* *32*, 257-283.
- Eichmann, R., Dechert, C., Kogel, K.H., and Huckelhoven, R. (2006). Transient over-expression of barley BAX Inhibitor-1 weakens oxidative defence and MLA12-mediated resistance to *Blumeria graminis f.sp. hordei*. *Molecular Plant Pathology* *7*, 543-552.
- Enstone, D.E., Peterson, C.A., and Ma, F.S. (2002). Root endodermis and exodermis: Structure, function, and responses to the environment. *J Plant Growth Regul* *21*, 335-351.
- Farmer, E.E., Pearce, G., and Ryan, C.A. (1989). In vitro phosphorylation of plant plasma membrane proteins in response to the proteinase inhibitor inducing factor. *Proc Natl Acad Sci USA* *86*, 1539-1542.

Literature

- Faulkner, C., and Robatzek, S. (2012). Plants and pathogens: putting infection strategies and defence mechanisms on the map. *Current Opinion in Plant Biology* 15, 699-707.
- Felix, G., Duran, J.D., Volko, S., and Boller, T. (1999). Plants have a sensitive perception system for the most conserved domain of bacterial flagellin. *The Plant Journal* 18, 265-276.
- Feng, F., Yang, F., Rong, W., Wu, X., Zhang, J., Chen, S., He, C., and Zhou, J.M. (2012a). A *Xanthomonas* uridine 5'-monophosphate transferase inhibits plant immune kinases. *Nature* 485, 114-118.
- Feng, F., Yang, F., Rong, W., Wu, X.G., Zhang, J., Chen, S., He, C.Z., and Zhou, J.M. (2012b). A *Xanthomonas* uridine 5'-monophosphate transferase inhibits plant immune kinases. *Nature* 485, 114-U149.
- Fitzner, D., Schneider, A., Kippert, A., Möbius, W., Willig, K. I., Hell, S. W., Bunt, G., Gaus, K. and Simons, M. (2006). Myelin basic protein-dependent plasma membrane reorganisation in the formation of myelin. *EMBO Journal* 25 (21); 5037-5048.
- Friml, J., Benkova, E., Blilou, I., Wisniewska, J., Hamann, T., Ljung, K., Woody, S., Sandberg, G., Scheres, B., Jurgens, G., *et al.* (2002a). AtPIN4 mediates sink-driven auxin gradients and root patterning in *Arabidopsis*. *Cell* 108, 661-673.
- Friml, J., Vieten, A., Sauer, M., Weijers, D., Schwarz, H., Hamann, T., Offringa, R., and Jurgens, G. (2003). Efflux-dependent auxin gradients establish the apical-basal axis of *Arabidopsis*. *Nature* 426, 147-153.
- Friml, J., Wisniewska, J., Benkova, E., Mendgen, K., and Palme, K. (2002b). Lateral relocation of auxin efflux regulator PIN3 mediates tropism in *Arabidopsis*. *Nature* 415, 806-809.
- Fujiwara, T., Ritchie, K., Murakoshi, H., Jacobson, K., and Kusumi, A. (2002). Phospholipids undergo hop diffusion in compartmentalized cell membrane. *The Journal of Cell Biology* 157, 1071-1081.
- Galweiler, L., Guan, C.H., Muller, A., Wisman, E., Mendgen, K., Yephremov, A., and Palme, K. (1998). Regulation of polar auxin transport by AtPIN1 in *Arabidopsis* vascular tissue. *Science* 282, 2226-2230.
- Gaus, K., Gratton, E., Kable, E. P. W., Jones, A. S., Gelissen, I., Kritharides, L. and Jessup, W. (2003). Visualizing lipid structure and raft domains in living cells with two-photon microscopy. *Proc Natl Acad Sci U S A* 100 (26); 15554-15559.
- Geldner, N., Hyman, D.L., Wang, X., Schumacher, K., and Chory, J. (2007). Endosomal signaling of plant steroid receptor kinase BRI1. *Genes & Development* 21, 1598-1602.
- Gish, L.A., and Clark, S.E. (2011). The RLK/Pelle family of kinases. *The Plant Journal* 66, 117-127.
- Glebov, O.O., Bright, N.A., and Nichols, B.J. (2006). Flotillin-1 defines a clathrin-independent endocytic pathway in mammalian cells. *Nature Cell Biology* 8, 46-54.
- Gohre, V., and Robatzek, S. (2008). Breaking the barriers: microbial effector molecules subvert plant immunity. *Annual Review of Phytopathology* 46, 189-215.
- Gohre, V., Spallek, T., Haweker, H., Mersmann, S., Mentzel, T., Boller, T., de Torres, M., Mansfield, J.W., and Robatzek, S. (2008). Plant pattern-recognition receptor FLS2 is directed for degradation by the bacterial ubiquitin ligase AvrPtoB. *Current Biology* 18, 1824-1832.

Literature

- Gomez-Gomez, L., and Boller, T. (2002). Flagellin perception: a paradigm for innate immunity. *Trends in Plant Science* 7, 251-256.
- Gómez-Gómez, L., and Boller, T. (2000). FLS2: an LRR receptor-like kinase involved in the perception of the bacterial elicitor flagellin in *Arabidopsis*. *Molecular Cell* 5, 1003-1011.
- Gómez-Gómez, L., Felix, G., and Boller, T. (1999). A single locus determines sensitivity to bacterial flagellin in *Arabidopsis thaliana*. *The Plant Journal* 18, 277-284.
- Grossmann, G., Opekarova, M., Novakova, L., Stolz, J., and Tanner, W. (2006). Lipid raft-based membrane compartmentation of a plant transport protein expressed in *Saccharomyces cerevisiae*. *Eukaryotic Cell* 5, 945-953.
- Gutierrez, R., Lindeboom, J.J., Paredes, A.R., Emons, A.M., and Ehrhardt, D.W. (2009). *Arabidopsis* cortical microtubules position cellulose synthase delivery to the plasma membrane and interact with cellulose synthase trafficking compartments. *Nature Cell Biology* 11, 797-806.
- Hammond, A.T., Heberle, F.A., Baumgart, T., Holowka, D., Baird, B., and Feigenson, G.W. (2005). Crosslinking a lipid raft component triggers liquid ordered-liquid disordered phase separation in model plasma membranes. *Proc Natl Acad Sci USA* 102, 6320-6325.
- Hancock, J.F. (2006). Lipid rafts: contentious only from simplistic standpoints. *Nature Reviews Molecular Cell Biology* 7, 456-462.
- Haney, C.H., and Long, S.R. (2010). Plant flotillins are required for infection by nitrogen-fixing bacteria. *Proc Natl Acad Sci USA*, pp. 478-483.
- Haney, C.H., Riely, B.K., Tricoli, D.M., Cook, D.R., Ehrhardt, D.W., and Long, S.R. (2011). Symbiotic rhizobia bacteria trigger a change in localization and dynamics of the *Medicago truncatula* receptor kinase LYK3. *The Plant Cell* 23, 2774-2787.
- Hao, H., Fan, L., Chen, T., Li, R., Li, X., He, Q., Botella, M.A., and Lin, J. (2014). Clathrin and Membrane Microdomains Cooperatively Regulate RbohD Dynamics and Activity in *Arabidopsis*. *The Plant Cell*.
- Harder, T., and Simons, K. (1997). Caveolae, DIGs, and the dynamics of sphingolipid-cholesterol microdomains. *Current Opinion in Cell Biology* 9, 534-542.
- Hartlova, A., Cervený, L., Hubalek, M., Krocova, Z., and Stulik, J. (2010). Membrane rafts: a potential gateway for bacterial entry into host cells. *Microbiology and Immunology* 54, 237-245.
- Hauck, P., Thilmony, R., and He, S.Y. (2003). A *Pseudomonas syringae* type III effector suppresses cell wall-based extracellular defense in susceptible *Arabidopsis* plants. *Proc Natl Acad Sci USA* 100, 8577-8582.
- Hayashi, F., Smith, K.D., Ozinsky, A., Hawn, T.R., Yi, E.C., Goodlett, D.R., Eng, J.K., Akira, S., Underhill, D.M., and Aderem, A. (2001). The innate immune response to bacterial flagellin is mediated by Toll-like receptor 5. *Nature* 410, 1099-1103.
- He, K., Gou, X., Powell, R.A., Yang, H., Yuan, T., Guo, Z., and Li, J. (2008). Receptor-like protein kinases, BAK1 and BKK1, regulate a light-dependent cell-death control pathway. *Plant Signaling & Behavior* 3, 813-815.
- He, K., Gou, X., Yuan, T., Lin, H., Asami, T., Yoshida, S., Russell, S.D., and Li, J. (2007). BAK1 and BKK1 regulate brassinosteroid-dependent growth and

Literature

- brassinosteroid-independent cell-death pathways. *Current Biology* *17*, 1109-1115.
- He, P., Shan, L., Lin, N.C., Martin, G.B., Kemmerling, B., Nurnberger, T., and Sheen, J. (2006). Specific bacterial suppressors of MAMP signaling upstream of MAPKKK in *Arabidopsis* innate immunity. *Cell* *125*, 563-575.
- He, Z., Wang, Z.Y., Li, J., Zhu, Q., Lamb, C., Ronald, P., and Chory, J. (2000). Perception of brassinosteroids by the extracellular domain of the receptor kinase BRI1. *Science* *288*, 2360-2363.
- Hecht, V., Vielle-Calzada, J.P., Hartog, M.V., Schmidt, E.D., Boutilier, K., Grossniklaus, U., and de Vries, S.C. (2001). The *Arabidopsis* SOMATIC EMBRYOGENESIS RECEPTOR KINASE 1 gene is expressed in developing ovules and embryos and enhances embryogenic competence in culture. *Plant Physiology* *127*, 803-816.
- Heerklotz, H. (2002). Triton promotes domain formation in lipid raft mixtures. *Biophysical Journal* *83*, 2693-2701.
- Heese, A., Hann, D.R., Gimenez-Ibanez, S., Jones, A.M., He, K., Li, J., Schroeder, J.I., Peck, S.C., and Rathjen, J.P. (2007a). The receptor-like kinase SERK3/BAK1 is a central regulator of innate immunity in plants. *Proc Natl Acad Sci USA* *104*, 12217-12222.
- Hemsley, P.A., Weimar, T., Lilley, K.S., Dupree, P., and Grierson, C.S. (2013). A proteomic approach identifies many novel palmitoylated proteins in *Arabidopsis*. *The New Phytologist* *197*, 805-814.
- Hoffmann, J.A., and Reichhart, J.M. (2002). *Drosophila* innate immunity: an evolutionary perspective. *Nature Immunology* *3*, 121-126.
- Hogue, I.B., Grover, J.R., Soheilian, F., Nagashima, K., and Ono, A. (2011). Gag induces the coalescence of clustered lipid rafts and tetraspanin-enriched microdomains at HIV-1 assembly sites on the plasma membrane. *Journal of Virology* *85*, 9749-9766.
- Homann, U., Meckel, T., Hewing, J., Hutt, M.T., and Hurst, A.C. (2007). Distinct fluorescent pattern of KAT1::GFP in the plasma membrane of *Vicia faba* guard cells. *European Journal of Cell Biology* *86*, 489-500.
- Iizasa, E., Mitsutomi, M., and Nagano, Y. (2010). Direct binding of a plant LysM receptor-like kinase, LysM RLK1/CERK1, to chitin in vitro. *The Journal of Biological Chemistry* *285*, 2996-3004.
- Ikonen, E. (2008). Cellular cholesterol trafficking and compartmentalization. *Nature Reviews Molecular Cell Biology* *9*, 125-138.
- Imler, J.L., and Hoffmann, J.A. (2001). Toll receptors in innate immunity. *Trends in Cell Biology* *11*, 304-311.
- Inohara, N., and Nunez, G. (2001). The NOD: a signaling module that regulates apoptosis and host defense against pathogens. *Oncogene* *20*, 6473-6481.
- Irani, N.G., Di Rubbo, S., Mylle, E., Van den Begin, J., Schneider-Pizon, J., Hnilikova, J., Sisa, M., Buyst, D., Vilarrasa-Blasi, J., Szatmari, A.M., *et al.* (2012). Fluorescent castasterone reveals BRI1 signaling from the plasma membrane. *Nature Chemical Biology* *8*, 583-589.
- Jacinto, T., Farmer, E.E., and Ryan, C.A. (1993). Purification of Potato Leaf Plasma Membrane Protein pp34, a Protein Phosphorylated in Response to Oligogalacturonide Signals for Defense and Development. *Plant Physiology* *103*, 1393-1397.

Literature

- Jacobson, K., Mouritsen, O.G., and Anderson, R.G. (2007). Lipid rafts: at a crossroad between cell biology and physics. *Nature Cell Biology* 9, 7-14.
- Janssens, B., and Chavrier, P. (2004). Mediterranean views on epithelial polarity. *Nature Cell Biology* 6, 493-496.
- Jarsch, I.K., Konrad, S.S., Stratil, T.F., Urbanus, S.L., Szymanski, W., Braun, P., Braun, K.H., and Ott, T. (2014). Plasma Membranes Are Subcompartmentalized into a Plethora of Coexisting and Diverse Microdomains in *Arabidopsis* and *Nicotiana benthamiana*. *The Plant Cell*.
- Jarsch, I.K., and Ott, T. (2011). Perspectives on remorin proteins, membrane rafts, and their role during plant-microbe interactions. *Molecular Plant-Microbe Interactions* 24, 7-12.
- Jeong, Y.J., Shang, Y., Kim, B.H., Kim, S.Y., Song, J.H., Lee, J.S., Lee, M.M., Li, J., and Nam, K.H. (2010). BAK7 displays unequal genetic redundancy with BAK1 in brassinosteroid signaling and early senescence in *Arabidopsis*. *Molecules and Cells* 29, 259-266.
- Johnson, N.L., Gardner, A.M., Diener, K.M., Lange-Carter, C.A., Gleavy, J., Jarpe, M.B., Minden, A., Karin, M., Zon, L.I., and Johnson, G.L. (1996). Signal transduction pathways regulated by mitogen-activated/extracellular response kinase kinase kinase induce cell death. *The Journal of Biological Chemistry* 271, 3229-3237.
- Jones, J.D.G., and Dangl, J.L. (2006). The plant immune system. *Nature* 444, 323-329.
- Journot-Catalino, N., Somssich, I.E., Roby, D., and Kroj, T. (2006). The transcription factors WRKY11 and WRKY17 act as negative regulators of basal resistance in *Arabidopsis thaliana*. *The Plant Cell* 18, 3289-3302.
- Kadota, Y., Sklenar, J., Derbyshire, P., Stransfeld, L., Asai, S., Ntoukakis, V., Jones, J.D., Shirasu, K., Menke, F., Jones, A., *et al.* (2014). Direct Regulation of the NADPH Oxidase RBOHD by the PRR-Associated Kinase BIK1 during Plant Immunity. *Molecular Cell* 54, 43-55.
- Karlova, R., Boeren, S., Russinova, E., Aker, J., Vervoort, J., and de Vries, S. (2006). The *Arabidopsis* SOMATIC EMBRYOGENESIS RECEPTOR-LIKE KINASE1 protein complex includes BRASSINOSTEROID-INSENSITIVE1. *The Plant Cell* 18, 626-638.
- Keinath, N.F., Kierszniowska, S., Lorek, J., Bourdais, G., Kessler, S.A., Asano, H., Grossniklaus, U., Schulze, W., Robotzek, S., and Panstruga, R. (2010). PAMP-induced changes in plasma membrane compartmentalization reveal novel components of plant immunity. *The Journal of Biological Chemistry*.
- Kemmerling, B., Schwedt, A., Rodriguez, P., Mazzotta, S., Frank, M., Qamar, S.A., Mengiste, T., Betsuyaku, S., Parker, J.E., Müssig, C., *et al.* (2007). The BR1-associated kinase 1, BAK1, has a brassinolide-independent role in plant cell-death control. *Current Biology* 17, 1116-1122.
- Kierszniowska, S., Seiwert, B., and Schulze, W.X. (2009). Definition of *Arabidopsis* sterol-rich membrane microdomains by differential treatment with methyl-beta-cyclodextrin and quantitative proteomics. *Molecular & Cellular Proteomics* 8, 612-623.
- Kilian, J., Whitehead, D., Horak, J., Wanke, D., Weinl, S., Batistic, O., D'Angelo, C., Bornberg-Bauer, E., Kudla, J., and Harter, K. (2007). The AtGenExpress global stress expression data set: protocols, evaluation and model data analysis of UV-B light, drought and cold stress responses. *The Plant Journal* 50, 347-363.

Literature

- Kim, M.G., da Cunha, L., McFall, A.J., Belkhadir, Y., DebRoy, S., Dangl, J.L., and Mackey, D. (2005). Two *Pseudomonas syringae* type III effectors inhibit RIN4-regulated basal defense in *Arabidopsis*. *Cell* *121*, 749-759.
- Kinoshita, T., Cano-Delgado, A., Seto, H., Hiranuma, S., Fujioka, S., Yoshida, S., and Chory, J. (2005). Binding of brassinosteroids to the extracellular domain of plant receptor kinase BRI1. *Nature* *433*, 167-171.
- Knodler, L.A., and Steele-Mortimer, O. (2003). Taking possession: biogenesis of the Salmonella-containing vacuole. *Traffic* *4*, 587-599.
- Knodler, L.A., Vallance, B.A., Hensel, M., Jackel, D., Finlay, B.B., and Steele-Mortimer, O. (2003). Salmonella type III effectors PipB and PipB2 are targeted to detergent-resistant microdomains on internal host cell membranes. *Molecular Microbiology* *49*, 685-704.
- Koncz, C., Martini, N., Mayerhofer, R., Koncz-Kalman, Z., Korber, H., Redei, G.P., and Schell, J. (1989). High-frequency T-DNA-mediated gene tagging in plants. *Proc Natl Acad Sci USA* *86*, 8467-8471.
- Konrad S. S. A. , Popp C., Stratil T. F. , Jarsch I. K., Thallmair V., Folgmann J., Marín M. and Ott T., (2014). S-acylation anchors Remorin proteins to the plasma membrane but does not primarily determine their localization in membrane domains. *New Phytologist*, *in press*
- Koornneef, A., and Pieterse, C.M. (2008). Cross talk in defense signaling. *Plant Physiology* *146*, 839-844.
- Korhonen, J.T., Puolakkainen, M., Haivala, R., Penttila, T., Haveri, A., Markkula, E., and Lahesmaa, R. (2012). Flotillin-1 (Reggie-2) contributes to *Chlamydia pneumoniae* growth and is associated with bacterial inclusion. *Infection and immunity* *80*, 1072-1078.
- Kunze, G., Zipfel, C., Robatzek, S., Niehaus, K., Boller, T., and Felix, G. (2004). The N terminus of bacterial elongation factor Tu elicits innate immunity in *Arabidopsis* plants. *The Plant Cell* *16*, 3496-3507.
- Kusumi, A., Fujiwara, T.K., Morone, N., Yoshida, K.J., Chadda, R., Xie, M., Kasai, R.S., and Suzuki, K.G. (2012). Membrane mechanisms for signal transduction: the coupling of the meso-scale raft domains to membrane-skeleton-induced compartments and dynamic protein complexes. *Seminars in Cell & Developmental Biology* *23*, 126-144.
- Kusumi, A., Ike, H., Nakada, C., Murase, K., and Fujiwara, T. (2005). Single-molecule tracking of membrane molecules: plasma membrane compartmentalization and dynamic assembly of raft-philic signaling molecules. *Seminars in Immunology* *17*, 3-21.
- Kusumi, A., Koyama-Honda, I., and Suzuki, K. (2004). Molecular dynamics and interactions for creation of stimulation-induced stabilized rafts from small unstable steady-state rafts. *Traffic* *5*, 213-230.
- Kusumi, A., and Sako, Y. (1996). Cell surface organization by the membrane skeleton. *Current Opinion in Cell Biology* *8*, 566-574.
- Kusumi, A., Sako, Y., Fujiwara, T., and Tomishige, M. (1998). Application of laser tweezers to studies of the fences and tethers of the membrane skeleton that regulate the movements of plasma membrane proteins. *Methods in Cell Biology* *55*, 173-194.

Literature

- Kusumi, A., and Suzuki, K. (2005). Toward understanding the dynamics of membrane-raft-based molecular interactions. *Biochimica et Biophysica Acta* 1746, 234-251.
- Laloi, M., Perret, A.-M., Chatre, L., Melsner, S., Cantrel, C., Vaultier, M.-N., Zachowski, A., Bathany, K., Schmitter, J.-M., Vallet, M., *et al.* (2007). Insights into the role of specific lipids in the formation and delivery of lipid microdomains to the plasma membrane of plant cells. *Plant Physiology* 143, 461-472.
- Lamb, C., and Dixon, R.A. (1997). The Oxidative Burst in Plant Disease Resistance. *Annual review of Plant Physiology and Plant Molecular Biology* 48, 251-275.
- Langhorst, M.F., Solis, G.P., Hannbeck, S., Plattner, H., and Stuermer, C.A. (2007). Linking membrane microdomains to the cytoskeleton: regulation of the lateral mobility of reggie-1/flotillin-2 by interaction with actin. *FEBS Letters* 581, 4697-4703.
- Lee, S.W., Han, S.W., Sririyanyum, M., Park, C.J., Seo, Y.S., and Ronald, P.C. (2009). A type I-secreted, sulfated peptide triggers XA21-mediated innate immunity. *Science* 326, 850-853. → retracted
- Lefebvre, B., Furt, F., Hartmann, M.-A., Michaelson, L.V., Carde, J.-P., Sargueil-Boiron, F., Rossignol, M., Napier, J.A., Cullimore, J., Bessoule, J.-J., *et al.* (2007). Characterization of lipid rafts from *Medicago truncatula* root plasma membranes: a proteomic study reveals the presence of a raft-associated redox system. *Plant Physiology* 144, 402-418.
- Lefebvre, B., Timmers, T., Mbengue, M., Moreau, S., Hervé, C., Tóth, K., Bittencourt-Silvestre, J., Klaus, D., Deslandes, L., Godiard, L., *et al.* (2010). A remorin protein interacts with symbiotic receptors and regulates bacterial infection. *Proc Natl Acad Sci USA* 107, 2343-2348.
- Lherminier, J., Elmayan, T., Fromentin, J., Elaraqui, K.T., Vesa, S., Morel, J., Verrier, J.L., Cailleteau, B., Blein, J.P., and Simon-Plas, F. (2009). NADPH oxidase-mediated reactive oxygen species production: subcellular localization and reassessment of its role in plant defense. *Molecular Plant-Microbe Interactions* 22, 868-881.
- Li, J., Wen, J., Lease, K.A., Doke, J.T., Tax, F.E., and Walker, J.C. (2002). BAK1, an *Arabidopsis* LRR receptor-like protein kinase, interacts with BRI1 and modulates brassinosteroid signaling. *Cell* 110, 213-222.
- Li, Q., Zhang, Q., Wang, C., Li, N., and Li, J. (2008). Invasion of enteropathogenic *Escherichia coli* into host cells through epithelial tight junctions. *The FEBS Journal* 275, 6022-6032.
- Li, R., Liu, P., Wan, Y., Chen, T., Wang, Q., Mettbach, U., Baluska, F., Samaj, J., Fang, X., Lucas, W.J., *et al.* (2012). A membrane microdomain-associated protein, *Arabidopsis* Flot1, is involved in a clathrin-independent endocytic pathway and is required for seedling development. *The Plant Cell* 24, 2105-2122.
- Li, X., Lin, H., Zhang, W., Zou, Y., Zhang, J., Tang, X., and Zhou, J.M. (2005). Flagellin induces innate immunity in nonhost interactions that is suppressed by *Pseudomonas syringae* effectors. *Proc Natl Acad Sci USA* 102, 12990-12995.
- Lin, W., Lu, D., Gao, X., Jiang, S., Ma, X., Wang, Z., Mengiste, T., He, P., and Shan, L. (2013). Inverse modulation of plant immune and brassinosteroid signaling pathways by the receptor-like cytoplasmic kinase BIK1. *Proc Natl Acad Sci USA* 110, 12114-12119.

Literature

- Lingwood, D., Ries, J., Schwille, P., and Simons, K. (2008). Plasma membranes are poised for activation of raft phase coalescence at physiological temperature. *Proc Natl Acad Sci USA* *105*, 10005-10010.
- Lingwood, D., and Simons, K. (2010). Lipid rafts as a membrane-organizing principle. *Science* *327*, 46-50.
- Liu, J., Elmore, J.M., Fuglsang, A.T., Palmgren, M.G., Staskawicz, B.J., and Coaker, G. (2009). RIN4 functions with plasma membrane H⁺-ATPases to regulate stomatal apertures during pathogen attack. *PLoS Biology* *7*, e1000139.
- Lu, D., Lin, W., Gao, X., Wu, S., Cheng, C., Avila, J., Heese, A., Devarenne, T.P., He, P., and Shan, L. (2011). Direct ubiquitination of pattern recognition receptor FLS2 attenuates plant innate immunity. *Science* *332*, 1439-1442.
- Lu, D., Wu, S., Gao, X., Zhang, Y., Shan, L., and He, P. (2010). A receptor-like cytoplasmic kinase, BIK1, associates with a flagellin receptor complex to initiate plant innate immunity. *Proc Natl Acad Sci USA* *107*, 496-501.
- Lu, Y.J., Schornack, S., Spallek, T., Geldner, N., Chory, J., Schellmann, S., Schumacher, K., Kamoun, S., and Robatzek, S. (2012). Patterns of plant subcellular responses to successful oomycete infections reveal differences in host cell reprogramming and endocytic trafficking. *Cellular Microbiology* *14*, 682-697.
- Luna, E., Pastor, V., Robert, J., Flors, V., Mauch-Mani, B., and Ton, J. (2011). Callose Deposition: A Multifaceted Plant Defense Response. *Mol Plant Microbe In* *24*, 183-193.
- Luschnig, C., Gaxiola, R.A., Grisafi, P., and Fink, G.R. (1998). EIR1, a root-specific protein involved in auxin transport, is required for gravitropism in *Arabidopsis thaliana*. *Genes & Development* *12*, 2175-2187.
- Mackey, D., Holt, B.F., Wiig, A., and Dangl, J.L. (2002). RIN4 interacts with *Pseudomonas syringae* type III effector molecules and is required for RPM1-mediated resistance in *Arabidopsis*. *Cell* *108*, 743-754.
- Manders, E.M., Stap, J., Brakenhoff, G.J., van Driel, R., and Aten, J.A. (1992). Dynamics of three-dimensional replication patterns during the S-phase, analysed by double labelling of DNA and confocal microscopy. *Journal of Cell Science* *103 (Pt 3)*, 857-862.
- Manders, E.M.M., Verbeek, F.J., and Aten, J.A. (1993). Measurement of Colocalization of Objects in Dual-Color Confocal Images. *J Microsc-Oxford* *169*, 375-382.
- Marin, M., and Ott, T. (2012). Phosphorylation of intrinsically disordered regions in remorin proteins. *Frontiers in Plant Science* *3*, 86.
- Marin, M., Thallmair, V., and Ott, T. (2012). The intrinsically disordered N-terminal region of AtREM1.3 remorin protein mediates protein-protein interactions. *The Journal of Biological Chemistry* *287*, 39982-39991.
- Marmagne, A., Rouet, M.-A., Ferro, M., Rolland, N., Alcon, C., Joyard, J., Garin, J., Barbier-Brygoo, H., and Ephritikhine, G. (2004). Identification of new intrinsic proteins in *Arabidopsis* plasma membrane proteome. *Molecular & Cellular Proteomics* *3*, 675-691.
- Martiniere, A., Lavagi, I., Nageswaran, G., Rolfe, D.J., Maneta-Peyret, L., Luu, D.T., Botchway, S.W., Webb, S.E., Mongrand, S., Maurel, C., *et al.* (2012). Cell wall constrains lateral diffusion of plant plasma-membrane proteins. *Proc Natl Acad Sci USA* *109*, 12805-12810.

Literature

- Melotto, M., Underwood, W., Koczan, J., Nomura, K., and He, S.Y. (2006). Plant stomata function in innate immunity against bacterial invasion. *Cell* *126*, 969-980.
- Metz, M., Dahlbeck, D., Morales, C.Q., Al Sady, B., Clark, E.T., and Staskawicz, B.J. (2005). The conserved *Xanthomonas campestris* pv. *vesicatoria* effector protein XopX is a virulence factor and suppresses host defense in *Nicotiana benthamiana*. *The Plant Journal* *41*, 801-814.
- Meyers, B.C., Kozik, A., Griego, A., Kuang, H., and Michelmore, R.W. (2003). Genome-wide analysis of NBS-LRR-encoding genes in *Arabidopsis*. *The Plant Cell* *15*, 809-834.
- Miller, G., Schlauch, K., Tam, R., Cortes, D., Torres, M.A., Shulaev, V., Dangl, J.L., and Mittler, R. (2009). The plant NADPH oxidase RBOHD mediates rapid systemic signaling in response to diverse stimuli. *Science Signaling* *2*, ra45.
- Miya, A., Albert, P., Shinya, T., Desaki, Y., Ichimura, K., Shirasu, K., Narusaka, Y., Kawakami, N., Kaku, H., and Shibuya, N. (2007). CERK1, a LysM receptor kinase, is essential for chitin elicitor signaling in *Arabidopsis*. *Proc Natl Acad Sci USA* *104*, 19613-19618.
- Monaghan, J., and Zipfel, C. (2012). Plant pattern recognition receptor complexes at the plasma membrane. *Current Opinion in Plant Biology* *15*, 349-357.
- Mongrand, S., Morel, J., Laroche, J., Claverol, S., Carde, J.-P., Hartmann, M.-A., Bonneu, M., Simon-Plas, F., Lessire, R., and Bessoule, J.-J. (2004). Lipid rafts in higher plant cells: purification and characterization of Triton X-100-insoluble microdomains from tobacco plasma membrane. *The Journal of Biological Chemistry* *279*, 36277-36286.
- Morbitzer, R., Elsaesser, J., Hausner, J., and Lahaye, T. (2011). Assembly of custom TALE-type DNA binding domains by modular cloning. *Nucleic Acids Research* *39*, 5790-5799.
- Morel, J., Claverol, S., Mongrand, S., Furt, F., Fromentin, J., Bessoule, J.-J., Blein, J.-P., and Simon-Plas, F. (2006). Proteomics of plant detergent-resistant membranes. *Molecular & Cellular Proteomics* *5*, 1396-1411.
- Mostov, K.E. (2003). Epithelial polarity and morphogenesis. *Methods* *30*, 189-190.
- Muller, A., Guan, C., Galweiler, L., Tanzler, P., Huijser, P., Marchant, A., Parry, G., Bennett, M., Wisman, E., and Palme, K. (1998). AtPIN2 defines a locus of *Arabidopsis* for root gravitropism control. *The EMBO Journal* *17*, 6903-6911.
- Munro, S. (2003). Lipid rafts: elusive or illusive? *Cell* *115*, 377-388.
- Murphy, S.C., Fernandez-Pol, S., Chung, P.H., Prasanna Murthy, S.N., Milne, S.B., Salomao, M., Brown, H.A., Lomasney, J.W., Mohandas, N., and Haldar, K. (2007). Cytoplasmic remodeling of erythrocyte raft lipids during infection by the human malaria parasite *Plasmodium falciparum*. *Blood* *110*, 2132-2139.
- Nagy, F., and Schafer, E. (2000). Nuclear and cytosolic events of light-induced, phytochrome-regulated signaling in higher plants. *The EMBO Journal* *19*, 157-163.
- Nakagawa, T., Kurose, T., Hino, T., Tanaka, K., Kawamukai, M., Niwa, Y., Toyooka, K., Matsuoka, K., Jinbo, T., and Kimura, T. (2007). Development of series of gateway binary vectors, pGWBs, for realizing efficient construction of fusion genes for plant transformation. *Journal of Bioscience and Bioengineering* *104*, 34-41.

Literature

- Nam, K.H., and Li, J. (2002). BRI1/BAK1, a receptor kinase pair mediating brassinosteroid signaling. *Cell* *110*, 203-212.
- Navarro, L., Dunoyer, P., Jay, F., Arnold, B., Dharmasiri, N., Estelle, M., Voinnet, O., and Jones, J.D. (2006). A plant miRNA contributes to antibacterial resistance by repressing auxin signaling. *Science* *312*, 436-439.
- Navarro, L., Zipfel, C., Rowland, O., Keller, I., Robatzek, S., Boller, T., and Jones, J.D. (2004). The transcriptional innate immune response to flg22. Interplay and overlap with Avr gene-dependent defense responses and bacterial pathogenesis. *Plant Physiology* *135*, 1113-1128.
- Neff, M.M., and Chory, J. (1998). Genetic interactions between phytochrome A, phytochrome B, and cryptochrome 1 during *Arabidopsis* development. *Plant Physiology* *118*, 27-35.
- Nelson, C.J., Hegeman, A.D., Harms, A.C., and Sussman, M.R. (2006). A quantitative analysis of *Arabidopsis* plasma membrane using trypsin-catalyzed (18)O labeling. *Molecular & Cellular Proteomics* *5*, 1382-1395.
- Nolen, B., Taylor, S., and Ghosh, G. (2004). Regulation of protein kinases; controlling activity through activation segment conformation. *Molecular Cell* *15*, 661-675.
- Nurnberger, T., and Kemmerling, B. (2006). Receptor protein kinases--pattern recognition receptors in plant immunity. *Trends in Plant Science* *11*, 519-522.
- Oh, H.S., and Collmer, A. (2005). Basal resistance against bacteria in *Nicotiana benthamiana* leaves is accompanied by reduced vascular staining and suppressed by multiple *Pseudomonas syringae* type III secretion system effector proteins. *The Plant Journal* *44*, 348-359.
- Oh, M.H., Wang, X., Wu, X., Zhao, Y., Clouse, S.D., and Huber, S.C. (2010). Autophosphorylation of Tyr-610 in the receptor kinase BAK1 plays a role in brassinosteroid signaling and basal defense gene expression. *Proc Natl Acad Sci USA* *107*, 17827-17832.
- Otto, G.P., and Nichols, B.J. (2011). The roles of flotillin microdomains--endocytosis and beyond. *Journal of Cell Science* *124*, 3933-3940.
- Panstruga, R., Parker, J.E., and Schulze-Lefert, P. (2009). SnapShot: Plant immune response pathways. *Cell* *136*, 978.e971-973.
- Panter, S., Thomson, R., de Bruxelles, G., Laver, D., Trevaskis, B., and Udvardi, M. (2000). Identification with proteomics of novel proteins associated with the peribacteroid membrane of soybean root nodules. *Molecular Plant-Microbe Interactions* *13*, 325-333.
- Park, C.J., Peng, Y., Chen, X., Dardick, C., Ruan, D., Bart, R., Canlas, P.E., and Ronald, P.C. (2008). Rice XB15, a protein phosphatase 2C, negatively regulates cell death and XA21-mediated innate immunity. *PLoS Biology* *6*, e231.
- Parton, R.G., and Richards, A.A. (2003). Lipid rafts and caveolae as portals for endocytosis: new insights and common mechanisms. *Traffic* *4*, 724-738.
- Pawson, T., and Nash, P. (2000). Protein-protein interactions define specificity in signal transduction. *Genes & Development* *14*, 1027-1047.
- Pelkmans, L. (2005). Secrets of caveolae- and lipid raft-mediated endocytosis revealed by mammalian viruses. *Biochimica et Biophysica Acta* *1746*, 295-304.
- Perraki, A., Cacas, J.L., Crowet, J.M., Lins, L., Castroviejo, M., German-Retana, S., Mongrand, S., and Raffaele, S. (2012a). Plasma membrane localization of *Solanum tuberosum* remorin from group 1, homolog 3 is mediated by

Literature

- conformational changes in a novel C-terminal anchor and required for the restriction of potato virus X movement]. *Plant Physiology* *160*, 624-637.
- Petrasek, J., Mravec, J., Bouchard, R., Blakeslee, J.J., Abas, M., Seifertova, D., Wisniewska, J., Tadele, Z., Kubes, M., Covanova, M., *et al.* (2006). PIN proteins perform a rate-limiting function in cellular auxin efflux. *Science* *312*, 914-918.
- Petutschnig, E.K., Jones, A.M., Serazetdinova, L., Lipka, U., and Lipka, V. (2010). The lysin motif receptor-like kinase (LysM-RLK) CERK1 is a major chitin-binding protein in *Arabidopsis thaliana* and subject to chitin-induced phosphorylation. *The Journal of Biological Chemistry* *285*, 28902-28911.
- Pike, L.J. (2006). Rafts defined: a report on the Keystone Symposium on Lipid Rafts and Cell Function. *Journal of Lipid Research* *47*, 1597-1598.
- Postel, S., K ufner, I., Beuter, C., Mazzotta, S., Schwedt, A., Borlotti, A., Halter, T., Kemmerling, B., and N urnberger, T. (2010). The multifunctional leucine-rich repeat receptor kinase BAK1 is implicated in *Arabidopsis* development and immunity. *European Journal of Cell Biology* *89*, 169-174.
- Pratelli, R., Sutter, J.U., and Blatt, M.R. (2004). A new catch in the SNARE. *Trends in Plant Science* *9*, 187-195.
- Raffaele, S., Bayer, E., Lafarge, D., Cluzet, S., German Retana, S., Boubekeur, T., Leborgne-Castel, N., Carde, J.-P., Lherminier, J., Noiro, E., *et al.* (2009). Remorin, a solanaceae protein resident in membrane rafts and plasmodesmata, impairs potato virus X movement. *The Plant Cell* *21*, 1541-1555.
- Raffaele, S., Mongrand, S., Gamas, P., Niebel, A., and Ott, T. (2007). Genome-wide annotation of remorins, a plant-specific protein family: evolutionary and functional perspectives. *Plant Physiology* *145*, 593-600.
- Reinhardt, D., Pesce, E.R., Stieger, P., Mandel, T., Baltensperger, K., Bennett, M., Traas, J., Friml, J., and Kuhlemeier, C. (2003). Regulation of phyllotaxis by polar auxin transport. *Nature* *426*, 255-260.
- Reuff, M., Mikosch, M., and Homann, U. (2010). Trafficking, lateral mobility and segregation of the plant K channel KAT1. *Plant Biology (Stuttg)* *12 Suppl 1*, 99-104.
- Reymond, P., Kunz, B., Paul-Pletzer, K., Grimm, R., Eckerskorn, C., and Farmer, E.E. (1996). Cloning of a cDNA encoding a plasma membrane-associated, uronide binding phosphoprotein with physical properties similar to viral movement proteins. *The Plant Cell* *8*, 2265-2276.
- Robatzek, S., and Saijo, Y. (2008). Plant immunity from A to Z. *Genome Biology* *9*, 304.
- Rodriguez-Boulan, E., Kreitzer, G., and Musch, A. (2005). Organization of vesicular trafficking in epithelia. *Nature Reviews Molecular Cell Biology* *6*, 233-247.
- Ron, M., and Avni, A. (2004). The receptor for the fungal elicitor ethylene-inducing xylanase is a member of a resistance-like gene family in tomato. *The Plant Cell* *16*, 1604-1615.
- Roppolo, D., De Rybel, B., Tendon, V.D., Pfister, A., Alassimone, J., Vermeer, J.E., Yamazaki, M., Stierhof, Y.D., Beekman, T., and Geldner, N. (2011). A novel protein family mediates Casparian strip formation in the endodermis. *Nature* *473*, 380-383.
- Rosenberger, C.M., Brumell, J.H., and Finlay, B.B. (2000). Microbial pathogenesis: lipid rafts as pathogen portals. *Current Biology* *10*, R823-825.

Literature

- Russinova, E. (2004). Heterodimerization and Endocytosis of *Arabidopsis* Brassinosteroid Receptors BRI1 and AtSERK3 (BAK1). *The Plant Cell ONLINE* 16, 3216-3229.
- Saalbach, G., Erik, P., and Wienkoop, S. (2002). Characterisation by proteomics of peribacteroid space and peribacteroid membrane preparations from pea (*Pisum sativum*) symbiosomes. *Proteomics* 2, 325-337.
- Sako, Y., and Kusumi, A. (1995). Barriers for lateral diffusion of transferrin receptor in the plasma membrane as characterized by receptor dragging by laser tweezers: fence versus tether. *The Journal of Cell Biology* 129, 1559-1574.
- Sako, Y., Nagafuchi, A., Tsukita, S., Takeichi, M., and Kusumi, A. (1998). Cytoplasmic regulation of the movement of E-cadherin on the free cell surface as studied by optical tweezers and single particle tracking: corralling and tethering by the membrane skeleton. *The Journal of Cell Biology* 140, 1227-1240.
- Salmon, M.S., and Bayer, E.M. (2012). Dissecting plasmodesmata molecular composition by mass spectrometry-based proteomics. *Frontiers in Plant Science* 3, 307.
- Sauer, M., Balla, J., Luschnig, C., Wisniewska, J., Reinohl, V., Friml, J., and Benkova, E. (2006). Canalization of auxin flow by Aux/IAA-ARF-dependent feedback regulation of PIN polarity. *Genes & Development* 20, 2902-2911.
- Sazuka, T., Keta, S., Shiratake, K., Yamaki, S., and Shibata, D. (2004). A proteomic approach to identification of transmembrane proteins and membrane-anchored proteins of *Arabidopsis thaliana* by peptide sequencing. *DNA Res* 11, 101-113.
- Scarpella, E., Marcos, D., Friml, J., and Berleth, T. (2006). Control of leaf vascular patterning by polar auxin transport. *Genes & Development* 20, 1015-1027.
- Schlessinger, J. (2000). Cell signaling by receptor tyrosine kinases. *Cell* 103, 211-225.
- Schneider-Poetsch, H.A. (1992). Signal transduction by phytochrome: phytochromes have a module related to the transmitter modules of bacterial sensor proteins. *Photochemistry and Photobiology* 56, 839-846.
- Schroeder, R., London, E., and Brown, D. (1994). Interactions between saturated acyl chains confer detergent resistance on lipids and glycosylphosphatidylinositol (GPI)-anchored proteins: GPI-anchored proteins in liposomes and cells show similar behavior. *Proc Natl Acad Sci USA* 91, 12130-12134.
- Schulze, B., Mentzel, T., Jehle, A.K., Mueller, K., Beeler, S., Boller, T., Felix, G., and Chinchilla, D. (2010). Rapid heteromerization and phosphorylation of ligand-activated plant transmembrane receptors and their associated kinase BAK1. *The Journal of Biological Chemistry* 285, 9444-9451.
- Schwacke, R., and Hager, A. (1992). Fungal elicitors induce a transient release of active oxygen species from cultured spruce cells that is dependent on Ca(2+) and protein-kinase activity. *Planta* 187, 136-141.
- Schwessinger, B., Roux, M., Kadota, Y., Ntoukakis, V., Sklenar, J., Jones, A., and Zipfel, C. (2011). Phosphorylation-dependent differential regulation of plant growth, cell death, and innate immunity by the regulatory receptor-like kinase BAK1. *PLoS Genetics* 7, e1002046.
- Schwessinger, B., and Zipfel, C. (2008). News from the frontline: recent insights into PAMP-triggered immunity in plants. *Current Opinion in Plant Biology* 11, 389-395.
- Shin, J.S., Gao, Z., and Abraham, S.N. (2000). Involvement of cellular caveolae in bacterial entry into mast cells. *Science* 289, 785-788.

Literature

- Shiu, S.H., and Bleecker, A.B. (2001a). Plant receptor-like kinase gene family: diversity, function, and signaling. *Science's STKE : signal transduction knowledge environment* 2001, re22.
- Shiu, S.H., and Bleecker, A.B. (2001b). Receptor-like kinases from *Arabidopsis* form a monophyletic gene family related to animal receptor kinases. *Proc Natl Acad Sci USA* 98, 10763-10768.
- Shiu, S.H., and Bleecker, A.B. (2003). Expansion of the receptor-like kinase/Pelle gene family and receptor-like proteins in *Arabidopsis*. *Plant Physiology* 132, 530-543.
- Silverman, N., and Maniatis, T. (2001). NF-kappaB signaling pathways in mammalian and insect innate immunity. *Genes & Development* 15, 2321-2342.
- Simons, K., and Gerl, M.J. (2010). Revitalizing membrane rafts: new tools and insights. *Nature Reviews Molecular Cell Biology* 11, 688-699.
- Simons, K., and Ikonen, E. (1997). Functional rafts in cell membranes. *Nature* 387, 569-572.
- Singer, S.J., and Nicolson, G.L. (1972). The fluid mosaic model of the structure of cell membranes. *Science* 175, 720-731.
- Singh, P., Kuo, Y.C., Mishra, S., Tsai, C.H., Chien, C.C., Chen, C.W., Desclos-Theveniau, M., Chu, P.W., Schulze, B., Chinchilla, D., *et al.* (2012). The Lectin Receptor Kinase-VI.2 Is Required for Priming and Positively Regulates *Arabidopsis* Pattern-Triggered Immunity. *The Plant Cell* 24, 1256-1270.
- Song, L., Shi, Q.M., Yang, X.H., Xu, Z.H., and Xue, H.W. (2009). Membrane steroid-binding protein 1 (MSBP1) negatively regulates brassinosteroid signaling by enhancing the endocytosis of BAK1. *Cell Research* 19, 864-876.
- Sorek, N., Poraty, L., Sternberg, H., Bar, E., Lewinsohn, E. and Yalovsky, S. (2007). Activation status-coupled transient S-acylation determines membrane partitioning of a plant Rho-related GTPase. *Molecular Cell Biology* 27 (6); 2144-2154.
- Souter, M., Topping, J., Pullen, M., Friml, J., Palme, K., Hackett, R., Grierson, D., and Lindsey, K. (2002). hydra mutants of *Arabidopsis* are defective in sterol profiles and auxin and ethylene signaling. *The Plant Cell* 14, 1017-1031.
- Spira, F., Mueller, N.S., Beck, G., von Olshausen, P., Beig, J., and Wedlich-Soldner, R. (2012). Patchwork organization of the yeast plasma membrane into numerous coexisting domains (vol 14, pg 640, 2012). *Nature Cell Biology* 14, 890-890.
- Spoel, S.H., and Dong, X. (2012). How do plants achieve immunity? Defence without specialized immune cells. *Nature Reviews Immunology* 12, 89-100.
- Staswick, P.E. (2008). JAZing up jasmonate signaling. *Trends in Plant Science* 13, 66-71.
- Sun, Y., Han, Z., Tang, J., Hu, Z., Chai, C., Zhou, B., and Chai, J. (2013a). Structure reveals that BAK1 as a co-receptor recognizes the BRI1-bound brassinolide. *Cell Research* 23, 1326-1329.
- Sun, Y., Li, L., Macho, A.P., Han, Z., Hu, Z., Zipfel, C., Zhou, J.M., and Chai, J. (2013b). Structural basis for flg22-induced activation of the *Arabidopsis* FLS2-BAK1 immune complex. *Science* 342, 624-628.
- Sutter, J.U., Campanoni, P., Tyrrell, M., and Blatt, M.R. (2006). Selective mobility and sensitivity to SNAREs is exhibited by the *Arabidopsis* KAT1 K⁺ channel at the plasma membrane. *The Plant Cell* 18, 935-954.

Literature

- Sutter, J.U., Sieben, C., Hartel, A., Eisenach, C., Thiel, G., and Blatt, M.R. (2007). Abscisic acid triggers the endocytosis of the *Arabidopsis* KAT1 K⁺ channel and its recycling to the plasma membrane. *Current Biology* *17*, 1396-1402.
- Swarup, R., Friml, J., Marchant, A., Ljung, K., Sandberg, G., Palme, K., and Bennett, M. (2001). Localization of the auxin permease AUX1 suggests two functionally distinct hormone transport pathways operate in the *Arabidopsis* root apex. *Genes & Development* *15*, 2648-2653.
- Sweere, U., Eichenberg, K., Lohrmann, J., Mira-Rodado, V., Baurle, I., Kudla, J., Nagy, F., Schafer, E., and Harter, K. (2001). Interaction of the response regulator ARR4 with phytochrome B in modulating red light signaling. *Science* *294*, 1108-1111.
- Tanner, W., Malinsky, J., and Opekarova, M. (2011). In plant and animal cells, detergent-resistant membranes do not define functional membrane rafts. *The Plant Cell* *23*, 1191-1193.
- Tavernier, E., Wendehenne, D., Blein, J.P., and Pugin, A. (1995). Involvement of Free Calcium in Action of Cryptogein, a Proteinaceous Elicitor of Hypersensitive Reaction in Tobacco Cells. *Plant Physiology* *109*, 1025-1031.
- Tena, G., Asai, T., Chiu, W.L., and Sheen, J. (2001). Plant mitogen-activated protein kinase signaling cascades. *Current Opinion in Plant Biology* *4*, 392-400.
- Thilmony, R., Underwood, W., and He, S.Y. (2006). Genome-wide transcriptional analysis of the *Arabidopsis thaliana* interaction with the plant pathogen *Pseudomonas syringae* pv. *tomato* DC3000 and the human pathogen *Escherichia coli* O157:H7. *The Plant Journal* *46*, 34-53.
- Tòth, K., Stratil, T.F., Madsen, E.B., Ye, J., Popp, C., Antolin-Llovera, M., Grossmann, C., Jensen, O.N., Schussler, A., Parniske, M., *et al.* (2012). Functional domain analysis of the Remorin protein LjSYMREM1 in *Lotus japonicus*. *PloS One* *7*, e30817.
- Tsuda, K., Qi, Y., Nguyen le, V., Bethke, G., Tsuda, Y., Glazebrook, J., and Katagiri, F. (2012). An efficient Agrobacterium-mediated transient transformation of *Arabidopsis*. *The Plant Journal* *69*, 713-719.
- Uppalapati, S.R., Ayoubi, P., Weng, H., Palmer, D.A., Mitchell, R.E., Jones, W., and Bender, C.L. (2005). The phytotoxin coronatine and methyl jasmonate impact multiple phytohormone pathways in tomato. *The Plant Journal* *42*, 201-217.
- Urbanus, S.L., and Ott, T. (2012). Plasticity of plasma membrane compartmentalization during plant immune responses. *Frontiers in Plant Science* *3*, 181.
- Utsuno, K., Shikanai, T., Yamada, Y., and Hashimoto, T. (1998). Agr, an Agravitropic locus of *Arabidopsis thaliana*, encodes a novel membrane-protein family member. *Plant & Cell Physiology* *39*, 1111-1118.
- Valot, B., Dieu, M., Recorbet, G., Raes, M., Gianinazzi, S., and Dumas-Gaudot, E. (2005). Identification of membrane-associated proteins regulated by the arbuscular mycorrhizal symbiosis. *Plant Molecular Biology* *59*, 565-580.
- Valot, B., Negroni, L., Zivy, M., Gianinazzi, S., and Dumas-Gaudot, E. (2006). A mass spectrometric approach to identify arbuscular mycorrhiza-related proteins in root plasma membrane fractions. *Proteomics* *6 Suppl 1*, S145-155.
- van der Hoorn, R.A., and Kamoun, S. (2008). From Guard to Decoy: a new model for perception of plant pathogen effectors. *The Plant Cell* *20*, 2009-2017.
- Varma, R., and Mayor, S. (1998). GPI-anchored proteins are organized in submicron domains at the cell surface. *Nature* *394*, 798-801.

Literature

- Wang, D., Pajerowska-Mukhtar, K., Culler, A.H., and Dong, X. (2007). Salicylic acid inhibits pathogen growth in plants through repression of the auxin signaling pathway. *Current Biology* *17*, 1784-1790.
- Wang, X., and Chory, J. (2006). Brassinosteroids regulate dissociation of BKI1, a negative regulator of BRI1 signaling, from the plasma membrane. *Science* *313*, 1118-1122.
- Wang, X., Kota, U., He, K., Blackburn, K., Li, J., Goshe, M.B., Huber, S.C., and Clouse, S.D. (2008). Sequential transphosphorylation of the BRI1/BAK1 receptor kinase complex impacts early events in brassinosteroid signaling. *Developmental Cell* *15*, 220-235.
- Watson, B.S., Asirvatham, V.S., Wang, L., and Sumner, L.W. (2003). Mapping the proteome of barrel medic (*Medicago truncatula*). *Plant Physiology* *131*, 1104-1123.
- Went, F.W. (1974). Reflections and Speculations. *Annual review of Plant Physiology and Plant Molecular Biology* *25*, 1-26.
- Widjaja, I., Naumann, K., Roth, U., Wolf, N., Mackey, D., Dangl, J.L., Scheel, D., and Lee, J. (2009). Combining subproteome enrichment and Rubisco depletion enables identification of low abundance proteins differentially regulated during plant defense. *Proteomics* *9*, 138-147.
- Willemsen, V., Friml, J., Grebe, M., van den Toorn, A., Palme, K., and Scheres, B. (2003). Cell polarity and PIN protein positioning in *Arabidopsis* require STEROL METHYLTRANSFERASE1 function. *The Plant Cell* *15*, 612-625.
- Willmann, R., Lajunen, H.M., Erbs, G., Newman, M.A., Kolb, D., Tsuda, K., Katagiri, F., Fliegmann, J., Bono, J.J., Cullimore, J.V., *et al.* (2011). *Arabidopsis* lysin-motif proteins LYM1 LYM3 CERK1 mediate bacterial peptidoglycan sensing and immunity to bacterial infection. *Proc Natl Acad Sci USA* *108*, 19824-19829.
- Wisniewska, J., Xu, J., Seifertova, D., Brewer, P.B., Ruzicka, K., Blilou, I., Rouquie, D., Benkova, E., Scheres, B., and Friml, J. (2006). Polar PIN localization directs auxin flow in plants. *Science* *312*, 883-883.
- Xiang, T., Zong, N., Zhang, J., Chen, J., Chen, M., and Zhou, J.M. (2011). BAK1 is not a target of the *Pseudomonas syringae* effector AvrPto. *Molecular Plant-Microbe Interactions* *24*, 100-107.
- Xiang, T., Zong, N., Zou, Y., Wu, Y., Zhang, J., Xing, W., Li, Y., Tang, X., Zhu, L., Chai, J., *et al.* (2008). *Pseudomonas syringae* effector AvrPto blocks innate immunity by targeting receptor kinases. *Current Biology* *18*, 74-80.
- Yamada, H., Hanaki, N., Imamura, A., Ueguchi, C., and Mizuno, T. (1998). An *Arabidopsis* protein that interacts with the cytokinin-inducible response regulator, ARR4, implicated in the His-Asp phosphorylay signal transduction. *FEBS Letters* *436*, 76-80.
- Yeh, K.C., Wu, S.H., Murphy, J.T., and Lagarias, J.C. (1997). A cyanobacterial phytochrome two-component light sensory system. *Science* *277*, 1505-1508.
- Zacharias, D.A., Violin, J.D., Newton, A.C., and Tsien, R.Y. (2002). Partitioning of lipid-modified monomeric GFPs into membrane microdomains of live cells. *Science* *296*, 913-916.
- Zhang, J., Li, W., Xiang, T., Liu, Z., Laluk, K., Ding, X., Zou, Y., Gao, M., Zhang, X., Chen, S., *et al.* (2010). Receptor-like cytoplasmic kinases integrate signaling

Literature

- from multiple plant immune receptors and are targeted by a *Pseudomonas syringae* effector. *Cell Host & Microbe* 7, 290-301.
- Zhang, S., and Klessig, D.F. (2001). MAPK cascades in plant defense signaling. *Trends in Plant Science* 6, 520-527.
- Zhang, Y., Immink, R., Liu, C.M., Emons, A.M., and Ketelaar, T. (2013). The *Arabidopsis* exocyst subunit SEC3A is essential for embryo development and accumulates in transient puncta at the plasma membrane. *The New Phytologist* 199, 74-88.
- Zhou, J.M., and Chai, J. (2008). Plant pathogenic bacterial type III effectors subdue host responses. *Current Opinion in Microbiology* 11, 179-185.
- Zinchuk, V., Zinchuk, O., and Okada, T. (2007). Quantitative colocalization analysis of multicolor confocal immunofluorescence microscopy images: Pushing pixels to explore biological phenomena. *Acta Histochem Cytoc* 40, 101-111.
- Zipfel, C., and Felix, G. (2005). Plants and animals: a different taste for microbes? *Current Opinion in Plant Biology* 8, 353-360.
- Zipfel, C., Kunze, G., Chinchilla, D., Caniard, A., Jones, J.D.G., Boller, T., and Felix, G. (2006). Perception of the bacterial PAMP EF-Tu by the receptor EFR restricts *Agrobacterium*-mediated transformation. *Cell* 125, 749-760.
- Zipfel, C., Robatzek, S., Navarro, L., Oakeley, E.J., Jones, J.D., Felix, G., and Boller, T. (2004). Bacterial disease resistance in *Arabidopsis* through flagellin perception. *Nature* 428, 764-767.

Publications:

Parts of this work have been published in the following peer-reviewed scientific articles:

Jarsch IK and Ott T (2011), review article

Perspectives on remorin proteins, membrane rafts and their role during plant-microbe interactions

Molecular Plant Microbe Interactions, 24(1): 7-12

Jarsch IK et al., scientific article

Plasma Membranes Are Subcompartmentalized into a Plethora of Coexisting and Diverse Microdomains in Arabidopsis and Nicotiana benthamiana

The Plant Cell; doi:10.1105/tpc.114.124446

Konrad SSA, Popp C, Stratil TF, **Jarsch IK** et al., scientific article

S-acylation anchors Remorin proteins to the plasma membrane but does not primarily determine their localization in membrane domains.

New Phytologist, *in press*

Appendix

List of constructs

Insert	Vector	Resistance	Origin
AtREM1.2 – stop cds	pENTR-D®	Kan	Jarsch 2009
AtREM1.2 + stop cds	pKSi	Gent	Karl-Heinz Braun
AtREM1.2ΔREMCA -stop cds	pDONR207	Gent	this study
proAtREM1.2:AtREM1.2 – stop gDNA	pDONR207	Gent	this study
AtREM1.2:CFP cds	pAM-PAT-35S:GW:CFP	Carb	Jarsch 2009
AtREM1.2ΔREMCA:CFP cds	pAM-PAT-35S:GW:CFP	Carb	this study
CFP:AtREM1.2 cds	pAM-PAT-35S:CFP:GW	Carb	this study
YFP:AtREM1.2 cds	pAM-PAT-35S:YFP:GW	Carb	this study
YFP:AtREM1.2 cds	pUbi:YFP:GW	Kan/Hyg	this study
GAL4 AD:AtREM1.2 cds	pGADT7	carb	this study
proAtREM1.2:AtREM1.2 gDNA	pH7YGW2	Spec/Hyg	this study
proAtREM1.2:YFP:AtREM1.2 gDNA	pGWB1	Kan/Hyg	Sebastian Konrad
AtREM1.3 – stop cds	pENTR-D®	Kan	Jarsch 2009
AtREM1.3 + stop cds	pKSi	Gent	Karl-Heinz Braun
AtREM1.3ΔREMCA -stop cds	pDONR207	Gent	this study
proAtREM1.3:AtREM1.3 – stop gDNA	pDONR207	Gent	this study
AtREM1.3:CFP cds	pAM-PAT-35S:GW:CFP	Carb	Jarsch 2009
CFP:AtREM1.3 cds	pAM-PAT-35S:CFP:GW	Carb	this study
YFP:AtREM1.3 cds	pAM-PAT-35S:YFP:GW	Carb	Seeholzer, 2012
GAL4 AD:AtREM1.3 cds	pGADT7	carb	this study
AtREM1.3ΔREMCA:CFP cds	pAM-PAT-35S:GW:CFP	Carb	this study

Appendix

proAtREM1.3:AtREM1.3 gDNA	pH7YGW2	Spec/Hyg	this study
proAtREM1.3:YFP:AtREM1.3 gDNA	pGWB1	Kan/Hyg	Sebastian Konrad
AtREM1.4 – stop cds	pDONR207	Gent	Macarena Marin
AtREM1.4 + stop cds	pDONR207	Gent	this study
AtREM1.4:CFP cds	pAM-PAT-35S:GW:CFP	Carb	this study
CFP:AtREM1.4 cds	pAM-PAT-35S:CFP:GW	Carb	this study
AtREM3.1 – stop cds	pDONR207	Gent	Macarena Marin
AtREM3.1 + stop cds	pKSi	Gent	Karl-Heinz Braun
proAtREM3.1:AtREM3.1 – stop gDNA	pDONR207	Gent	this study
AtREM3.1:CFP cds	pAM-PAT-35S:GW:CFP	Carb	this study
CFP:AtREM3.1 cds	pAM-PAT-35S:CFP:GW	Carb	this study
GAL4 AD:AtREM3.1 cds	pGADT7	carb	this study
proAtREM3.1:AtREM3.1 gDNA	pH7YGW2	Spec/Hyg	this study
AtREM3.2 – stop cds	pENTR-D®	Kan	Jarsch 2009
AtREM3.2 + stop cds	pKSi	Gent	Karl-Heinz Braun
proAtREM3.2:AtREM3.2 – stop gDNA	pDONR207	Gent	this study
AtREM3.2:CFP cds	pAM-PAT-35S:GW:CFP	Carb	Jarsch 2009
CFP:AtREM3.2 cds	pAM-PAT-35S:CFP:GW	Carb	this study
YFP:AtREM3.2 CDS	pAM-PAT-35S:YFP:GW	Carb	this study
YFP:AtREM3.2 cds	pUbi:YFP:GW	Kan/Hyg	this study
GAL4 AD:AtREM3.2 cds	pGADT7	carb	this study
proAtREM3.2:AtREM3.2 gDNA	pH7YGW2	Spec/Hyg	this study
AtREM4.1 – stop cds	pENTR-D®	Kan	Jarsch 2009
AtREM4.1 + stop cds	pKSi	Gent	Karl-Heinz Braun
AtREM4.1:CFP cds	pAM-PAT-35S:GW:CFP	Carb	Jarsch 2009

Appendix

CFP:AtREM4.1cds	pAM-PAT-35S:CFP:GW	Carb	this study
YFP:AtREM4.1 cds	pAM-PAT-35S:YFP:GW	Carb	this study
YFP:AtREM4.1 cds	pUbi:YFP:GW	Kan/Hyg	this study
GAL4 AD:AtREM4.1 cds	pGADT7	carb	this study
AtREM4.2 – stop cds	pENTR-D®	Kan	Jarsch 2009
AtREM4.2 + stop cds	pKSi	Gent	Karl-Heinz Braun
AtREM4.2ΔREMCA -stop cds	pDONR207	Gent	this study
AtREM4.2:CFP cds	pAM-PAT-35S:GW:CFP	Carb	Jarsch 2009
CFP:AtREM4.2cds	pAM-PAT-35S:CFP:GW	Carb	this study
YFP:AtREM4.2 cds	pAM-PAT-35S:YFP:GW	Carb	this study
YFP:AtREM4.2 cds	pUbi:YFP:GW	Kan/Hyg	this study
AtREM4.2ΔREMCA:CFP cds	pAM-PAT-35S:GW:CFP	Carb	this study
GAL4 AD:AtREM4.2 cds	pGADT7	carb	this study
AtREM5.1 – stop cds	pENTR-D®	Kan	Jarsch 2009
AtREM5.1 + stop cds	pENTR-D®	Kan	this study
AtREM5.1:CFP cds	pAM-PAT-35S:GW:CFP	Carb	Jarsch 2009
CFP:AtREM5.1cds	pAM-PAT-35S:CFP:GW	Carb	this study
YFP:AtREM5.1 cds	pAM-PAT-35S:YFP:GW	Carb	this study
YFP:AtREM5.1 cds	pUbi:YFP:GW	Kan/Hyg	this study
AtREM6.1 – stop cds	pENTR-D®	Kan	Jarsch 2009
AtREM6.1 + stop cds	pKSi	Gent	Karl-Heinz Braun
AtREM6.1ΔREMCA -stop cds	pDONR207	Gent	this study
AtREM6.1:CFP cds	pAM-PAT-35S:GW:CFP	Carb	Jarsch 2009
CFP:AtREM6.1cds	pAM-PAT-35S:CFP:GW	Carb	this study
YFP:AtREM6.1 cds	pAM-PAT-35S:YFP:GW	Carb	this study
YFP:AtREM6.1 cds	pUbi:YFP:GW	Kan/Hyg	this study

Appendix

AtREM6.1ΔREMCA:CFP cds	pAM-PAT-35S:GW:CFP	Carb	this study
AtREM6.2 – stop cds	pENTR-D®	Kan	Jarsch 2009
AtREM6.2 + stop cds	pENTR-D®	Kan	this study
AtREM6.2:CFP cds	pAM-PAT-35S:GW:CFP	Carb	Jarsch 2009
CFP:AtREM6.2cds	pAM-PAT-35S:CFP:GW	Carb	this study
YFP:AtREM6.2 cds	pAM-PAT-35S:YFP:GW	Carb	this study
YFP:AtREM6.2 cds	pUbi:YFP:GW	Kan/Hyg	this study
AtREM6.3 – stop cds	pENTR-D®	Kan	Jarsch 2009
AtREM6.3 + stop cds	pENTR-D®	Kan	this study
AtREM6.3:CFP cds	pAM-PAT-35S:GW:CFP	Carb	Jarsch 2009
CFP:AtREM6.3cds	pAM-PAT-35S:CFP:GW	Carb	this study
YFP:AtREM6.3 cds	pAM-PAT-35S:YFP:GW	Carb	this study
YFP:AtREM6.3 cds	pUbi:YFP:GW	Kan/Hyg	this study
AtREM6.4 – stop cds	pENTR-D®	Kan	Jarsch 2009
AtREM6.4 + stop cds	pDONR207	Gent	this study
AtREM6.4ΔREMCA -stop cds	pDONR207	Gent	this study
AtREM6.4ΔREMCA +stop cds	pDONR207	Gent	this study
AtREM6.4REMCA -stop cds	pDONR207	Gent	this study
AtREM6.4ΔC-term -stop cds	pDONR207	Gent	this study
AtREM6.4ΔN-term -stop cds	pDONR207	Gent	this study
AtREM6.4ΔN-term +stop cds	pDONR207	Gent	this study
AtREM6.4ΔN-termΔREMCA -stop cds	pDONR207	Gent	this study
AtREM6.4T215A + stop cds	pDONR207	Gent	this study
AtREM6.4T215D + stop cds	pDONR207	Gent	this study
proAtREM6.4:AtREM6.4 – stop gDNA	pDONR207	Gent	this study
AtREM6.4:CFP cds	pAM-PAT-35S:GW:CFP	Carb	Jarsch 2009
AtREM6.4ΔREMCA:CFP cds	pAM-PAT-35S:GW:CFP	Carb	this study
CFP:AtREM6.4 cds	pAM-PAT-	Carb	this study

Appendix

	35S:CFP:GW		
YFP:AtREM6.4 cds	pAM-PAT-35S:YFP:GW	Carb	this study
YFP:AtREM6.4 cds	pUbi:YFP:GW	Carb	this study
AtREM6.4ΔREMCA +stop cds	pDONR207	Carb	this study
AtREM6.4REMCA:CFP	pAM-PAT-35S:GW:CFP	Carb	this study
YFP:AtREM6.4REMCA	pAM-PAT-35S:YFP:GW	Carb	Sebastian Konrad
AtREM6.4ΔC-term:CFP cds	pAM-PAT-35S:GW:CFP	Carb	this study
AtREM6.4ΔN-term:CFP cds	pAM-PAT-35S:GW:CFP	Carb	this study
YFP:AtREM6.4ΔN-term cds	pAM-PAT-35S:YFP:GW	Carb	this study
AtREM6.4ΔN-termΔREMCA:YFP cds	pAM-PAT-35S:GW:YFP	Carb	this study
YFP:AtREM6.4T215A cds	pAM-PAT-35S:YFP:GW	Carb	this study
YFP:AtREM6.4T215D cds	pAM-PAT-35S:YFP:GW	Carb	this study
YFPc:AtREM6.4T215A cds	pAM-PAT-35S:YFPc:GW	Carb	this study
YFPc:AtREM6.4T215D cds	pAM-PAT-35S:YFPc:GW	Carb	this study
YFPn:AtREM6.4T215A cds	pAM-PAT-35S:YFPn:GW	Carb	this study
YFPn:AtREM6.4T215D cds	pAM-PAT-35S:YFPn:GW	Carb	this study
GAL4 AD:AtREM6.4ΔREMCA cds	pGADT7	carb	this study
proAtREM6.4:AtREM6.4 gDNA	pH7YGW2	Spec/Hyg	this study
proAtREM6.4:YFP:AtREM6.4 gDNA	pGWB1	Kan/Hyg	Sebastian Konrad
AtREM6.5 – stop cds	pENTR-D®	Kan	this study
AtREM6.5 + stop cds	pENTR-D®	Kan	this study
AtREM6.6:YFP cds	pAM-PAT-35S:GW:YFP	Carb	this study
YFP:AtREM6.5 cds	pAM-PAT-35S:YFP:GW	Carb	this study
YFP:AtREM6.5 cds	pUbi:YFP:GW	Kan/Hyg	this study
AtREM6.6 – stop genomic	pDONR207	Gent	this study

Appendix

AtREM6.6 + stop genomic	pDONR207	Gent	this study
AtREM6.6:CFP genomic	pAM-PAT-35S:GW:CFP	Carb	this study
YFP:AtREM6.6 genomic	pAM-PAT-35S:YFP:GW	Carb	this study
YFP:AtREM6.6 genomic	pUbi:YFP:GW	Kan/Hyg	this study
AtREM6.7 – stop cds	pENTR-D®	Kan	Jarsch 2009
AtREM6.7 + stop cds	pDONR207	Gent	Macarena Marin
AtREM6.7:CFP cds	pAM-PAT-35S:GW:CFP	Carb	Jarsch 2009
CFP:AtREM6.7 cds	pAM-PAT-35S:CFP:GW	Carb	this study
YFP:AtREM6.7 cds	pAM-PAT-35S:YFP:GW	Carb	this study
YFP:AtREM6.7 cds	pUbi:YFP:GW	Kan/Hyg	this study
BAK1 –stop genomic	pDONR201	Kan	Jarsch 2009
BAK1:YFPc genomic	pAM-PAT-35S:GW:YFPc	Carb	Jarsch 2009
BAK1:YFPn genomic	pAM-PAT-35S:GW:YFPn	Carb	Jarsch 2009
BRI1 –stop cds	pENTR-D®	Kan	Jarsch 2009
BRI1:YFPc	pAM-PAT-35S:GW:YFPc	Carb	Jarsch 2009
BRI1:YFPc	pAM-PAT-35S:GW:YFPn	Carb	Jarsch 2009
FLS2 –stop cds	pENTR-D®	Kan	Jarsch 2009
FLS2:YFPc	pAM-PAT-35S:GW:YFPc	Carb	Jarsch 2009
FLS2:YFPc	pAM-PAT-35S:GW:YFPn	Carb	Jarsch 2009
EFR –stop cds	pENTR-D®	Kan	Jarsch 2009
EFR:YFPc	pAM-PAT-35S:GW:YFPc	Carb	Jarsch 2009
EFR:YFPc	pAM-PAT-35S:GW:YFPn	Carb	Jarsch 2009
KAT1-CFP genomic	pAM-PAT-35S:GW:CFP	Carb	Sebastian Konrad
KAT1-YFP genomic	pAM-PAT-35S:GW:YFP	Carb	Sebastian Konrad
FLOT1A-CFP genomic	pAM-PAT-	Carb	Sebastian

Appendix

	35S:GW:CFP		Konrad
FLOT1A-YFP genomic	pAM-PAT-35S:GW:YFP	Carb	Sebastian Konrad
FLOT1B-CFP genomic	pAM-PAT-35S:GW:CFP	Carb	Sebastian Konrad
FLOT1B-YFP genomic	pAM-PAT-35S:GW:YFP	Carb	Sebastian Konrad
Free YFP + stop	pAM-PAT-35S:YFP w/o GW	Carb	Sebastian Konrad
YFP:SYMREM1REMCA cds	pUbi:YFP:GW	Kan/Hyg	Claudia Popp
GAL4 BD:At1g51820KDSC	pGBKT7	Kan	B. Kemmerling, Tübingen
GAL4 BD:At4g28490KDSC	pGBKT7	Kan	B. Kemmerling, Tübingen
GAL4 BD:At3g28450KDSC	pGBKT7	Kan	B. Kemmerling, Tübingen
GAL4 BD:At2g13790KDSC	pGBKT7	Kan	B. Kemmerling, Tübingen
GAL4 BD:At5g48380KDSC	pGBKT7	Kan	B. Kemmerling, Tübingen
GAL4 BD:At1g51860KDSC	pGBKT7	Kan	B. Kemmerling, Tübingen
GAL4 BD:At1g56140KDSC	pGBKT7	Kan	B. Kemmerling, Tübingen
GAL4 BD:At3g02880KDSC	pGBKT7	Kan	B. Kemmerling, Tübingen
GAL4 BD:At1g51790KDSC	pGBKT7	Kan	B. Kemmerling, Tübingen
GAL4 BD:At1g09970KDSC	pGBKT7	Kan	B. Kemmerling, Tübingen
GAL4 BD:At1g17750KDSC	pGBKT7	Kan	B. Kemmerling, Tübingen
GAL4 BD:At5g53320KDSC	pGBKT7	Kan	B. Kemmerling, Tübingen
GAL4 BD:At1g17230KDSC	pGBKT7	Kan	B. Kemmerling, Tübingen
GAL4 BD:At1g34420KDSC	pGBKT7	Kan	B. Kemmerling, Tübingen
GAL4 BD:At1g55610KDSC	pGBKT7	Kan	B. Kemmerling, Tübingen
GAL4 BD:At1g56130KDSC	pGBKT7	Kan	B. Kemmerling, Tübingen
GAL4 BD:At2g13800KDSC	pGBKT7	Kan	B. Kemmer-

Appendix

			ling, Tübingen
GAL4 BD:At1g53420KDSC	pGBKT7	Kan	B. Kemmerling, Tübingen
GAL4 BD:At2g41820KDSC	pGBKT7	Kan	B. Kemmerling, Tübingen
GAL4 BD:At2g24130KDSC	pGBKT7	Kan	B. Kemmerling, Tübingen
GAL4 BD:At1g67510KDSC	pGBKT7	Kan	B. Kemmerling, Tübingen
GAL4 BD:At1g66830KDSC	pGBKT7	Kan	B. Kemmerling, Tübingen
GAL4 BD:At1g73080KDSC	pGBKT7	Kan	B. Kemmerling, Tübingen
GAL4 BD:At1g56120KDSC	pGBKT7	Kan	B. Kemmerling, Tübingen
GAL4 BD:At1g71830KDSC	pGBKT7	Kan	B. Kemmerling, Tübingen
GAL4 BD:At1g24650KDSC	pGBKT7	Kan	B. Kemmerling, Tübingen
GAL4 BD:At5g25930KDSC	pGBKT7	Kan	B. Kemmerling, Tübingen
GAL4 BD:At2g25790KDSC	pGBKT7	Kan	B. Kemmerling, Tübingen
GAL4 BD:At1g53440KDSC	pGBKT7	Kan	B. Kemmerling, Tübingen
GAL4 BD:At1g51870KDSC	pGBKT7	Kan	B. Kemmerling, Tübingen
GAL4 BD:At1g51800KDSC	pGBKT7	Kan	B. Kemmerling, Tübingen
GAL4 BD:At1g53430KDSC	pGBKT7	Kan	B. Kemmerling, Tübingen
GAL4 BD:At3g14840KDSC	pGBKT7	Kan	B. Kemmerling, Tübingen
GAL4 BD:At1g12460KDSC	pGBKT7	Kan	B. Kemmerling, Tübingen
GAL4 BD:At4g33430KDSC	pGBKT7	Kan	B. Kemmerling, Tübingen
GAL4 BD:At1g69270KDSC	pGBKT7	Kan	B. Kemmerling, Tübingen
GAL4 BD:At4g03390KDSC	pGBKT7	Kan	B. Kemmerling, Tübingen
GAL4 BD:At1g69990KDSC	pGBKT7	Kan	B. Kemmerling, Tübingen

Appendix

GAL4 BD:At2g23300KDSC	pGBKT7	Kan	B. Kemmerling, Tübingen
GAL4 BD:At3g13380KDSC	pGBKT7	Kan	B. Kemmerling, Tübingen
GAL4 BD:At3g56100KDSC	pGBKT7	Kan	B. Kemmerling, Tübingen
GAL4 BD:At5g07280KDSC	pGBKT7	Kan	B. Kemmerling, Tübingen
GAL4 BD:At3g25560KDSC	pGBKT7	Kan	B. Kemmerling, Tübingen
GAL4 BD:At1g34210KDSC	pGBKT7	Kan	B. Kemmerling, Tübingen
GAL4 BD:At1g75640KDSC	pGBKT7	Kan	B. Kemmerling, Tübingen
GAL4 BD:At5g59670KDSC	pGBKT7	Kan	B. Kemmerling, Tübingen
GAL4 BD:At1g51880KDSC	pGBKT7	Kan	B. Kemmerling, Tübingen
GAL4 BD:At3g46370KDSC	pGBKT7	Kan	B. Kemmerling, Tübingen
GAL4 BD:At2g31880KDSC	pGBKT7	Kan	B. Kemmerling, Tübingen
GAL4 BD:At3g47580KDSC	pGBKT7	Kan	B. Kemmerling, Tübingen
GAL4 BD:At1g51830KDSC	pGBKT7	Kan	B. Kemmerling, Tübingen
GAL4 BD:At1g35710KDSC	pGBKT7	Kan	B. Kemmerling, Tübingen
GAL4 BD:At3g02130KDSC	pGBKT7	Kan	B. Kemmerling, Tübingen
GAL4 BD:At5g46330KDSC	pGBKT7	Kan	B. Kemmerling, Tübingen
GAL4 BD:At1g51850KDSC	pGBKT7	Kan	B. Kemmerling, Tübingen

Appendix

List of primers

cloning of overexpression constructs

	F	R	
AtREM1.2	CACC ATG GCGGAGGAACAGAAGA	TTA GAAACATCCACAAGTTGCCTT	2
atREM1.3	CACC ATG GCGGAGGAGCAAAAGAC	TTA GAAACATCCACACGTTGCCTT	2
AtREM1.4	GGGACAAGTTTGTACAAAAAAGCAGGCTC CATG GCTGAAGAGGAACCG	GGGGACCACTTTGTACAAGAAAGCTGGGTTT T ACATGCATCCGAAAAGC	3
AtREM3.1	GGGACAAGTTTGTACAAAAAAGCAGGCTC CATG AACGAATCCACAGTGC	GGGGACCACTTTGTACAAGAAAGCTGGGTT T AGAGGCATGTAGAGGGTTCC	3
AtREM3.2	GGCGCGCTACC ATG GAGCCAAATATTCCG ATCC	CGTTTAAAC CTTA GAAAGAGAGAAGAATGTA	1
AtREM4.1	GGCGCGCTACC ATG TTGACTTTGTACGGTC A	CGTTTAAAC CTTA GAAAGAGAGAAGAATGTA C	1
AtREM4.2	GGCGCGCTACC ATG CTGACTCTTACCATC AAG	CGTTTAAAC CTTA GGAGAAAGAGAAGAAGGA GC	1
AtREM5.1	GGCGCGCTACC ATG CCGTGGAGTCATCG TAC	CGTTTAAAC CTTA GAAATACATGGCAGGTGAAG C	1
AtREM6.1	GGCGCGCTACC ATG GATTACGAACGAATC GG	GGCGCGC CTTA AGAACAAAAGCTAAAGC	1
AtREM6.2	GGCGCGCTACC ATG GATTACGAGAGGATA CAG	CGTTTAAAC CTTA TGAGAACCAACCACAACA	1
ATREM6.3	GGCGCGCTACC ATG GACTTCACAAGAAAC AG	CGTTTAAAC CTTA ATGACAAGTATTATTGC	1
AtREM6.4	GGGACAAGTTTGTACAAAAAAGCAGGCTC CATG AGAAAGACTTCTGTTTC	GGGGACCACTTTGTACAAGAAAGCTGGGTT T AGAGAGCAGAAGAAGATTTTC	3
AtREM6.5	CACC ATG AGATCTAGTGTAGAAG	TTA TTGACACCAACAACGAG	2
AtREM6.6	GGGACAAGTTTGTACAAAAAAGCAGGCTC CATG GATACCTTAATCAAGC	GGGGACCACTTTGTACAAGAAAGCTGGGTT T AGAAACAGCATGCATTTTC	3
AtREM6.7	GGGACAAGTTTGTACAAAAAAGCAGGCTC CATG GATAATTTGGTTAAGC	GGGGACCACTTTGTACAAGAAAGCTGGGTT T AGTAACACCGAAAAGCAGAAA	3
KAT1	GGGACAAGTTTGTACAAAAAAGCAGGCTT AATG TCGATCTCTGGACTCG	GGGGACCACTTTGTACAAGAAAGCTGGG TTAT TTGATGAAAAATACAAATGATCACC	3
FLOT1A	TTTGGTCTCTACC ATG TTCAAAGTTGCAAG AGC	AAAGGTCTCACCTTCTGCTGAGTCACTTGC	4
FLOT1B	TTTGGTCTCTACC ATG TTCAAAGTTGCAAG AGC	AAAGGTCTCACCTTCTGCTTAGAGTACCGATC C	4

cloning of truncation constructs

AtREM1.2ΔREMCA	GGGACAAGTTTGTACAAAAAAGCAGGC TCC ATG GCGGAGGAACAGAAG	GGGGACCACTTTGTACAAGAAAGCTGGGTT T TTACTTAGCTTCAATCATGCTCTTCTC	3
AtREM1.3ΔREMCA	GGGACAAGTTTGTACAAAAAAGCAGGC TCC ATG GCGGAGGAGCAAAAG	GGGGACCACTTTGTACAAGAAAGCTGGGTT T TTATTTAGCTTCAACCATGCTCTC	3
AtREM4.2ΔREMCA	GGGACAAGTTTGTACAAAAAAGCAGGC TCC ATG CTGACTCTTACCATCAAG	GGGGACCACTTTGTACAAGAAAGCTGGGTT T TTACTTTGCCTCTGCCGCTC	3
AtREM6.1ΔREMCA	GGGACAAGTTTGTACAAAAAAGCAGGC TCC ATG GATTACGAACGAATCGG	GGGGACCACTTTGTACAAGAAAGCTGGGTT T TTACTTTGCTTCAAGCCGCTGCT	3
AtREM6.4ΔREMCA	GGGACAAGTTTGTACAAAAAAGCAGGC TCC ATG AGAAAGACTTCTGTTTC	GGGGACCACTTTGTACAAGAAAGCTGGGTT T TTACTTTGCTTCAAGCCGCTGCT	3
AtREM6.4ΔC-term	GGGACAAGTTTGTACAAAAAAGCAGGC TCC ATG AGAAAGACTTCTGTTTC	GGGGACCACTTTGTACAAGAAAGCTGGGTT T TTACTTTGCTTCAAGCCGCTGCT	3
AtREM6.4ΔNterm	GGGACAAGTTTGTACAAAAAAGCAGGC TCC ATG TCTGCTTCTTCTTCTTCTTGGG	GGGGACCACTTTGTACAAGAAAGCTGGGTT T TTACTTTGCTTCAAGCCGCTGCT	3
AtREM6.4ΔNtermΔREMCA	GGGACAAGTTTGTACAAAAAAGCAGGC TCC ATG TCTGCTTCTTCTTCTTCTTGGG	GGGGACCACTTTGTACAAGAAAGCTGGGTT T TTACTTTGCTTCAAGCCGCTGCT	3

cloning of pro:YFP:ORF constructs

proAtREM1.2	TTTGGTCTCTACCGTTGGCCGCTGTTG	AAAGGTCTCTGTGCTGCTCAGCCGCTCAGCC	4
AtREM1.2	TTTGGTCTCGAAT ATG GCGGAGGAACAG	AAAGGTCTCACCT TTA GAAACATCCACAAGTT GC	4
proAtREM1.3	TTTGGTCTCTACCGGTATTCCTATGCTCAA ATC	AAAGGTCTCTGTGCTGCTCAGCCGAAGAA GAAG	4
AtREM1.3	TTTGGTCTCAGAAT ATG GCGGAGGAGCAAA AG	AAAGGTCTCACCT TTA GAAACATCCACAGTT GC	4

Appendix

proAtREM6.4	TTTGGTCTCTCACCTGCGTTGCATCGTTCGT GA	AAAGGTCTCTTGTCTGTTGGTTTCTCAAAGAAC AAAATC	4
AtREM6.4	TTTGGTCTCAGAATATGAGAAAGACTTCTGT TTC	AAAGGTCTCACCTTACTGAGAGCAGAAGAAGA TTTTC	4
YFP	TTTGGTCTCTGACAATGGTGAGCAAGGGCG AGG	AAAGGTCTCTATTCCCTGTACAGCTCGTCCATG C	4

1= for cloning into pksi

2= for cloning into pENTR-D

3= for cloning into pDONR207

4= for cloning into pENTR-D Bsal

Appendix

Biological material:

bacterial and yeast strains

species	strain	Marker	growth cond.	purpose of use
<i>Agrobacterium tumefaciens</i>	Agl1	Rif, Carb	28°C	transient and stable transformation of <i>A. thaliana</i> and <i>N. benthamiana</i>
<i>Agrobacterium tumefaciens</i>	GV3101 mp90RT	Rif, Kan, Gent	28°C	transient transformation
<i>Agrobacterium tumefaciens</i>	UJA143	Rif, Kan, Gent	28°C	stable transformation of <i>A. thaliana</i>
<i>Escherichia coli</i>	DH5a	-	37°C	plasmid multiplication and maintenace
<i>Escherichia coli</i>	TOP10	-	37°C	plasmid multiplication and maintenace
<i>Escherichia coli</i>	DB3.1	-	37°C	plasmid multiplication and maintenace
<i>Saccharomyces cerevisiae</i>	pJ69-4a	Leu, Trp, His, Ala	30°C	interaction studies

plant lines

species	Ecotype	Background	marker	Transgene	Id.
<i>A. thaliana</i>	Col-0	Wildtype	-	-	-
<i>A. thaliana</i>	Col-0	<i>Atrem1.2-1</i>	Kan	SALK-TDNA	SALK_117637.50.50.x
<i>A. thaliana</i>	Col-0	<i>Atrem1.2-2</i>	Kan	SALK-TDNA	SALK_117639.51.85.x
<i>A. thaliana</i>	Col-0	<i>Atrem1.3-2</i>	Kan	SALK-TDNA	SALK_117448.53.95.x
<i>A. thaliana</i>	Col-0	<i>Atrem1.4-3</i>	Kan	SALK-TDNA	SALK_063841.47.35.x
<i>A. thaliana</i>	Col-0	<i>Atrem3.1-2</i>	Kan	SALK-TDNA	SALK_038891
<i>A. thaliana</i>	Col-0	<i>Atrem3.2-1</i>	Kan	FLAG-TDNA	SALK_045695
<i>A. thaliana</i>	Ws-0	<i>Atrem3.2-4</i>	Kan	SALK-TDNA	FLAG275H05
<i>A. thaliana</i>	Col-0	<i>Atrem4.1-1</i>	Kan	SALK-TDNA	SALK_043600.49.90.x
<i>A. thaliana</i>	Col-0	<i>Atrem4.2-2</i>	Kan	SALK-TDNA	SALK_064620.54.00.x
<i>A. thaliana</i>	Col-0	<i>Atrem6.3-2</i>	Kan	SALK-TDNA	SALK_017747
<i>A. thaliana</i>	Col-0	<i>Atrem6.4-1</i>	Kan	SALK-TDNA	SALK_037050.55.00.x
<i>A. thaliana</i>	Col-0	<i>Atrem6.6-1</i>	Kan	SALK-TDNA	SALK_039171
<i>A. thaliana</i>	Col-0	<i>Atrem6.7-1</i>	Kan	SALK-TDNA	SALK_059946
<i>A. thaliana</i>	Col-0	<i>Atrem1.2-2</i>	Kan, Hyg	SALK-TDNA, <i>proAt3g61260:YFP:At3g61260</i>	SALK_117639.51.85.x; <i>proAtREM1.2:YFP:AtREM1.2</i>
<i>A. thaliana</i>	Col-0	<i>Atrem1.3-2</i>	Kan, Hyg	SALK-TDNA, <i>proAt2g45820:YFP:At2g45820</i>	SALK_117448.53.95.x; <i>proAtREM1.3:YFP:AtREM1.3</i>
<i>A. thaliana</i>	Col-0	<i>Atrem6.4-1</i>	Kan, Hyg	SALK-TDNA, <i>proAt4g36970:YFP:At4g36970</i>	SALK_037050.55.00.x; <i>proAtREM6.4:YFP:AtREM6.4</i>
<i>A. thaliana</i>	Col-0	<i>Atrem1.2-</i>	Kan	SALK-TDNAs	SALK_117637.50.50.x;

Appendix

		<i>1/Atrem1.3-2</i>			SALK_117448.53.95.x
<i>A. thaliana</i>	Col-0	<i>Atrem1.2-1/Atrem1.3-2/Atrem1.4-3</i>	Kan	SALK-TDNAs	SALK_117637.50.50.x; SALK_117448.53.95.x; SALK_063841.47.35.x
<i>A. thaliana</i>	Col-0	<i>fls2</i>	kan	SAIL-TDNA	SAIL-691C04
<i>N. benthamiana</i>	-	wildtype	-	-	-

Macros created for Fiji

Quantitative analysis of single domains: Creation of masks for segmentation:

```
run("Mean...", "radius=2");
run("Subtract Background...", "rolling=20");
setAutoThreshold("Default");
//run("Threshold...");
setThreshold(0, 22);
setOption("BlackBackground", false);
run("Convert to Mask");
run("Make Binary");
run("Erode");
run("Erode");
run("Dilate");
run("Dilate");
run("Watershed");
run("Save");
run("Close");
```

Kymographs: Creation of stacks for each time-point:

```
run("Images to Stack", "name=Stack title=[] use");
run("Z Project...", "start=1 stop=14 projection=[Max Intensity]");
saveAs("Tiff", "/Users/ijarsch/Desktop/paper die zweite/kymographs/1.2/MAX_Stack
t09.tif");
close();
selectWindow("Stack");
close();
```

Kymographs: Combination of timepoints and shift correction between time-points:

```
run("Images to Stack", "name=Stack title=[] use");
run("StackReg", "transformation=[Rigid Body]");
run("Properties...", "channels=1 slices=10 frames=1 unit=µm pixel_width=0.15
pixel_height=0.15 voxel_depth=10000.000000 frame=[0 sec] origin=0,0");
saveAs("Tiff", "/Users/ijarsch/Desktop/paper die zweite/kymographs/1.3/StackReg
t00t09.tif");
close();
```

Kymographs: Creation of kymographs from shift-corrected stacks:

```
run("Reslice [/]...", "output=10000.000 slice_count=1 avoid");
saveAs("Jpeg", "/Users/ijarsch/Desktop/paper die zweite/kymographs/1.2/Reslice of
StackReg.jpg");
close();
selectWindow("StackReg t00t09.tif");
close();
```

Funding and fellowships

This work has been financially supported by the German Research Foundation (Deutsche Forschungsgemeinschaft) with grants of the Emmy-Noether Programme to Dr. Thomas Ott (OT423/2-1) and the Collaborative Research Centre 924 (Sonderforschungsbereich 924).

Further funding was provided by the following fellowships:

2009 – 2011: PHD fellowship by the University of Bavaria (Graduiertenförderung nach dem bayrischen Eliteförderungsgesetz)

2011 - 2012: Prolongation of the PHD fellowship by the University of Bavaria (Graduiertenförderung nach dem bayrischen Eliteförderungsgesetz)

2009: Travel grant by the „Bayrisch-Kalifornisches Hochschulzentrum“ (BaCaTeC)

2012: EMBO short-term fellowship for a research stay at the Sainsbury Laboratory

2014: Short term fellowship by the Center for advanced studies (CAS) LMU

Curriculum vitae

PERSONAL INFORMATION

Name	Iris Katharina Jarsch
Contact address	Emil-Geis-Strasse 32; 81379 München
Phone	+49-(0)89-54899770
E-mail	iris.jarsch@biologie.uni-muenchen.de
Date of birth	02.09.1985
Place of birth	Munich
Nationality	German

ACADEMIC CAREER

Since 09/2009	Ludwig-Maximilians-Universität München, Munich, Germany PHD thesis in the research group of Dr. Thomas Ott
Since 10/2009	Enrolled at the International Graduate School of Life Sciences Munich (LSM)
07/2009	Diploma exams (final grade: 1,0)
2004-2009	Ludwig-Maximilians-Universität München, Munich, Germany Studies in Biology, main emphasis on Genetics, cell biology and biochemistry (including Diploma thesis in the research group of Dr. Thomas Ott)
05/2004	Abitur (final grade: 1,1)
1994-2004	Gymnasium Penzberg, High School Graduation

RESEARCH

08/2014 -	Research associate with Dr. Jenny Gallop at The Gurdon Institute/Wellcome Trust, Cambridge, UK
Since 09/2009	PHD thesis in the research group of Dr. Thomas Ott <i>Cell biological and genetic characterization of Arabidopsis thaliana remorin proteins and their role in plant - pathogen interactions</i>
09/2008- 07/2009	Diploma thesis in the research group of Dr. Thomas Ott <i>Characterization of remorin proteins in Arabidopsis thaliana with respect to their localization, oligomerisation and interaction with receptor proteins</i>
11/2007-	Internship at Max Planck Institute for Neurobiology, Martinsried, Germany; Research Group of Dr. Florian

Appendix

02/2008	Kurschus; Studies on <i>“Spontaneous relapsing-remitting EAE in the SJL/J mouse: MOG-reactive transgenic T cells recruit endogenous MOG-specific B cells”</i>
02/2007- 04/2007	Internship at the Institute for molecular Parasitology at the University of Bordeaux II Victor Ségalen; Research project: <i>“Studies on two RNAi double knock-down mutants of metabolic enzymes of Trypanosoma brucei”</i>
05/2006- 12/2006	Internship at the Ludwig Maximilians-Universität München, Germany; Research group of Prof. Dr. Boshart; <i>Creation of a library of stable transgenic RNAi knock-down mutant lines of tyrosine kinases in the model organism Trypanosoma brucei</i>

TEACHING, SUPERVISION OF MASTER, BACHELOR AND LAB ROTATION PROJECTS

WS 2012/2013	Lab rotation project (Student: Christina Carola Weiß); complete supervision <i>Characterization of AtREM6.4 and its interaction with BAK1</i>
2012	Master project (Student: Corinna Hofer); complete supervision <i>„Characterization of a Remorin-interacting receptor-like kinase during plant-pathogen interactions“</i>
SS2012	Practical course: <i>Methods to study protein-protein interactions</i> ; 2 lectures, supervision
SS2011	Lab rotation project (Student: Alexander Buschle); complete supervision <i>The role of AtREM1.2 and AtREM1.3 in early plant defence</i> Practical course: <i>Methods to study protein-protein interactions</i> ; 2 lectures, course preparation and supervision
WS10/11	Practical course Genetik 2; supervision
SS2010	Bachelor project (Student: Elisabeth Dittmer); shared supervision <i>„ Subcellular localizations of the Arabidopsis thaliana remorins AtREM3.1 und AtREM3.2 and investigation of their putative functions“</i> Practical course: <i>Methods to study protein-protein interactions</i> ; supervision
WS09/10	Practical course Genetik 2; supervision

Appendix

SCIENTIFIC PUBLICATIONS

Jarsch IK and Ott T (2011), review article

Perspectives on remorin proteins, membrane rafts and their role during plant-microbe interactions

Molecular Plant Microbe Interactions, 24(1): 7-12

Jarsch IK et al., scientific article

Plasma Membranes Are Subcompartmentalized into a Plethora of Coexisting and Diverse Microdomains in Arabidopsis and Nicotiana benthamiana

The Plant Cell; doi:10.1105/tpc.114.124446

Konrad SSA, Popp C, Stratil TF, **Jarsch IK** et al., scientific article

S-acylation anchors Remorin proteins to the plasma membrane but does not primarily determine their localization in membrane domains.

New Phytologist, *in press*

POSTERS, CONFERENCES AND TALKS

2013	21.10: University of Heidelberg, Germany; COS Special Seminar (invited speaker) 08. – 10.07: PHD seminar of the SFB924 student initiative “Molecular mechanisms regulating yield and yield stability in plants”, Herrsching, Germany (talk)
2012	29. – 31.10: PHD seminar of the SFB924 student initiative “Molecular mechanisms regulating yield and yield stability in plants”, Königsdorf, Germany (talk, poster) 27. – 30.11: Dijon Domain Meeting; Dijon, France (poster) 02. – 05.09: 10 th European Nitrogen fixation conference, Ludwig-Maximilians-Universität, München, Germany 29.07. – 02.08.: XV International Congress of Molecular Plant-Microbe Interactions, Kyoto, Japan (poster)
2011	14. – 16.09: 12 th International Symposium on Plant Protein Phosphorylation (talk)
2010	14. – 19.03: Keystone Symposium on Receptors and Signaling in Plant Development and Biotic Interactions, Tahoe, USA (poster)

FELLOWSHIPS AND PRIZES

2014	Short-term fellowship by the Centre for Advanced Studies (CAS), LMU
2012	EMBO Short-Term Fellowship for a research stay at the group of Dr. Cyril Zipfel, The Sainsbury Laboratory, Norwich, UK DAAD travel stipend for the flight to the XV International

Appendix

	Congress of Plant-Microbe Interactions, Kyoto, Japan
2011	Prize for best poster at PHD seminar of the SFB924 student initiative "Molecular mechanisms regulating yield and yield stability in plants", Königsdorf, Germany
2009-2012	PhD fellowship: University of Bavaria: Graduiertenförderung nach dem Eliteförderungsgesetz der Universität Bayern e.V
2004-2006	E-fellows Stipendium
2004	Apollinaire-Prize for extraordinary achievements in the subject French (Abitur)

HONORARY ENGAGEMENTS

2011-2012	1 st elected president of the student initiative of the SFB924 "Molecular mechanisms regulating yield and yield stability in plants"
2010-2011	Mentoring with the non-profit organization "Die Komplizen: Mentoring für Schüler GmbH"
SS2008	Mentoring for the first Bachelor year at the Faculty for Biology, LMU
2005-2009	Active engagement at the student representative of the Faculty for Biology, LMU, 2007 – 2008 elected member of the student board
08-09/2005	"Green Volunteer" with the Hebridian Whale and Dolphin Trust ("Cetacean Reseach Project"), Tobermory, Scotland, UK